Retinoic Acid Plays Critical Roles in the Late Development of the Heart

By

Suya Wang

Submitted to the graduate degree program in Pharmacology and Toxicology and the Graduate Faculty of the University of Kansas in partial fulfillment of the requirements for the degree of Doctor of Philosophy.

Chair: Honglian Shi, Ph.D.

Alexander R. Moise, Ph.D.

Shirley Shidu Yan, Ph.D.

Mizuki Azuma, Ph.D.

Erik A. Lundquist, Ph.D.

Date Defended: December 6, 2017

The Dissertation Committee for Suya Wang certifies that this is the approved version of the following dissertation:

Retinoic Acid Plays Critical Roles in the Late Development of the Heart

Chair, Honglian Shi, Ph.D.

Date Approved: December 6, 2017

Abstract

Vitamin A, via its active metabolite retinoic acid (RA), actively participates in many biological processes including cardiogenesis. Yet RA was found to be highly teratogenic as both excess and deficiency of this critical morphogen result in congenital heart defects. Studies presented here aims to gain insight in mechanisms regulating RA metabolism during embryogenesis and enrich our knowledge of the critical roles of RA during late heart development. Previously, our lab reported that a short-chain dehydrogenase/reductase, i.e. *DHRS3,* is required for preventing excessive accumulation of RA and thus safeguarding mouse embryogenesis during mid-gestation. The current study expanded the investigation and studied the physiological importance of *DHRS3* in RA metabolism at multiple embryonic stages. Consistent with the elevated RA synthesis and signaling at E14.5, genetic ablation of *Dhrs3* results in an expansion of RA signaling at E10.5 and E12.5 globally; as well as in the fetal hearts at E10.5, 12.5 and 13.5. *Dhrs3*-null mutants display a spectrum of congenital defects, including defects in the heart, skeleton and cranial nerves, which collectively result in mid-gestational lethality in *Dhrs3*$^{-/-}$ embryos. Reduction of maternal intake of vitamin A successfully rescued the *Dhrs3*$^{-/-}$ fetuses and allows them to survive into full-size adults with normal growth rate. These data jointly demonstrated the indispensability of DHRS3 in reducing the accumulation of RA in various developmental stages and in the formation of fetal organs.

With the advancement of knowledge in RA metabolism gained in the first part of this dissertation, the critical roles of RA in cardiogenesis was further explored in the current work. During late cardiogenic stages, the major source of RA is the epicardium. Epicardium contributes greatly to the formation of coronary vessels and the myocardium via 1) giving rise to migratory epicardial cells that differentiate into perivascular cells, and 2) secreting cardiogenic factors. This dissertation employed multiple *in vivo* and *in vitro* models to determine the influence of RA on epicardial behaviors and the subsequent epicardial-regulated cardiogenic events. *In vitro* studies demonstrated that inhibition of RA synthesis in epicardial cell disrupted cytoskeletal reorganization and preserved epithelial characteristics, which resulted in a reduction of migration of epicardial cells. On the contrary, addition of RAR agonist to activate RA

signaling strongly induced remodeling of cytoskeleton represented by the formation of stress fibers as well as filopodia marked by polymerized F-actin. RA signaling also abolished the membranous distribution of epithelial markers and induces expression of numerous metalloproteases to pave the way for cell migration. Data from *in vivo* models showed consistent observation in the regulation of epicardial migration by RA: excess RA in *Dhrs3*$^{-/-}$ embryos enhances the intramyocardial invasion of epicardial cells whereas deficiency of RA largely retained epicardial cells in the intact epicardium on the surface of the myocardium. To further understand the molecular mechanisms underlying the regulation of epicardial EMT by RA, we employed transcriptomic analysis, which in combination with further molecular assays clearly demonstrated that RhoA pathway is activated by RA and proves to be critical for RA-induced morphological changes in epicardial cells. Furthermore, potentially as a consequence of altered epicardial behavior and functions in response to aberrant RA signaling, both deficiency and excess RA led to compromised coronary vessel formation and hypoplastic ventricular myocardium *in vivo*. Vascular hierarchy was severely impaired and density of intramyocardial vessels was drastically diminished by altered RA signaling. Lack of proper recruitment and differentiation of vascular smooth muscle cells further acerbated the malformations in coronary vessels in response to abnormal RA signaling. These observations provided novel evidence of the teratogenic nature of RA and collectively demonstrated that RA signaling is not only actively involved but also critically important in the late heart development, which may shed light on the discovery of methods in preventing congenital heart diseases as well as the identification of novel targets for treating cardiovascular diseases.

Acknowledgement

During my graduate studies at the University of Kansas, I have received enormous help from kind people that made this dissertation possible. Thus I would like to express my most sincere appreciation to all of them.

First and foremost, I would like to express my deepest appreciation and gratitude to my advisor, Dr. Alexander Moise for his wise guidance, continuous support and encouragement. His enthusiasm in research, persistent pursuit of truth as well as perseverance in work set him a true role model which I highly respect. I am truly grateful to him for the great mentorship during the past years, from which I benefit greatly. He has provided insightful suggestions to me about both my projects as well as career. When there's down time, he always brings hope and cheers me up. In addition, he and his lovely family treated me warmly and made me feel home. Indeed it has been my honor and greatest fortune to be his student. I cherish every discussion we had; those golden days when we worked together will be engraved in my memory.

I would like to extend my appreciation to my committee chair, Dr. Honglian Shi, for his kind help with our lab and me during a period of unstable time before my graduation. Dr. Shi's lab is another home of mine at KU and without this strong support of him, this dissertation will be much more difficult to complete. I would like to thank my committee members, Dr. Shirley ShiDu Yan, Dr. Mizuki Azuma as well as Dr. Erik Lundquist for their precious suggestions and constant support during my graduate studies.

I would also like to thank people outside of the department and my committee for their help in my research. I would like to express my appreciation to Heather Shinogle in the Microscopy and Analytical Imaging Core facility for training me on using microscopes, analyzing data and helping me with troubleshooting immunostaining experiments. I would like to thank Dr. Maureen Kane and her lab

members for their help with the proteomics study, Dr. Paul Trainor and Dr. José Xavier Neto for their invaluable suggestions to the current study.

My experience at KU has been joyful largely due to my dearest friends who have been by my side during even the toughest time. I would like to thank my friends, Shuman Chen, Xinyun Liu, Sarah Schmidt, Cristina Parra and Xin Zhang for their warm accompany. Special thanks to my labmates and good friends Mohammed Almutairi, Jiani Chen and Siying Li for sharing my life and providing suggestions to help me troubleshoot at work.

Last but definitely not the least, I wholeheartedly thank my family for their unfailing love and unconditional trust in me. My parents are my best friends and their wisdom in life and resilience in the face of difficulty has taught me the most valuable lesson in my life. This work will not be possible without the good characteristics I learned from them. I would like to thank my boyfriend, Siyu Ou, for his support and encouragement, which has been an inexhaustible source of strength of mine.

This work is supported by the grant R01HD077260 (A.R.M., M.A.K., P.A.T) from the National Institutes of Health.

Table of contents

List of Figures

Supplementary Figures

List of Tables

List of Abbreviation

AKR	aldo-keto-reductases
BCDO1	beta-carotene 15, 15-dioxygenase 1
BMP	bone morphogenetic protein
CNCC	cardiac neural crest cells
CRABP	cellular retinoic acid binding protein
CV	cranial nerve
CYP26A1	Cytochrome P450 family 26 subfamily A member 1
DHRS3	dehydrogenase/reductase 3
DR	direct repeat
EMT	epithelial to mesenchymal transition
EPDC	epicardial derived cells
EpiMT	epicardial epithelial to mesenchymal transition
EPO	erythropoietin
EPOR	erythropoietin receptor
FGF	fibroblast growth factor
GATA	GATA Binding Protein
HOX	Homeobox
IGF	Insulin-like growth factor
IGFR	insulin-like growth factor receptor
ISL1	ISL LIM Homeobox 1
ISX	intestine specific homeobox
LC	liquid chromatography
LPL	lipoprotein lipase
LRAT	lecithin retinol acyltransferase
MEC1	mouse epicardial cells
MS	mass-spectrometry
NKX2.5	NK2 Homeobox 5
OFT	outflow tract
PDGFBB	platelet derived growth factor BB
PDGFRA/B	platelet derived growth factor receptor alpha/beta
PE	proepicardium
PHF	primary heart field
RA	retinoic acid
RAL	retinaldehyde
RALDH	retinaldehyde dehydrogenase
RAR	retinoic acid receptor
RARE	retinoic acid responsive element
RBP4	retinol binding protein 4
RBPR2	RBP4 receptor-2
RDH10	retinol dehydrogenase 10
RE	retinyl esters
REH	retinyl ester hydrolase
RHOA	Ras homolog family member A

RND3	Rho family GTPase 3,
ROCK	Rho associated coiled-coil containing protein kinase 1
ROL	retinol
RT-PCR	quantitative real-time polymerase chain reaction
RXR	retinoid X receptor
SCARB1	scavenger receptor class B member 1
SDR	short-chain dehydrogenase/reductases
SHF	second heart field
STRA6	stimulated by retinoic acid 6
TBX	T-box transcription factor
TCF21	transcription factor 21
TGFβ	transforming growth factor β
VAD	vitamin a deficiency
VAS	vitamin a sufficient
VEGF	vascular endothelial growth factor
VLDL	very low density lipoprotein
VSMC	vascular smooth muscle cells
WT1	Wilms-tumor 1
WGA	Wheat germ agglutinin

Chapter 1 : Introduction

Vitamin A, is required for multiple biological processes during both embryonic development and postnatal life. In adults, vitamin A deficiency (VAD) results in growth arrest, blindness, and impaired immunity. Both excess and deficiency of vitamin A during fetal life can result in a variety of congenital defects (Dickman & Smith, 1996; Hale, 1937; Lammer et al., 1985; Mason, 1935; Shenefelt, 1972; Tickle, Lee, & Eichele, 1985; J. S. Waxman, B. R. Keegan, R. W. Roberts, K. D. Poss, & D. Yelon, 2008; Wilson, Roth, & Warkany, 1953a). Vitamin A exerts its biological functions primarily through two of its metabolites: 11-*cis*-retinaldehyde and all-*trans*-retinoic acid (ATRA) (Collins & Mao, 1999; Lohnes et al., 1994; Wilson & Warkany, 1948). While 11-*cis* retinaldehyde is required in visual phototransduction, ATRA participates in transcriptional regulation via its cognate retinoic acid receptors (RARs) which form heterodimers with the retinoid X receptors (RXRs) (Giguere, Ong, Segui, & Evans, 1987; Kliewer, Umesono, Mangelsdorf, & Evans, 1992; Petkovich, Brand, Krust, & Chambon, 1987). Considering the adverse consequences of altered ATRA-signaling, it becomes clear that the levels of ATRA within target cells need to be very tightly controlled. Therefore, it is imperative that we develop a better understanding of the metabolic pathways that control ATRA formation, transport and breakdown and of the transcriptional pathways controlled via ATRA-signaling within target tissues.

The heart is the first organ to form during embryogenesis, and the success in establishing cardiovascular system lays the foundation of further development of other organs and systems. Perturbation of cardiogenesis leads to congenital heart defects (CHDs). CHDs are the most common birth defects in humans, affecting nearly 1% of newborns in the United States and resulting in 30% loss of embryos prenatally (Bruneau, 2008; Hoffman, 1995; Hoffman & Kaplan, 2002). Previous studies have revealed a delicate network of genes that regulate cardiogenesis and multiple signaling molecule have been involved, including ATRA (Collop et al., 2006; Heine, Roberts, Munoz, Roche, & Sporn, 1985; Niederreither, Subbarayan, Dolle, & Chambon, 1999; Osmond, Butler, Voon, & Bellairs, 1991). In this

review, we aim to provide an update of the current understanding of the connection between altered RA metabolism and / or signaling and several major aspects of congenital cardiac defects, as well as recent efforts in unveiling the underlying mechanisms by which RA regulates the cardiac development.

1.1. RA metabolism and signaling

Homeostasis of vitamin A is maintained by proper controlled absorption and transport of vitamin A from diet. Dietary sources of vitamin A include both preformed vitamin A such as retinol and retinyl esters (REs), as well as provitamin A carotenoids such as β-carotene and β-cryptoxanthin, which have unsubstituted β-ionone rings. Both forms of vitamin A are absorbed in the intestine and transported to the liver by chylomicrons through lymphatic circulation. Upon arrival at the liver, REs are hydrolyzed and taken up by the liver to be esterified and stored in the stellate cells for storage in the form of REs. Alternatively, retinol in hepatocytes can be secreted in association with serum retinol binding protein 4 (RBP4), which forms a complex with transthyretin and retinol for further delivery to other tissues (Moasser & Dmitrovsky; Shirakami, Lee, Clugston, & Blaner, 2012). Independent of RBP4, vitamin A can also be transported as RE in association with VLDL and chylomicrons for delivery to peripheral tissues via the lipoprotein lipase (LPL). Clinical studies showed that total loss of RBP4 function in patients was associated with VAD-like symptoms (Cukras et al., 2012). Yet in some clinical cases, such a mutation was found to be non-symptomatic or cause only mild symptoms, possibly because the lack of transport of vitamin A via RBP4 was compensated by circulating REs and β-carotene in these patients (Biesalski et al., 1999). During embryogenesis, VLDL and chylomicrons-associated RE and retinol-bound RBP4 are also the major pathways for delivery of retinoids to the embryo (Moasser & Dmitrovsky; Quadro et al., 2005; Sapin, Bègue, Dastugue, Chambon, & Dollé, 1998). Loss of either maternal or fetal-derived RBP4 can results in VAD-like symptoms in embryos (Båvik, Ward, & Chambon, 1996; Quadro et al., 2005). These defects observed in embryos with *Rbp4* null mutation displayed with various severity, which could be attributed to different maternal levels of REs and provitamin A carotenoids that can be delivered across the placenta in a RBP4-independent manner. Interestingly, maternal transmission of the

mutation of Rbp4 was noticed to cause much stronger phenotypes in offspring than the mutation transmitted by the father. This is because in addition to defects associated with fetal derived non-functional RBP4, maternally derived defective RBP4 further disrupts the transport of retinoids cross the placenta thus reducing the amount of retinoids the embryos get from the mother via RBP4 (Chou et al., 2015). Though previous studies have clearly demonstrated the importance of RBP4 in delivery of maternal vitamin A to the embryo, the mechanism of how vitamin A is transported in the placenta remains mysterious because neither maternal nor fetal RBP4 crosses the placental barrier (Quadro et al., 2004). In addition, when derived from dams reared on vitamin A sufficient diet, *Rbp4*$^{-/-}$ embryos display normal growth in most organs besides the heart, suggesting that additional transport proteins and receptors play a role in retinol transport, and that proper delivery of retinol by RBP4 is required for cardiogenesis. Indeed, it was found that the concentration of RE in circulation surged in *Rbp4*$^{-/-}$ mice reared on vitamin A sufficient diet, which is not seen in fasted *Rbp4*$^{-/-}$ mice, indicating that REs transported in the conjunction with lipoproteins may compensate for the loss of *Rbp4* in most organs (Quadro et al., 2004; Quadro et al., 2005; Wendler et al., 2003).

At target tissue, retinol is imported into cells and either esterified to RE for storage or metabolized to ATRA to exert its biological functions. The retinol-RBP4 complex is recognized by the RBP4 receptors, such as Stimulated by Retinoic Acid 6 (STRA6) and Retinol Binding Protein Receptor 2 (RBPR2) (Alapatt et al., 2013). STRA6 can bind to RBP4 with high affinity and function as a bidirectional transporter of retinol by mediating influx or efflux of retinol, depending on the levels of intracellular retinol and the ratio of holo- to apo-RBP4 (Isken et al., 2008). STRA6 has also been found to be responsible for transferring retinol across the blood-tissue barrier in adults (M. Kelly, Widjaja-Adhi, Palczewski, & von Lintig, 2016). Yet, *Stra6* null mutant mice display profound retinoid deficiency and impaired development of the visual tissues but otherwise develop normally, possibly due to a compensatory effect of other *RBP4* receptors such as *RBPR2* or other modes of retinol uptake by non-visual target tissues (Berry et al., 2013). In fact, Rbpr2 has distinct expression domain from Stra6, and has

been shown to facilitate retinol import in tissues where Stra6 is absent, such as adult liver and intestine (Bouillet et al., 1997).

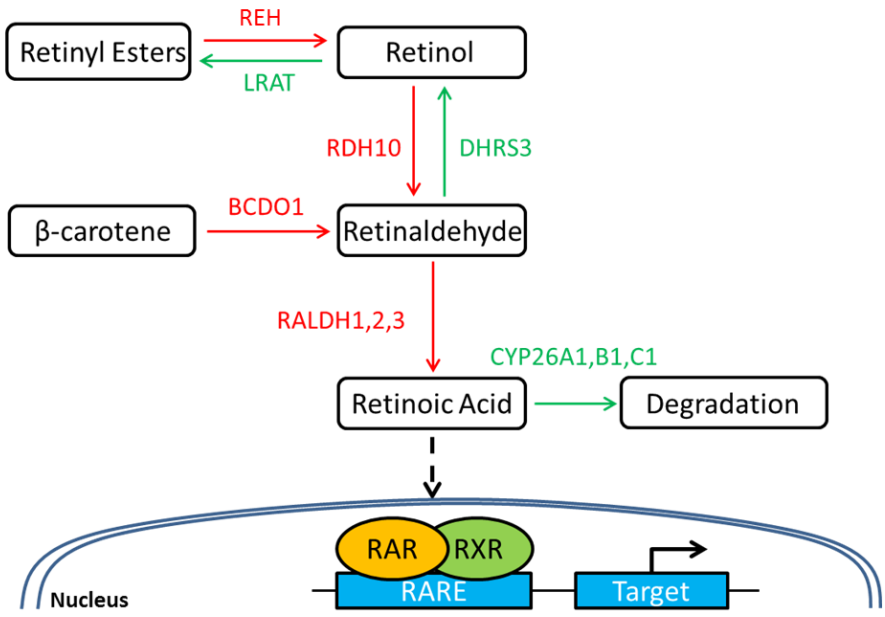

Figure 1.1 Overview of RA metabolism and signaling

Intracellular retinol is metabolized to RA through a two-step oxidation (Fig 1.1). Retinol is first reversibly oxidized to an intermediate, i.e. retinaldehyde, by either medium-chain alcohol dehydrogenases (ADHs), or short-chain dehydrogenase/reductase (SDR) enzymes. Of the latter, retinol dehydrogenase 10 (RDH10), has been shown to be critical for RA synthesis during embryogenesis. Mouse embryos lacking *Rdh10* die at E9.5 of a variety of congenital defects similar to those observed in embryonic models lacking sufficient RA, such as craniofacial defects and malformed forelimbs (Clagett-Dame & DeLuca, 2002; Niederreither, Subbarayan, Dollé, & Chambon, 1999; L. L. Sandell et al., 2007). Maternal supplementation of either RA or retinaldehyde successfully postponed the embryonic lethality in *Rdh10* null mice. The first oxidation of retinol to retinaldehyde is reversible and the reductive reaction is essential for fine-tuning the rate of ATRA formation and to prevent ATRA-induced teratogenic effects. Retinol produced as a result of reduction of retinaldehyde can be sequestered as RE for storage internally or exported externally to other tissues. Previously, we and others have demonstrated that the reduction of

retinaldehyde in embryos is primarily carried out by short-chain dehydrogenase/reductase family member 3 (DHRS3) (Adams, Belyaeva, Wu, & Kedishvili, 2014; Billings et al., 2013; Feng, Hernandez, Waxman, Yelon, & Moens, 2010; R. K. T. Kam et al., 2013). Global deletion of *Dhrs3* in mouse embryos results in an elevated level of ATRA, which leads to late-gestational lethality as well as congenital defects such as cleft palate, heart malformations and skeletal defects (Billings et al., 2013). Interestingly, a recent study reported that DHRS3 and RDH10 have overlapped expression patterns in the limb bud where they associated and reciprocally activated each other (Adams et al., 2014), which allows for the fine-tuning of the production of RA in embryonic tissues. Other enzymes, such as some aldo-keto-reductase, have also been shown to participate in the reduction of retinaldehyde *in vitro* however their importance during embryogenesis needs further investigation (Gallego et al., 2007; Ruiz et al., 2009; Ruiz et al., 2011).

The second oxidation step, converting retinaldehyde to RA, occurs quickly and irreversibly. Though multiple enzymes have been found to be able to catalyze this reaction *in vitro*, genetic evidence identified retinaldehyde dehydrogenase (RALDH) 1, 2 and 3 as the major RA-synthesizing enzymes in embryogenesis (Kumar, Sandell, Trainor, Koentgen, & Duester, 2012). RALDHs have distinct expression patterns and thus are in charge of RA synthesis at different time points and in various tissues. Among these enzymes, RALDH2 is the most critical for cardiogenesis, since *Raldh2* mutant mouse embryos die around E9.0 and display a wide range of severe defects in the heart (Niederreither et al., 2001; Karen Niederreither et al., 1999). RALDH3 is found in the embryonic retina, nasal area as well as skeletal muscle. Absence of *Raldh3* leads to perinatal lethality, primarily because of respiratory distress induced by insufficient ATRA signaling reference. On the contrary, a lack of *Raldh1*, which expresses in the brain, retina and cardiac valves, does not cause embryonic death, possibly because of the compensation by the other RALDHs (Deltour, Foglio, & Duester, 1999). Besides RALDH1-3, another RALDH-independent ATRA synthetic enzyme has also been reported, i.e. CYP1B1, whose expression overlaps with RALDH2 in the mesoderm and can compensate for the lack of RALDH2. This compensation might

be responsible for the ameliorated phenotypes in *Raldh2*$^{-/-}$ embryos when compared to complete VAD quail model.

Degradation of retinoic acid is catalyzed by cytochrome P450 family member, CYP26 A1, B1 and C1, which hydrolyze excess retinoic acid to inactive metabolites. Oxidative products of RA were proposed to mediate signaling functions but evidence derived from genetic models demonstrates that deficiency in the Cyp26a1 can be rescued by a reduction in the expression of Raldh2. This suggests that oxidative metabolites do not carry out essential roles in embryogenesis (Niederreither, Abu-Abed, et al., 2002). Loss of function studies, highlight the necessity of these enzymes to limit the concentration of RA and act to prevent the expansion of RA-signaling domains. *Cyp26a1*$^{-/-}$ embryos have truncated posterior structures and die during mid-gestation (Suzan Abu-Abed et al., 2001); *Cyp26b1*$^{-/-}$ mice display craniofacial and limb defects and die right after birth (Glenn Maclean, Dollé, & Petkovich, 2009; Yashiro et al., 2004); while ablation of *Cyp26c1* does not result in any embryonic defect (M. Uehara et al., 2007). Similar to Raldh1-3, Cyp26a1-c1 has distinct expression domains. Interestingly, their expression patterns have been observed to be complementary to ATRA synthesizing enzymes: Raldh2-enriched regions are neighbored with Cyp26-expressing regions, for example in the developing anteroposterior axis and tailbud (Sakai et al., 2001; Swindell et al., 1999). While Raldhs-expressing domains act as the source of producing ATRA, Cyp26-expressing regions function as a sink to constrain the distribution of ATRA and thus control its endogenous level at distinct regions and windows of development. These complex expression patterns of Raldhs and Cyp26 create a gradient of ATRA in the embryo, which provides guidance to the anteroposterior patterning of the body axis and hindbrain (Suzan Abu-Abed et al., 2001; Ribes, Fraulob, Petkovich, & Dolle, 2007; Sakai et al., 2001). As mentioned before, the levels of RA are further fine-tuned at the level of interconversion of retinol-retinaldehyde (Adams et al., 2014).

Beside retinol, provitamin A carotenoids can also be converted to retinaldehyde to participate in retinoid metabolism. Provitamin A carotenoids, such as β-carotene, serves as the major source of retinoids in herbivores. Uptake of carotenoids is mediated by Scavenger receptor class B member 1

(SCARB1) in the intestinal epithelial cells. Upon absorption, carotenoids undergo oxidative cleavage by β-carotene-15,15-dioxygenase 1 (BCDO1) to produce retinaldehyde, which is either reduced to retinol for redistribution into other organs or oxidized to RA for signaling (Hessel et al., 2007; von Lintig & Vogt, 2000; Wyss et al., 2000). Since the conversion of β-carotene to retinaldehyde and that of retinaldehyde to RA are both irreversible and RA levels have to be tightly controlled to prevent toxic effects, enzymes that can convert retinaldehyde to retinol and thus prevent the relentless accumulation of RA, for example DHRS3, are of critical importance especially in herbivorous animals.

As a potent teratogen, RA maintains its own homeostasis by regulating metabolic enzymes through feedback mechanisms. It was noticed that the levels of absorption of carotenoids are sensitive to the status of retinoids. Mice reared on VAD diet have much higher absorption of β-carotene and elevated expression levels of *Scarb1* and *Bcdo1,* suggesting a self-adjusting homeostasis of the metabolism of retinoids (Lobo et al., 2010). Further analysis identified a RA-responsive transcription factor, namely Intestine Specific Homeobox (ISX), to be exclusively expressed in the epithelial cells of the gut where carotenoids are absorbed. Activated RAR induces the expression of *Isx* through binding to a regulatory *cis*-element in the promoter of *Isx*, while *Isx* efficiently binds and suppresses the expression of *Scarb* and *Bcdo1*. Consistently, *Isx*-null mutant mice absorb higher amount of β-carotene. Thus, RA controls the absorption of β-carotene through transcriptionally inducing the expression of Isx, which down-regulates the transcription of Scarb and Bcdo1. In addition, RA regulates its metabolism by directly or indirectly modulating the transcription of critical enzymes involved in RA metabolism. For example, activation of RA signaling strongly up-regulates the transcription of enzymes that either degrade RA or prevent the formation of RA, i.e. Cyp26a1 and Dhrs3, respectively; and down-regulates the expression of RA synthetic enzymes, such as Rdh10 and Raldh2, was found to be suppressed by excess RA (Abu-Abed et al., 1998; Billings et al., 2013; Emoto, Wada, Okamoto, Kudo, & Imai, 2005; Feng et al., 2010).

The complex regulation of RA in biological processes ensures that RA signaling can transcriptionally modulate gene expression in a precise spatial and temporal manner. ATRA regulates the transcription of

target genes through binding as a ligand to nuclear receptor RAR and RXR. In the absence of ATRA, RAR and RXR form heterodimer which have been found to be associated with a DNA sequence termed retinoic acid response element (RARE) in the promoter of RA target gene. The RAR/RXR complex also recruits transcriptional co-repressors to suppress gene expression in such a non-ligand silent phase. Once ATRA is present, the conformational changes brought by the binding of ligand to the RAR/RXR complex lead to dissociation of the co-repressors and the recruitment of co-activators to relax the chromatin and to facilitate gene transcription. Though binding of ATRA to the RAR/RXR heterodimer generally results in the activation of transcription of target genes, there is evidence that in some cases it can lead to suppression of some targets, for example Fibroblast growth factor 8 (Fgf8) (Kumar & Duester, 2014). Recent studies have proposed that the mode of regulation of gene transcription by RA (activation versus repression) is dictated by the type of RARE and its local environment. Analysis of the occupancy of RAR on genome revealed that a typical RARE consists of direct repeats of 5'-PuGGTCA-3' that are spaced by 1, 2 or 5 nucleotides, namely DR1, 2 and 5. Novel RAREs are being continuously identified such as DR0 and DR8 (Emmanuel Moutier et al., 2012). Most DRs were found to be capable of regulating transcription independently upon ligand binding to RAR, and DR0-RARE was noticed to Therefore, the distribution of RA signaling depends on the expression of both RA metabolic enzymes and the signaling elements. RAR and RXR each have 3 isoforms, α, β and γ (Kliewer et al., 1992; Krust, Kastner, Petkovich, Zelent, & Chambon, 1989; Petkovich et al., 1987); each has distinct spatiotemporal expression patterns and biological functions during embryogenesis (Lohnes et al., 1994; Mollard et al., 2000). Yet these receptors also possess some level of redundancy in their physiological roles, since genetic deletion of a single RAR has mild phenotype when compared to a double knock-out mutant and does not result in a full spectrum of VAD syndrome, most likely due to a compensatory effect by other isoforms of existing RARs (Ghyselinck et al., 1997; Hutson & Kirby, 2007; E. Li, Sucov, Lee, Evans, & Jaenisch, 1993; Subbarayan et al., 1997).

1.2. Cardiogenesis and its dependence on RA signaling

The formation and maturation of the heart is achieved by contribution from cells derived distinct origins including the mesoderm and ectoderm. At E7.5, the myocardial progenitor cells starts to develop from the splanchnic lateral plate mesoderm and form the cardiac crescent, which is also known as the primary heart field (PHF) (Figure 1.2). Another population of cardiogenic cells derived from the pharyngeal mesoderm reside medial to the PHF and form the second heart field (SHF). Progenitor cells arising from PHF/cardiac crescent and SHF contribute different to the morphogenesis of the heart. In mouse embryos at E8, cardiac crescent folds and fuses medially to form the primitive heart tube, through which blood can flow to establish systemic circulation. The heart tube elongates with the addition of cells from the SHF and neural crest to the anterior region of the heart. As the heart tube grows, it loops to the right at E9 and start to develop septation between chambers at E10. Whereas cells from PHF contribute primarily to the myocardium, progenitor cells derived from the SHF facilitates the development of the atrium, outflow tract (OFT) and right ventricle (Galli et al., 2008; S. Zaffran, Kelly, Meilhac, Buckingham, & Brown, 2004). The neural crest cells that contribute to the formation of the heart are termed cardiac neural crest cells and they play an important role in the septation of OFT (Minoux & Rijli, 2010). During E9.0 to E9.5, cells derived from the proepicardium (PE), a cluster of cardiac progenitor cells that originate from mesothelium and reside adjacent to sinus venosus, migrate and cover primitive heart tube to form the epicardium, which promotes development and maturation of myocardium and coronary vessels (Ingo Stuckmann, Samuel Evans, & Andrew B. Lassar, 2003). With the addition of these progenitor cells, the primitive heart tube finally develops to a well-segregated four-chambered organ that can pump blood to peripheral tissues to provide nutrients and take away waste, which is fundamentally important for embryos when diffusion is not sufficient. This elaborate cardiogenic process requires the coordination of multiple signaling molecules, including RA, which can modulate cell proliferation, differentiation and apoptosis (Azambuja et al., 2010; Ghyselinck et al., 1998; Ingo Stuckmann et al., 2003).

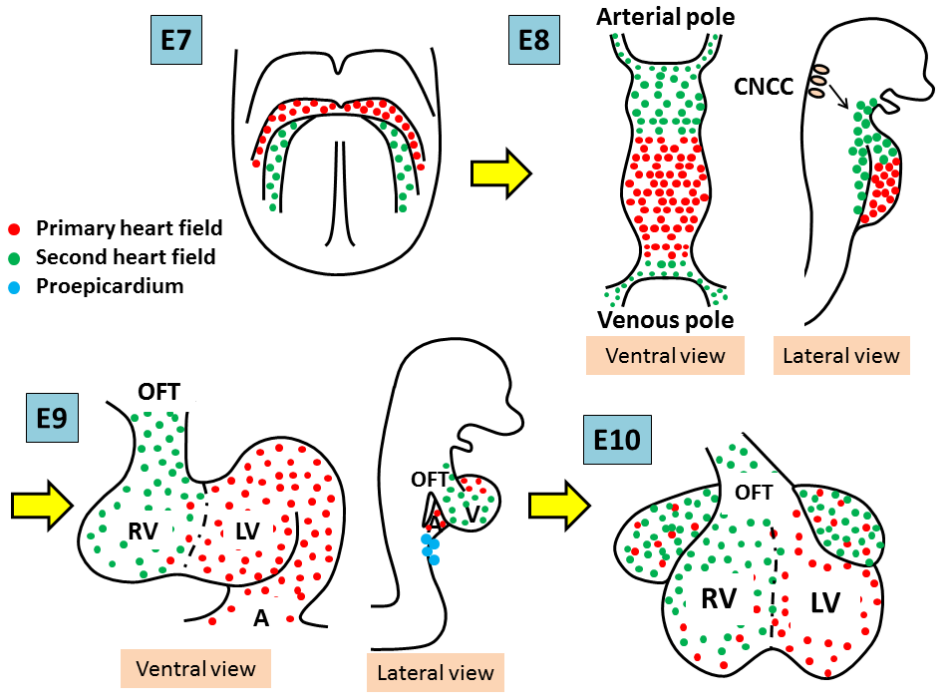

Figure 1.2 Heart morphogenesis in mouse embryos.

Cardiogenic progenitor cells populate the cardiac crescent (green) and the SHF (red) at embryonic day (E) 7. At E8, cardiac crescent fuses to form the primitive heart tube and progenitors derived from SHF are added to both poles of heart tube to facilitate the elongation of the heart. Cardiogenic CNCCs start to migrate to cardiogenic fields to assist heart formation. Primitive heart tube loops to the right at E9 and cells from PE (blue) start to migrate to the surface of the looping heart to form epicardium. At E10, septation between cardiac chambers begins to form and the heart develops into a four-chambered organ.

The requirement of RA during cardiogenesis has been well established in multiple models. Dietary approaches have been historically most common method to study the role of vitamin A in development animals. Avian embryo lacking vitamin A displays severe cardiovascular defects, most notably a lack of inflow tract due to the closure of posterior heart tube (Heine et al., 1985). Genetic ablation of genes involved in RA metabolism and signaling was frequently employed to study the roles of RA in cardiogenesis and results derived from those genetically modified models suggest that perturbation of RA signaling can lead to various cardiac malformations. Ablation of *Raldh2* or *Rdh10* in mice leads to early embryonic lethality with severe malformations in early heart development, such as dilation and failed looping of the heart tube (K. Niederreither et al., 1999; Lisa L. Sandell, Lynn, Inman, McDowell, &

Trainor, 2012). Maternal supplementation of RA postpones the lethality induced by deficiency of RA signaling in those mutant embryos and the rescued *Raldh2* and *Rdh10* null mutants display other spectrum of cardiac defects, which include double outlet ventricle, common arterial trunk, thin ventricular wall and hypoplastic atria; as well as defective coronary vessel formation and misaligned great arteries (Azambuja et al., 2010; Hoover, Burton, Brooks, & Kubalak, 2008; Kastner et al., 1997; S.-C. Lin et al., 2010; M. Rhinn, Schuhbaur, Niederreither, & Dolle, 2011; Muriel Rhinn & Dollé, 2012). Genetic or pharmacological approaches have also been employed to test the necessity of RA signaling during cardiogenesis and due to the redundancy between different isotypes of RARs and RXRs, two or more RARs/RXRs have to be deleted to effectively abolish RA signaling. Loss of function of RAR and/or RXR recapitulates cardiac defects observed in VAD models, further supporting the requirement of sufficient RA signaling in the formation of the heart (Chazaud, Chambon, & Dolle, 1999; Romeih, Cui, Michaille, Jiang, & Zile, 2003) . On the other hand, overexposure of chicken embryos to high levels of RA results in a variety of cardiac defects including cardia bifida, abnormal looping of the heart tube and even duplicated hearts in severe cases (S. M. Smith, Dickman, Power, & Lancman, 1998; Zile, 1999). Hyperactivation of RA signaling achieved by genetic deletion of enzymes that prevent accumulation of RA, i.e. CYP26 and/or DHRS3, can also impair cardiogenesis (Billings et al., 2013; Niederreither et al., 2001; Pennimpede et al., 2010). Mouse embryos lacking *Cyp26a1* manifest defective cardiac looping; *Cyp26a1* and *c1* double mutation increases the number of atrial cells; *Dhrs3* null mice display several defects including double outlet ventricle, septal defects and impaired looping (Suzan Abu-Abed et al., 2001; Billings et al., 2013; A. B. Rydeen & Waxman, 2014). Interestingly, embryos with excess or deficient RA signaling share a largely overlapping spectrum of symptoms (Billings et al., 2013; Kolodzinska, Heleniak, & Ratajska, 2013; G. Maclean, Dolle, & Petkovich, 2009; M. Uehara et al., 2007), the basis of which is worthy of further investigation.

1.3. RA and early cardiogenesis

Early embryonic development of the heart involves the contribution from progenitor cells from two distinct cardiogenic fields. Precursors derived from the PHF build up the primitive heart tube and are the first to differentiate into cardiomyocytes. These cells contribute primarily to the prospective left ventricle. A second wave of splanchnic mesodermal-derived progenitors is the cardiogenic cell population from the SHF. During the formation of the cardiac crescent the SHF progenitor cells remain undifferentiated and highly proliferative thus facilitating the growth of the heart tube. Strikingly, studies have found that SHF cells are pre-patterned before migrating to the initial heart tube. In pharyngeal mesoderm, while LIM transcription factor Islet1 being a pan-SHF marker (Cai et al., 2003), the expression of Fgf10 and/or T-box 1(Tbx1) specifies the anterior SHF and that of Tbx5 marks the posterior portion. Fate-tracing experiment using Fgf10 promoter-driven lacZ transgene indicated that the rostral SHF cells contribute to the right ventricle and the myocardium of OFT (S. Zaffran et al., 2004). Fluorescent dye based-cell tracing in chicken embryos later showed that the posterior SHF progenitor cells give rise to the atria and sinus venosus (Galli et al., 2008; R. G. Kelly, 2012). Previous studies have demonstrated that surgical ablation of SHF results in defects in OFT such as overriding aorta and pulmonary atresia (Ward, Stadt, Hutson, & Kirby, 2005) and the genetic deletion of SHF-specific genes such as Isl1 and Fgf8 leads to defective septation and misalignment of the OFT, as well as failure in heart looping and elongation (Cai et al., 2003; Ilagan et al., 2006; Xu et al., 2004). These data clearly demonstrated the importance of SHF in the heart morphogenesis.

Sufficient and appropriate RA signaling is critical for the early development of the primitive heart tube. Embryos with severe VAD display early mortality; for example, *Raldh2*$^{-/-}$ mice and quail VAD embryos die before E9.5 and E4, respectively (Dersch & Zile, 1993; Kostetskii et al., 1999; Twal, Roze, & Zile, 1995). Analysis of the gross morphology of these embryos found that the hearts fail to loop and occasionally exhibit situs inversus. The posterior portion of the quail embryonic heart tube is severely affected by VAD: the inflow tract is closed and thus not connected to the embryonic or extra-embryonic

blood circulation. Detailed examination of cardiac markers demonstrated that shortage of vitamin A supply leads to a loss of left-right asymmetry and the disorganization of the A-P axis in the heart tube (Karen Niederreither et al., 1999). The early mortality of embryos lacking sufficient RA can be rescued by administration of exogenous RA. Maternal replenishment of RA corrected most cardiac abnormalities in *Raldh2*$^{-/-}$ mouse embryos besides the septal defect of OFT (Niederreither et al., 2001). Addition of ATRA at the 5-somite stage fully recovered cardiogenic programs in VAD quail embryos, suggesting a critical retinoid-sensitive window during early avian development (Kostetskii et al., 1998). From the point of view of RA-signaling, the RA receptors RARα, RARγ and RXRα are expressed in the precardiogenic mesoderm at 5-somite stage and the major RA synthetic enzyme *Raldh2* was found to be expressed adjacent to the sino-atrial region of the early heart from E8.25 and on in mouse embryos (Jennifer B Moss et al., 1998). In conclusion, all the components of RA signaling are present in early cardiogenesis (Kostetskii et al., 1998). Contrary to VAD models, excess RA applied to chicken embryos leads to a misshaped and abnormally looped heart tube. Situs inversus and duplication of the heart are also observed when teratogenic dose of RA (100μg/ml) is added (Dickman & Smith, 1996; Osmond et al., 1991). However, the teratogenic effect of RA in heart looping seems to be position-dependent; ATRA added to the right precardiac field disrupts the heart rightward looping while the same dose added to the left has no significant effect (S. M. Smith et al., 1997). Therefore precisely controlled amount of RA at the right time and place is indispensable for normal early cardiogenesis (Xavier-Neto et al., 2015).

1.4. The role of RA in specification of cardiac progenitor pool

Studies from multiple animal models suggest RA limits the size of cardiac progenitor pool especially in the SHF. *Raldh2*-null mutant mouse embryos display an expansion of the cardiac marker *Nkx2.5*, pan-SHF markers *Isl1* as well as several anterior SHF makers (Lucile Ryckebusch et al., 2008; Sirbu, Zhao, & Duester, 2008). Zebrafish embryos with reduced RA synthesis or signaling exhibit an increased Nkx2.5-positive cardiogenic cell population and while addition of exogenous RA has the opposite effect on the size of progenitor pool (Keegan, Feldman, Begemann, Ingham, & Yelon, 2005). Similarly, *Xenopus*

embryos treated with an RA antagonist have transient increase in the size of Nkx2.5-expressing cardiogenic domain (Collop et al., 2006). In contrast to RA-deficient models, addition of RA to SHF in chicken embryos down-regulates the expression of SHF markers Isl1 and Fgf8 (Narematsu, Kamimura, Yamagishi, Fukui, & Nakajima, 2015). As consequences of the changes in early cardiogenesis, the later cardiac development shows consistent alteration in heart sizes in response to abnormal RA signaling. Blocking either synthesis or signaling of RA leads to enlarged cardiac chambers with significant increase in cell number (J. S. Waxman et al., 2008; Waxman & Yelon, 2009). However observation made in zebrafish model treated with various doses of RA suggested that RA seemed to have dual roles in the formation of heart at different concentrations and that ventricular and atrial cardiomyocytes showed different sensitivity to RA signaling. Waxman *et al.* reported that while addition of teratogenic dose of RA (high dose) could dramatically reduce both cardiac chambers in zebrafish embryos, low dose of RA paradoxically increased the number of cell in the atrium but did not alter the formation of ventricle (J. S. Waxman et al., 2008; Waxman & Yelon, 2009). The authors reasoned that the regulation of the size of primitive cardiogenic pool requires higher RA signaling while the A-P patterning of heart tube and subsequent determination of chamber sizes are more sensitive to RA signaling and requires only low levels of RA. Though this hypothesis might explain the observation, it needs to be considered with caution and information about spatiotemporal distribution of RA synthesis and signaling in the cardiogenic region, as well as the information of physiological concentrations of RA during early heart formation. Despite the paradoxical observation with low dose of RA in zebrafish, previous studies have clearly demonstrated a critical role of RA in affecting the size of cardiac progenitor pool during early heart formation.

In zebrafish models, a new mechanism was recently proposed that RA signaling affects the cardiac progenitor pool through influencing the fate decision of mesodermal-derived progenitor cells. Embryos lacking sufficient RA signaling have expanded cardiac progenitor pool and severely reduced forelimb, indicating a converse relationship between the development of the heart and the forelimb (Grandel et al.,

2002). Zebrafish models have been broadly used in aspect of studying the influence of RA-regulated non-cardiogenic lineage in cardiogenesis. Unlike mouse and chick embryos where RA synthesizing enzyme Raldh2 is expressed in the posterior cardiac field at the cardiac crescent stage (Tatiana Hochgreb et al., 2003; Sirbu et al., 2008), in zebrafish Raldh2 is expressed in the forelimb field posterior to the cardiogenic region. Consistent with this distribution of RA synthesizing enzyme, several RA-responsive genes are expressed in the forelimb field but not the heart, for example Homeobox b5b (Hoxb5b) (Joshua S. Waxman, Brian R. Keegan, Richard W. Roberts, Kenneth D. Poss, & Deborah Yelon, 2008). These observations imply that the functions of RA in regulating cardiac progenitor pool might be indirect and acting in non-cell-autonomous fashion. Results from fate mapping technique that marks the multipotential blastomeres demonstrated that in response to blocked RA signaling, pluripotent progenitor cells commit to cardiac-lineage two times as frequently compared to the control group, suggesting that RA functions to limit cardiogenic fate decision and promote non-cardiac lineage commitment (Keegan et al., 2005). Later studies from the same lab further reported that the expanding cardiac progenitors in RA-deficient zebrafish embryos occupy the domain where normally forelimb progenitor cells would reside, indicating a balance between cardiac and forelimb lineages that is RA-responsive. However, even though in the transplant study, donor cells contribute more to cardiogenic progenitors and less to fin mesenchyme in response to a lack of RA signaling, no fate transformation between these two lineage populations have been observed (Joshua S. Waxman et al., 2008). Therefore, RA can influence fate decision of the pluripotent progenitor cells independently before their fate decision, but not after.

Molecular analysis identified Tbx5 to be critical in carrying out the roles of RA in regulating limb versus cardiac lineage specification. As discussed above, cell fate decision between limb and cardiogenic populations greatly affects the development of the heart and RA signaling may indirectly limit cardiogenic pool by promoting forelimb progenitor formation. One of the genes that are RA-responsive and regulate forelimb development is Tbx5 (Mercader, Fischer, & Neumann, 2006; Lucile Ryckebusch et al., 2008). Similar to Nkx2.5 and Gata4, Tbx5 is one of the earliest expressed genes in cardiogenic

mesoderm (Chapman et al., 1996; Liberatore, Searcy-Schrick, & Yutzey, 2000). Embryos lacking sufficient RA or RA signaling consistently show a reduced Tbx5 domain and a loss of forelimbs, while loss of Tbx5 greatly compromised the limb formation (Agarwal et al., 2003; Grandel et al., 2002; K. Niederreither et al., 1999; Niederreither et al., 2001; Lucile Ryckebusch et al., 2008). In zebrafish model, activation of RA-signaling was found to promote fin development through activating Wnt, Tbx5 and Fgf10 sequentially in the fin bud-forming zone (Mercader et al., 2006), thus potentially inhibiting the cardiogenic potential of pluripotent progenitor cells.

Another candidate downstream of RA signaling in mediating the formation of heart and forelimb is Fgf8. Deficiency of RA signaling leads to increased expression of cardiogenic SHF marker Fgf8 (Mercader et al., 2006; Sirbu et al., 2008) while activation of RA signaling directly suppressed Fgf8 transcription by modulating the activity of a repressive RARE in the promoter of Fgf8 (Kumar & Duester, 2014; Sorrell & Waxman, 2011). Previous studies have demonstrated that Fgf8 is capable of increasing the number of cardiogenic progenitors but limiting the formation of forelimb (Marques, Lee, Poss, & Yelon, 2008; Sorrell & Waxman, 2011). Molecular analysis further suggests that Fgf8 induces the expression of key cardiogenic transcription factors such as Isl1 and Nkx2.5 (Marques et al., 2008; Reifers, Walsh, Leger, Stainier, & Brand, 2000; Sirbu et al., 2008). Meanwhile, the cardiogenic Fgf signaling was noticed to antagonize the expression of Tbx5 that favors limb formation (Marques et al., 2008). More importantly, reducing Fgf8 level rescued the heart and forelimb defects in those RA signaling-deficient embryos (Kumar & Duester, 2014; Sorrell & Waxman, 2011). Therefore, it was plausible that in the forelimb-developing region RA sustains the expression level of Tbx5 through suppressing Fgf8, while in the cardiogenic region where RA signaling is reduced, cardiogenic molecule Fgf8 is highly expressed to promote the cardiogenesis.

Besides Tbx5 and Fgf8, Hoxb5b has also been found to be an RA-inducible gene that promotes fin development and restrict the formation of atrial cardiomyocytes. Due to the absence of Hoxb5b in the heart field, the inhibitory effect Hoxb5b on the number of atrial cardiomyocytes is then believed to be

non-autonomous. Strikingly, overexpression of Hoxb5b recapitulate phenotypes seen in zebrafish treated with high dose of exogenous RA (0.3μM), such as a reduction in the number of cardiomyocytes in ventricles and atria (J. S. Waxman et al., 2008). Thus Hoxb5b has also been considered as a candidate for transducing RA signaling from non-cardiac tissue to guide the development of cardiogenic pool.

Last but not least, the expansion of cardiac progenitor pool in response to reduced RA signaling has also been proposed to be attributed to a LIM domain protein, Ajuba. In undifferentiated P9 cells, RA induces the expression of Ajuba in a dose-dependent manner (Yu, Levi, Siegel, & Noy, 2012). Hagen *et al.* recently reported Ajuba modulates the number of cardiomyocytes in zebrafish not by affecting their proliferation but through limiting the number of the Isl1+ cardiac progenitors. Transcriptional activity assay suggested that Ajuba binds Isl1 and represses the transcription of Isl1 *in vitro*. As consistent with previous studies that RA deficiency expands the Isl1 expression domain, addition of RA potentiates the interaction between Ajuba and Isl1 and increase the abundance of this complex, thus reducing the expression of Isl1. Therefore, RA restricts the size of Isl1+ cardiogenic pool possibly through mediating the Ajuba-Isl1 complex.

1.5. The role of RA in determining the A-P patterning of heart tube

During early cardiogenesis, anteroposterior (A-P) patterning in fetal heart is tightly correlated with RA metabolism and signaling. Immunohistochemistry analysis of RALDH2 in quail embryo demonstrated that this critical RA-synthesizing enzyme is highly expressed at the venous pole of the avian heart tube and that its expression gradually fades out anteriorly (J. B. Moss et al., 1998; Karen Niederreither et al., 1999; Xavier-Neto, Shapiro, Houghton, & Rosenthal, 2000). This expression pattern of RALDH2 also overlaps with the marker of the posterior heart tube, atrial-specific myosin heavy chain 1 (AMHC1), in the cardiogenic region which is destined to develop into atria and sinus venosus (Xavier-Neto et al., 2000). Moreover, RA signaling revealed by *RARE*-reporter mouse models was shown to be activated in the posterior region of cardiogenic splanchnic mesoderm, which corresponds to the posterior SHF and the prospective sinus venosus and atria (Dolle, Fraulob, Gallego-Llamas, Vermot, &

Niederreither, 2010; J. B. Moss et al., 1998). The restricted localization of the RA synthetic enzyme and RA signaling to the caudal region of the heart tube suggests that RA promotes posterior cardiac identity.

Multiple approaches have been used to understand the role of RA in the A-P patterning of the heart. In *Raldh2* deficient mice, the sinoatrial region of the heart tube is severely affected. In *Raldh2*$^{-/-}$ embryos, anterior cardiac markers expand caudally, for instance *Fgf8* and the expression of posterior cardiac marker *Tbx5* is reduced (Niederreither et al., 2001; L. Ryckebusch et al., 2008; Lucile Ryckebusch et al., 2008). VAD quail embryos exhibit severe truncation of the posterior region of the heart, leading to early embryonic lethality (Heine et al., 1985). In contrast, chicken embryos treated with exogenous RA have expanded expression domains of Amhc1 (Yutzey, Rhee, & Bader, 1994). As a consequence of altered A-P patterning of the early heart tube caused by abnormal RA signaling, the morphogenesis of cardiac structures which derive from specific anterior or posterior regions of the heart is also affected by changed RA signaling. For example, *Raldh2*$^{-/-}$ mice have compromised atrial development and embryos treated with an RAR-antagonist lack atrial chambers (D'Aniello & Waxman, 2014). Similarly, VAD quail embryos show a significantly shortened caudal portion of heart tube that cannot link to the extra-embryonic circulation system, which leads to early embryonic lethality (Dersch & Zile, 1993; Heine et al., 1985). On the contrary, with increasing doses of exogenous RA in zebrafish embryos, the anterior portion of the embryonic heart tube, corresponding to the nascent ventricle, is truncated progressively (Calmont et al., 2009). Administration of exogenous RA to avian hearts during or before the fusion of heart primordia evidently expands the atrial domain, even occupying the entire heart tube (Yutzey et al., 1994). Similar expansion of sino-atrial marker in response to exogenous RA during the fusion of cardiac crescent is observed in mouse and zebrafish embryos (Waxman & Yelon, 2009; Xavier-Neto et al., 1999). Moreover, an accumulation of RA in Cyp26-deficient zebrafish embryos results in an increase of the number of atrial cells (A. B. Rydeen & Waxman, 2014). Altogether, the caudally distributed RA signaling is linked to the establishment of the posterior cardiac domain.

Molecular analysis has indicated that RA regulates the early cardiogenesis through interacting with other developmentally important signaling pathways. VAD quail embryos express significantly low level of the key cardiogenic morphogen, Gata-4, and *Raldh2*$^{-/-}$ mice show a reduction in the expression of *Bmp2* (Kostetskii et al., 1999) (Lucile Ryckebusch et al., 2008). Interestingly, administration of exogenous GATA-4 and BMP2 rescues the cardiac defects in VAD quails, indicating the cross-talk between RA signaling and BMP2 as well as GATA-4. In contrast, another cardiogenic factor, Nkx2.5, has been found to be involved in RA-mediated early cardiogenesis. Genetic deletion of Raldh2 significantly up-regulates Nkx2.5 but down-regulates Tbx5 and Bmp2 (Keegan et al., 2005; Lucile Ryckebusch et al., 2008). Loss of function of Nkx2.5 in the *Raldh2*$^{-/-}$ background, however, restores the expression of Tbx5 and Bmp2, indicating that Nkx2.5 may function downstream of RA signaling but upstream of Tbx5 and Bmp2 in early heart formation (Lucile Ryckebusch et al., 2008). Furthermore, RA signaling has been found to negatively regulate the expression of transforming growth factor β2 (Tgfβ2), which is critical in heart tube formation. The expression levels of Tgfβ2 have been found to be up-regulated in both VAD quail embryos and *Raldh2*-null mice (S. K. Ghatpande et al., 2010; Paschaki et al., 2013). Consistently, administration of TGFβ2 to normal quail embryos recapitulates the severe truncation of heart tube observed in the VAD quail model (S. K. Ghatpande et al., 2010). In contrary, application of a TGFβ2-blocking antibody successfully rescues the deleterious cardiac phenotype in posterior heart tube in VAD quail embryos (S. K. Ghatpande et al., 2010), suggesting that RA may convey its biological effects through suppression of Tgfβ2 signaling during early heart formation. Though multiple potential pathways have been proposed to interact with RA signaling, the exact molecular mechanisms by which RA regulates the process of heart patterning and early formation have not yet been clearly demonstrated.

It is now believed that the A-P patterning of the heart tube is generated largely by a well-organized SHF through the regulation of RA. As mentioned earlier, cardiac progenitor cells from the SHF migrate to the primary heart tube, adding to both arterial and venous poles (R. G. Kelly, 2012). In fate tracing analysis, cells derived from anterior SHF contribute mainly to the rostral side of the heart tube, including

ventricle and OFT, and those from posterior SHF facilitate the development of atrium and the venous pole (Galli et al., 2008; S. Zaffran et al., 2004). Accordingly, a disorganized SHF can result in a defective heart tube patterning and development, as demonstrated in fetuses with abnormal RA signaling levels (Dersch & Zile, 1993; Niederreither et al., 2001; Park et al., 2006). In *Raldh2*$^{-/-}$ mice embryos, expression of anterior SHF markers, such as *Tbx1* and *Fgf9*, are expanded into caudal region while the expression of posterior marker *Tbx5* is greatly reduced (Niederreither et al., 2001; L. Ryckebusch et al., 2008; Vincent & Buckingham, 2010). Similar expansion of anterior SHF markers has been observed in both VAD quail (L. Ryckebusch et al., 2008) and zebrafish treated with RA antagonists (Collop et al., 2006). On the other hand, an enlarged region marked by *Tbx5* as well as a sino-atrial specific marker *smooth myosin heavy chain 3 (sMyHC3)* was shown in fetal mice and chicken exposed to exogenous RA (Bruneau et al., 1999; D'Aniello & Waxman, 2014; Yutzey et al., 1994). Therefore, the proper patterning of SHF modulated by RA creates the foundation of the development of a well-organized heart tube.

Due to such a correspondence between the SHF and the heart tube, the mechanisms by which RA influences the SHF patterning may also contribute to the development of the heart tube. One of the well-known RA target signaling pathway is the Hox family. Hox genes have been well-characterized in determination of the patterning of body axis and the hindbrain under the regulation of RA signaling (Glover, Renaud, & Rijli, 2006; Koop et al., 2010). In the heart, it is now identified that RA-target genes Hoxa1, Hoxb1 and Hoxb3 are expressed in distinct regions in the SHF, potentiating the regulation of RA signaling in patterning of the heart tube (Bertrand et al., 2011). Recent studies also revealed that embryos lacking Hox A and Hox B sister cluster genes display multiple embryonic defects that mimic those observed in VAD embryos and *Raldh2* null mutants, such as dilation of heart tube and failure in cardiac looping (Soshnikova, Dewaele, Janvier, Krumlauf, & Duboule, 2013). Taken together, Hox genes contribute to the heart tube patterning by regulation of RA signaling.

Aside from Hox genes, Fgf8 has also been identified to be an RA-responsive modulator of the SHF development (Kumar & Duester, 2014). As mentioned above, Fgf8 is transcriptionally repressed by RA

and can affect the cell fate determination during early cardiogenesis (Sorrell & Waxman, 2011). Besides, FGF8 is also known as an anterior SHF marker that is critical for the development of cardiac structures derived from the SHF (Abu-Issa, Smyth, Smoak, Yamamura, & Meyers, 2002; Ilagan et al., 2006). *Fgf8* null mutant exhibits DORV and persistent truncus arteriosus, as a result of perturbation of anterior SHF. Similarly, conditional deletion of Fgf8 in Nkx2.5-expressing and/or Isl1-expressing cells results in severe truncation of OFT and RV region, primarily due to reduced proliferation of cardiogenic cells and increased cell death in the splanchnic mesoderm and pharyngeal endoderm (Ilagan et al., 2006; Park et al., 2006). Besides, Fgf8 is also found to promote cell migration through regulating cadherin expression, facilitating the migration of SHF progenitors and the elongation of the heart tube (Sun, Meyers, Lewandoski, & Martin, 1999). Therefore, the role of RA in promoting posterior identity of the heart tube during early heart development may be carried out by suppressing the transcription of anterior marker Fgf8, which further affects proliferation and apoptosis of the cardiogenic cells and influence the prospective cardiac structures such as the OFT.

Tbx5 has also been proposed to carry out RA functions in patterning the heart tube. As explained in last section, Tbx5 is RA-responsive and can regulate early cardiogenic pool by influencing cell fate choices (Agarwal et al., 2003). Expression of Tbx5 is highly dynamic and was found to be exclusively confined to the posterior SHF during the heart tube formation (Chapman et al., 1996). Loss of functional Tbx5 leads to severe hypoplasia in sinoatrial structures and persistent expression of *Tbx5* in the ventricle abrogates the expression of ventricular markers, suggesting the requirement of proper Tbx5 signaling in promoting the development of posterior heart tube (Liberatore et al., 2000). During the patterning of the heart, Tbx5 is highly responsive to the level of RA signaling: maternal administration of RA caused anterior expansion of the expression of Tbx5 and an increased expression of an atrial marker AMHC1 (Bruneau et al., 1999; Liberatore et al., 2000; Niederreither et al., 2001; Karen Niederreither et al., 1999; Lucile Ryckebusch et al., 2008; Yutzey et al., 1994). Tbx5 thus may function as a mediator of RA functions in SHF patterning, presumably by promoting commitment of a cardiogenic cell to a

posterior/atrial fate. Recently reported, the expression of *Tbx5* can be directly regulated by Hox genes since a Hox response element sequence was identified within the promoter of Tbx5 where Hox4 and Hox5 have been found to bind (Kane & Napoli, 2010). Since RA is a well-known regulator of Hox genes expression, it is plausible that RA may convey its essential roles in the patterning of the SHF and heart tube through Hox genes, which transcriptionally regulate the further downstream target Tbx5. However, mutation of *hoxb5* results in a partial list of the defects associated with RA-deficiency (Franco, Farooqui, Seto, & Wei, 2001), which indicates the involvement of other RA-responsive effectors in heart formation (S. Ghatpande, Brand, Zile, & Evans, 2006; Kostetskii et al., 1999).

Though progress has been made, basic questions about physiological behavior of cardiac progenitor cells need to be addressed. One of the key questions to ask is whether the pre-patterned progenitor cells move in concert as a sheet to maintain their relative position, or whether they migrate individually and re-pattern on the heart tube under the guidance of an RA gradient in the new environment. Another important question to be answered is if levels of RA signaling function as indicators of current location in the migrating path for these cells and if so, how is this map of cell migration regulated. Altogether, current studies demonstrated an indispensable role of RA in the patterning of the heart tube.

1.6. RA and the formation of outflow tract (OFT)

During normal cardiogenesis, the septum of the OFT is formed by two types of cells under the tight regulation of RA signaling: endocardial cells and cardiac neural crest cells (CNCCs). In the OFT, endocardial cells undergo epithelial-mesenchymal transition (EMT) and migrate to the middle of endocardium and myocardium to form the endocardial cushions (von Gise & Pu, 2012). The cushions eventually form the septa and valves that separate the aorta and pulmonary trunk, as well as the chambers in heart (Mendez, Kojima, & Goldman, 2010). CNCCs mainly migrate to the anterior heart tube and facilitate the formation of endocardial cushions. Ablation of premigratory CNCCS in chicken embryos severely impairs the septation of the pulmonary trunk and aorta, which is a congenital defect known as common arterial trunk (CAT) (Hutson & Kirby, 2007). Similar to the results of ablating CNCCs, lack of

proper RA signaling also leads to congenital heart defects in OFT septation (Jiang et al., 2002; Sakabe, Kokubo, Nakajima, & Saga, 2012). Intriguingly, defective formation of OFT septum in response to RA deficiency cannot be rescued by repletion of RA which increases the embryonic levels of RA in a global manner. This further reflects the specific requirement of a spatially controlled distribution of RA during the proper formation of OFT (Niederreither et al., 2001).

Alterations in RA signaling can cause defects of endocardial EMT, which is a frequent cause of OFT defects (Sakabe et al., 2012). Ectopic RA signaling delays endocardial EMT and suppresses Tbx2/ Tgfβ2 pathway. Consistently, addition of recombinant TGFβ2 in the RA-treated mouse embryos can restore the attenuated migration of endocardial cells, suggesting that RA represses endocardial EMT through down-regulation of *Tgfβ2*. Further molecular analyses suggest that *Tbx2* transcriptionally induces the expression of *Tgfβ2* and that the expression of *Tbx2* is most likely a direct transcriptional target of RA signaling, since a repressive *RARE* was identified in the promoter of *Tbx2* (Sakabe et al., 2012). Thus, excess RA can directly repress transcription of *Tbx2*, and further decrease expression of *Tgfβ2*, which influences the endocardial EMT. Moreover, decreased RA signaling due to *Rarα1/Rarβ* double ablation in mice also resulted in CAT (P. Li, Pashmforoush, & Sucov, 2010). Such a reduction in RA signaling increased the activity of the *Tbx2/ Tgfβ2* pathway and deleting one *Tgfβ2* allele ameliorates the septal defect. To sum up, these data suggest that lack of septation in the OFT can be at least partially attributed to the disrupted *Tbx2/Tgfβ2* pathway by altered levels of RA.

Alteration in CNCC behavior can be a major contributor to the defective OFT in RA-deficient models. The migration pattern of CNCCs was impaired in *Raldh2*$^{-/-}$ mice even when exogenous RA was applied maternally (Niederreither et al., 2001). Likewise, the proliferation of CNCCs was decreased after the RA administration to zebrafish larvae (Giovannone et al., 2012). However, these observations conflict with the results which showed that mutations of *Rarα1/Rarβ* in fetal mice do not cause changes in the distribution and proliferation of CNCCs (Jiang et al., 2002). These conflicting data may be explained by the fact that the effects RA deficiency lead to a different repertoire of gene expression changes than the

deletion of the RA receptors. To put this simply, RAR is still “active” even in the absence of its ligand by carrying out repression of target genes. However, the absence of RAR causes repression of target genes which become expressed. Another explanation for the discrepancy between the RA and RAR-deficient models could be that the proliferation of CNCCs is mainly controlled by other isoforms of RARs than RARα1 and RARβ, thus CNCCs might still proliferate and migrate in the absence of these two RAR isoforms. Importantly, since the RA synthetic enzyme Raldh2 is not expressed in CNCC (Calmont et al., 2009; T. Hochgreb et al., 2003), the RA signaling that orchestrates CNCCs function and migration is mediated by RA- produced and secreted by RA in the surrounding neighboring cells (Jiang et al., 2002).

To sum up, the specific distribution of RA regulates the development of the OFT septum. Since abnormalities in OFT caused by RA signaling deficiency cannot be rescued by global supplementation of RA, it is clear that RA must carry out a strictly positional or gradient-based effect in the development of OFT (Niederreither et al., 2001). To demonstrate this putative RA gradient in the OFT, a more sensitive and reliable RA signaling reporter will be needed to image RA distribution in the developing heart tube as well as along the path of CNCC migration.

1.7. RA and the myocardial proliferation in the ventricle

The growth of the myocardium depends on the normal function of the epicardium. Epicardium is critical to cardiomyocyte proliferation as a lack of epicardium results in arrested myocardial growth (David J. Pennisi, Ballard, & Mikawa, 2003; Ingo Stuckmann et al., 2003). Epicardium is a thin layer of epithelial cells that develop from a transient extra-cardiac tissue, namely the proepicardium (PE). PE-derived mesothelial cells migrate and populate the surface of the heart to form the epicardium. Upon stimulation, epicardial cells undergo epithelial-to-mesenchymal transition (EMT) to become migratory and invade into the myocardium where these epicardial-derived progenitor cells (EPDCs) differentiate into multiple cell types to facilitate late heart development. Besides its role as a source of cardiac progenitor pool, the epicardium also functions as a signaling center and actively produces multiple developmentally important signaling molecules to orchestrate the heart maturation, especially the

myocardial growth (von Gise & Pu, 2012). One of these epicardial-derived morphogens is RA. RA synthesis, as demonstrated by the expression of *Raldh2*, and RA signaling, visualized by the expression of *RARE-lacZ* transgene (Rossant, Zirngibl, Cado, Shago, & Giguere, 1991), are both localized in cells in the epicardium and subepicardial space. Though RA is exclusively made in the epicardium, we still have very limited knowledge of the biological significance of RA signaling in epicardial-regulated morphogenic events, including the myocardial growth and the development of coronary vessels.

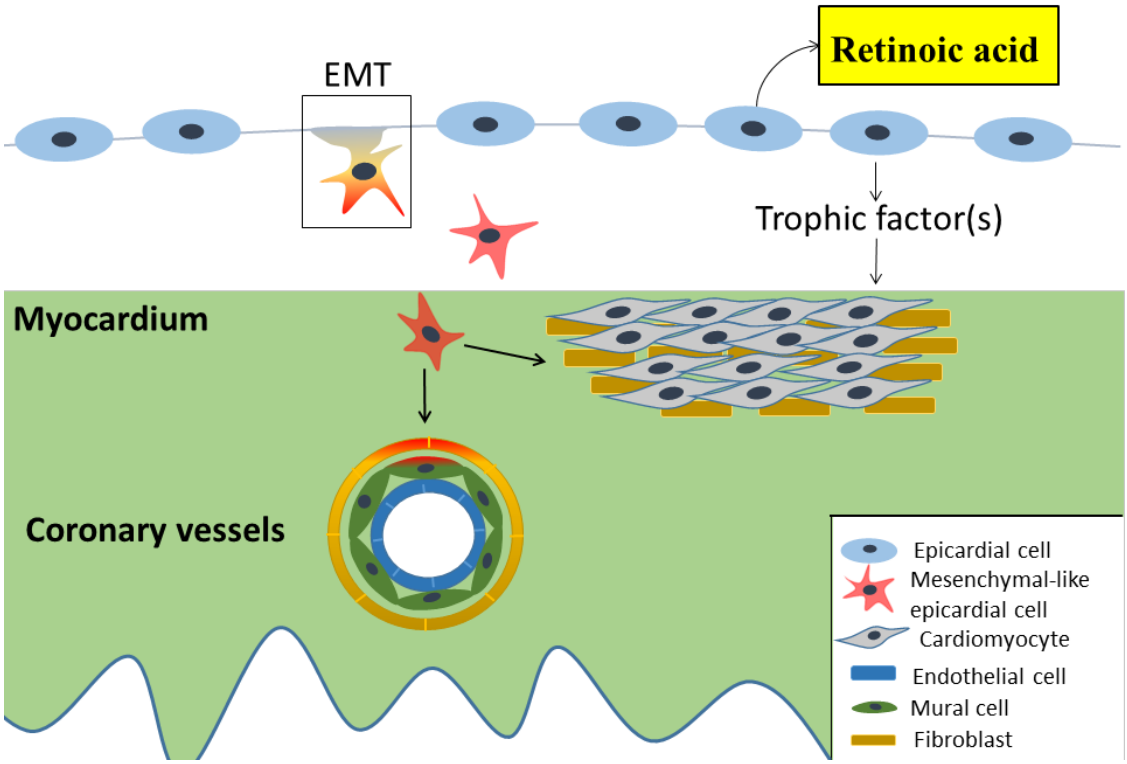

Figure 1.3 Contribution of epicardium during late heart development.

Epicardial cells (EPDCs) undergo epithelial-to-mesenchymal transition (EMT) to gain migratory capacity and invade into myocardium. Intramyocardial EPDCs differentiate into fibroblasts and perivascular vascular smooth muscle cells to facilitate the development of coronary vessels and assist the contraction of the heart. Epicardium secretes essential morphogens, including RA, to promote cardiomyocyte proliferation and heart maturation.

Previously, multiple lines of evidence have demonstrated the importance of RA and its signaling in the development of myocardium. Short-term repletion of RA from E7.5 to E8.5 to *Raldh2* null mouse embryos postpones their embryonic lethality, yet, still results in a thin ventricular myocardium at E12.5.

Considering RA has short half-life (less than 12 hrs) *in vivo* (Lee et al., 2012; Satre & Kochhar, 1989) and that the *Raldh2*$^{-/-}$ heart is devoid of RA signaling at E12.5 revealed by the absence of expression of *RARE-LacZ* transgene in the heart, the hypoplastic ventricular myocardium was attributed to a lack of RA in the heart (Niederreither et al., 2001). Similar hypoplastic ventricles have been also observed in mouse embryos that have reduced RA signaling, such as embryos with genetic ablation of *Rxrα*, those expressing a dominant-negative *RAR* or embryos with *Rarα/Rarγ* compound loss of function mutation (Thomas Brade et al., 2011; T. Chen et al., 2002; Kastner et al., 1997). In addition, Cre-guided epicardial-specific ablation of *Rxrα* using GATA5 promoter or the expression of the dominant-negative *Rarα* in the epithelial epicardium (Merki et al., 2005) (T. Chen et al., 2002), results in thin ventricular myocardium, while deficiency of *Rxrα* in the cardiomyocytes does not alter heart morphology (J. Chen, Kubalak, & Chien, 1998). These observations suggest that RA signaling within the epicardium is required to promote myocardial growth.

Previous *ex vivo* studies suggested that RA promotes myocardial growth by stimulating epicardium to secrete trophic factors. Surgical removal of the epicardium abolishes the pro-proliferative function of RA in cardiomyocytes (Ingo Stuckmann et al., 2003). In addition, conditioned media from RA-treated epicardial cell cultures was collected and applied to cultured cardiomyocytes (T. Chen et al., 2002). The epicardial-conditioned media potently boosted the proliferation of cardiomyocytes and heat abolished the effect of the epicardial-conditioned media, indicating that 1) RA promotes the proliferation of cardiomyocytes through stimulating the epicardium to produce trophic factor(s) and 2) the epicardial-derived RA-responsive factor(s) responsible for promoting cardiomyocyte proliferation is peptide-based. Though multiple studies have proposed potential candidates, heated discussion on the identity of this trophic factor is still ongoing.

FGF proteins were thought to be possible epicardial derived mitogens yet their trophic effects were questioned by *in vivo* studies. FGF2 and FGF9 has been previously found to be mitogenic in culture and were responsive to alteration of epicardial RA signaling (Kardami & Fandrich, 1989; Kory J. Lavine et

al., 2005; Merki et al., 2005; David J. Pennisi et al., 2003). However *Fgf2* null embryos display normal cardiac morphology, which excludes the role of Fgf2 in the development of the heart (M. Zhou et al., 1998). *Fgf9* null mutation on the other hand results in hypoplasia in the ventricular myocardium. Yet the spatiotemporal expression pattern of Fgf9 is not compatible with the requirement of being an epicardial-derived mitogen. The myocardial thickness typically increases from E11.5 to E14.5 in mouse embryos, but at E12.5 Fgf9 is not expressed in the epicardium but exclusively in the endocardium, questioning the possibility of FGF9 as an epicardial-derived mitogen in promoting thickening of the myocardium (Kory J. Lavine et al., 2005). In addition, Peng *et al.* performed a screening of secretome of an immortalized epicardial cell line, MEC1, to identify the presence of possible mitogens. The MEC1 cells were capable of producing trophic factors, yet the authors did not detect FGF2 or FGF9 in the MEC1-conditioned culture media, which leaves the role of these two proteins as epicardial-derived mitogens uncertain (Peng Li et al., 2011). However, though MEC1 cells do not spontaneously secrete FGF2 or FGF9, it is still possible that upon stimulation of RA, the production of these two mitogens might be increased. Therefore, this lack of FGFs in the secretome of MEC1 cells needs to be re-examined in conditions where the key epicardial stimulant, RA, is applied.

PDGF-A was also once proposed to transduce the RA signaling in myocardial proliferation. PDGF-A is the primary mitogen produced in rat atrial epicardial cell line, namely EMC cells, in response to RA stimulation (Kang et al., 2008). However mutation of *Pdgfrs* in the myocardium and epicardium results in normal ventricular myocardium (Kang et al., 2008). Additionally, *Pdgfa* is barely expressed in the epicardium *in vivo* and its expression was not detected in the ventricular epicardial cell line, MEC1 (Kang et al., 2008; Peng Li et al., 2011). Therefore, PDGF-A may not carry out the proliferative function of RA signaling on ventricular myocardium.

Recent studies proposed a new model where extra-cardiac (liver) -derived RA promotes myocardial growth. In this model liver-generated RA upregulated the expression of *liver erythropoietin* (*EPO*), which then induces the epicardium to secrete *IGF2* and promote myocardial growth. Support for this model

comes from evidence that inactivation of *Epo* or its receptor led to ventricular hypoplasia, resembling the cardiac phenotype observed in mouse embryos lacking sufficient RA signaling (Thomas Brade et al., 2011; T. Chen et al., 2002; Kastner et al., 1997; H. Wu, Lee, Gao, Liu, & Iruela-Arispe, 1999). *Epo* was found to be expressed in the liver but not heart and ChIP assay studies suggest that the *Epo* gene is a potential direct transcriptional target of RA signalEing (Thomas Brade et al., 2011). Next, it was noticed that *Rxrα*$^{-/-}$ embryos have reduced expression of *Epo* in the liver, and addition of *EPO* to cultured *Raldh2*$^{-/-}$ and *Rxrα*$^{-/-}$ embryos successfully restored their myocardial proliferation (Thomas Brade et al., 2011). The proliferative effects of RA and EPO on the cardiomyocytes are seemingly redundant in an explant model: exogenous RA can resume myocardial proliferation when the EPO receptor is blocked, while EPO partially restore the proliferative response in cells treated an RAR antagonist (Ingo Stuckmann et al., 2003). Such a partial restoration also suggests other trophic factors may respond to RA to promote myocardial proliferation, independent of EPO. In addition, the thinned myocardium in either *Raldh2*$^{-/-}$ or *Rxrα*$^{-/-}$ embryonic hearts can be rescued in heart explant culture by the addition of EPO, which further strengthens the tie between RA and EPO signaling in regulating myocardial growth (Thomas Brade et al., 2011). Based on the fact that *Epo* is expressed primarily by the fetal liver, not the heart, a hypothesis was raised that an extra-cardiac source of RA may be involved in the regulation of hepatic EPO secretion which is responsible myocardial development (Kambe et al., 2000; Peng Li et al., 2011). Consistent with the hypothesis, expression of a dominant negative *Rarα* in the cardiogenic mesoderm leads to normal ventricular myocardium, while blocking RA signaling in liver results in an underdeveloped thin ventricular myocardium (Shen et al., 2015). However, to rule out the possible roles of cardiac/epicardial RA signaling in the development of myocardium, animal models with combination of mutation in multiple RARs need to be employed because redundancy of RAR functions in the heart formation has been frequently reported and deletion of a single receptor may not be effective in abolishing RA signaling. Due to the closure of diaphragm and subsequent loss of direct transport of hepatic molecule to the heart by perfusion, the regulation of ventricular myocardium by hepatic RA and EPO can only exist between E10-11 in mouse embryos. Therefore, even though it is clear that hepatic RA signaling through

RARα is critical for ventricular myocardial growth, in face with the wealth of evidence from isolated epicardial cells inducing myocardial growth in culture, one cannot completely rule out the requirement of epicardial RA signaling in mediating cardiomyocyte proliferation.

A recently rising candidate of epicardial-derived mitogen is IGF2. The pro-proliferative characteristics of IGF2 have been previously demonstrated in both *in vitro* and *in vivo* models. Application of IGF2 to cardiomyocytes potently induces their proliferation (Liu et al., 1996). *Igf2* null embryos show reduced myocardial proliferation while excess *IGF2*, due to the lack of degradation in *Igf2r*$^{-/-}$ mutant mice, results in hyperplastic ventricles (Eggenschwiler et al., 1997; Peng Li et al., 2011). Not only qualified as a mitogen on cardiomyocytes, IGF2 has been reported to be the most abundantly secreted mitogen in MEC1 cells and the epicardium *in vivo* (Peng Li et al., 2011). However, the induction of Igf2 in the epicardium is dependent on EPO but not RA in MEC1 cell line, excluding the possibility of IGF2 as a RA responsive mitogen (Thomas Brade et al., 2011). It is even more confusing that though IGF2 is not RA-responsive, knocking down of Igf2 or blocking IGF signaling greatly reduced the proliferative response of cardiomyocytes to the conditioned media from MEC1 cells pretreated with RA. Nevertheless, inhibition of IGF signaling did not completely abolish the proliferation of cardiomyocyte treated with MEC1-conditioned media, suggesting the existence of non-IGF mitogen produced by epicardial cells in response to RA treatment (Peng Li et al., 2011).

Despite all the findings these years by multiple models, the identity of RA-stimulated epicardial-derived mitogen(s) remains mysterious and we still have poor understanding of the roles of RA signaling in the heart during late cardiogenesis.

1.8. RA and the development of coronary vessels

Great efforts have been recently made to elucidate the complex program of the formation coronary vessels, which has been discussed in several excellent reviews (Lamalice, Le Boeuf, & Huot, 2007; Lie-Venema et al., 2007; Schmidt, Brixius, & Bloch, 2007). Briefly, the development of coronary circulation involves the establishment of a primary endothelial plexus network which is then followed by remodeling

and the addition of perivascular cells. Endothelial precursors, i.e. angioblasts, transform to become migratory and migrate to form a primitive vascular network at E11.5, which functions as a scaffold for further expansion and branching of growing vessels on the surface of the heart and into the myocardium (Vrancken Peeters et al., 1997). In the meantime, epicardial cells that derive from the proepicardium undergo epithelial-to-mesenchymal transition (EMT) migrate towards the heart and spread to cover the myocardium. The epicardium is essential in the development of coronary vessels, shown by failure in the establishment of coronary vessels in mouse models lacking proper development of epicardium (Tevosian et al., 2000; von Gise et al., 2011; Yang, Rayburn, & Hynes, 1995). As the vascular network forms, the coronary vessels connect to the system circulation by ostia that are localized in the sinuses of the aortic valves to get oxygenated blood. The shear stress created from the blood flow further refines the existing vasculature and facilitate its final maturation.

Lineage tracing approaches have been used in the past to elucidate the origin of cellular component of coronary vessels. Studies using the Wt1-Cre system reported the contribution of EPDCs to cardiomyocytes and endothelial cells (Cai et al., 2008; Gittenberger-de Groot, Vrancken Peeters, Mentink, Gourdie, & Poelmann, 1998; J.-M. Perez-Pomares et al., 2002; B. Zhou et al., 2008), which is however being debated due to the questionable specificity of the "epicardial markers" that were utilized in those studies: $WT1^{Cre\text{-}EGFP}$ show ectopic signal which is inconsistent with the physiological Wt1 expression; endothelial cells endogenously express Wt1 and cardiomyocytes naturally express Tbx18, which doubted their origin from epicardial cells (Christoffels et al., 2009; Carsten Rudat & Kispert, 2012; Bin Zhou & Pu, 2012). In addition the PE contains heterogenous populations of cells and the most popular PE/epicardial markers, for example Wt1, Tbx18 and Tcf21, do not mark completely identical domains in the PE (Caitlin M. Braitsch, Michelle D. Combs, Susan E. Quaggin, & Katherine E. Yutzey, 2012). Therefore, the discrepancy in lineage tracing experiment from various studies might be explained by different expression patterns of these markers (Acharya et al., 2012; Cano et al., 2016; Grieskamp, Rudat, Lüdtke, Norden, & Kispert, 2011; Katz et al., 2012; B. Zhou et al., 2008). Interspecific difference

also accounts for the distinct conclusions gained from mouse and avian models (Cai et al., 2008; Juan A Guadix, Carmona, Muñoz‐Chápuli, & Pérez‐Pomares, 2006; Mikawa & Fischman, 1992; B. Zhou et al., 2008). Besides endothelial cells, epicardial-derived cells (EPDCs) also give rise to perivascular cells recruited to the coronary vessels. Multiple lineage tracing studies have clearly demonstrated that in response to endothelial and epicardial signals, migrating EPDCs are recruited to the immature vessels where they differentiate into vascular smooth muscle cells (VSMCs) and fibroblasts to stabilize the immature endothelial tubes (Cai et al., 2008; Lie-Venema et al., 2007). Additionally, EPDCs also contribute to fibroblasts in myocardium and anulus fibrosus cordis, which facilitates heart contraction (Gittenberger-de Groot et al., 1998; Lie-Venema et al., 2008; Bin Zhou, von Gise, Ma, Hu, & Pu, 2010).

RA signaling has been implicated in the development of coronary vasculature. RALDH2 and RXRα are both detected in endothelial cells in the immature vessels and in EPDCs prior to their differentiation into VSMCs and fibroblasts (Juan A. Guadix, Carmona, Muñoz-Chápuli, & Pérez-Pomares, 2006; Pérez-Pomares et al., 2002). Consistent with this, insufficient RA synthesis due to the genetic ablation of *Raldh2*, leads to retarded vessel growth and patterning in the coronary system and epicardial mutation of *Rxrα* results in defective branching of coronary artery (S.-C. Lin et al., 2010; Merki et al., 2005). Interestingly, once the immature vessels develop, the expression of Raldh2 and Rxrα is gradually lost and becomes undetectable in fully developed vessels that are wrapped with mature perivascular cells (Pérez-Pomares et al., 2002). Similarly, Raldh2 is actively expressed in the EPDCs delaminated from the epicardium and is gradually lost as they migrate away from the epicardium and invade deep into the myocardium (Lockhart, Phelps, van den Hoff, & Wessels, 2014). Moreover, cardiac expression of Raldh2 and levels of RA signaling surge at E12.5, which stage correlates with active epicardial EMT, myocardial compaction and coronary vessel development (Jennifer B Moss et al., 1998). However, despite the information of the dynamic changes and specific localization of RA metabolism and signaling in the epicardium and coronary vessels, our knowledge of the exact roles of RA in epicardial behavior and coronary vasculature is by far very limited.

Previously, genetic mouse models have suggested critical roles of RA and its signaling in epicardial EMT. In the epicardial-specific *Rxrα* null mutant mice, the migratory capacity of EMT in epicardial cells was found to be greatly reduced and molecular analysis demonstrated a concomitant down-regulation of *Wnt9b*, a key regulator in Wnt signaling that possibly regulates epicardial EMT through modulating the stability of *β-catenin* (Merki et al., 2005; von Gise et al., 2011). Indirect evidence derived from a *Wt1*-null mutant mouse model suggested that RA was required for proper epicardial migration *in vivo*. As a classic marker of the epicardium, Wt1 is critical to epicardial EMT through up-regulating the expression of Snail and down-regulating E-cadherin (Martínez-Estrada et al., 2010). In $Wt1^{-/-}$ mutant mice, the epicardial EMT was found attenuated and the subsequent coronary vessel formation was impaired (von Gise et al., 2011). Coincident with the defective EMT, the expression of RA-synthesizing enzyme *Raldh2* is drastically suppressed, which was proposed to result in low RA signaling in the $Wt1^{-/-}$ epicardial cells, though this remains unconfirmed. Nevertheless, maternal administration of RA partially rescued the defective EMT in *Wt1*-null mutants, strongly suggesting that WT1 conveys its regulatory role in EMT at least partially through RA signaling. Further molecular analysis has supported the idea that *WT1* transcriptionally regulates the expression of *Raldh2* (J. A. Guadix et al., 2011). The WT1-RA signaling interaction is mutual as RA also influences the expression of *Wt1*, increasing the complexity of this regulatory network in epicardial EMT (Caitlin M. Braitsch et al., 2012). Therefore, epicardial EMT could be regulated by RA acting downstream of WT1 and reinforcing its signal via positive feedback.

Currently, whether RA signaling influences epicardial EMT is still at debate and direct evidence of the roles of RA in the epicardium is of immediate need to answer this question. Opposing opinions of the involvement of RA in epicardial EMT came from a study using the "rescued" *Raldh2* mutant mice described above. In the "rescued" $Raldh2^{-/-}$ embryos, the expression level of *Wnt9b* was not altered and the collagen gel infiltration capacity of isolated $Raldh2^{-/-}$ epicardial cells was found to be comparable to the wildtype (S. C. Lin et al., 2010). However this model of RA deficiency was later proved to be leaky because RA signaling was not completely depleted in the heart of the "rescued" *Raldh2* null embryos due

to the presence of *Raldh2*-independent RA synthesizing enzymes (Felix A. Mic, Haselbeck, Cuenca, & Duester, 2002) (Niederreither, Vermot, Fraulob, Chambon, & Dolle, 2002). Other objectors against the necessity of RA signaling in epicardial migration based their opinions on observations derived from proepicardial explant culture. Addition of 1mM of RA to proepicardial cells didn't seem to induce evident accumulation of spindle-like mesenchymal cells. Inhibition of RA synthesis, on the other hand, does not obviously inhibit the proepicardial EMT induced by 5% FBS (Azambuja et al., 2010). Though morphological change is a critical step in EMT, the observation based solely on cell shape was subjective and conclusion is not solid unless molecular markers of epithelial/mesenchymal cells are examined. In addition, even if the involvement of RA signaling in the proepicardium is minimal, one cannot bluntly rule out the possible effects of RA in epicardial EMT suggested by several *in vivo* models discussed above. Last but not the least, as noticed by Shen *et al.*, at E10.5-E11.5, when the epicardial EMT is highly active, the embryonic heart forms under hypoxia (Shen et al., 2015), hence the regulation of EMT under hypoxia should also be evaluated and is worth investigation. Therefore, the roles of RA in epicardial EMT need to be analyzed systematically in more appropriate models.

Aside from epicardial EMT, RA has also been reported to control the differentiation of EPDCs into perivascular cells. Several previous studies suggested RA seemed to inhibit the development of VSMCs. In cultures of human coronary VSMCs, RA has been found to inhibit cell proliferation through regulating the cell cycle (Wakino et al., 2001). In embryonic proepicardial explants, RA eliminated the expression of several markers of VSMCs while inhibition of RA synthesis induced the VSMC differentiation of quail proepicardial cells (Azambuja et al., 2010). In contrast, over-expressing the RA-synthesizing enzyme Raldh2 in proepicardial cultures led inhibition of the differentiation of EPDCs into VSMCs (Azambuja et al., 2010). Later studies by Braitsch *et al.* reported that RA induces the expression of epicardial-specific transcription factor TCF21, which favors the differentiation of fibroblasts at the expense of VSMCs (Acharya et al., 2012; Caitlin M. Braitsch et al., 2012; Kazu Kikuchi et al., 2011; Quaggin, Vanden Heuvel, & Igarashi, 1998). Genetic ablation of *Tcf21* globally in mouse embryos results in premature of

VSMCs, which further supports the potential regulatory pathway in which RA delays VSMCs through up-regulating Tcf21 (Acharya et al., 2012; Caitlin M. Braitsch et al., 2012; Felicia Chen et al., 2014; Hector, Felicia, Yuxia, & Wellington, 2013). However, another *Tcf21*-null mouse model raised by Archarya *et al*. showed that ablation of Tcf21 does not affect the formation of VSMCs in the heart (Acharya et al., 2012; Caitlin M. Braitsch et al., 2012; Kazu Kikuchi et al., 2011; Quaggin et al., 1998). Thus, the exact roles of RA and Tcf21 in VSMC differentiation need further investigation. In addition to VSMCs, EPDCs also contribute to the formation of fibroblasts. Loss of *Tcf21* in mouse embryos also leaded to a significant reduction in the number of Col1a1-expressing fibroblasts (Acharya et al., 2012; Caitlin M. Braitsch et al., 2012; Kazu Kikuchi et al., 2011; Quaggin et al., 1998). Collectively, RA has clear involvement in the EPDC differentiation and the interaction between RA signaling and Tcf21 is worth of in-depth investigation.

1.9. RA and the heart regeneration

The regenerative capacity of heart after injury varies between species. In mammals, the heart is one of the least regenerative organs. Cardiac injury such as myocardial infarction (MI) leads to ventricular remodeling, including ventricular hypertrophy and deposition of collagen in the wound region, which results in partial loss of cardiac function due to a lack of contractile cardiomyocytes. In contrast, zebrafish and the air-breathing fish *Polypterus senegalus* can repair the injured heart by up-regulating the proliferation of cardiomyocytes near the border zone of wound and establishing new coronary vessels to nourish the newly formed muscles. Surprisingly, neonatal mice exhibit full regenerative capacity of the heart up to 7 days after birth, which presents the potential of mammalian heart regeneration and provides an invaluable model for exploration of potential targets that activate heart regeneration in adult human MI patients (Porrello et al., 2011). The cardiac repair program is tightly linked with the epicardium since the activation of expression of the epicardial-specific genes serves as the first response to heart wounding. In normal animal hearts, the adult epicardium remains quiescent and does not produce migratory EPDCs (Duim, Kurakula, Goumans, & Kruithof, 2015; van Wijk, Gunst, Moorman, & van den Hoff, 2012; Bin

Zhou et al., 2011). Upon cardiac injury, as observed in both mouse and zebrafish models, the embryonic program is once again activated in the epicardium and mesenchymal EPDCs are generated through EMT to migrate to the wound (Chablais & Jazwinska, 2012; Lepilina et al., 2006; van Wijk et al., 2012; Bin Zhou et al., 2011). The newly formed cardiomyocytes primarily come from undifferentiated progenitor cells in zebrafish (Lepilina et al., 2006), or potentially via reprogramming of cardiofibroblasts (Qian et al., 2012). Similar to their role in embryonic development, EPDCs also contribute to the re-establishment of postnatal coronary vessels by providing progenitors of perivascular cells (Kazu Kikuchi et al., 2011).

RA has been proposed to play a role in heart repair and regeneration. In the zebrafish heart regeneration model, after ventricular apex removal, the epicardium induces the expression of developmental epicardial markers, such as Wt1, Tbx18 as well as Raldh2, suggesting the activation of epicardium and the need for RA synthesis during heart repair (K. Kikuchi et al., 2011; Nicola Smart et al., 2011). Additionally, epicardial cells proliferate to cover the wound area and Raldh2-expressing EPDCs has been observed to invade into the injury zone and surround the myocardium to facilitate the repair of damaged myocardium. In mice subjected to ligation of the left anterior descending artery (LAD) - injury, both cardiac retinol levels as well as cardiac RA signaling were seen to increase (Dusan Bilbija et al., 2012). Concomitantly, the expression of RA-synthesizing enzyme *Raldh2* was found to be induced and that of the RA-catabolic enzyme *Cyp26a1* was noticed to be suppressed in hearts subjected to LAD ligation. Direct evidence of the necessity of RA signaling in heart repair comes from a zebrafish heart regeneration model, in which genetic disruption of RA signaling or increasing RA degradation dramatically reduced the proliferation of cardiomyocytes in the wounded heart (K. Kikuchi et al., 2011). Interestingly, in zebrafish, RA signaling is rapidly initiated in both endocardium and epicardium while in mouse adult heart RA signaling is only detected in the epicardium, but not the endocardium. The difference in the expression patterns of Raldh2 between zebrafish and mice may account for the differences in their regenerative capacity. Factors that can augment cardiac RA signaling may constitute novel targets in an attempt to promote mammalian heart regeneration after MI. Altogether, these results

support a potential role of RA signaling in the repair and potentially in the treatment of cardiac injury. In contrast, other studies reported that RA restricts the proliferation of cardiofibroblasts, potentially reducing the formation of fibrotic scars that disrupt the signaling transduction in the cardiac conductive system (Dusan Bilbija et al., 2012).

Support for a role of RA in ventricular remodeling and heart repair also comes from other models. In rats, RA treatment was reported to lead to ventricular remodeling and enhanced myocardial function, while vitamin A-deficiency led to adverse ventricular remodeling after myocardial infarction (de Paiva et al., 2003; Minicucci et al., 2010; Paiva et al., 2005). *In vitro*, RA antagonized the cardiomyocyte hypertrophy induced by angiotensin II which is also a contributor to hypertrophy in post-MI hearts (Rosenkranz, 2004; Wang, Zhu, & Yao, 2002). Interestingly, the re-activated epicardium in injured adult mice seems to largely recapitulate its embryonic effects in secreting paracrine factors to promote the formation of new vessels and cardiomyocytes (Bin Zhou et al., 2011). Similar to what happens during embryogenesis, the expression of IGF2 is up-regulated in the injured area in zebrafish, and IGF-signaling is indispensable for cardiomyocyte proliferation and heart repair in zebrafish (Y. Huang et al., 2013). Whether RA signaling is involved in the secretion of IGF2 by the injured epicardium remains to be explored, as does many of the facets of the complex role of RA in heart regeneration.

1.10. Conclusion

The teratogenic effects of altered RA signaling on cardiogenesis have been frequently reported and the underlying mechanisms are under intensive investigation. As discussed above, RA signaling actively participates in the early cardiogenic events including the determination of cell fate between cardiogenic versus non-cardiac lineages; regulation of sizes of cardiogenic progenitor pool; as well as the anteroposterior patterning of the primitive heart tube. Despite numerous studies aiming at unveiling roles of RA in early cardiogenesis, defects associated with altered RA signaling during mid- to late-gestational cardiogenesis have been reported, however the underlying mechanisms have been rarely studied due to a lack of appropriate models. The temporal requirement of RA and the exact effect of RA signaling in late

heart morphogenesis remain ambiguous. Because of the critical roles of RA in early cardiogenesis, it is indeed difficult to separate the phenotypes that are truly attributed to mid-gestational RA deficiency or excess from those that are secondary to early cardiogenic defects. In addition, there is a critical need for a better understanding of the maturation of the embryonic heart under the regulation of RA signaling, which would be beneficial to the study of heart regeneration in mammalian systems. In this thesis, I sought to establish novel models for the study of RA-mediated heart maturation using mammalian models and investigate the teratogenic effects of excess RA in the development of coronary vessels. With the help of multiple *in vivo* and *in vitro* models, I investigated the roles of RA in late heart formation to better understand heart development and to shed light on the potential role of RA signaling during heart regeneration and repair.

Chapter 2 : Roles of DHRS3 in Retinoic Acid Metabolism in Early Embryogenesis

Abstract

Vitamin A embryopathy has been frequently reported in the development of multiple organs. Thus the precise amount of the active metabolite of vitamin A, namely RA, needs to be exquisitely controlled throughout embryogenesis. Homeostasis of RA is maintained by well-balanced network of RA metabolism comprising catabolic enzymes either synthesizing or breaking down RA. Previously our lab has demonstrated the physiological role of a short-chain dehydrogenase/reductase, DHRS3, in preventing excessive accumulation of RA during mid-gestation. Genetic ablation of *Dhrs3* in mouse embryos resulted in significant elevation in the amount of endogenous RA and increase in both domain sizes and levels of RA signaling in the *Dhrs3*$^{-/-}$ mice at E14.5. As a result, *Dhrs3*$^{-/-}$ embryos display mid-gestational lethality accompanied with multiple cardiac and skeletal defects. Here, we explored the importance of DHRS3 during early embryogenesis and its roles in neuronal development. Our results indicated that *DHRS3* protected the developing mouse embryos from excessive RA signaling as early as E10 and that deletion of *Dhrs3* caused neuronal defects associated with malformations of cranial nerves during early embryogenesis. Moreover, by rearing the *Dhrs3*$^{+/-}$ dam on a vitamin A deficient (VAD) diet, we were able to improve the skeletal defects observed in *Dhrs3*$^{-/-}$ embryos receiving normal levels of maternal vitamin A. Not only correcting the phenotype, prolonged VAD dietary treatment was found to successfully rescue the embryonically lethal *Dhrs3*$^{-/-}$ mice to fully grown adults with normal body weight and life span. Altogether, data presented here further strengthened the indispensability of Dhrs3 in preventing excessive accumulation of RA *in vivo* during mouse embryogenesis.

2.1. Introduction

RA as an essential signaling molecule has been proved to be critical in many life processes, such as reproduction, vision, immune response and embryogenesis (Collins & Mao, 1999; Wilson, Roth, & Warkany, 1953b; Wilson & Warkany, 1948). Thus the proper distribution of RA needs to be maintained for normal fetal development. The requirement of vitamin A is illustrated by defects shown in animal models without sufficient retinol: fetal mice with inadequate vitamin A from maternal sources are not viable(Lucile Ryckebusch et al., 2008); even adult rats reared on a vitamin A deficient (VAD) diet are growth-arrested but resume growing upon subsequent provision of vitamin A (McCollum & Davis, 1913). On the other hand, excess intake of retinol or retinoic acid (RA) can be toxic: high dose RA treatment impairs fetal organogenesis, leading to various congenital defects (Dickman & Smith, 1996; Lammer et al., 1985; Rothman et al., 1995; Shenefelt, 1972). The adverse consequences of both deficiency and excess allude to the duality of vitamin A being both teratogenic yet essential for life. Thus, the proper distribution of RA needs to be maintained for normal fetal development.

Homeostasis of RA is precisely controlled by a well-orchestrated network of metabolic enzymes safeguarding the formation and degradation of such an essential, yet, teratogenic molecule. Synthesis of RA in embryonic tissues starts with the reversible oxidation of retinol to retinaldehyde by retinol dehydrogenase 10 (RDH10) (M. Rhinn et al., 2011; Lisa L. Sandell et al., 2012), which can be reversed by short-chain dehydrogenase/reductases (SDR) or aldo-keto-reductases (AKR) (Kedishvili, 2013; Porté et al., 2013). These two reactions constitute an important point of metabolic regulation to control the level of retinaldehyde, since the oxidation of retinaldehyde to RA by retinaldehyde dehydrogenases (RALDHs) 1, 2 and 3 is irreversible (Deltour et al., 1999; F. A. Mic, Molotkov, Fan, Cuenca, & Duester, 2000; Zhao et al., 1996). Excess RA is degraded by CYP26A1, B1 and C1, which are expressed in different tissues and time points (Pennimpede et al., 2010; Romand et al., 2006; Masayuki Uehara, Yashiro, Takaoka, Yamamoto, & Hamada, 2009). These specifically expressed enzymes function as “sinks” to prevent accumulation of RA and thus control its endogenous levels in distinct regions and windows of

development. Previous *in vitro* assays identified a short chain dehydrogenase-reductase, Dhrs3, to be capable of catalyzing the reduction of retinaldehyde to retinol (Haeseleer, Huang, Lebioda, Saari, & Palczewski, 1998). Further studies based on *in vivo* models from multiple labs, including our own, validated the physiological function of *Dhrs3* preventing teratogenic accumulation of RA and its indispensability in organogenesis and body patterning (Adams et al., 2014; Billings et al., 2013; Feng et al., 2010; Kam et al., 2010; R. K. T. Kam et al., 2013).

Here we explore and investigate the necessity of *Dhrs3* in the metabolism of RA during early embryogenesis and its roles in neuronal and skeletal development by utilizing *Dhrs3*-deficient mice. Our results indicated that, deficiency in *DHRS3* led to an evident expansion of RA signaling domains in the developing *Dhrs3*$^{-/-}$ embryos at E10.5, which was consistent with the increased RA signaling observed at E14.5 (Billings et al., 2013). As a consequence, *Dhrs3*$^{-/-}$ mutants displayed partially penetrant defects in the morphology and outgrowth of cranial nerves. A lack of *DHRS3* also resulted in fusion of C1-C2 cervical vertebrae and delayed ossification of cartilages in the rib cage, both of which phenotypes can be reversed by reducing the maternal intake of vitamin A in *Dhrs3*$^{-/-}$ embryos. Rearing the *Dhrs3*$^{+/-}$ dam on vitamin A deficient diet for three generations successfully rescued the embryonically lethality of *Dhrs3* deficient embryos to survive postnatally. The rescued *Dhrs3*$^{-/-}$ mice were observed to possess similar growth rate as their wild type littermates but were found to have behavioral defects and difficulty in breeding. Taken together, our data suggest that DHRS3 plays critical roles in preventing the excessive accumulation of RA during early embryogenesis and that well-controlled synthesis of RA is required for proper development of cranial nerves and skeleton.

2.2. Materials and Methods

Mice

Generation of *Dhrs3*$^{+/-}$ mice was previously described (Billings et al., 2013). Female *Dhrs3*$^{+/-}$ mice were maintained on vitamin A sufficient diet, containing 4 IU preformed vitamin A (D13112B, Research Diets) per gram of diet, while male *Dhrs3*$^{+/-}$ were on 2018 chow diet that contains 15 IU vitamin A/gram

of diet (Envigo). The *RARE-LacZ* carry a *LacZ* gene under the control of an RA-inducible promoter (Rossant et al., 1991) and are available at the Jackson Laboratories identified as strain *RARE-hsp68LacZ*, stock 008477. Timed matings were set up using female mice at proestrus stage and vaginal plugs were check on the following morning. Caesarean sections were performed at designated embryonic stages to collect embryonic tissues. All animal protocols were approved by the Institutional Animal Care and Use Committee at the University of Kansas.

Rescue study

Dhrs3$^{+/-}$ parent mice were kept on vitamin A sufficient diet (VAS) and their female *Dhrs3*$^{+/-}$ offsprings were reared on vitamin A deficient diet (VAD) from weaning. VAD-fed female *Dhrs3*$^{+/-}$ mice were bred overnight with male *Dhrs3*$^{+/-}$ mice fed on 2018 chow diet (Envigo) to generate VAD *Dhrs3*$^{-/-}$ embryos. Caesarean sections were performed at designated embryonic stages to harvest pups. Both VAS and VAD diets are derived from AIN-93G growing rodent diet (Reeves, 1997). VAS diet contains 4 IU preformed vitamin A (D13112B, Research Diets) per gram of diet whereas VAD diet is depleted with vitamin A (D13110GC, Research Diets).

X-Gal staining

Detection of LacZ reporter gene was carried out using previously established protocol (Billings et al., 2013). Embryos were stained under identical conditions to facilitate fair comparison. Stained tissues were post-fixed in 4% paraformaldehyde at 4°C overnight and embedded in paraffin blocks for sectioning. Samples were cut sagittally at 7μm, counterstained with eosin and mounted in Vectamount Permanent Mounting Medium (Vector Laboratories, Cat # H-5000).

Immunostaining

E10.5 mouse embryos were harvested and rinsed in ice-cold PBS and fixed in 4% paraformaldehyde at 4°C overnight. Endogenous HRP activity was quenched by incubating embryos in Dent's bleach (methanol: DMSO: 30%H_2O_2=4:1:1) for 4 hours at room temperature. Samples were then rehydrated

through a series of methanol solution with decreasing concentrations and blocked by 3% non-fat milk/ 0.1% Trion X-100/ PBS for two hours at room temperature. Subsequently primary antibody was diluted in blocking buffer (2H3 1:200; anti-Tuj1 1:1000) and applied to embryos at 4ºC overnight. On the following day embryos were washed with PBS for 3 times, one hour each at room temperature and HRP-conjugated secondary antibody recognizing the species of primary antibody was applied to embryos at 4ºC overnight. After being washed in PBS, DAB kit was used to detect HRP. Chromogenic reactions were allowed for 7 minutes for each sample and embryos were washed in PBS to stop the color reaction. Stained embryos were dehydrated through methanol, cleared by BABB reagent (benzyl alcohol: benzyl benzoate=1:1) and documented using a Leica DMS300 Dissection Microscope equipped with a digital camera.

Skeletal staining

Cartilages and ossified bones in E14.5 embryos were stained by Alcian blue and Alizarin red reagents according to previously described procedure (Billings et al., 2013). In brief, embryos were fixed in 95% ethanol overnight at 4ºC and subsequently incubated in washing solution containing 70% ethanol/5% acetic acid for 30min at room temperature. Staining was performed using 0.4% Alcian blue/1% Alizarin red solution at room temperature overnight. After staining, samples were rinsed in washing solution for 30 min and incubated in series of clearing reagent containing increasing concentrations of glycerol. The samples in both experimental and control groups were processed simultaneously using identical protocols to avoid artifacts due to staining and the images were documented using a Leica DMS300 Dissection Microscope equipped with a digital camera.

Microarray

Dhrs3$^{+/+}$ and *Dhrs3*$^{-/-}$ embryos were isolated at E14.5 on ice and snap-frozen in liquid nitrogen and stored at -80ºC for RNA isolation later. Extraction of tissue RNA was performed using TRIZOL reagent (Invitrogen) according to manufacturer's protocol. Before submission for microarray, RNA samples were

treated with DNase I (New England Biolabs, Cat # M0303S). Two embryos per genotype were utilized for the analysis.

2.3. Results

Deletion of *Dhrs3* leads to altered retinoid metabolism and RA signaling during early embryonic stages.

In order to visualize RA signaling, we employed a reporter mouse model carrying a transgene, *LacZ*, whose expression is under the control of a canonical RA-responsive element (RARE) in the promoter and can be detected by β-galactosidase staining (Jennifer B Moss et al., 1998). *RARE-LacZ* mice were crossed with *Dhrs3*$^{+/-}$ mice and used to generate *Dhrs3*$^{-/-}$*; RARE-LacZ* and *Dhrs3*$^{+/+}$*; RARE-LacZ* embryos as previously described (Billings et al., 2013). Mouse estrus cycle was determined by vaginal cytology using 0.1% crystal violet and female mice at proestrus stage were assigned to mate with *Dhrs3*$^{+/-}$*; RARE-LacZ* male for timed mating (Fig 2.1). Mouse embryos were isolated at E10.5 by caesarean section and processed for β-galactosidase staining. The results demonstrated that *Dhrs3* deficient embryos had expanded expression domains of the *RARE*-reporter, *LacZ*, in the frontonasal region, in the body trunk, in the limbs as well as in the tail (Fig 2.2 A, B vs. D, E). The expression of *RARE*-driven *LacZ* was found to be mild in the heart and limb buds in the wildtype embryos, but was much higher in the same tissues in *Dhrs3*$^{-/-}$ embryos. Sagittal sections of *Dhrs3*$^{-/-}$ embryos consistently exhibited a broader expression pattern of *RARE*-reporter in the spinal cord and within the heart (Fig 2.2 C vs. F). Therefore, ablation of *Dhrs3* causes expansion of RA signaling domains in mouse embryos as early as E10.5.

We also measured the abundance of retinoid metabolites in wild type, *Dhrs3*$^{+/-}$ and *Dhrs3*$^{-/-}$ embryos at E12.5 by LC-MS/MS. As expected, global levels of all-*trans*-RA (ATRA) were found to be higher in the *Dhrs3*-null embryos when compared to either wildtype or heterozygote controls (Fig 2.3 A). These results agree with the increased levels of RA observed in E14.5 *Dhrs3*$^{-/-}$ embryos versus controls (Fig 2.3 D) (Billings et al., 2013). The neutral retinoids (RE and retinol) were not altered in E12.5 *Dhrs3*$^{-/-}$ embryos versus wild type controls. This is in contrast to the observations that at E14.5, *Dhrs3*$^{-/-}$ embryos

have significantly lower levels of neutral retinoids compared to controls (Billings et al., 2013). The decrease in neutral retinoids in E14.5 *Dhrs3*$^{-/-}$ embryos cannot be accounted simply by their increase in their levels of RA. The 50% decreases in neutral forms of retinoids in E14.5 *Dhrs3*$^{-/-}$ embryos versus controls vastly exceeds their modest, 15%, increase in RA levels at the same stage. We propose that the dramatic increase in RE levels from E12.5-E14.5 seen in wildtype and heterozygous embryos coincides with the acquisition of hepatic functions by the wildtype embryonic liver which among other functions also includes storage of RE. However, in the case of *Dhrs3*$^{-/-}$ there is no apparent increase in RE between E12.5 and E14.5 suggesting a delay or an alteration in liver specification, however, such a possibility will require further studies.

***Dhrs3* deficiency leads to defects in the development of cranial nerves.**

Excess of RA has been frequently reported to induce craniofacial defect in embryos (Morriss-Kay, 1993; Maxence Vieux-Rochas et al., 2007) including defects in the development of cranial neural crest cells, neurocristopathies which contribute to craniofacial structure and cranial nerves (Cordero et al., 2011; Rothman et al., 1995). In addition to CNCC, RA was found to play important roles in the patterning of the neural system in multiple models (Chawla, Schley, Williams, & Bohnsack, 2016). Altered levels of RA affect hindbrain patterning as well as the neurite outgrowth from spinal cord and DRG (Maden, Gale, Kostetskii, & Zile, 1996; Niederreither et al., 2003; Jeffrey C. White, Highland, Kaiser, & Clagett-Dame, 2000). Teratology studies of RA has also revealed that maternal exposure to excess RA or deficiency of retinoid can result in defective cranial neural crest cell migration in mouse embryo models (Pratt, Goulding, & Abbott, 1987). We have previously reported that *Dhrs3*$^{-/-}$ embryos display severe malformation in palate and craniofacial bone ossification (Billings et al., 2013). Therefore, we sought to extend our investigation looking at the development of cranial nerves (CVs) in *Dhrs3*$^{-/-}$ mice at E10.5.

We examined the structure and morphology of CVs by wholemount immunostaining using an antibody (2H3) against neurofilament. We compared 7 CVs between *Dhrs3*$^{-/-}$ and wildtype: V, trigeminal;

VII, facial; VIII, vestibulocochlear; IX, glossopharyngeal; X, vagus; XI, accessory; and XII, hypoglossal. 89% (8 out of 9) *Dhrs3*$^{-/-}$ embryos examined showed evident neuronal malformation in CVs when compared to stage-matched wildtype embryos (Fig 2.4 A-C). Multiple CV defects were present in the mutant mice with various degrees of severity and penetrance (Fig 2.4 D). Within the examined mutant mice, 89% (8 in 9) exhibit disarray in the organization of neuronal fibers in anterior CV-XII (hypoglossal nerve). CV-IX and X were found to be fused or randomly distributed in 56% (5 in 9) Dhrs3$^{-/-}$ mice when compared to the wildtype. Nerve fiber density was found to be reduced in CV-VII and VIII and smaller sized CV-V was observed in 33% (3 in 9) Dhrs3$^{-/-}$ embryos. Some knockout embryos have double or more symptoms while some only present with defective structure in CV-XII. No obvious morphological alteration was seen in CV-XI between Dhrs3$^{-/-}$ and wildtype embryos. We also performed wholemount immunostaining of CVs using neuron-specific Class III β- (Tuj1) antibody. Tuj1 staining revealed relatively normal development of CVs in Dhrs3$^{-/-}$ embryos at E10.5 (Fig 2.5 A vs. B), except for disorganization of CV-XII and alteration in shape of CV-IX and X (Fig 2.5 C vs. D), similar to what was observed by neurofilament immunostaining. To sum up, ablation of *Dhrs3* in mouse embryos affects the development of specific cranial nerves at E10.5.

Deletion of *Dhrs3* leads to malformation in the cervical vertebrae and rib ossification.

RA embryopathy can often result in a series of congenital defects including skeletal malformations (Collins & Mao, 1999; Lammer et al., 1985). Our lab has previously reported that E14.5 *Dhrs3*$^{-/-}$ embryos consistently exhibit a distinguishing fusion of the neural arches of the C1 and C2 cervical vertebrae (Billings et al., 2013), which phenocopies another genetic mouse model, *Cyp26a1*$^{-/-}$, where RA accumulates as a result of a deficiency in its catabolic enzyme CYP26A1 (Suzan Abu-Abed et al., 2001). We further investigated the skeletal development in absence of *DHRS3* at E14.5 by Alcian blue to stain for cartilages and Alizarin red to stain for ossified bones. Our analysis found that the altered levels of RA and its signaling in *Dhrs3*$^{-/-}$ mice did not affect the number of cervical vertebrae (C1-C7) or the formation of the first rib at the location of thoracic vertebra T1 (Fig2.6 A vs. B). Yet, whereas the ossification of

cartilaginous thoracic rib was initiated normally from the dorsal end (next to the spine) to the ventral end in the wildtype embryos, the osteogenesis process was found to be delayed in *Dhrs3* null mutant embryos at E14.5, indicating a delayed ossification in the developing ribs.

DHRS3 regulates complement and coagulation cascades at E14.5.

In order to understand additional biological processes regulated by DHRS3 and RA, we performed microarray utilizing E14.5 *Dhrs3*$^{-/-}$ and *Dhrs3*$^{+/+}$ embryos. Specifically, liver functions were noticed to be drastically elevated in the *Dhrs3*-null mutant at E14.5 (Supplementary Figure 2.1). Amongst all the altered pathways complement and coagulation cascades represented the largest change. Though complement and coagulation are distinct pathways with different physiological functions, they share similarity on molecular level and function as critical barrier of the innate immune system against exogenous threat. Based on two embryos per phenotype, we generated preliminary results demonstrating that genes involved in both extrinsic and intrinsic coagulation pathways were evidently elevated in the *Dhrs3*$^{-/-}$ mutant mice and multiple critical proteins involved in completion pathway, such as complement component 2, 3 and 4, are up-regulated by increased RA signaling. Additional investigation of liver functions in *Dhrs3*$^{-/-}$ embryos at various time points is needed in the future to understand the progress of hepatic development in response to altered RA metabolism.

Maternal vitamin A deficient diet successfully rescues *Dhrs3* null mutant mice.

Previous studies from our lab has provided substantial evidence that ablation of *Dhrs3* causes excessive accumulation of RA and increased RA signaling in the mutant mice (Billings et al., 2013). Deficiency of *DHRS3* also results in various malformations in cardiac, palatal and skeletal development. However, previous studies did not provide evidence that the observed morphological congenital defects can be attributed to the biochemical defect of excess RA present in *Dhrs3*$^{-/-}$ mice. To reach this conclusion we performed a “rescue” study, in which we depleted the maternal vitamin A from diet of the dam to create a deficiency of RA precursors in the hope that this would then restore normal levels of RA and recover normal development in the *Dhrs3*- null embryos developing in this context.

Vitamin A deficient diet (VAD) was provided to *Dhrs3*$^{+/-}$ dam from weaning and throughout gestation. Feeding female *Dhrs3*$^{+/-}$mice with VAD diet within one generation did not alter their breeding capacity. VAD diet occasionally led to dystocia if the treatment was prolonged beyond two generations. Morphological analysis of the axial skeleton of E14.5 VAD-*Dhrs3*$^{-/-}$ embryos via Alcian blue and Alizarin red staining suggested that the reduced maternal intake of vitamin A could partially rescue the cervical defect. Though the C1 and C2 cervical vertebrae became discrete and separated in VAD-*Dhrs3*$^{-/-}$ embryos, the neural arches of the C2 and C3 vertebrae were found to be fused laterally on one side. Intriguingly, in VAD-*Dhrs3*$^{-/-}$ embryos, the morphology of the C3 vertebrae was found to be more similar to a normal C2 vertebra while the C2 vertebra came to resemble C1. Collectively, reducing maternal intake of vitamin A in *Dhrs3*$^{-/-}$ embryos ameliorated the skeletal defects in cervical vertebrae.

In contrast to both humans and other experimental models, mice are remarkably resistant to diet-induced vitamin A deficiency, being able to provide sufficient vitamin A from dam to fetus to last for the entire lifetime of the offspring. Mouse vitamin A deficiency requires the depletion of both preforemed and provitamin A carotenoids from the diet for several generations. By prolonging the dietary VAD treatment through three generation of *Dhrs3*$^{+/-}$ female mice, we were able to generate a sufficiently deficient vitamin A state in the dam to obtain viable *Dhrs3*$^{-/-}$ mice which survived to adulthood. Unlike *Dhrs3*$^{-/-}$ mice born to dams maintained on vitamin A sufficient diet, *Dhrs3*$^{-/-}$ mice from vitamin A-deficient dams were born with their eyelids still fused, did not exhibit clefting and were able to, breath, suckle and grow. We were not able to obtain sufficient living *Dhrs3*$^{-/-}$ mice to perform retinoid analysis to verify that the fetal RA levels of the rescued *Dhrs3*$^{-/-}$ mice was the same as wildtype littermates maintained on a normal diet. However, were able to examine the few living *Dhrs3*$^{-/-}$ mice were put on vitamin A sufficient (4 IU/g) diet and regularly examined for any signs of the potential postnatal effects of excess RA. Rescued *Dhrs3*$^{-/-}$ mice maintained on a vitamin A sufficient diet were able to grow into full-sized adult mice with a normal rate of weight gain compared to their wildtype littermates (Fig 2.7). Examination of the gross morphology of the surviving adult *Dhrs3*$^{-/-}$ mice indicated a shortening and

reduction in the length of skull when compared normal age-matched mice that have been fed only on VAS diet. These rescued mice were found to be easily agitated and displayed stereotypic circling behavior upon subtle stimulation, possibly suggesting vestibular dysfunction and/or striatal asymmetry (Ishiguro, Inagaki, & Kaga, 2007). Responsiveness to light was also evaluated and the surviving knockout mice did not respond to sudden light exposure, possibly due to freezing behavior, defects in neural processing or defective visual functions. Taken together, we were able to rescue embryonic lethal *Dhrs3*$^{-/-}$ embryos by removing maternal dietary intake of vitamin A, suggesting that the congenital defects observed in Dhrs3 mutant mice were attributed to excessive accumulation of RA.

In summary, our results demonstrate that genetic ablation of *Dhrs3* in developing mouse embryos causes alterations in RA signaling, suggesting an indispensable role of *Dhrs3* in safeguarding RA homeostasis during embryonic development. In addition to altered RA signaling, lack of function of *DHRS3* also results in embryonic lethality and malformations in cranial nerves and skeleton. Rearing *Dhrs3*$^{+/-}$ dams on VAD diet successfully corrected most of the phenotypes in *Dhrs3*$^{-/-}$ embryos and allowed the *Dhrs3*-null mutant to survive postnatally.

2.4. Discussion

DHRS3 plays critical roles in RA metabolism *in vivo*.

Genetic mutation of Dhrs3 increases RA signaling during early embryogenesis at E10.5. Homeostasis of RA is controlled by many critical enzymes to safeguard normal embryogenesis. DHRS3 was reported to reduce retinaldehyde in a NADPH-dependent manner *in vitro* (Haeseleer et al., 1998) and non-mammalian models demonstrated that deletion of *dhrs3* causes elevated levels of RA signaling and results in defects in early embryogenic pattering. Our lab previously reported that ablation of *Dhrs3* in mouse model led to increases in the embryonic level of RA and results in alteration in the extent of RA signaling during mid-gestation. In the current study, we continued our investigation of the necessity of *Dhrs3* in embryogenesis at E10.5. The expression of the RARE-driven reporter LacZ was detected in an expanded pattern in the frontonasal area and along the spine in the *Dhrs3*$^{-/-}$ embryos at E10.5, indicating

that *DHRS3* is required to prevent the accumulation of RA as early as E10.5. The expansion in RA signaling in the frontal nasal area in the Dhrs3 mutant mice is consistent with the observed craniofacial defects observed at E14.5 (Billings et al., 2013) and the alterations in the patterning of the vibrissae as noted in studies performed in collaboration with Dr. Denis Headon from the Roslin Institute (manuscript in preparation). The increased RA signaling in the heart of *Dhrs3*$^{-/-}$ embryos is consistent with the role of RA in heart development and with the etiologic role of altered RA in congenital heart diseases and is the subject of the following chapters. Though it is possible that the heart defects associated with *Dhrs3* deletion play a role in the mid- to late-gestational lethality observed in the *Dhrs3*$^{-/-}$ embryos but we cannot exclude other causes (Papaioannou & Behringer, 2005). Quantification of the levels of ATRA at E12.5 demonstrates that deletion of *Dhrs3* causes accumulation of RA and agrees with our previous report of RA increases in this model at E14.5.

Proper levels of RA are required for neuronal development.

Dhrs3$^{-/-}$ embryos exhibit defective formation of cranial nerve at E10.5. Previously, several reports have demonstrated the importance of proper levels of RA signaling in the embryonic development of cranial nerves. Rat embryos derived from vitamin A deficient dams display a loss of posterior cranial nerves (IX-XII), which can be corrected by maternal administration of all-*trans*-RA or retinol (J. C. White et al., 1998; Jeffrey C. White et al., 2000). Similar defects were observed in mice lacking sufficient RA synthesis as a result of genetic mutation of *Raldh2* (Niederreither et al., 2003). The posterior regions in the hindbrain of embryos deficient in vitamin A signaling were found to show abnormal expression of markers of anterior regions, which might contribute to the defects in the posterior cranial nerves (Jeffrey C. White et al., 2000). In the present study, deficiency of *Dhrs3* causes malformations in hindbrain-derived cranial nerves (V-XII). 89% examined mutant embryos display reduced nerve density or alteration in the shape of the nerves. In *Dhrs3*$^{-/-}$ embryos, the most affected nerve was the hypoglossal nerve (XII) and the second most frequently observed defect was fusion between glossopharyngeal (IX) and vagus (X) nerves, which is consistent with previous studies indicating that the posterior somatic

motor nerves are sensitive to altered levels of RA signaling. In addition, *Dhrs3*$^{-/-}$ embryos share similarity with the *Pax6* mutant embryos in the observed phenotypes in XII cranial nerve. *Pax6* was found to be RA-responsive and the eccentric expression and signaling of *Pax6* induced by anteriorly expanding RA signaling might be detrimental to the well-organized development of the hindbrain and the hindbrain-derived cranial nerves (Ericson et al., 1997; Osumi et al., 1997). In addition, over half of the examined *Dhrs3*$^{-/-}$ embryos show reduced density of cranial nerve fibers and lack of sufficient outgrowth of cranial nerves. Previous studies of the effects of RA on neurite outgrowth employed RA-deficient models; the current study provides evidence indicating that excess RA also causes deleterious effect of in the growth of nerve fibers.

Embryonic defects as well as mid-gestational lethality in *Dhrs3*$^{-/-}$ mice are attributed to excess RA.

Depletion of dietary vitamin A in the dam corrected most of the defects in the *Dhrs3*$^{-/-}$ embryos and successfully rescued *Dhrs3* mutants to survive postnatally. Previously, we have reported that *Dhrs3*$^{-/-}$ embryos possess malformations and fusions of the C1 and C2 cervical vertebrae t and delayed ossification in the skull at E17.5 (Billings et al., 2013). Rearing the *Dhrs3*$^{+/-}$ dam on VAD diet effectively prevented the fusion of the C1 and C2 vertebrae but also altered the identity and characteristics of C2 and C3 vertebrae. In the *Dhrs3*$^{-/-}$ embryos, and anteriorizing homeotic transformation (C2 to C1 and C3 to C2) was observed in the VAD-rescued *Dhrs3*$^{-/-}$ embryos. It is known that vertebrae display unique morphological characteristics according to their identities, which are determined by their localization relative to the anteroposteriorly patterned body axis. RA has been known to regulate the embryonic patterning of several organs as well as the whole body and homeotic transformation has been observed in animal models exposed to inappropriate levels of RA signaling. Exogenous treatment of RA to mouse embryos caused anteriorly enlarged expression domain of posterior Hox genes, which indicated the expansion of posterior somatic regions at the expense of anterior somites in response to activation of RA signaling (Kessel & Gruss, 1991). Thus it is plausible that anterior transformation in C2 and C3 vertebrae might be due to altered body patterning in response to changed levels of RA signaling.

Deficiency of *Dhrs3* also delays the ossification of ribs at E14.5, which is consistent with previous observation in the case of skull ossification at E17.5 (Billings et al., 2013). Similar to the defects in cervical vertebrae, this phenotype in rib skeleton ossification is also restore by reduced maternal intake of vitamin A. Most importantly, by feeding *Dhrs3*$^{+/-}$ dams on a VAD diet allowed us to circumvent the embryonic lethality associated with *Dhrs3* deletion. *Dhrs3*$^{-/-}$ pups survived to adulthood with normal body weight. More importantly, these findings suggest that the lethal defects observed in *Dhrs3*$^{-/-}$ embryos are truly due to excessive accumulation of RA and that lack of *Dhrs3* in adult mice is compatible with a normal growth and lifespan. However, several potential postnatal effects of *Dhrs3* deletion were noted. Adult *Dhrs3*$^{-/-}$ mice seemed to exhibit a minimal responsiveness to light stimulation. It is therefore possible that DHRS3, first described as retinal SDR1, retSDR1 which carries out the reduction of retinaldehyde may play a role in the regeneration of visual chromophore in the retina (Haeseleer et al., 1998). Further studies of the visual responses of the rescued *Dhrs3*$^{-/-}$ mice or retina-specific *Dhrs3* conditional knockout are warranted. Another observation is that when reared on VAS diet after weaning, *Dhrs3*$^{-/-}$ mice display spontaneous circling behavior, resembling defects observed in mice with vestibular dysfunction and striatal asymmetry. Further investigation of the neurological development and visual functions of adult *Dhrs3* deficient mice is needed to understand the postnatal roles of DHRS3 in vitamin A metabolism.

In summary, DHSR3 is required to safeguard embryonic development against the excess formation of RA during early and mid-gestation. DHSR3 via its effects on RA signaling plays critical, nonredundant roles in the development of the cranial nerves and the axial skeleton. Our results provide evidence supporting the physiological role of Dhrs3 in the metabolism of RA *in vivo* and of the teratogenic effects of excess RA in the development of skeleton and nervous system.

FIGURES

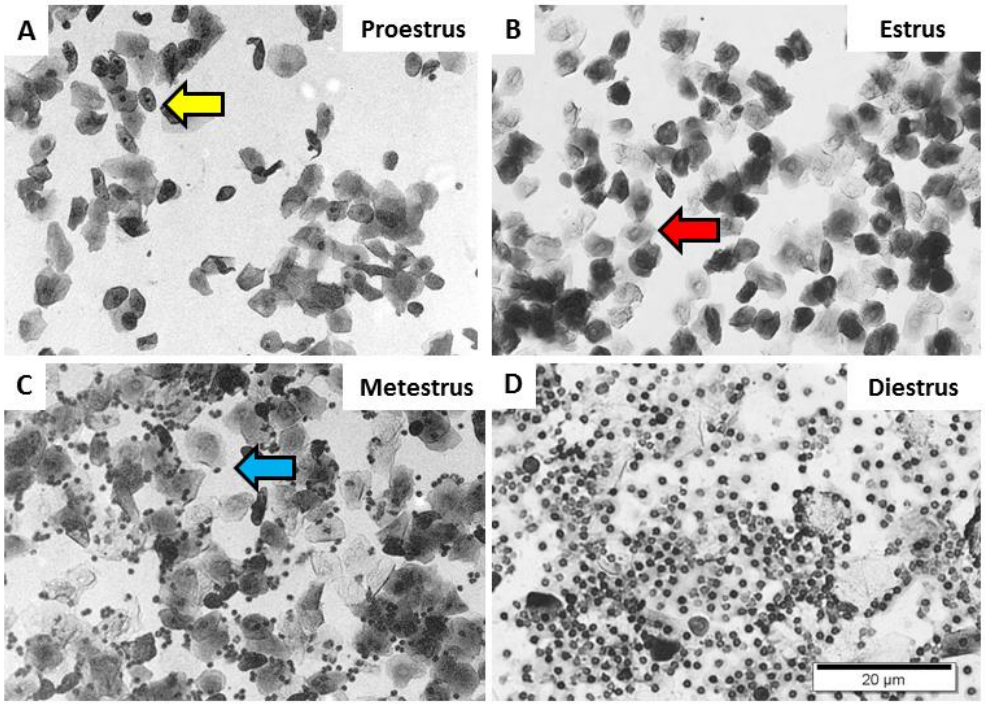

Figure 2.1 Determination of mouse estrus cycle.

Examination of vaginal cytology indicates that A) proestrus is characterized by the presence of nucleated epithelial cells (yellow arrow); B) nucleous-free conified epithelial cells dominate in estrus (red arrow); C) cells in metestrus contain both cornified epithelial cells and leukocytes (blue arrow); D) vaginal cells are primirily leukocytes during diestrus. Visualization of the cellular composition of vaginal smear helps identify different estrus stages of adult female mice and the successful timed mating.

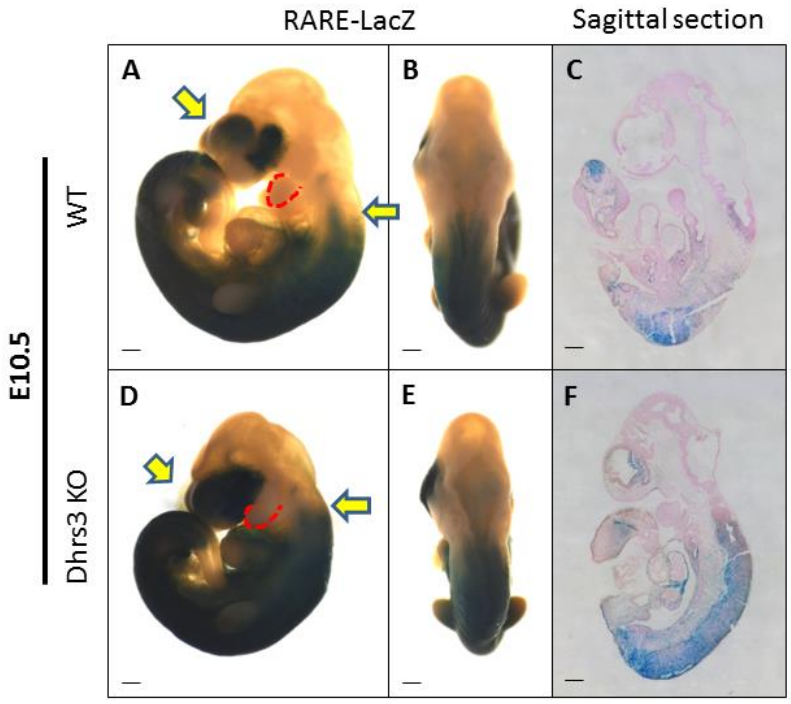

Figure 2.2 Ablation of *Dhrs3* causes expansion of RARE-driven RA signaling domains in E10.5 mouse embryos.

Wildtype (A-C) and Dhrs3 knockout (D-F) embryos carrying *RARE-LacZ* transgene were collected at E10.5 and processed for X-Gal staining to visualize β-Galactosidase (LacZ) activity. *Dhrs3*$^{-/-}$ *;RARE-LacZ* embryos display broader and more intense staining color in the dorsal body trunk and frontal nasal area (yellow arrows), suggesting an expansion of RARE-driven RA signaling domains in developing mutant embryos. Red dashed line marks the first pharyngeal arch. The expansion of LacZ expressing domain in *Dhrs3*$^{-/-}$ embryos reaches the posterior end of the first pharyngeal arch, which is in evident contrast to the wildtype. Scale bars represent 200μm. Images are representative of three individual embryos per genotype.

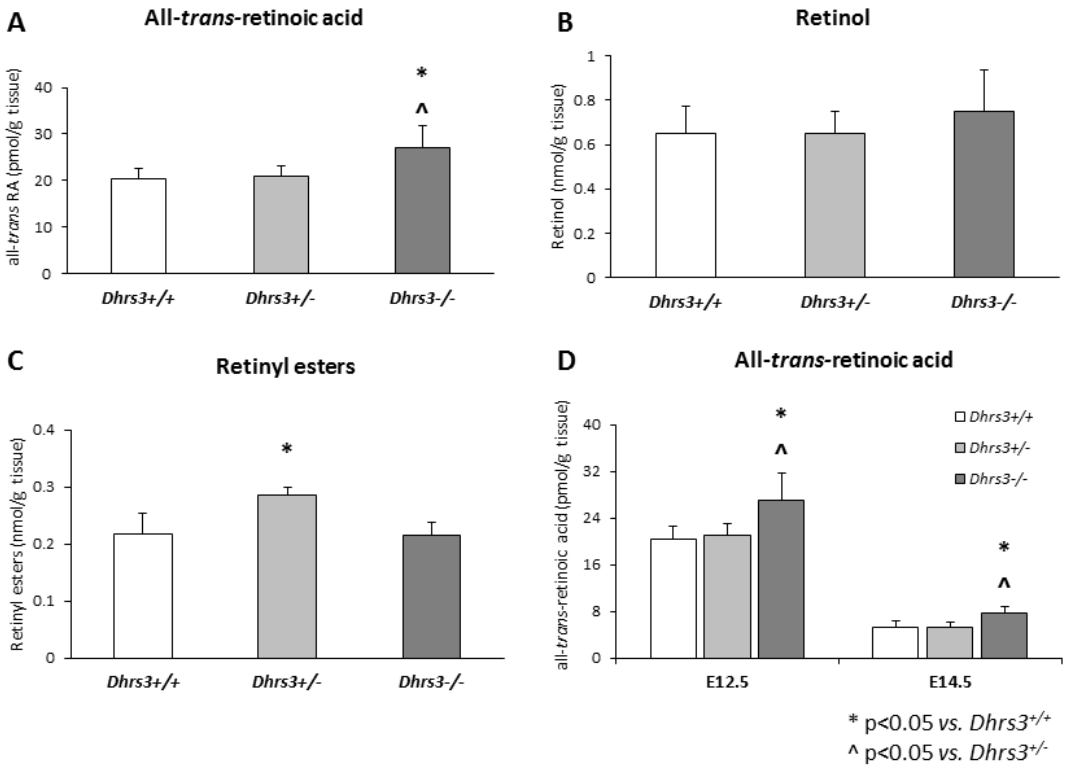

Figure 2.3 Mutation of *Dhrs3* leads to alterations in the levels of retinoids in developing embryos at E12.5.

Measurements were performed using LC-MS/MS and normalized by the weight of sample. At least 4 samples per genotype per stage were analyzed. * $p<0.05$ *vs.* $Dhrs3^{+/+}$;^ $p<0.05$ *vs.* $Dhrs3^{+/-}$.

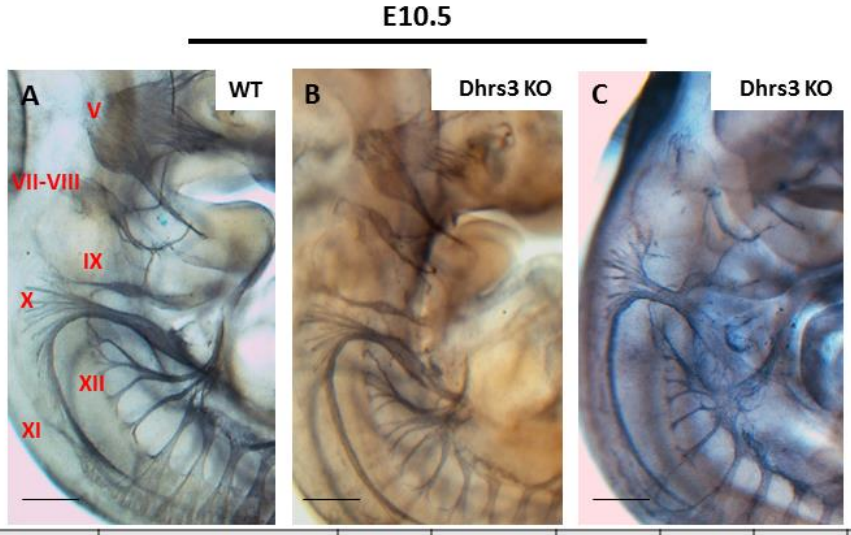

D

Defect in:	Total # of embryos examined	V	VII-VIII	IX-X	XI	XII	Overall
# of *Dhr3*$^{+/+}$ affected	3	0	0	0	0	0	0
# of *Dhrs3*$^{-/-}$ affected	9	3	3	5	0	8	8
Penetrance in *Dhrs3*$^{-/-}$	N/A	33%	33%	56%	0%	89%	89%

Figure 2.4 Wholemount immunostaining of Neurofilament reveals defective cranial nerve formation with partial penetrance in *Dhrs3*$^{-/-}$ mice.

Severity of neuronal defects varies in 9 examined *Dhrs3* mutant mice (A vs. B, C) and 89% mutant mice display malformations in the cranial nerves. Morphology of each individual cranial nerve was differentially affected by the ablation of *Dhrs3*. The percentage of mutant mice exhibiting a certain defect in a specific nerve is quantified and listed in D. V, trigeminal nerve; VII, facial nerve; VIII, vestibulocochlear nerve; IX, glossopharyngeal nerve; X, vagus nerve; XI, accessory nerve; and XII, hypoglossal nerve. Scale bars represent 500μm. Images are representative of 3 wildtype and 9 mutant embryos.

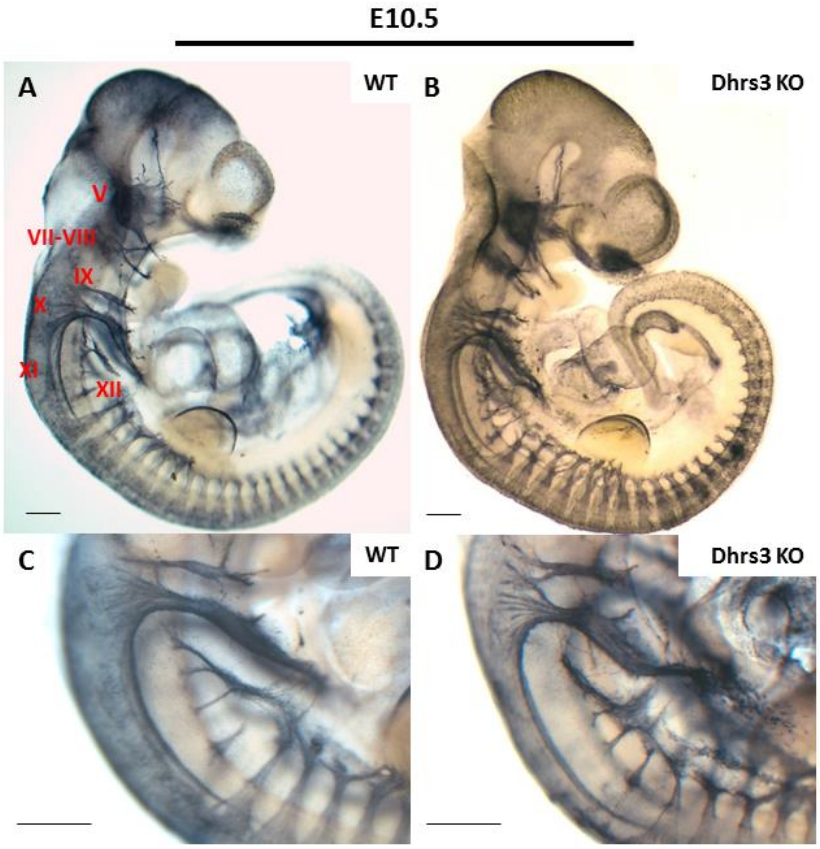

Figure 2.5 Wholemount immunostaining of neuron-specific Tubulin β 3 (Tuj1) in E10.5 embryos reveals the deleterious effect of ablation of *Dhrs3* on neuronal development.

Abnormal assembly and growth of hypoglossal nerve (XII) was observed in all examined Dhrs3 mutant mice (C vs. D, n=4). Scale bars represent 500μm. Images are representative of 3 individual embryos per genotype.

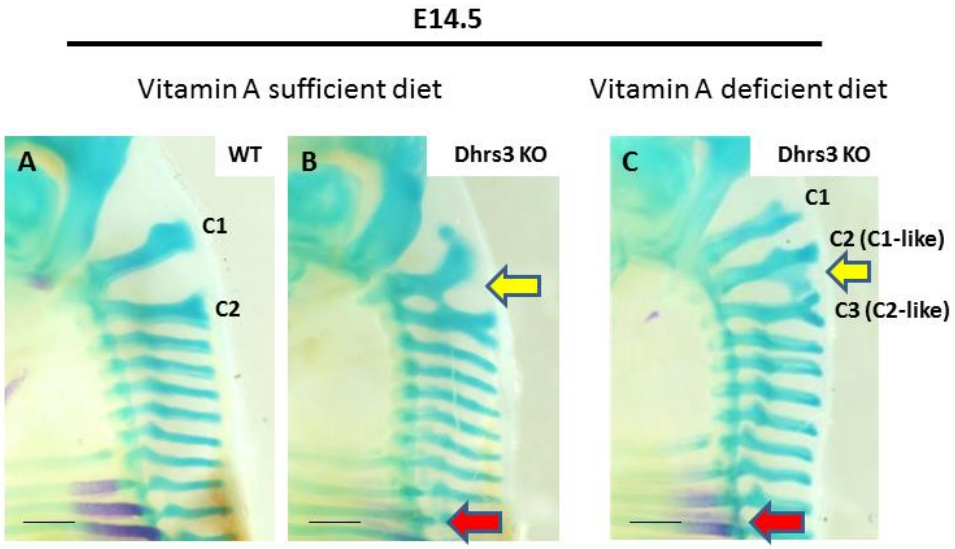

Figure 2.6 Malformations in cervical vertebrae and delayed ossification in *Dhrs3*$^{-/-}$ embryos are attributed to excessive accumulation of RA and can be rescued by reducing maternal intake of vitamin A.

Genetic deletion of *Dhrs3* causes evident fusion of C1 and C2 cervical vertebrae cartilage (yellow arrow) as well as delayed bone ossification (red arrow) in the rib cage of developing mouse embryos (A vs. B). Maternal vitamin A deficient (VAD) diet was able to partially correct the abnormal vertebrae fusion on one side of the body (yellow arrow in C) and restore the level of bone formation (red arrow in C) in *Dhrs3*$^{-/-}$ embryos. Yet, the VAD diet leaded to the transformation of the C3 cervical vertebrae into C2-like morphology with bifurcated extremity (B vs. C) in *Dhrs3*$^{-/-}$ mice, which indicates the requirement of tightly controlled amount of RA during skeletal development. Scale bars represent 500μm. Images are representative of three individual embryos per genotype.

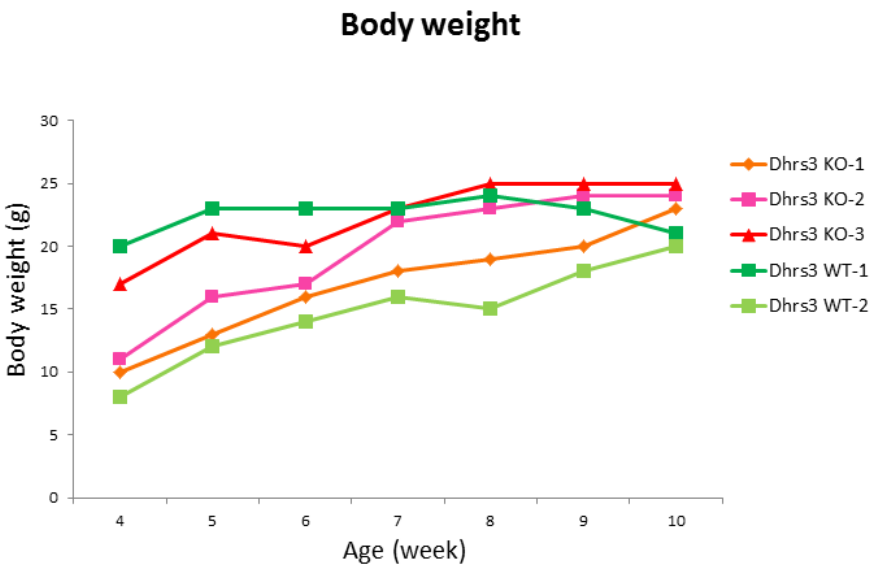

Figure 2.7 Maternal VAD diet rescued embryonically lethal Dhrs3 mutant embryos to adulthood.

Rescued *Dhrs3*$^{-/-}$ mice display normal growth on vitamin A sufficient diet when compared to their wildtype littermates. Three *Dhrs3* knockout mice and two wildtype mice were examined.

SUPPLEMENTARY FIGURES

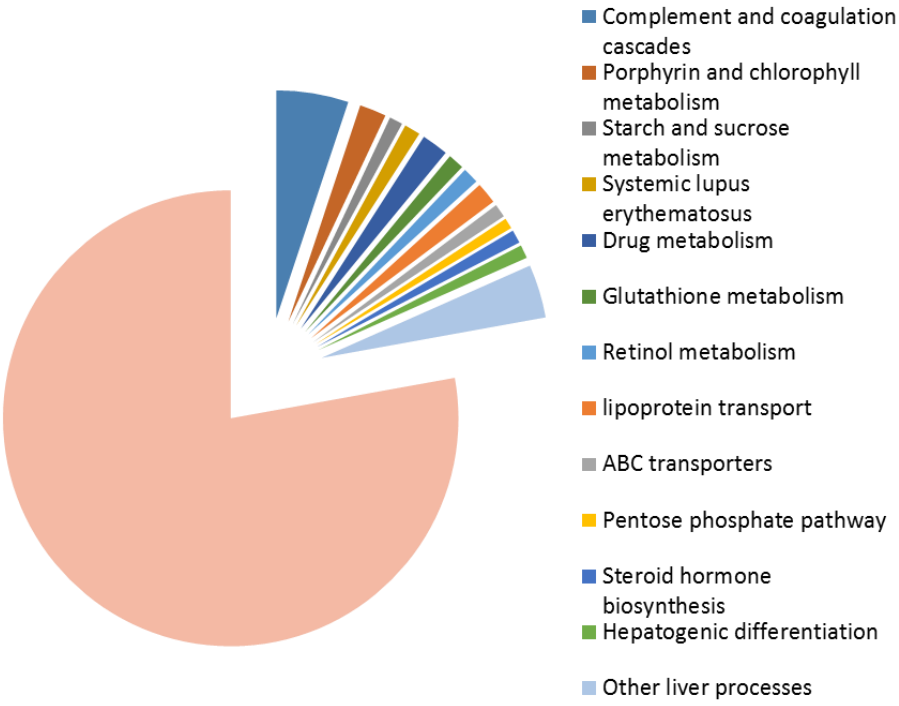

Supplementary Fig 2.1 Deletion of *Dhrs3* in mouse embryos altered hepatic functions at E14.5

Microarray analysis of genes that are differentially expressed in *Dhrs3*$^{-/-}$ *vs.* *Dhrs3*$^{+/+}$ embryos is presented as pie chart showing the gene ontology distribution of liver functions. Two embryos per genotype were employed in the microarray analysis.

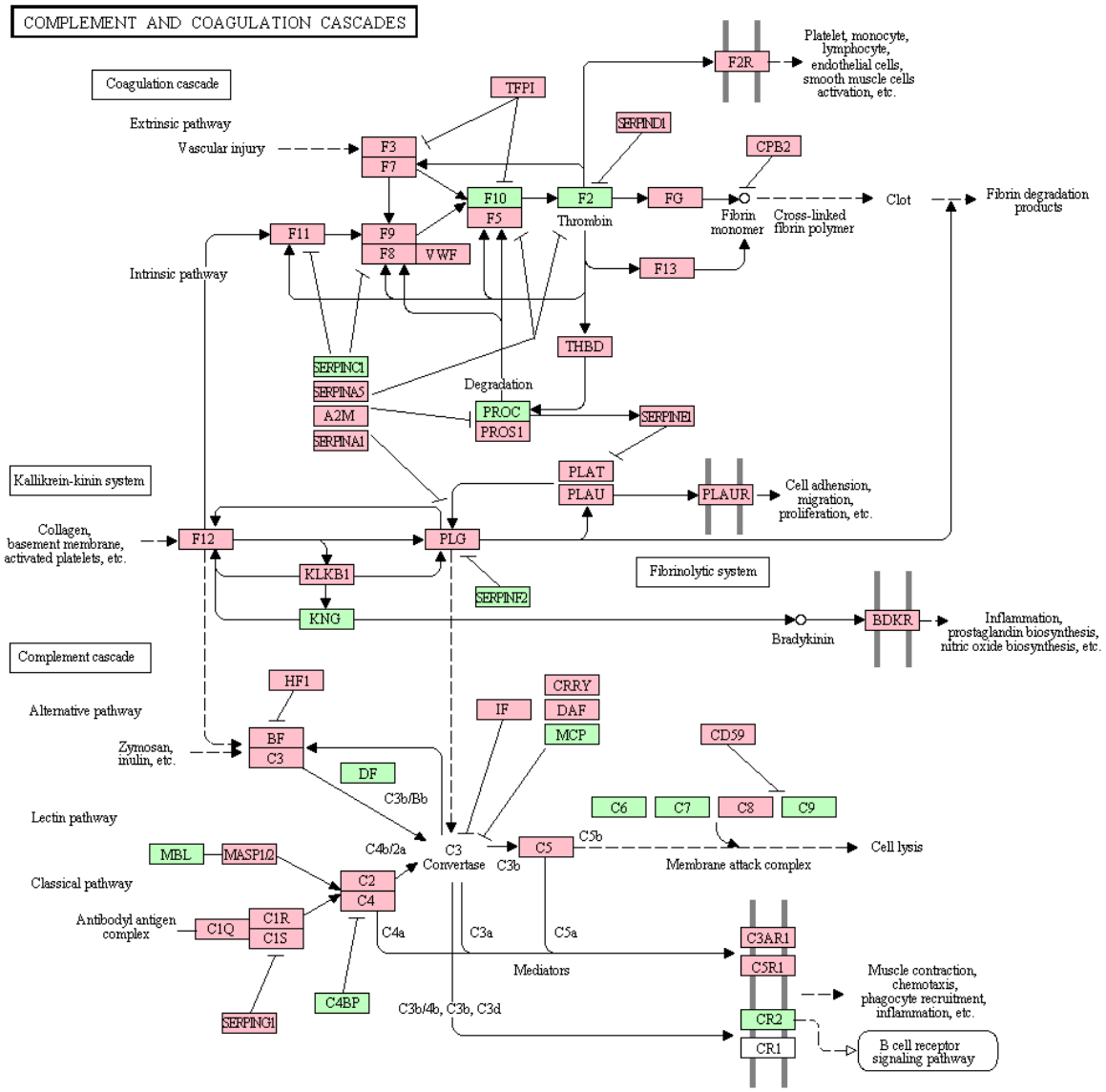

Supplementary Fig 2.2 KEGG analysis of genes involved in complement and coagulation cascades in *Dhrs3*$^{-/-}$ embryos.

Complement and coagulation cascades were found to be broadly activated in the *Dhrs3*$^{-/-}$ embryos when compared to wildtype controls at E14.5. Pink represents genes that are induced by the deficiency of *DHRS3* and green represents genes that are suppressed.

Chapter 3 : Retinoic Acid Regulates Cytoskeletal Reorganization in Epithelial to Mesenchymal Transition of Embryonic Epicardial Cells

Abstract

The epicardium is the main source of RA in the embryonic heart. Yet, the cardiogenic functions of epicardial-produced RA are not fully understood. Here, we investigated the roles of RA-signaling in the embryonic epicardium using *in vivo* and *in vitro* models of excess or deficiency of RA. Our results suggested that RA plays a critical role in regulating the cytoskeletal rearrangement required for the epicardial-to-mesenchymal transition (EpiMT) of epicardial-derived precursor cells (EPDCs). *In vivo*, treatment with an inhibitor of RA synthesis delayed the migration of EPDCs into the myocardium. In contrast, the opposite was seen in the case of *Dhrs3*$^{-/-}$ embryos, a mouse model of RA excess, in which EPDCs were localized deeper into the myocardium than in wild type controls. To understand the molecular mechanisms by which RA regulates EpiMT, we employed a whole transcriptome profiling approach which in combination with pull-down and inhibition assays demonstrated that the RhoA pathway is required for the morphological changes induced by RA in epicardial cells. Collectively, these data demonstrate that RA regulates EpiMT via a signaling cascade which involves the RhoA pathway.

3.1. Introduction

There are few therapeutic options for coronary vascular disease (CVD), despite it being the leading cause of death worldwide. The minimal regenerative capacity of the adult human heart is an important roadblock in the treatment of CVD. Species capable of effective cardiac regeneration rely on fast revascularization to supply nutrients and restore oxygen to the injured area (Marin-Juez et al., 2016). Thus, a better understanding of the developmental processes that guide the formation of coronary vasculature could help in the design of therapies to assist the formation of new vessels.

The epicardium is an epithelial layer of cells that covers the surface of the heart and plays a critical role in its development and regeneration. The main developmental contributions of the epicardium consist of cardiotrophic factors and epicardial-derived precursor cells (EPDCs) which give rise to several cardiac

lineages (reviewed in (Carmona et al., 2010)). Formed by a process of epicardial-to-mesenchymal transition (EpiMT), EPDCs migrate into the myocardium and differentiate mainly into vascular smooth muscle cells (VSMCs) and cardiac fibroblasts (reviewed in (Fang, Xiang, Braitsch, & Yutzey, 2016; Ruiz-Villalba & Perez-Pomares, 2012; von Gise & Pu, 2012)). Following birth, the epicardium becomes quiescent but, upon injury, its regulatory functions can be reactivated to sustain the wound repair process (Lepilina et al., 2006; B. Zhou et al., 2011). EpiMT is thus an integral process that leads to the generation of key precursor cells necessary for both the late development of the embryonic heart and for the response to injury in the adult heart.

All-*trans*-retinoic acid (RA), a metabolite of vitamin A, acting as a ligand of its cognate RA receptor (RAR), plays an important regulatory role in development of the heart (reviewed in (Stefanovic & Zaffran, 2017; Xavier-Neto et al., 2015)). RA produced by the lateral mesoderm determines the size of the cardiac progenitor pool and specifies the cells that contribute to the inflow versus the outflow tract (T. Hochgreb et al., 2003). After the heart forms, it becomes enveloped with a visceral pericardial layer of cells called the epicardium. The embryonic epicardium is the major source of cardiac RA as it expresses both the enzymes involved in the synthesis of RA (J. B. Moss et al., 1998; Niederreither, McCaffery, Drager, Chambon, & Dolle, 1997; Xavier-Neto et al., 2000) as well as the receptors for RA and 9-*cis*-RA, namely, RAR and RXR (Dolle, 2009; Merki et al., 2005). In fact, the embryonic RA biosynthetic enzyme, retinaldehyde dehydrogenase type II (RALDH2, officially designated ALDH1A2) is often used as a specific marker for the epicardium in the developing heart (J. M. Perez-Pomares et al., 2002; Xavier-Neto et al., 2000). Visualization of RA signaling in the embryonic heart has also revealed enriched RA signaling activity in the epicardium (Matt et al., 2005). However, in spite of earlier reports suggesting epicardial-derived RA to be required for the secretion of epicardial-derived trophic factors (T. Chen et al., 2002; Merki et al., 2005; Ingo Stuckmann et al., 2003), it appears that epicardial-mediated myocardial growth relies primarily on non-epicardial RA sources (Thomas Brade et al., 2011; Shen et al., 2015). This raises the question: what is the role of the RA produced by the epicardium in cardiogenesis?

The roles of epicardial-derived RA in heart development are still poorly understood. Studies from mouse models provide evidence of the requirement of Retinoid X Receptor-α (RXRα) in EpiMT (Merki et al., 2005) and of the involvement of RA-signaling in EpiMT mediated by Wilms-tumor 1 (WT1) (von Gise et al., 2011). Results based on avian models also suggest that epicardial-derived RA plays a role in the differentiation of EPDCs into VSMCs (Azambuja et al., 2010; Caitlin M. Braitsch et al., 2012). In adults, epicardial RA-signaling is required for the regeneration of the zebrafish heart and is involved in the injury response of the adult mammalian heart (D. Bilbija et al., 2012). In conclusion, several lines of evidence suggest that epicardial-derived RA may play important roles in cardiac developmental and regenerative processes but many of the mechanistic details of this regulation are still missing.

Here, we report that RA-signaling plays a critical role in the development and migration of EPDCs. These conclusions are derived from complementary models of excess or deficient RA-signaling which show that RA-signaling is required for the cytoskeletal reorganization of epicardial cells to facilitate cell movement. Our data clarifies a less well understood aspect of the role of RA-signaling in the development of the epicardial-derived cell lineages.

3.2. Materials and Methods

Mice

Heterozygote crosses of the previously described *Dhrs3*$^{+/-}$ mouse strain (Billings et al., 2013) were used to generate *Dhrs3*$^{-/-}$ homozygotes and *Dhrs3*$^{+/+}$ control embryos. The *RARE-LacZ* reporter mouse strain (Rossant et al., 1991) was obtained from Jackson Laboratories identified as strain *RARE-hsp68LacZ*, stock 008477. The mice were maintained on a regular chow diet Teklad 2018 (Envigo, Cambridgeshire, UK) that contains 15 IU vitamin A/ gram diet and housed in rooms providing controlled temperature and humidity on a 12-hour light-dark cycle. Female mice were examined daily for estrus cycle stages by vaginal smear and those at proestrus stage were mated to male mice overnight. Matings were broken the next morning and that noon was considered to be embryonic day (E0.5). Caesarean sections were performed at designated embryonic stages to harvest pups or embryonic tissues. The age of

the harvested embryos was also verified based on having achieved specific developmental milestones for each stage. All animal protocols were approved by the Institutional Animal Care and Use Committee at the University of Kansas.

Establishment of an RA-deficient mouse model

N'N'-bis(dichloroacetyl)-1,8-octamethylenediamine (Tocris Bioscience, Cat# 4736, CAS Number: 1477-57-2) also known as WIN18,446 (WIN), was dissolved in DMSO (ACROS Organics, Cat #61097-1000) to form a stock solution. Pregnant *RARE-LacZ* mice were orally gavaged with 51.6 mg/kg WIN mixed in corn oil once per day from E9.5 to E13.5. At E14.5 caesarean sections were performed to harvest embryos for various analyses.

Histology

Mouse embryos harvested at various developmental stages were fixed overnight in 4% paraformaldehyde at 4°C and then embedded in paraffin and cut as 7µm transversal sections using a Leica RM2255 microtome. The slides were stained using hematoxylin and eosin according to previously published protocol (Fischer, Jacobson, Rose, & Zeller, 2008) and documented by a dissecting microscope equipped with a digital camera. The heart morphology was evaluated as described in (Billings et al., 2013) to assess the effect of WIN treatment on heart tube elongation, looping and chamber formation.

RT-PCR

RNA was isolated using the QIAGEN RNeasy micro kit (Qiagen, Cat # 74104) according to manufacturer's instructions. 1µg of RNA was first treated with DNase I (New England Biolabs, Cat # M0303S) and then reverse-transcribed using SuperScript III reverse transcriptase (Invitrogen, Cat# 18080051) into complementary DNA (cDNA). Quantitative real-time PCR analysis using the Power SYBR Green Master Mix (Applied Biosystems, Cat# 4367659) was performed on an Applied Biosystems StepOnePlus Real-Time PCR system (Applied Biosystems, Foster City, CA). The primer sequences for each target gene are listed in Supplementary Table 3.2. The amplified regions of all used qRT-PCR

primer sets have been mapped and validated by UCSC In-Silico PCR database [Dec. 2011 (GRCm38/mm10), mouse genome] and the products have been examined by agarose gel electrophoresis to confirm the specificity of the primers. The relative expression levels of a gene have been calculated using the ΔΔCt method and normalized to that of *Gapdh* as an internal control.

Immunofluorescent staining

The embryos were fixed in 4% PFA overnight at 4°C and embedded in paraffin and then transversal sections were cut at 7µm. The slides were first deparaffinized and rehydrated at room temperature. Antigen retrieval was performed and endogenous horseradish peroxidase (HRP) activity was quenched with 3% H_2O_2 for 10 minutes. Slides were then blocked for an hour with blocking buffer (5% normal goat serum/ 0.1% Tween20/ PBS) at room temperature for an hour. The primary antibody was diluted in blocking buffer and applied to slides for overnight incubation at 4°C. After being washed in 0.1% Tween20/ PBS, HRP-conjugated secondary antibody recognizing the species of the primary antibody was applied to the slides. Detailed information of antibodies and dilution ratios are reported in **Table 2**. The specificity of the primary antibodies has been validated by western blotting revealing in each case recognition of a single protein band migrating at the expected molecular weight for the respective antigen. Subsequently, a tyramide-based signal amplification (TSA) method using the TSA Plus Fluorescein Evaluation Kit (PerkinElmer, Cat# NEL741E001KT) was used to amplify the fluorescent signal according to manufacturer's protocol. 1µM of DAPI (Life Technologies) was applied to counterstain the nuclei and the slides were mounted in Vectashield (Vector Laboratories, Cat# H-1000).

For WT1 immunofluorescent staining, slides were deparaffinized, rehydrated and boiled in pH6 10mM sodium citrate buffer containing 0.05% Tween 20 for 20 minutes. The sections were incubated with blocking buffer (5% BSA/ 0.2% Triton X-100/ PBS) for an hour, followed by overnight incubation with primary antibody (anti-Wilm's Tumor 1, Cat# ab89901, abcam) in antibody diluent (5% BSA/0.1% Triton X-100/PBS) at 4°C. The slides were then washed in PBS for 15 minutes and incubated with secondary antibody (Alexa Fluor 568-conjugated goat anti-rabbit antibody, Cat# A-11011, Invitrogen) in

antibody diluent for 1.5 hours at room temperature. After washing off excess secondary antibody, sections were mounted with Vectashield mounting medium supplemented with DAPI (Vector Laboratories, Cat# H-1200).

The fluorescent images were acquired on an inverted epifluorescent microscope (Olympus IX-81 with ZDC, Olympus Scientific Solutions Americas) using 10x air objective (0.3NA, Olympus Scientific Solutions Americas) and equipped with a Hamamatsu Flash 4.0 v1 CMOS camera (Hamamatsu Corporation). The images at higher magnification were collected on an Olympus 3I spinning disk confocal microscope (Olympus IX-81, Olympus Scientific Solutions Americas) using 40x oil objective (1.3NA, Olympus Scientific Solutions Americas) equipped with an Andor Zyla 4.2 CMOS camera (Andor Technology Ltd). Using SlideBook 6.0 (Intelligent Imaging Innovations) a Look-up table (LUT) tool was applied to adjust the images to the same level to facilitate a fair comparison of intensities of fluorescence between images.

Immunocytochemistry staining

For immunocytochemistry staining, the cultured cells were rinsed with warm phosphate-buffered saline (PBS) 3 times and fixed in 4% PFA for 10 minutes at room temperature. The cells were then blocked with blocking buffer (5% normal goat serum/ 0.1% Tween20/ PBS) and incubated with diluted primary antibody (dilution ratios are listed in Supplementary Table 3.1) at 4°C overnight. After being washed in 0.1% Tween20/ PBS, the cells were incubated with the respective secondary antibody diluted in blocking buffer and counterstained with 1μM of DAPI. The cells were mounted in mounting medium (glycerol: PBS=9:1). The immunostaining results were visualized and documented on an inverted epifluorescent microscope (Olympus IX-81 with ZDC, Olympus Scientific Solutions Americas) using 20x air objective (0.3NA, Olympus Scientific Solutions Americas) and Hamamatsu Flash 4.0 v1 CMOS camera (Hamamatsu Corporation). Images at higher magnification were collected on an Olympus 3I spinning disk confocal microscope (Olympus IX-81, Olympus Scientific Solutions Americas) using 40x oil objective (1.3NA, Olympus Scientific Solutions Americas) equipped with an Andor Zyla 4.2 CMOS

camera (Andor Technology Ltd). The LUT of each image was adjusted to the same level using SlideBook 6.0 (Intelligent Imaging Innovations) to facilitate a fair comparison of intensity of fluorescence. Quantification of the number of cells retaining tight cell-to-cell contact was performed by a blinded observer. Images (at least 4 separate fields per biological replicate) were scrambled and presented to an observer for counting the number of tightly contacting epithelial cells. At least 200 cells were counted for primary epicardial cells and 400 cells were counted for MEC1 cells for each biological replicate.

Primary explant culture

The isolation of primary epicardial cells has been performed according to a previously reported protocol (Amy M. Mellgren et al., 2008). In brief, embryonic mouse hearts were collected at E12.5 in Hanks buffered salt solution and incubated on collagen coated iBidi plates (Cat # 80826, iBidi, Martinsried, Germany) in explant medium (DMEM:M199=1:1) supplemented with 10% heat-inactivated FBS. 12 to 15 hr later the hearts were removed to leave a monolayer of primary epicardial cells attached to the plate. The morphology and identity of isolated primary cells has been assessed by immunostaining of the epicardial marker WT1 to confirm their epicardial origin. Only wells with sufficient numbers of attached epicardial cells and no mesenchymal-like cells were used for experiments.

Assessment of EpiMT

Primary epicardial cells isolated from C57BL/6 embryos were cultured with explant medium supplemented with 5% heat-inactivated FBS and 1% antibiotic-antimycotic reagent (Gibco, Cat # 15240062) and pretreated with 2.5μM ALK5 inhibitor (SB431542, Cat # 616461, Calbiochem, San Diego, CA, USA) for 5 hr to synchronize and restore the colony to a minimal level of EpiMT. After the removal of the ALK5 inhibitor, primary epicardial cells were either treated with vehicle (DMSO) vs. 10 nM TTNPB (Sigma, Cat # T3757) for an additional 48 hr or pretreated with vehicle (DMSO) vs. 8μM WIN for 5 hr to inhibit the enzymatic activity of RALDH enzymes. Cells pretreated with vehicle (DMSO) or WIN were then cultured in the presence of 50ng/ml PDGFBB (R&D systems, Cat # 220-BB) to induce EpiMT. Primary cells were cultured with PDGFBB alone or PDGFBB in combination with

8μM of WIN for additional 48 hr and then subjected to immunocytochemistry staining or scratch wound migration assay.

Similar treatments were also applied to the MEC1 epicardial cells. MEC1 cells were cultured with DMEM supplemented with 10% FBS and 1% antibiotic-antimycotic reagent. After being plated in culture chambers, MEC1 cells were pretreated with 2.5μM ALK5 inhibitor (SB431542, Cat # 616461, Calbiochem, San Diego, CA, USA) for up to 24 hr. In the experiment depicted in Fig 3.1, MEC1 cells were pretreated with either vehicle (DMSO) or 8μM WIN for up to 24 hr followed by induction of EpiMT with 50ng/ml PDGFBB (R&D systems, Cat # 220-BB) for an additional 72 hr. Alternatively, in experiments depicted in Fig 3.5 and 3.6 aiming to examine the effect of TTNPB on EpiMT, MEC1 cells were pretreated with 2.5μM ALK5 inhibitor for 24 hr and then stimulated with either vehicle (DMSO) vs. 10 nM TTNPB for additional 72 hr. Cell were examined by scratch wound migration assay or immunocytochemistry staining to assess their migratory capacity and level of EpiMT.

In the case of primary epicardial cells derived from *Dhrs3*$^{+/+}$ and *Dhrs3*$^{-/-}$ mice, these explants were incubated in serum-reduced explant medium supplemented with 1% heat-inactivated FBS to minimize the basal EpiMT process and to allow us to assess their inherent migratory capacity. Following 48 hr incubation in serum-reduced explant medium the migratory capacity of *Dhrs3*$^{+/+}$ and *Dhrs3*$^{-/-}$ primary epicardial cells as assesses by a scratch wound migration assay in conjunction with immunocytochemistry staining.

Scratch wound migration assay

The migratory capacity of primary epicardial cells derived from *Dhrs3*$^{+/+}$ and *Dhrs3*$^{-/-}$ mice or from C57BL/6 mice was assessed by scratch wound migration assay. For this, a scratch was made through the monolayer of epicardial cells to create a cell-free zone. The width of the gap was measured at 0 hrs and 12 hrs after the scratch was made and the percentage of wound closure was calculated to evaluate the migratory capacity of primary epicardial cells. In the case of the MEC1 cell line, the width of the gap was measured every 2 hours after the scratch was created. As in the case of primary epicardial cells, the

migration ability of MEC1 cells was calculated by comparing the percentage of wound closure. Statistical analysis of the results was based on three independent biological replicates per experimental group.

LacZ staining

The embryos or fetal hearts harvested from *RARE-LacZ* reporter mice were isolated at various developmental stages to assess the activity of the LacZ-reporter as per previously described protocols (Billings et al., 2013). The X-gal stained slides were counterstained with eosin Y. The samples in both experimental and control groups were processed simultaneously using identical protocols to avoid artifacts due to staining and the images were documented using a Leica DMS300 Dissection Microscope equipped with a digital camera.

Western blotting

Treated cultures of MEC1 cells were rinsed twice with ice-cold Hank's Balanced Salt Solution (HBSS) and lysed with radioimmunoprecipitation assay buffer (RIPA) buffer composed of 25mM Tris pH 7.6, 150 mM NaCl, 1% NP-40, 1% sodium deoxycholate, 0.1% SDS and containing a protease inhibitor cocktail (cOmplete ULTRA Tablet, Roche; Cat # 05892791001). The cell lysate was sonicated three times on ice. After centrifugation, the protein concentration in the supernatant was quantified by Coomassie Protein Assay Reagent (Thermo scientific, Cat #1856209). Samples were prepared by mixing protein supernatants (10 µg protein per sample) with NuPAGE LDS sample buffer (Invitrogen, Cat # NP0007) and reducing agent (Invitrogen, Cat # NP0004) and heating at 70°C for 10 minutes to denature the proteins. Protein samples were loaded on a 4-12% SDS-PAGE gradient gel (Invitrogen, Cat # NP0321BOX). Protein electrophoresis and transfer to PVDF membranes were performed according to manufacturer's protocol (Invitrogen, CA). Immunoblotting and signal detection was conducted using the WesternBreeze Chemiluminescent Immunodetection System (Novex, Cat # WB7104). The primary antibodies used in western blotting include anti-RND3 (1:1000, ab50316; Abcam) and anti-β-actin (1:4000, sc-47778; Santa Cruz Biotechnology). Alkaline phosphatase- conjugated secondary antibodies include anti-rabbit (Invitrogen, Cat # WP20007) and anti-mouse (Invitrogen, Cat # 46-7006).

RhoA pull-down assay

Affinity purification of RhoA-GTP from the lysates of TTNPB- or DMSO-treated MEC1 cells was performed using the Rho activation assay kit (MD Millipore; Cat #17-294) following manufacturer's protocol. Lysis of TTNPB- or DMSO-treated MEC1 in 125mM HEPES, pH 7.5, 750mM NaCl, 5% Igepal CA-630, 50mM MgCl2, 5mM EDTA and 10% glycerol (Mg^{2+} Lysis/Wash Buffer; Cat # 20-168, EMD Millipore) was performed in the presence of phosphatase inhibitors, 25mM NaF and 1mM orthovanadate, and protease inhibitors, 10µg/ml leupeptin and 10µg/ml aprotinin. The GTP-bound Rho proteins were purified from the lysates using recombinant Rhotekin Rho Binding Domain (RBD) -bound agarose beads. The resulting purified fractions from each treatment were loaded on a 4-12% SDS-PAGE gradient gel (Invitrogen, Cat # NP0323BOX) transferred to PVDF membranes and immunoblotted with anti-RhoA antibody (NewEast Biosciences, Cat # 26007) to detect RhoA-GTP. Non-hydrolyzable GTPγS was used to induce the association and purification of all available Rho protein from the lysate. We confirmed that we used the same amount of starting protein from each of the lysates by immunoblotting of each lysate with anti-actin antibody (SantaCruz Biosciences, Cat # sc-47778).

LC-MS/MS

Embryos were collected at E12.5 or E14.5, snap frozen in liquid nitrogen and stored in -80°C till extraction. The levels of RA were measured using a previously published protocol (Kane, Chen, Sparks, & Napoli, 2005). For E12.5 embryos, RA levels were measured using 4 *Dhrs3*$^{+/+}$, 5 *Dhrs3*$^{+/-}$ and 5 *Dhrs3*$^{-/-}$ embryos. RA levels present in E14.5 embryos WIN-treated embryos were established using 5 embryos for each the DMSO or WIN-treated groups.

Transcriptome analysis

MEC1 cells were treated with vehicle (DMSO) or 10nM TTNPB for 48 hours and total RNA was isolated using TRIZOL reagent according to manufacturer's protocol. RNA was pretreated with DNA-free™ DNA Removal Kit (Invitrogen, Cat # AM1906) before submission for cDNA library assembly.

Image analysis using CellProfiler

All the immunostaining-based images were acquired non-biasedly on the same day under identical conditions (identical microscope and camera; same laser intensity, exposure time and 1x1 Binning mode). Cells were double-labeled with wheat germ-agglutinin (WGA) that marks the cell membrane, and the target protein for measurement and comparison, namely ZO-1. Relative expression of ZO-1 on cell membrane was measured and represented by the relative fluorescent intensity of ZO-1 localized on the cell border marked by WGA. The quantification of membranous expression of ZO-1 was performed by three main steps in CellProfiler: identification of whole cells using whole-cell-stained images (WGA-based), identification of border of each cell (edge of cell membrane) using WGA-based images, and measurements of relative fluorescent intensity of ZO-1 on the edge of cell membrane. Detailed pipeline and module settings are provided in supplementary materials and the identical quantification pipeline was applied non-biasedly to all cases. To be more specific, after whole cell was identified based on WGA staining, intracellular area that was 0.39μm (5 pixel) away from the cell boundary was subtracted and the remaining area (a 0.39μm-wide loop) was defined as the edge of a cell membrane. Mean intensity of ZO-1 fluorescence in this defined membranous region was subsequently quantified and used to compare the relative localization of ZO-1 on cell membrane between different experimental groups.

Statistical analysis

Each experiment contains at least three biological replicates. For assays containing two experimental groups, the statistical analysis was performed using unpaired Student's *t*-test between groups. For tests that contain more than two experimental groups, one way ANOVA was performed followed by post-hoc analysis. The data were represented as means ± standard deviation.

3.3. Results

Inhibition of RA synthesis impairs the response of epicardial cells to PDGFBB

We began our investigation of the role of RA in EpiMT using a well-characterized epicardial cell line, MEC1, derived from the ventricular epicardium of E13.5 embryos of the ICR/CD1 outbred mouse strain (P. Li et al., 2011). When plated at 60-80% confluency and in the absence of EpiMT inducers, the MEC1 cells retained many of the features of resting embryonic epicardial cells. This included the expression of the epicardial markers, WT1 and transcription factor 21 (TCF21, also known as POD-1, or epicardin) (Supplementary Fig 3.1A-B), and the epithelial markers ZO-1 and beta-catenin at their cell border (Fig 3.1A for ZO-1, Supplementary Fig 3.1C for beta-catenin). Uninduced MEC1 cells had a cobblestone epithelial morphology, with tight cell-to-cell contact, and showed minimal formation of stress fibers, and no detectable expression of markers of VSMC differentiation (Supplementary Fig 3.1E and Fig 3.1F). Importantly, MEC1 cells also expressed the dehydrogenase/reductase 3 (DHRS3) (Supplementary Fig 3.1D), an enzyme required for controlling the formation of embryonic RA (Billings et al., 2013). This observation was consistent with the existence of ongoing RA metabolism within MEC1 cells, just as previously described in the case of epicardial cells (J. B. Moss et al., 1998; Niederreither et al., 1997; Xavier-Neto et al., 2000).

PDGFR-signaling is a critical regulator of EpiMT. Epicardial-specific ablation of PDGFRA or PDGFRB, or of both PDGFRA/B, leads to compromised EpiMT and reduced migration of EPDCs into the myocardium (Bax et al., 2010; Amy M. Mellgren et al., 2008; C. Rudat, Norden, Taketo, & Kispert, 2013; C. L. Smith, Baek, Sung, & Tallquist, 2011). Addition of the PDGFRA/PDGFRB ligand, PDGFBB, to epicardial cells induces EpiMT and EPDC differentiation into VSMCs (Lu et al., 2001). Upon addition of PDGFBB at 50ng/ml MEC1 cells efficiently underwent EpiMT-relevant programs including cytoskeletal reorganization, as evidenced by the loss of the expression of the epithelial marker, ZO-1 (Fig 3.1A vs. B) and the formation of smooth muscle α-actin (SMAα)-positive stress fibers (Fig 3.1K vs. L). In order to examine the expression level and the intracellular localization of ZO-1 relative to

the cell membrane, we performed double labeling of ZO-1 and wheat germ agglutinin (WGA), which binds glycoproteins on the cell membrane, on MEC1 cells (Fig 3.1 D-I). Relative expression of ZO-1 on cell membrane was evaluated and represented by the fluorescent intensity of ZO-1 on the cell membrane marked by WGA. Measurement of relative expression of ZO-1 on cell membrane revealed that PDGFBB caused 50% of reduction in ZO-1 immunofluorescence on the cell membrane, shown in Fig 3.1 J, suggesting that PDGFBB can induce the loss of epithelial characteristics.

Due to the critical roles of PDGFR-signaling in EpiMT in embryogenesis and in heart regeneration (Kim et al., 2010), we studied the role of RA-signaling in PDGFBB-induced EpiMT. To test whether RA-signaling is necessary for the process of PDGFBB-induced EpiMT *in vitro*, we blocked RA synthesis in MEC1 cells using WIN18,446 (WIN), a potent bis-dichloroacetyldiamine inhibitor of the enzymes of the aldehyde dehydrogenase 1A family (ALDH1A). The ALDH1A family includes the enzymes ALDH1A1, ALDH1A2, and ALDH1A3, also known as RALDH1, RALDH2 and RALDH3, respectively, RALDH2 being the main RA synthetic enzyme during embryogenesis (Arnold et al., 2015; Niederreither et al., 2001; Paik et al., 2014). Using WIN to treat cells prior to PDGFBB-induction, we found that WIN pretreatment effectively counteracted the morphological changes induced by PDGFBB in MEC1 cells based on ZO-1 staining (Fig 3.1B vs. C, expression levels of ZO-1 on cell membrane was quantified in J). This suggests that production of RA was required for the loss of the epithelial marker caused by PDGFBB. In addition, WIN pretreatment also prevented the accumulation of SMAα-positive stress fibers induced by PDGFBB (Fig 3.1L-M).

Using a scratch wound migration assay, we next assayed the effect of WIN on the migration of PDGFBB-induced MEC1 cells. The level of wound closure was examined every 2 hours over 12 hr period following PDGFBB treatment to estimate the extent of cell migration (Supplementary Fig 3.2 A-F). PDGFBB treatment significantly accelerates the closure of scratch wound when compared with DMSO group, starting from 2 hours post-scratch. In comparison to MEC1 cells stimulated with PDGFBB alone, MEC1 cells treated with PDGFBB+WIN displayed reduction in percentage of wound closure over

time (Supplementary Fig G). To understand the reasons for the slower gap closure in the PDGFBB+WIN group versus the PDGFBB group, we performed Ki67 immunostaining to assess the effect of WIN on the rate of cell proliferation. Quantification of Ki67-positive proliferating cells suggested that WIN did not affect PDGFBB-induced cell proliferation (Supplementary Fig 3.3D). Thus, the reduced migration in response to PDGFBB+WIN versus PDGFBB alone cannot be attributed to reduced proliferation and was most likely caused by a reduced level in cytoskeletal reorganization due to WIN treatment.

To investigate the cause of reduced epicardial cell migration in WIN-treated cells, we next examined the cytoskeletal structure and formation of focal adhesions that are a site of interaction of cells with the extracellular matrix during the process of cell migration (Couchman & Rees, 1979). By phalloidin staining of migrating cells 5 hr after the scratch was made, we observed that PDGFBB alone treatment increased F-actin bundle formation presumably facilitating the formation of stress fibers. In the case of PDGBB-alone treated cells, the stress fibers were aligned with the direction of cell migration, i.e. towards the closure of the wound (Fig 3.1N vs. O). Meanwhile, focal adhesion proteins, which mediate the interaction between cells and the extracellular matrix, accumulated and relocated to the leading edge of the PDGFBB alone treated cells, as visualized by vinculin staining (Fig 3.1Q vs. R). In contrast, MEC1 cells treated with PDGFBB+WIN formed F-actin stress fibers that were disorganized and not aligned with the direction of cell migration (Fig 3.1O vs. P), while vinculin-positive focal adhesions remained diffusely distributed throughout the cell (Fig 3.1R vs. S). Taken together these data suggest that RA is required for reorganization of the cytoskeleton and the loss of epithelial morphology which is necessary to facilitate the process of EpiMT and cell migration.

To confirm that the effects of WIN on EpiMT were due to a reduced level of RA-signaling, we stimulated the PDGFBB+WIN-treated cells with 10 nM TTNPB, a stable pan-RAR agonist (Beard et al., 1995), and we tested whether addition of TTNPB can recover the ability of PDGFBB+WIN-treated MEC1 cells to undergo EpiMT. Immunostaining results demonstrated that addition of TTNPB to PDGFBB+WIN led to reduced expression of ZO-1 at cell border and a loss of cell-to-cell contact

(Supplementary Fig 3.4A-D), and a similar restoration of the formation of stress fibers (Supplementary Fig 3.4E-H). This was indicative of a higher level of cytoskeletal reorganization in MEC1 cells treated with TTNPB in addition to PDGFBB+WIN when compared to cells treated with PDGFBB+WIN. Therefore, while WIN prevented the response of MEC1 cells to PDGFBB, the addition of TTNPB restored the response of WIN-pretreated MEC1 cells to PDGFBB suggesting that the effects of WIN were indeed caused by a reduction in the levels of RA-signaling.

The interference of WIN treatment with the PDGFBB-induced response of MEC1 cells could also be observed by examining the expression of genes involved in RA-signaling and EpiMT (Fig 3.1T). First, qRT-PCR analysis using mRNA isolated from MEC1 cells treated with PDGFBB alone or PDGFBB+WIN demonstrated that WIN treatment reduced RA-signaling by down-regulation of the direct RAR target, *Rarb*. Secondly, cells treated with PDGFBB and WIN had a higher expression level of the epithelial marker *Cdh1* than MEC1 cells treated with PDGFBB alone. WIN-pretreatment also led to a reduced level of the canonical Wnt target, *Axin2*, which was proposed to be involved in EpiMT (von Gise et al., 2011), Taken together, our data suggest that RA-signaling is critical and indispensable for the loss of epithelial characteristics and the process of cytoskeletal reorganization during EpiMT.

We next examined whether the effects of reduced RA signaling on PDGFBB-induced EpiMT observed in MEC1 cells are relevant to the EpiMT of primary epicardial cultured cells. Primary epicardial cells isolated from E12.5 C57BL/6 embryos and treated with PDGFBB at 50 ng/ml exhibited a reduction in surface expression of the epithelial marker ZO-1, together with formation of stress fibers as visualized via phalloidin staining (Supplementary Fig 3.5A, C). As in the case of the MEC1 cell model, we pretreated primary epicardial cells with WIN to block RA synthesis and modulate RA-signaling. In comparison to treatment with PDGFBB-alone, PDGFBB+WIN treatment led to preservation of the epithelial characteristics of primary epicardial cells. This included a cobblestone-like morphology with evident cell-to-cell contact, maintenance of ZO-1 expression at the cell border, together with minimal accumulation of stress fibers (Supplementary Fig 3.5A-D). Based on ZO-1 staining the WIN-pretreated

group had a 45-fold higher percentage of epithelial-like cell, maintaining tight cell-to-cell contact than the cells treated solely with PDGFBB (Supplementary Fig 3.5G). In addition, we also observed that PDGFBB+WIN treatment resulted in reduced formation of SMAα-positive stress fibers in primary epicardial cells (Supplementary Fig 3.5E *vs*. F) when compared to PDGFBB-treated controls. Consistent with the reduced formation of stress fibers, we found that primary epicardial cells treated with PDGFBB+WIN exhibited an 80% reduction in their ability to close a wound when compared to PDGFBB alone group (Supplementary Fig 3.5H). Thus, our data derived from primary epicardial explants corroborate our findings using MEC1 cells, in that inhibition of RA synthesis attenuated the EpiMT of primary epicardial cells in response to PDGFBB.

EpiMT and differentiation can also be induced using tumor-derived transforming growth factor-β2 (TGFβ2) (Austin, Compton, Love, Brown, & Barnett, 2008). Therefore, we examined whether WIN pretreatment affected the reorganization of the cytoskeleton and differentiation of MEC1 cells in response to TGFβ2. MEC1 cells treated with WIN and TGFβ2 resembled MEC1 cells treated with TGFβ2 alone in terms of both the loss of ZO-1 surface expression (Supplementary Fig 3.6A-G) and the expression of stress fiber actin SMAα (Supplementary Fig 3.6H-N). Hence, RA synthesis is required for the reorganization of the cytoskeleton induced by PDGFBB, but not by TGFβ2.

Both deficiency and excess of RA affect the migration of EPDCs *in vivo*

Given that, *in vitro*, a reduction in RA-signaling prevented the cytoskeletal reorganization and migration of EPDCs, we decided to examine the effects of altered RA-signaling on the formation and migration of the EPDCs derived by EpiMT *in vivo*.

To dissect the role of RA-signaling in epicardial cell behavior, we employed models of altered RA-signaling in which epicardial-dependent cardiogenesis was affected. We initially used *in vivo* pharmacological treatment with WIN to block RA synthesis during mid-gestation. When administered early in pregnancy in rats WIN exposure causes various cardiac malformations and early embryonic lethality (Oster, Salgo, & Taleporos, 1974), however, if administered to rats at mid-gestation, WIN

treatment consistently results in coronary vascular defects (Hanato et al., 2011; Nishijima et al., 2000). It is important to note that neither the mechanism by which WIN causes congenital heart defects, nor the relationship of the WIN-caused heart defects and RA signaling are currently known.

We empirically determined the optimal course of WIN-treatment necessary to result in alterations in RA levels and RA-signaling without causing the aforementioned WIN-associated early embryonic death (Oster et al., 1974). By direct measurement of embryonic RA levels by LC-MS/MS, we established that daily treatment of pregnant dams with 51.6 mg/kg body weight of WIN from E9.5 to E13.5 led to a 60% reduction in RA at E14.5 (Fig 3.2A). Using the same WIN-treatment of pregnant *RARE-LacZ* reporter mice we found that the reduced levels of embryonic RA were associated with a decrease in the extent of RARE-reporter activity, hence, RA-signaling, in the heart of WIN-treated embryos at E14.5 relative to vehicle-treated controls (Fig 3.2B, C). Consistent with this finding, the transcription of the direct RAR target, *Rarb*, was found to be down-regulated in the E14.5 fetal hearts in the WIN-treated group compared to controls (Fig 3.2D). Importantly, delaying WIN treatment till E9.5 allowed the embryos to survive to midgestation. Thus, we confirmed that daily WIN treatment from E9.5 to E13.5 embryonic led to reduced embryonic RA synthesis and concomitantly reduced RA-signaling in the heart of WIN-treated embryos without causing death or any noticeable abnormalities associated with heart tube elongation, looping and chamber formation which could confound our analysis. Further reductions in WIN dosage or less frequent treatment schedules did not result in any noticeable inhibition of RA-signaling in the heart, while, in contrast, an earlier time course or a higher dosage led to embryonic death and resorption of fetuses before E14.5.

Next, we examined the biological consequences of the late onset RA deficiency mediated by WIN treatment on the migration of EPDCs. We first immunostained EPDCs using the classic epicardial marker WT1. Staining of WT1 in DMSO- and WIN-treated embryos demonstrated that at E14.5 inhibition of RA synthesis in the heart restricted most WT1-expressing cells to the surface of the heart, suggesting an attenuated migration of epicardial cells in WIN-treated group (Fig 3.2E *vs.* F). Quantification of the

density of WT1-positive EPDCs that are localized away from the surface of the heart suggested that WIN treatment resulted in a 44% reduction in the density of intramyocardial EPDCs (Fig 3.2G). We further utilized another set of epicardial markers PDGFRA and PDGFRB for visualization of EPDCs. Though, PDGFRA and PDGFRB are both expressed in embryonic epicardial cells, they mark distinct populations of EPDCs which employ a different timeframe for EpiMT and migration in the myocardium (Amy M. Mellgren et al., 2008; C. L. Smith et al., 2011). PDGFRB-positive EPDCs, which constitute the "first wave of migrating EPDCs", leave the epicardium at E13.5 and differentiate into VSMCs and pericytes. PDGFRA-positive EPDCs migrate as the "second wave of EPDCs" at E14.5 and contribute to the coronary and interstitial fibroblast populations (C. Rudat et al., 2013; C. L. Smith et al., 2011). We observed that by E14.5, PDGFRA-positive cells in the vehicle-treated embryos had migrated into the myocardium, whereas in the WIN-treated group PDGFRA-positive cells remained confined to the epicardial epithelium and subepicardial space (Fig 3.2H vs. I). Number of PDGFRA-positive EPDCs per mm^2 in the heart was measured and embryos treated with WIN display a 50% reduction in the density of PDGFRA-positive EPDCs in the myocardium (Fig 3.2J). A similar WIN-caused delay was also observed in the case of the myocardial invasion by the PDGFRB-positive EPDCs (not shown). We evaluated the expression of *Pdgfra* and *Pdgfrb* in the hearts of WIN- or vehicle-treated embryos by qRT-PCR and we found no significant changes in the expression of these markers. Although, we cannot rule out variations in the expression of these markers amongst individual cells, these results suggest that while the localization of PDGFRA and PDGFRB-positive EPDC was affected by WIN treatment, the overall expression of these markers in the embryonic heart remained the same.

The above findings suggest that RA deficiency impairs the migration of EPDCs *in vivo*. As RA-signaling is equally sensitive to both excess or deficiency of RA, we hypothesized that RA excess would also affect the development of EPDCs. To test this idea, we employed a genetic mouse model deficient in DHRS3, which maintains RA homeostasis by converting the RA precursor retinaldehyde, to retinol (Adams et al., 2014; Billings et al., 2013; Feng et al., 2010; R. K. Kam et al., 2013). As previously

described by our lab, *Dhrs3*-deficient embryos accumulate excess RA at E14.5 and display altered and expanded RA-signaling domains in conjunction with cardiac and skeletal malformations and embryonic lethality ((Billings et al., 2013) and Chapter 2). By examining *Dhrs3*$^{-/-}$ embryos at earlier stages of development, we discovered that genetic ablation of leads to the elevated levels of RA earlier than we had previously reported. By measuring the amount of global embryonic RA via LC-MS/MS we found that deletion of *Dhrs3* led to an increase of 33% in the levels of RA in E12.5 *Dhrs3*$^{-/-}$ embryos when compared to their wild type littermates (Fig 3.3A). Next, using *Dhrs3*$^{+/-}$ mice crossed with the *RARE-LacZ* reporter mouse strain, we found that *Dhrs3*-ablation led to increased RA-signaling based on *RARE*-driven reporter activity as early as E10.5 (Fig 3.3B, and (Shannon, Moise, & Trainor, 2017)) as the heart becomes invested in epicardium. Thus, these data suggest that genetic deletion of *Dhrs3* leads to consistent increases in RA-signaling during the late development of the heart.

We next examined the effect of the increased levels of embryonic RA on the development of epicardial derived structures in *Dhrs3*$^{-/-}$ embryos. As reported previously, *Dhrs3*$^{-/-}$ embryos display mid- to late-gestational lethality accompanied by multiple severe malformations, such as double-outlet right ventricle, and ventricular and atrial septal defects, (Billings et al., 2013). In addition, *Dhrs3*$^{-/-}$ embryos display subcutaneous edema, indicative of cardiac dysfunction, a thin myocardial compact zone and malformations of the coronary vasculature (Chapter 4). By examining the expression and localization of EPDCs in *Dhrs3*$^{-/-}$ embryos, we observed that RA excess affected the migration of EPDCs into the myocardium. Immunostaining of the epicardial marker WT1 in embryonic hearts revealed that *Dhrs3*$^{-/-}$ hearts display 2-fold increase in the density of EPDCs that localized away from the surface of the heart, i.e. the epithelial layer of epicardium, suggesting that the delamination of WT1-positive EPDCs was accelerated by excessive RA signaling in the *Dhrs3*$^{-/-}$ hearts. Moreover, we observed that cells from another epicardial population marked by expression of PDGFRA, localized deeper in the myocardium of *Dhrs3*$^{-/-}$ hearts in comparison to those of littermate controls (Fig 3.3H vs. I, quantified in J) suggesting that excess RA present in *Dhrs3*$^{-/-}$ hearts altered the migration ability and/or timing of the invasion of

PDGFRA-positive cells. By examining the expression of epithelial markers in the embryonic hearts, we found that the classic epithelial marker *Cdh1* was down-regulated by 97% in E13.5 *Dhrs3*$^{-/-}$ hearts compared to the hearts of *Dhrs3*$^{+/+}$ littermates (Fig 3.3D), implying a higher level of EMT in *Dhrs3*$^{-/-}$ embryos. Predictably, the expression of genes which are direct targets of RAR, namely, *Rarb* and *Cyp26a1*, were found to be up-regulated by 1.7 and 2.6-fold respectively in the *Dhrs3*$^{-/-}$ hearts compared to controls. These results suggest that EPDCs undergo a higher level of EpiMT in response to excess RA in *Dhrs3*$^{-/-}$ embryos.

Excess RA augments the cytoskeletal rearrangement of EPDCs

To better understand the effect of excess RA on epicardial cells, we isolated primary epicardial cells from *Dhrs3*$^{-/-}$ and *Dhrs3*$^{+/+}$ embryos. Epicardial cells isolated from *Dhrs3*$^{+/+}$ control embryos appeared to have a cobblestone-like epithelial morphology. In contrast, even in the absence of PDGFBB, epicardial cells isolated from the *Dhrs3*$^{-/-}$ embryos displayed spindle-like mesenchymal morphology particularly at the border of the explant (Supplementary Fig 3.7A vs. B). Cell membrane was stained by WGA and the double labeling of ZO-1 and WGA on EPDCs revealed that the epithelial marker ZO-1 was not localized on the cell membrane but internalized in *Dhrs3*$^{-/-}$ EPDCs (Fig 3.4 A-C *vs*. E-G). The relative expression of ZO-1 on cell membrane was quantified in Fig 3.4 I and *Dhrs3*$^{-/-}$ EPDCs displayed a 65% reduction in the levels of ZO-1 that was localized on the cell membrane, when compared to the wildtype control. Formation of filopodia and gaps between cells was readily seen in Fig 3.4F marked by arrowheads. Similar internalization was observed in the expression of beta-catenin in *Dhrs3*$^{-/-}$ EPDCs (Fig 3.4D *vs*. H). These results suggested that the lack of *Dhrs3* caused acceleration in cytoskeletal rearrangement in epicardial cells *in vitro* (Fig 3.4A-H). In addition, as evaluated by a scratch wound migration assay, *Dhrs3*$^{-/-}$ epicardial cells closed the wound faster than primary epicardial cells isolated from *Dhrs3*$^{+/+}$ controls (Fig 3.4J). Collectively, our data suggest that the loss of *Dhrs3* leads to accumulation of RA and a higher rate of cytoskeletal reorganization.

By manipulating the production of RA via genetic or pharmacological approaches we found that RA-

signaling affected the migration of EPDCs *in vivo*. To obtain a better mechanistic understanding of the role of RA in EpiMT, we investigated whether RA directly facilitates EpiMT by treating MEC1 cells with the pan-RAR agonist TTNPB. Using moderate levels of TTNPB approaching the physiological levels observed in the case of the endogenous RAR agonist, all-*trans*-retinoic acid (Billings et al., 2013), we found that 10 nM TTNPB treatment led to the increased expression of several genes known to be up-regulated by RAR, including *Dhrs3*, *Cyp26a1* and *Rarb*, and down-regulation of the expression of the RA synthetic enzyme, *Raldh2*, in accordance with the known negative feedback regulation of RA metabolism (Supplementary Fig 3.8A). Consistent with its increased transcription in the TTNPB-treated group, the level of DHRS3 protein was also found to be up-regulated (Supplementary Fig 3.8B-C). These results demonstrated that 10 nM TTNPB was able to activate RA-signaling in MEC1 cells.

We next tested whether activation of RAR by 10 nM TTNPB could lead to the cytoskeletal reorganization in MEC1 cells. Through immunostaining for the cell junction marker proteins ZO-1 in combination with membrane marker WGA, we observed that TTNPB treatment resulted in their internalization and loss of cell-to-cell contact (Fig 3.5A vs. G for ZO-1 and B-C vs. H-I for WGA; filopodia are marked with arrowheds). Expression of beta-catenin on cell border was also found to be diminished by TTNPB (Fig D vs. J). Moreover, activation of RA-signaling by TTNPB actively regulates the cytoskeleton evidence by accumulation of F-actin (Fig 3.5E vs. K) as well as the increased acquisition of SMAα-positive stress fibers (Fig 3.5F vs. L). Comparison of relative expression of ZO-1 on cell membrane between DMSO and TTNPB groups showed that TTNPB treatment significantly reduced the localization of ZO-1 on cellular domains on and adjacent to the cell membrane (Fig 3.5M). Besides morphological changes, we also found that activation of RAR resulted in down-regulation of the epithelial markers *Cdh1*, *Krt17* and *Ppl*, and upregulation of the mesenchymal marker *N-cadherin* and the EpiMT positive regulator *Axin2* (Fig 3.5N). Increased RA-signaling was also associated with induction of the VSMC marker *Sm22α*. Thus, activation of RA-signaling in MEC1 triggers events associated with EpiMT in MEC1 cells including repressed epithelial characteristics while concomitantly promoting

cytoskeletal reorganization and acquisition of VSMC markers.

To better characterize the effect of TTNPB treatment on epicardial cells we examined primary epicardial cells isolated from the *RARE-LacZ* mouse embryos that were treated with TTNPB. We observed that 10nM TTNPB enhanced the expression of *RARE*-driven *LacZ* reporter gene in primary epicardial cells (Supplementary Fig 3.9G-I), which was indicative of RA signaling activation. Consequently, the number of epithelial-like cells which maintained tight cell-to-cell contact was reduced by 49% (Supplementary Fig 3.9H) and the area occupied by such epithelial-like cells was reduced by 52% (Supplementary Fig 3.9A *vs*. D, quantified in J) in TTNPB-treated cultures compared to the vehicle control group. In addition to reduced number of epithelial cells, epicardial cells treated with TTNPB also displayed evident reduction in the expression levels of ZO-1 and beta-catenin throughout the culture including the epithelial zone (Supplementary Fig 3.9B *vs*. E for ZO-1 staining; Supplementary Fig 3.9C *vs.* F for beta-catenin). Collectively, our results suggest that activation of RA-signaling facilitates cytoskeletal rearrangement *in vitro* in both primary epicardial cells and MEC1 cells.

RA promotes cytoskeletal rearrangement of EPDCs via the RhoA-ROCK pathway

Using TTNPB to induce cytoskeletal reorganization in MEC1 cells, we surveyed the effects of TTNPB on pathways that govern EpiMT. To globally assess the changes in gene expression elicited by TTNPB treatment, we performed transcriptome profiling of MEC1 cells stimulated with TTNPB compared with cells stimulated with vehicle alone (Fig 3.6A). This analysis revealed that RA-signaling affects a multitude of pathways in MEC1 cells including many previously implicated in the EpiMT and differentiation of EPDCs, such as cell cycle, focal adhesion, Hippo-signaling, and RAP1-signaling (Artamonov et al., 2015; Singh et al., 2016).

Focusing on pathways that control cytoskeletal rearrangement, we identified several regulatory proteins that participate in the RhoA-Rho kinase (ROCK) pathway and whose expression was found to be significantly affected by TTNPB treatment. The Rho family of GTPases are primarily controlled through GTPase exchange factors (GEFs) or GTP activating proteins (GAPs) which activate or antagonize RhoA,

respectively. In addition to RhoA, Rac and Cdc42, there are also atypical Rho family members, such as Rnd1 and Rnd3, which are constitutively GTP bound and which inhibit RhoA-ROCK signaling (reviewed in (Riento, Villalonga, Garg, & Ridley, 2005)). Importantly, the Rho pathway has been shown to be a regulator of EpiMT (Lu et al., 2001). As summarized in the diagram depicted in Fig 3.6B, TTNPB-treatment of MEC1 cells led to the up-regulation of the expression of genes coding for Rho-effectors such as, *cofilin*, *kalirin*, *Limk2*, *Mlck1* and *3*, *Rhoc*, *Rock2*, *Arhgef2* and *Arhgef28*, or down-regulation of those coding for Rho-inhibitors such as, *Arhgap11a*, *Arhgap19*, *Arhgap31*, and *Rnd 2* and *3*. For a few selected members of the Rho pathway, we validated the findings derived from gene expression profiling by qRT-PCR and/or immunoblotting and immunocytochemistry. Our results suggest that TTNPB treatment led to up-regulation of the expression of the central Rho-effector ROCK2 and suppresses the expression of the ROCK inhibitor, RND3 (Fig 3.6C). The decreased expression of RND3 in response to TTNPB was also observed by immunoblotting and immunocytochemistry of TTNPB- or vehicle treated MEC1 cells (Fig 3.6D; Supplementary Fig 3.10). Therefore, our results suggest that one of the mechanisms by which RA-signaling modulates cytoskeletal reorganization and EpiMT involves activation of the Rho pathway through transcriptionally regulation of the expression of critical Rho regulatory proteins.

To further investigate the involvement of the Rho pathway in the RA-mediated cytoskeletal reorganization of epicardial cells, we first determined the effect of TTNPB treatment on the formation of active GTP-bound RhoA. The levels of RhoA-GTP formed in TTNPB- versus DMSO-treated cells were determined by affinity purification of Rho-GTP using agarose beads coupled to the Rhotekin-RBD and by immunoblotting of the purified fractions with anti-RhoA antibody. Our results suggest that TTNPB induces the binding of GTP to RhoA and hence the activation of RhoA signaling pathway (Fig 3.6E). To explore the necessity of the active RhoA-ROCK pathway in RA-induced morphological changes in MEC1 epicardial cells, we tested whether a selective p160ROCK inhibitor, Y-27632, would interfere with the morphological changes induced by TTNPB. Through immunostaining of ZO-1 and beta-catenin, we observed that Y-27632 prevented the cytoskeletal reorganization induced by TTNPB and restored the

expression of epithelial markers at the cell junctions (Fig 3.6G-O, relative expression of ZO-1 on cell membrane was quantified in F). We also observed that activation of RA-signaling no longer induced the expression of SMAα-positive stress fibers in the presence of the ROCK inhibitor (Fig 3.6P-R), suggesting that ROCK plays a critical role downstream of RA-signaling in promoting cytoskeletal reorganization and the loss of epithelial characters in MEC1 cells. Altogether, our results suggest that the RhoA-ROCK pathway is activated by RA and that its activation is required for the RA-induced morphological changes in MEC1 cells.

Analysis of transcriptomic changes in MEC1 cells in response to activated RA signaling

Our RNAseq analysis revealed that activation of RA signaling leads to broad and vast alternation in gene expression pattern in MEC1 cells (Fig 3.6A). In summary, 3493 genes were found to be down-regulated while 3438 up-regulated by 48hr TTNPB treatment (Fig 3.7A), amongst which multiple gene pathways were concluded by KEGG analysis and noticed to be evidently altered in response to elevated RA signaling. Both GO term (Fig 3.6A) and KEGG pathway analysis (Fig 3.7B) identified that Hippo pathway was found to be activated, evidenced by the transcriptional induction of key components of Hippo pathway, for example Mst1/2, Lats1/2 and Yap/Taz, as well as up-regulation of multiple known downstream target genes of Hippo pathway, including Ctgf and Smad genes. Moreover, genes that are known to retain Yap/Taz from the nucleus were suppressed by the activated RA signaling, such as 14-3-3 and α-Catenin. An overview of all the affected genes involved in Hippo pathway demonstrated that the transcription of many Hippo effectors and/or regulators was found to be changed in the TTNPB-treated group, suggesting an interesting interaction of Hippo pathway with RA signaling (Fig 3.7C, altered genes are listed in Supplementary Table 3.3). Besides the Hippo pathway, another developmentally important pathway, the serum response factor (SRF) signaling, has been observed to be broadly initiated by the activation of RAR in MEC1 cells (Fig 3.7D). SRFs have been known to work with other nuclear receptors and function as co-regulator to mediate multiple developmental processes including the epiMT as well as the coronary vessel formation; its function depends on the specific transcription factor that

SRFs interact with. Additionally, we have observed that the multiple key metalloproteases (MMPs), which digest the extracellular matrix to prime the microenvironment for mesenchymal-like cells to migrate and thus facilitate EMT, were detected to be significantly up-regulated by the activation of RA signaling (Fig 3.7E), which cooperates with the ongoing cytoskeletal reorganization orchestrated by RA to accelerate the gain of migratory capacity of epicardial cells. Last but not the least, our results from RNAseq revealed that, instead of promoting epicardial cell differentiation to both VSMCs and fibroblasts, RA signaling interestingly favors VSMC differentiation and suppresses the development of mature fibroblasts (Fig 3.7F). Collagen production, which is a hallmark of fibroblast, was found to be significantly down-regulated by the activation of RA signaling, while the expression of every established marker for mature VSMCs was detected to be drastically induced. The imbalance between VSMC and fibroblast differentiation could possibly leads to alterations in heart functionality as well as coronary vessel formation in embryos experiencing excess or deficiency of RA, thus may provide clue of the teratogenic effects of altered RA signaling in the heart maturation.

3.4. Discussion

In findings presented here, we demonstrate that RAR activation plays an important role in the development and migration of EPDCs. Our results derived from *in vitro* models of RA deficiency suggest that proper synthesis of RA in the epicardium is required for the morphological changes associated with the process of EpiMT. Conversely, RA excess induces the down-regulation of epithelial markers and reorganizes cytoskeletal actin to potentiate the migration of epicardial cells. Our conclusions were substantiated by data derived from *in vivo* models. In *Dhrs3*$^{-/-}$ mouse embryos, a model of RA excess (Billings et al., 2013), PDGFRA-positive EPDCs penetrate deeper into the myocardium than in wild-type controls. When cultured *in vitro*, primary *Dhrs3*-deficient EPDCs also manifest a higher intrinsic rate in cytoskeletal remodeling and enhanced migration capacity. The opposite is seen in the case of WIN-treated embryos, a model of RA deficiency, where PDGFRA-positive EPDCs remain close to the epicardium. Finally, through transcriptome profiling we found that RAR activation leads to changes in the

expression of factors that control the RhoA-ROCK pathway, the activation of which mediates the effects of RA on epicardial cells. In conclusion, our findings suggest that RA-signaling is critical for the EpiMT and the migration of EPDCs during mouse heart development.

Epicardial RA plays a critical role in the cytoskeletal reorganization of EPDCs

Our results provide evidence that the EpiMT is influenced by epicardium mediated RA-signaling. Since our results are based on isolated explants, this role could be attributed to the local production of RA by the epicardium. But even though it seems plausible that RA mediates the initial events of EpiMT via a cell-autonomous signaling mechanism, it is likely that the migration and differentiation of EPDCs is mediated by a non-cell autonomous RA-signaling from the undifferentiated epithelial epicardium. This mode of signaling can be invoked based on the well-established fact that epicardial cells cease to express RALDH2 after having undergone EpiMT and differentiation (J. M. Perez-Pomares et al., 2002). In this case, RA produced by the undifferentiated epicardium would promote the migration of EPDCs to distance themselves from the epicardial layer before settling in the myocardium or being recruited by vessels to differentiate into fibroblasts and VSMCs, as previously proposed by Azambuja *et al.* and Braitsch *et al.* (Azambuja et al., 2010; Caitlin M. Braitsch et al., 2012).

Cytoskeletal remodeling is a critical step in EpiMT, providing a scaffold of extending protrusions and creating the mechanical force needed to facilitate the movement of cells. Our results suggest that inhibition of the synthesis of RA abolishes the bundle aggregation of F-actin, proper alignment of focal adhesion actin and the formation of filopodia in transitioning EPDCs whereas activation of RA-signaling facilitates the accumulation of F-actin and the formation of stress fibers. Similar effects on cytoskeletal remodeling have been observed in neurons where RA-signaling stimulated dendritic protrusions (N. Chen & Napoli, 2008). The EpiMT-promoting role of RA described here is supported by the previous observation that supplementation with RA can partially correct the EpiMT defect caused by epicardial-specific ablation of WT1 (von Gise et al., 2011) and by the observation that epicardial-specific RXRα-ablation impairs EpiMT (Merki et al., 2005).

EpiMT is necessary for the subsequent differentiation of EPDCs into VSMCs and fibroblasts. In both mouse primary epicardial cells and the mouse epicardial cell line MEC1, we observed that RA-signaling not only promoted EpiMT but also to higher expression of VSMC markers. Depending on the precursor cells involved, RA-signaling has been associated with either induction of repression of SMC marker expression (F. Chen et al., 2014; Manabe & Owens, 2001). In the case of avian epicardial and proepicardial cells, RA was reported to block their differentiation into VSMCs by activating TCF21 (Azambuja et al., 2010; Caitlin M. Braitsch et al., 2012). Indeed, we also observed up-regulation of the expression of TCF21 in the TTNPB-treated MEC1 cells, yet, this was accompanied by an increased expression of multiple VSMC markers based on both their transcript and protein levels. Since, we did not observe an increase in the expression of mature VSMC markers in response to higher levels of RA *in vivo* in *Dhrs3*$^{-/-}$ embryos, we propose that the differentiation-promoting effects of RA observed in our *in vitro* studies should still be interpreted with caution. Further analyses of vessel-mural cell communication and/or recruitment are required to achieve a better understanding of the mechanisms by which RA regulates VSMC differentiation *in vivo*. Nevertheless, both our *in vitro* and *in vivo* data argue strongly that epicardial-derived RA is required for EpiMT through promoting the cytoskeletal reorganization of EPDCs.

RA mediates epicardial cytoskeletal reorganization via RhoA-ROCK

Findings presented here suggest that RA-mediated cytoskeletal rearrangement of epicardial cells requires activation of the Rho pathway (Fig 3.6). Rho family small GTPases, including Rho, modulate actin filaments in the cytoskeleton, cell contractility, and polarity to facilitate cell movement (Amano et al., 1997). Specifically, the RhoA pathway has been implicated in EpiMT as it is induced by PDGFBB (Kim et al., 2010; Lu et al., 2001). Results from our *in vitro* model suggest that RA-signaling activates the Rho pathway, and that this pathway is required for the morphological changes induced by RA in epicardial cells. Amongst the RA-responsive genes in epicardial cells, we identified several critical Rho pathway factors, namely ROCK2 and RND3, both of which been implicated in the Rho-signaling

pathways that drive EpiMT (Artamonov et al., 2015). Notably, ChIP-sequencing studies have identified direct binding of RAR to RA-response elements (RARE), within the promoters of *Rock2*, *Rnd3* and other Rho effectors, implicating the Rho-signaling pathway as a direct target of RAR (Delacroix et al., 2010; E. Moutier et al., 2012) and suggesting a potential mechanism for the effect of RA-signaling on EpiMT.

Experimental models to study the role of RA in late heart development

The approaches described here are relevant in understanding the roles of RA-signaling in the development of the EPDCs, a role which, thus far, has been difficult to discern. The reason for this is that many of the existing mouse models deficient in enzymes involved in RA synthesis or breakdown either manifest early lethality (S. Abu-Abed et al., 2001; K. Niederreither et al., 1999), precluding the analysis of the effect of RA on late heart development or have no discernible cardiac defects as a result of redundant enzyme activities or tissue specificity of the enzymes involved (reviewed in (Metzler & Sandell, 2016)).

By employing the previously described *Dhrs3*$^{-/-}$ mouse, a model of modest RA excess which exhibits globally altered RA-signaling in most tissues including the heart (Fig 3.3 and (Billings et al., 2013)), we could obtain *Dhrs3*-null embryos surviving to late gestation. This allowed us to examine the effects of RA excess on late events in heart development. Conversely, by taking advantage of a well characterized inhibitor of RALDH2, we could observe the effects of RA deficiency on late stages of cardiogenesis. As previously shown in the case of WIN-exposed rat embryos (Hanato et al., 2011), WIN-treatment causes coronary vascular defects associated with a reduction in the migration and differentiation of EPDCs. Although, the reasons for impaired myocardial infiltration of EPDCs in WIN-treated rats was not understood, our data presented here suggest that WIN-treatment results in reduced RA-signaling causing deficits in EpiMT and ensuing differentiation of EPDCs.

An important precaution in the use of any RA-treated or genetic model of RA excess or deficiency is that it should always include a careful evaluation of the levels of retinoids and RA-signaling patterns in the particular model. In both mice and zebrafish, RA-supplementation or enhanced RA-signaling can

paradoxically lead to RA deficiency and loss of RA-signaling through excessive negative feedback (Lee et al., 2012; A. Rydeen et al., 2015). To confirm that the WIN-treated and *Dhrs3*$^{-/-}$ embryos represent models of embryonic RA deficiency or excess, respectively, we directly examined the levels of RA and the patterns of RA-signaling. Additionally, by correcting the EpiMT defect induced by WIN-treatment through provision of an RAR agonist, we causally implicated reduced RA signaling in the effects of WIN on EPDCs.

Role of EPDC derived cell lineages in embryonic development and in the adult heart

EpiMT is necessary for the development of EPDC-derived cell lineages which include the pericytes and VSMCs that stabilize the coronary vasculature and the cardiac fibroblast population. The data presented here suggest that RA produced by the epicardium acts to promote reorganization of epicardial cytoskeleton and the migration of EPDCs deep into the myocardium. In addition to the altered behavior of EPDCs exposed to sub- or supraoptimal levels of RA, both WIN-treated and *Dhrs3*$^{-/-}$ mouse models exhibit defects in coronary vascular development ((Hanato et al., 2011; Nishijima et al., 2000) and Wang *et al.* manuscript in preparation).

The adult epicardium is an important tissue in mediating the wound repair and regeneration following cardiac injury (reviewed in (Kennedy-Lydon & Rosenthal, 2015)). In zebrafish, which have a remarkable cardiac regenerative capacity, the epicardium is critical in mediating the regeneration of the heart relying on PDGF and RA-signaling to do so (K. Kikuchi et al., 2011; Kim et al., 2010). With the exception of neonates, postnatal mammalian hearts have a very modest regenerative response following cardiac injury, yet, even in this case, epicardial RA-signaling may play a key role in the post-ischemic remodeling and repair (D. Bilbija et al., 2012). Though wound repair is an important component of heart regeneration, it can lead to unchecked collagen deposition/fibrosis and scar formation (Fang et al., 2016; Tallquist & Molkentin, 2017). Importantly, the expression of RALDH2 in the epicardium is controlled by C/EBP and inhibition of C/EBP leads to an improvement in cardiac function following ischemia reperfusion (G. N. Huang et al., 2012). Given the evidence supporting a role for RA-signaling in regulating the

development, migration and differentiation of embryonic EPDCs, an important future area of investigation should be to examine the role of RA-signaling in the function of adult EPDCs and to use of knowledge to promote repair of the heart and/or reduce scar formation following injury.

FIGURES

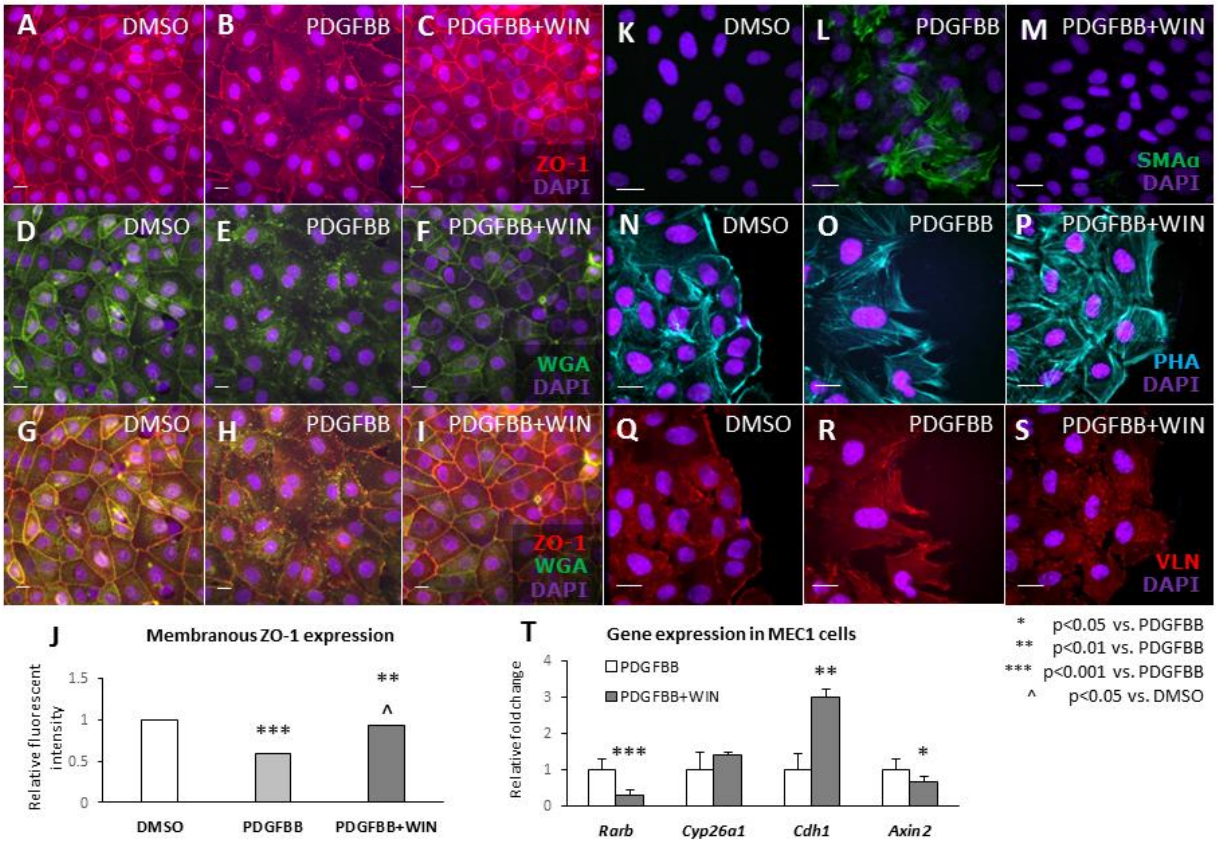

Figure 3.1 RA is required for the PDGFBB-cytoskeletal reorganization of MEC1 epicardial cells.

Treatment with PDGFBB induced loss of expression of the epithelial marker ZO-1 (**A-B**) and enhanced the expression of stress fiber actin SMAα (**K-M**) in cultured MEC1 cells. Cotreatment of PDGFBB and WIN (**PDGFBB+WIN**) reverted the changes induced by PDGFBB alone (**PDGFBB**) (**A-C** for ZO-1, **K-M** for SMAα). The relative expression of ZO-1 on cell membrane marked by WGA (**D-F**) was quantified in **J**, being normalized to the percent of contacting cells in DMSO control-treated cells. Compared to DMSO, PDGFBB treatment of MEC1 cells robustly induced the polymerization and fiber bundle formation of F-actin as shown by phalloidin immunostaining (**N** *vs*. **O**), and vinculin-positive focal adhesion (**Q** *vs*. **R**). Actin fibers and vinculin-positive adhesion bundles were aligned in the direction of cell migration in the PDGFBB-treated cells but displayed a more random distribution in cells

treated with PDGFBB+WIN (phalloidin in **O** *vs*. **P**; vinculin in **R** *vs*. **S**). Combination treatment of MEC1 cells with PDGFBB+WIN led to decreased expression of the RAR-target gene *Rarb* and the positive regulator of EpiMT *Axin2* and a higher expression level of the epithelial marker *Cdh1* in comparison with MEC1 cells treated with PDGFBB alone, as assessed by qRT-PCR (**T**). Scale bars are 50μm in K-P and 20μm in A-I and Q-S. * $p<0.05$ vs. PDGFBB, ** $p<0.01$ vs. PDGFBB, *** $p<0.001$ vs. PDGFBB, ^ $p<0.05$ vs. DMSO, ^^ $p<0.01$ vs DMSO, ^^^ $p<0.001$ vs DMSO. The error bars indicate the standard deviation; all experiments were repeated at least twice with three biological replicates each time.

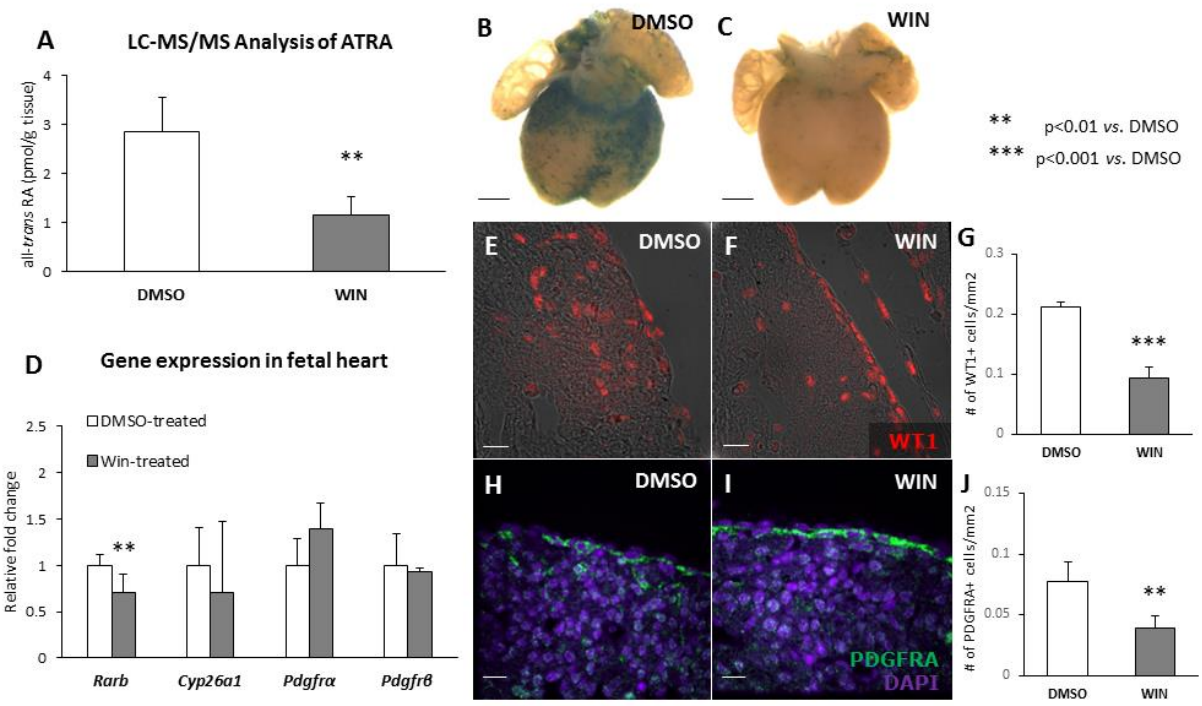

Figure 3.2 RA deficiency is associated with altered localization of PDGFRA-positive EPDCs within the myocardium.

As quantified by LC-MS/MS, E14.5 embryos collected from dams treated daily from E9.5-E13.5 with **WIN** had reduced levels of RA compared to embryos collected from dams treated with **DMSO**-vehicle control (**A**). **WIN**-treatment led to reduced RA-signaling within the heart of embryos collected from *RARE-LacZ* dams treated daily from E9.5-E13.5 with either **WIN** versus **DMSO**-vehicle control as seen by beta galactosidase staining (seen as blue stain) of E14.5 embryonic hearts (**B** *vs.* **C**). **WIN**-treatment also led to a reduction in the expression of the direct RAR target gene, *Rarb*, within the heart of E14.5 embryos derived from dams treated with **WIN** compared to **DMSO**-controls, however, the expression of *Cyp26a1* was not significantly altered by the **WIN** treatment (**D**). **WIN**-treatment led to accumulation of WT1-positive epicardial cells on the surface of the heart (**E-F**, density of WT1+ cells that delaminated from the surface of the heart was quantified in **G**), and an altered distribution of PDGFRA-positive cells in the myocardium of embryos derived from **WIN**-treated dams compared to embryos harvested from **DMSO**-treated dams (**G** vs. **H**, density of PDGFRA+ cells that delaminated

from the surface of the heart was quantified in **J**). Scale bars in B and C are 200 μm and in E-F 20 μm. ** $p<0.01$ vs DMSO, *** $p<0.001$ vs DMSO. Retinoid levels were determined in n=5 of each group (WIN or DMSO). The error bars indicate the standard deviation for each measurement set in each experimental group; images and gene expression assays are based on observations derived from three embryos for each treatment.

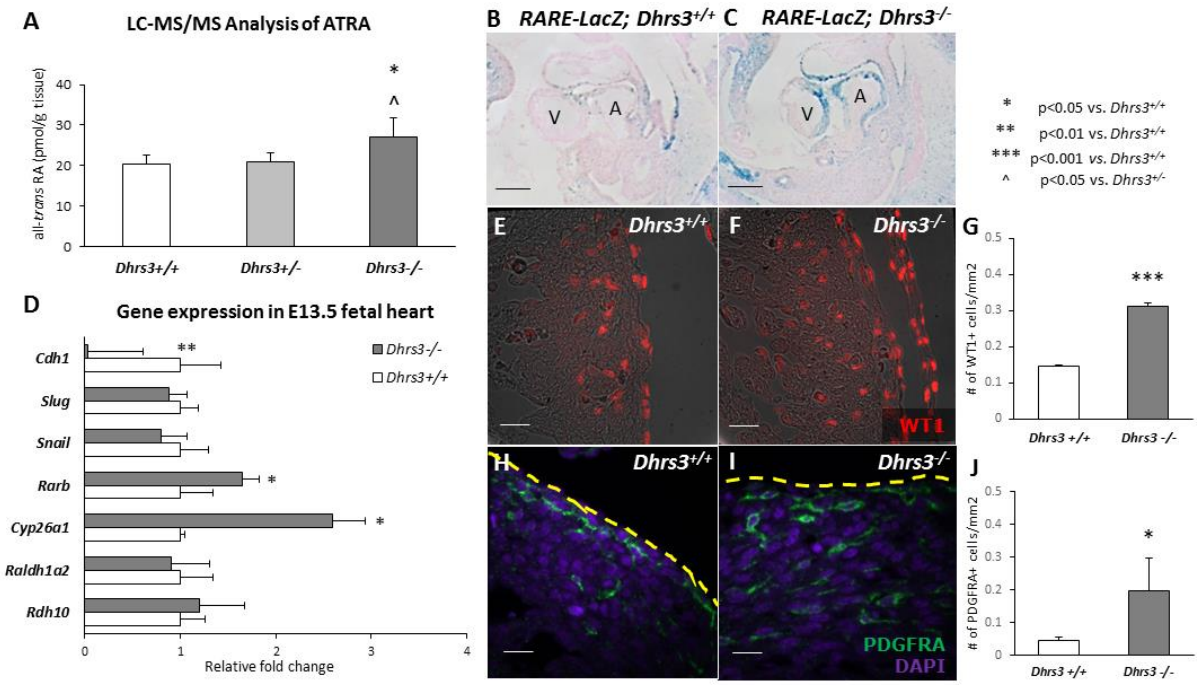

Figure 3.3 *Dhrs3*–deficiency leads to RA-excess and altered localization of PDGFRA-positive EPDCs in the myocardium.

A) E12.5 *Dhrs3*$^{-/-}$ embryos had higher levels of endogenous RA compared to the *Dhrs3*$^{+/-}$ or *Dhrs3*$^{+/+}$ littermate controls as measured by LC-MS/MS analysis. *RARE-LacZ; Dhrs3*$^{-/-}$ embryos displayed more extensive domains of RA-signaling in the heart at E10.5 than the pattern observed in in *RARE-LacZ; Dhrs3*$^{+/+}$ embryos based on the expression of the RARE-driven reporter LacZ (blue stain) (**B** vs**. C**). *Dhrs3*-ablation led to an increased expression of the direct RAR-targets *Cyp26a1* and *Rarb* and a reduced expression of the epithelial marker *Cdh1* in the *Dhrs3*$^{-/-}$ embryonic hearts at E13.5 as measured by qRT-PCR (**D**). Both WT1-positive EPDCs (**E** vs. **F**, density of WT1+ cells that delaminated from the surface of the heart was quantified in **G**) and PDGFRA-positive EPDCs (**H** vs. **I**, density of PDGFRA+ cells that delaminated from the surface of the heart was quantified in **J**) exhibited an altered localization pattern within the myocardium of the *Dhrs3*$^{-/-}$ embryonic hearts versus those of wild type controls. Scale bars in B-C represent 200µm and 20µm in E-F as well as H-I. The yellow dashed-lines mark the outer surface of the heart in H and I. * p<0.05 vs. *Dhrs3*$^{+/+}$ and ^ p<0.05 vs. *Dhrs3*$^{+/-}$; ** p<0.01 vs. *Dhrs3*$^{+/+}$, *** p<0.001

vs. *Dhrs3*$^{+/+}$. The error bars indicate the standard deviation for each measurement set in each experimental group. Retinoids levels were measured using n=4 *Dhrs3*$^{+/+}$, n=5 *Dhrs3*$^{+/-}$ and n=5 *Dhrs3*$^{-/-}$. The images and measurements are based on observations derived from three embryos for each genotype.

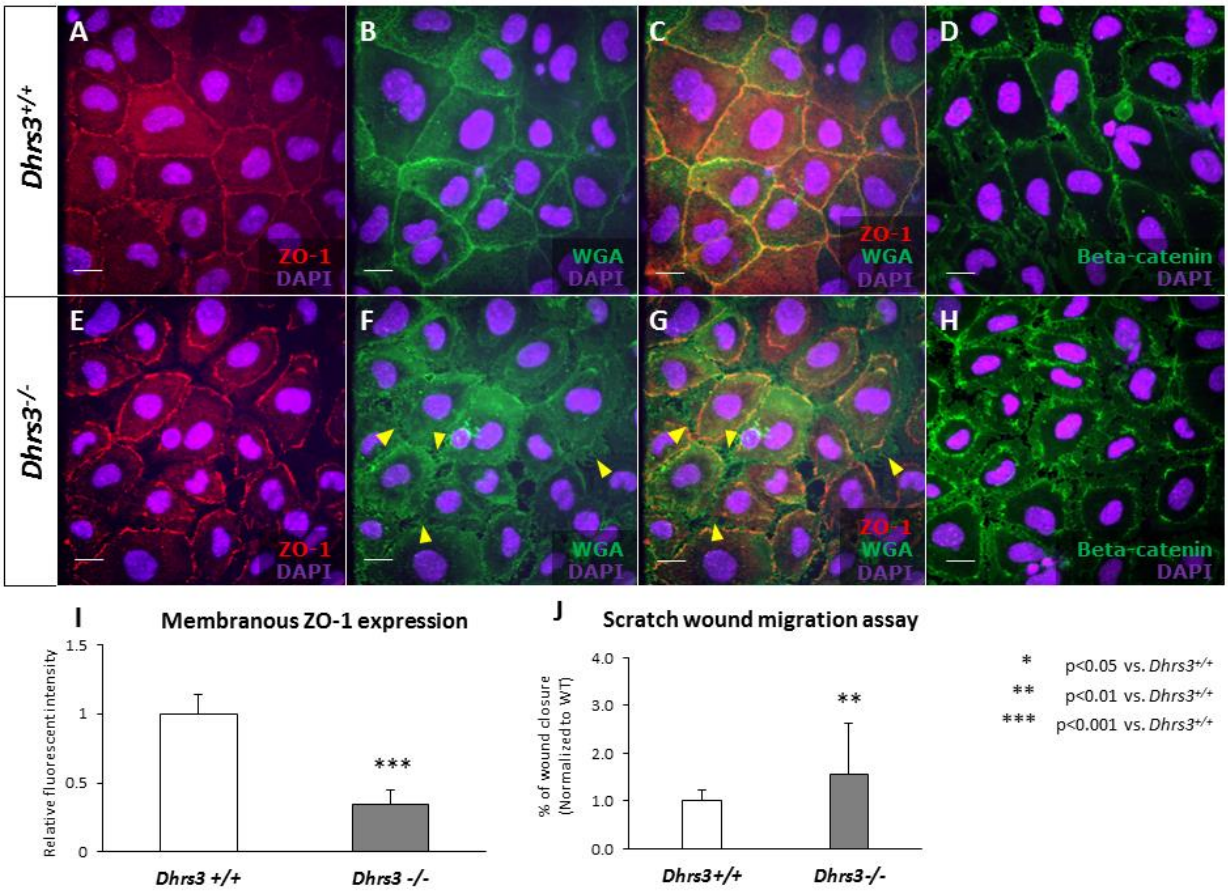

Figure 3.4 Altered cytoskeletal rearrangement and cell migration of *Dhrs3*$^{-/-}$ primary epicardial cells.

Primary epicardial cells derived from E12.5 *Dhrs3*$^{-/-}$ and *Dhrs3*$^{+/+}$ embryonic hearts were cultured in the presence of 1% fetal calf serum. Double labeling of the epithelial markers ZO-1 (**A** vs**. E**) and cell membrane dye (WGA) revealed that the expression of ZO-1 was internalized in cultured *Dhrs3*$^{-/-}$ EPDCs (**E-G**) compared to their localization at the plasma membrane of epicardial cells isolated from wild type controls (**A-C**). Similar internalization from cell border is observed in the expression pattern of beta-catenin (**D** vs**. H**) in *Dhrs3*$^{-/-}$ epicardial cells. Relative expression of ZO-1 on cell membrane was quantified in **I**. Formation of filopodia is indicated with yellow arrows in **F** and **G**. As evaluated by scratch wound migration, *Dhrs3*$^{-/-}$ epicardial cells closed the wound faster in 24 hr compared to epicardial cells derived from wild type littermates (**J**). Scale bars in A-D are 20 μm. * $p<0.05$ vs. *Dhrs3*$^{+/+}$; **

$p<0.01$ vs. *Dhrs3*$^{+/+}$, *** $p<0.001$ vs. *Dhrs3*$^{+/+}$. The images and quantification in I are based on EPDCs derived from 3 *Dhrs3*$^{+/+}$ vs. 4 *Dhrs3*$^{-/-}$ embryos. Scratch wound migration assays employed 4 biological replicates per genotype. The error bars indicate the standard deviation for each measurement set in each experimental group.

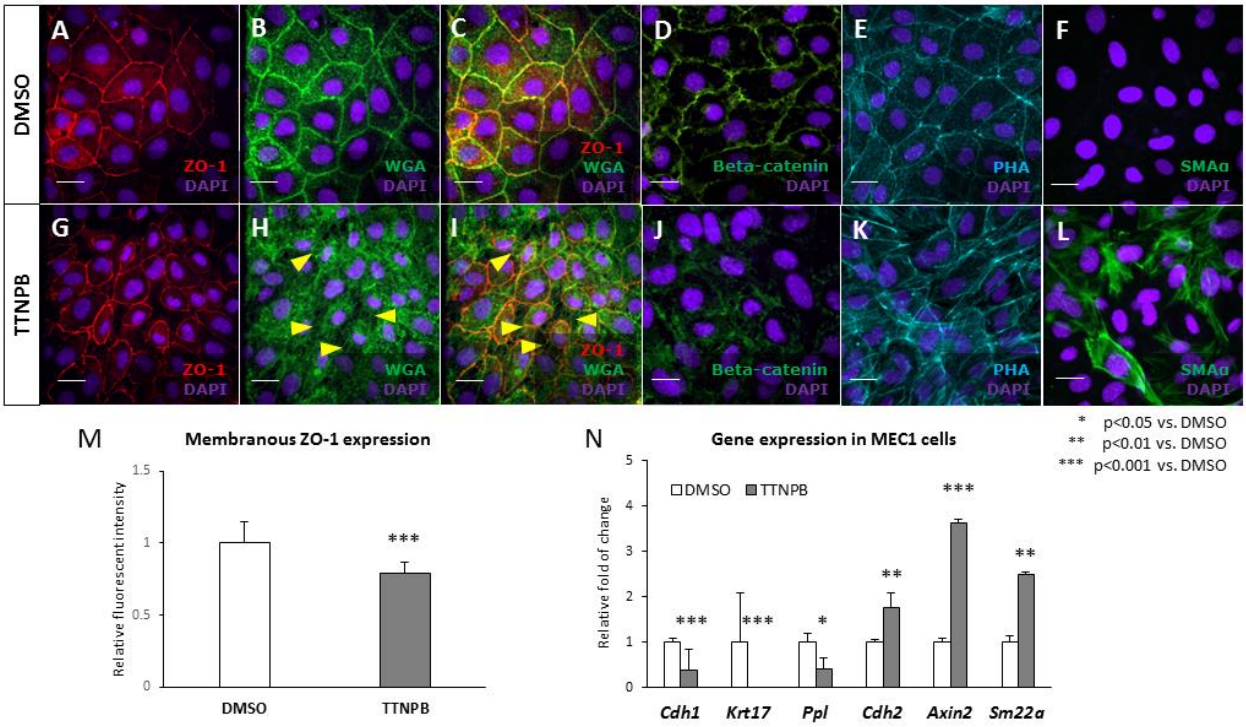

Figure 3.5 RA-signaling promotes cytoskeletal rearrangement in MEC1 cells.

Treatment of MEC1 cells with 10 nM TTNPB, a pan-RAR agonist, led to internalization of epithelial markers, ZO-1 (**A** vs. **G**) and beta-catenin (**D** vs. **J**) and increased formation of stress fibers as evidenced by phalloidin and SMAα staining (**E** vs. **K** for phalloidin; **F** vs. **L** for SMAα). TTNPB-treatment of MEC1 cells led to reduced expression of ZO-1 on cell membrane stained with WGA, which is quantified in **M**. Formation of filopodia revealed by WGA staining is indicated with yellow arrows in **H** and **I**. qRT-PCR results in **N** indicated that RAR activation via TTNPB led to down-regulation of the expression of epithelial markers (*Cdh1*, *Krt17*, *Ppl*) and up-regulation of the expression of a mesenchymal marker (*Cdh2*), a VSMC marker (*Sm22α*) and of *Axin2*, a positive regulator of EpiMT. Scale bars represent 20 μm. *p<0.05 *vs* DMSO, **p<0.01 *vs* DMSO, ***p<0.001 *vs* DMSO. The error bars indicate the standard deviation for each measurement set in each experimental group. All experiments were repeated at least twice with three biological replicates each time.

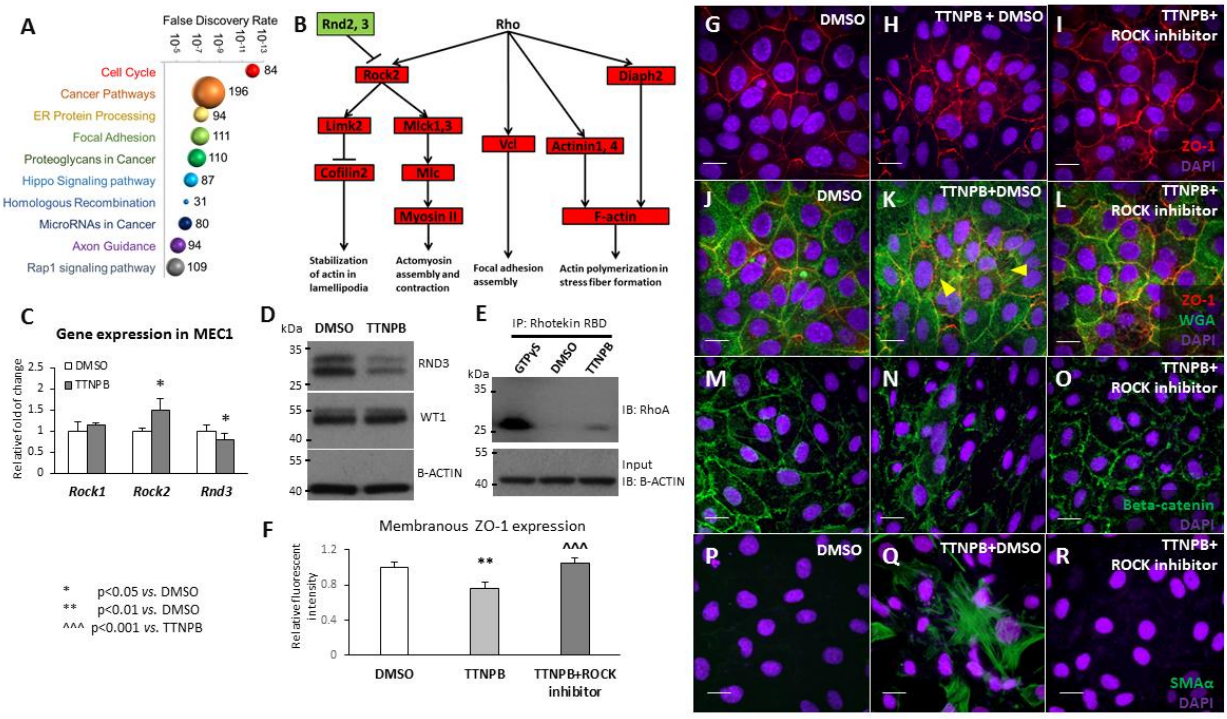

Figure 3.6 Activation of RAR leads to cytoskeletal reorganization via the RhoA-ROCK pathway.

KEGG enrichment analysis based on RNAseq data derived from MEC1 cells treated with either TTNPB or DMSO suggests that RA-signaling led to global changes in multiple signaling pathways in MEC1 cells (**A**). The y-value of each bubble represents the level of enrichment in each pathway while the size of the bubble reflects the number of genes belonging to the pathway whose expression was altered by TTNPB treatment (the gene count mapped to each pathway is also listed numerically besides each bubble). Schematic representation of the Rho pathway indicating genes whose expression was upregulated (red colour) or downregulated (green colour) by TTNPB treatment (**B**). qRT-PCR results indicated that RAR activation led to upregulation of *Rock2* and downregulation of *Rnd3* in MEC1 cells compared to controls (**C**). TTNPB treatment led to decreased expression of RND3 but not WT1 as seen by immunoblot analysis examined by western blotting (**D**). TTNPB treatment of MEC1 cells led to increased association of RhoA with GTP in comparison to cells treated with DMSO (**E**). The levels of GTP-RhoA were examined by affinity-purification of GTP-Rho proteins via agarose beads coupled to the Rhotekin-RBD. The amount of Rho-GTP purified from cell lysates incubated with non-hydrolyzable GTPγS was used to assess the total amount of available Rho, while immunoblotting of the lysates using anti-actin antibody was used to verify that the amount of starting protein in each lysate was the same. Addition of the pan-ROCK inhibitor, Y27632, blocked the TTNPB-induced internalization of the

epithelial markers, ZO-1 (**G-L**) and beta-catenin (**M-O**), as well as the TTNPB-induced expression of SMAα (**P-R**). Yellow arrowheads marks the formed filopodia evidenced by the WGA staining (**K**). Relative expression of ZO-1 on cell membrane was measured and compared amongst DMSO, TTNPB and TTNPB+ROCK inhibitor groups (**F**). Scale bars are 20 μm. * $p<0.05$ vs. DMSO, ** $p<0.01$ vs. DMSO, ^^^ $p<0.001$ vs. TTNPB. The error bars indicate the standard deviation for each measurement set in each experimental group. Staining results are representative from three biological replicates and have been repeated three times. Gene expression measurements and pull-down assays were based on three biological replicates. Western blotting was performed using 4 biological replicates per experimental group and has been repeated twice.

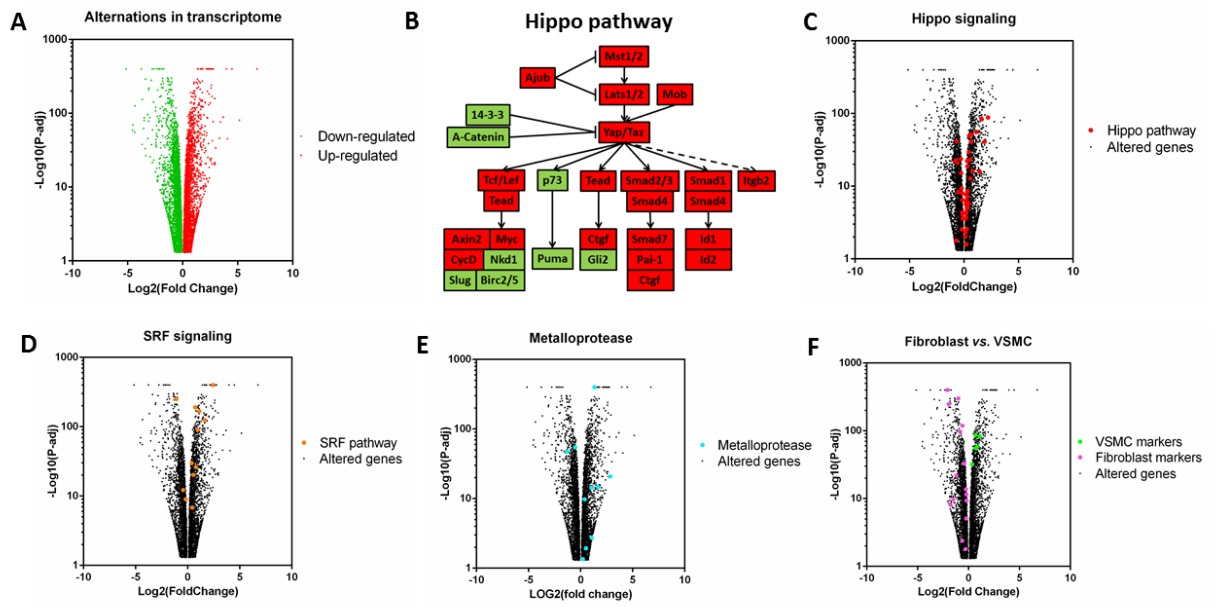

Figure 3.7 Activation of RAR leads to alterations in transcriptome in MEC1 cells.

MEC1 cells were treated with vehicle or 10nM RAR agonist TTNPB for 48 hours before RNA was isolated and submitted for RNAseq. Analysis of the sequencing results showed drastic changes in transcriptome of epicardial cells in response to RA. **A**. Within the significantly altered genes, 3493 are down-regulated (Green) and 3438 genes are induced (Red) by active RA signaling. **B-C.** KEGG analysis and volcano plot demonstrated that Hippo pathway is broadly induced by RA signaling. Green indicates genes that are suppressed and red indicates genes that are up-regulated by RA signaling. **D-E.** Activation of RAR induces SRF signaling pathway and expression of multiple metalloproteases. **F.** Elevated RA signaling induces the expression of mature VSMC markers while suppresses the differentiation of fibroblast cells. Four independent biological repeats were submitted per treatment for RNA-sequencing.

SUPPLEMENTARY FIGURE LEGENDS

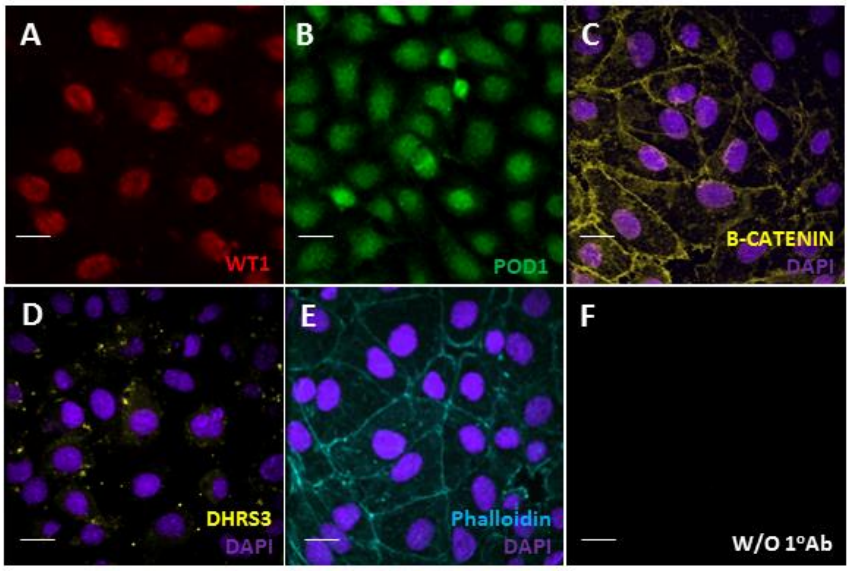

Supplementary Fig 3.1 MEC1 cells express epicardial markers and resemble epithelioid epicardial cells in the absence of induction.

(**A**-**D**) As evidenced by immunocytochemistry with specific antibodies, the MEC1 cells express epicardial markers WT1 (**A**), POD1 (**B**), epithelial marker Beta-catenin (**C**) as well as the retinaldehyde reductase DHRS3 (**D**). Uninduced MEC1 cells also display minimal stress fiber formation as visualized by phalloidin staining (**E**). Negative control group contains MEC1 cells stained in the absence of primary antibodies shown in (**E**).

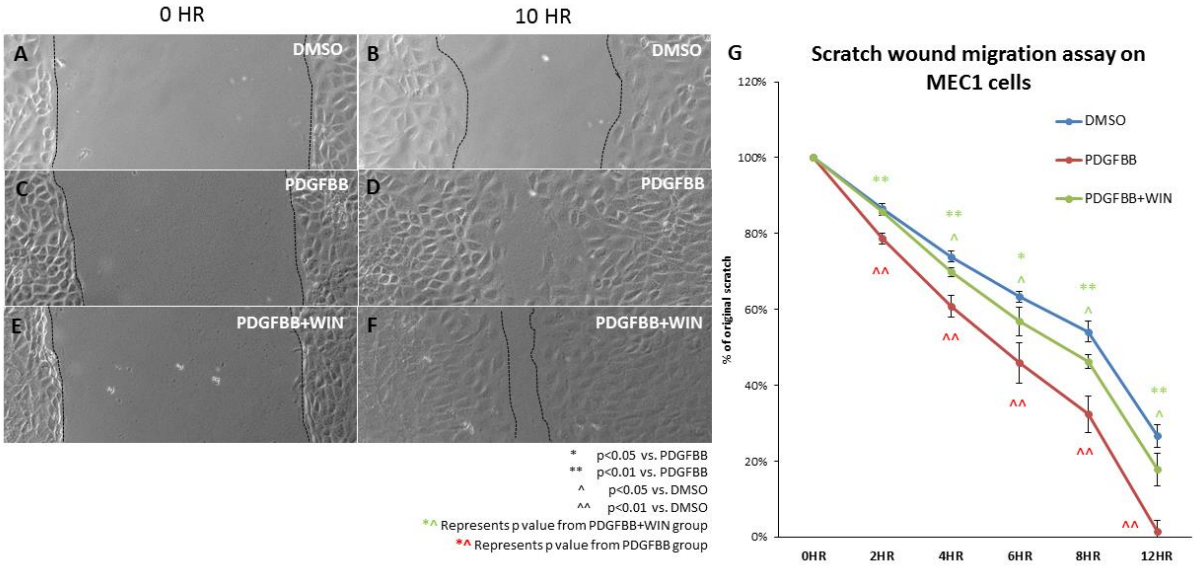

Supplementary Fig 3.2 Inhibition of RA synthesis attenuates PDGFBB-induced cell migration in MEC1 cells.

A scratch wound was made in MEC1 cells treated with DMSO (**A**-**B**), PDGFBB (**C**-**D**) and PDGFBB+WIN (**E**-**F**). Widths of wound were evaluated in each group every 2 hours and the percentage of remaining gap compared to the original scratch was plotted in **G**. PDGFBB accelerated the wound closure in MEC1 cells as early as 2 hours. From 4 hours to 12 hours after the scratch was created, WIN treatment significantly attenuated the rapid wound closure caused by PDGFBB.

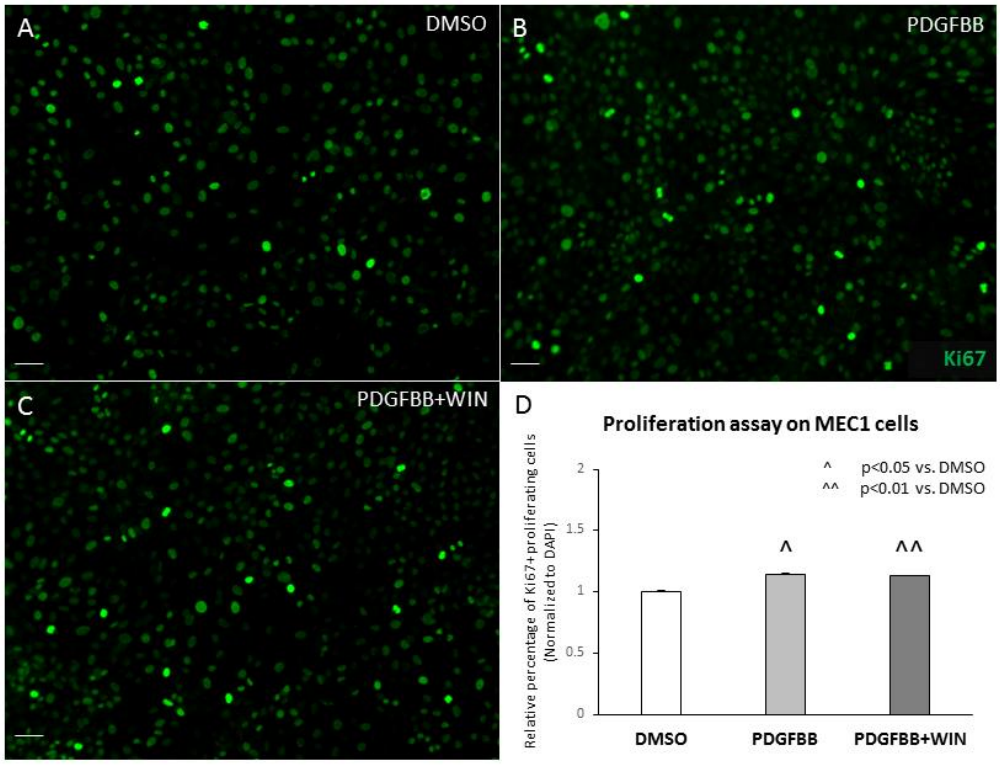

Supplementary Fig 3.3 Inhibition of RA synthesis does not alter MEC1 cell proliferation.

PDGFBB significantly enhances MEC1 cell proliferation as evaluated by the percentage of Ki67-positive cells (**A** *vs*. **B**). 8μM WIN compound does not alter the proliferation induced by PDGFBB (**B** *vs*. **C**). Scale bars represent 50μm. ^ $p<0.05$ *vs*. DMSO, ^^ $p<0.01$ *vs*. DMSO. Error bars represent standard deviation for each measurement set in each experimental group. Results are representative from 4 biological replicates.

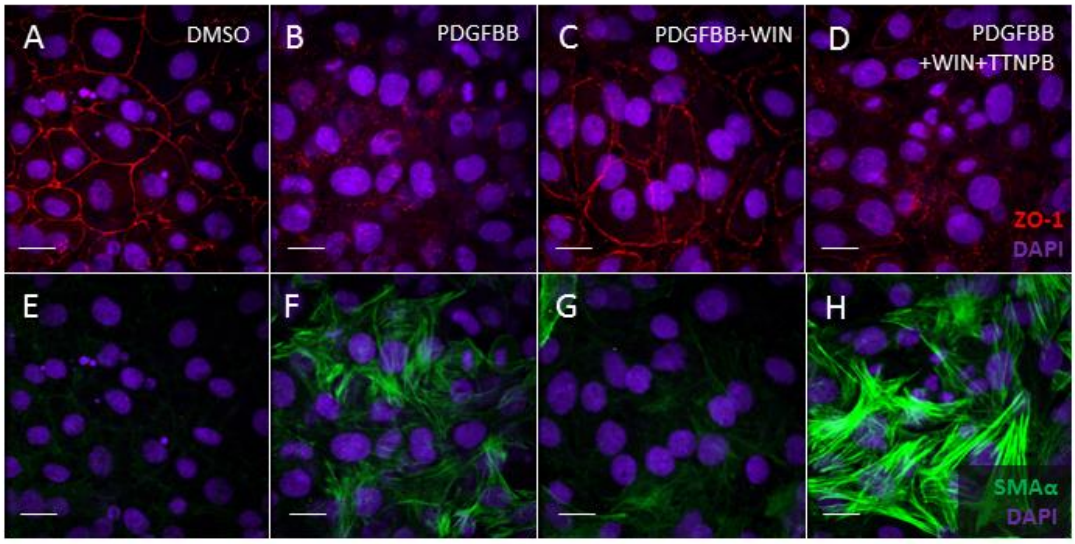

Supplementary Fig 3.4 WIN attenuates PDGFBB-induced EMT through repressing RA synthesis.

Addition of RA (TTNPB) reverses the inhibitory effect of WIN on PDGFBB-induced loss of the epithelial marker, ZO-1, (**A**-**D**) in MEC1 cells. TTNPB also reverses the inhibitory effect of WIN on PDGFBB-induced expression of the VSMC differentiation marker SMAα (**E**-**H**) in MEC1. Scale bars represent 20μm. Each experiment contained two biological replicates per treatment and has been repeated three times.

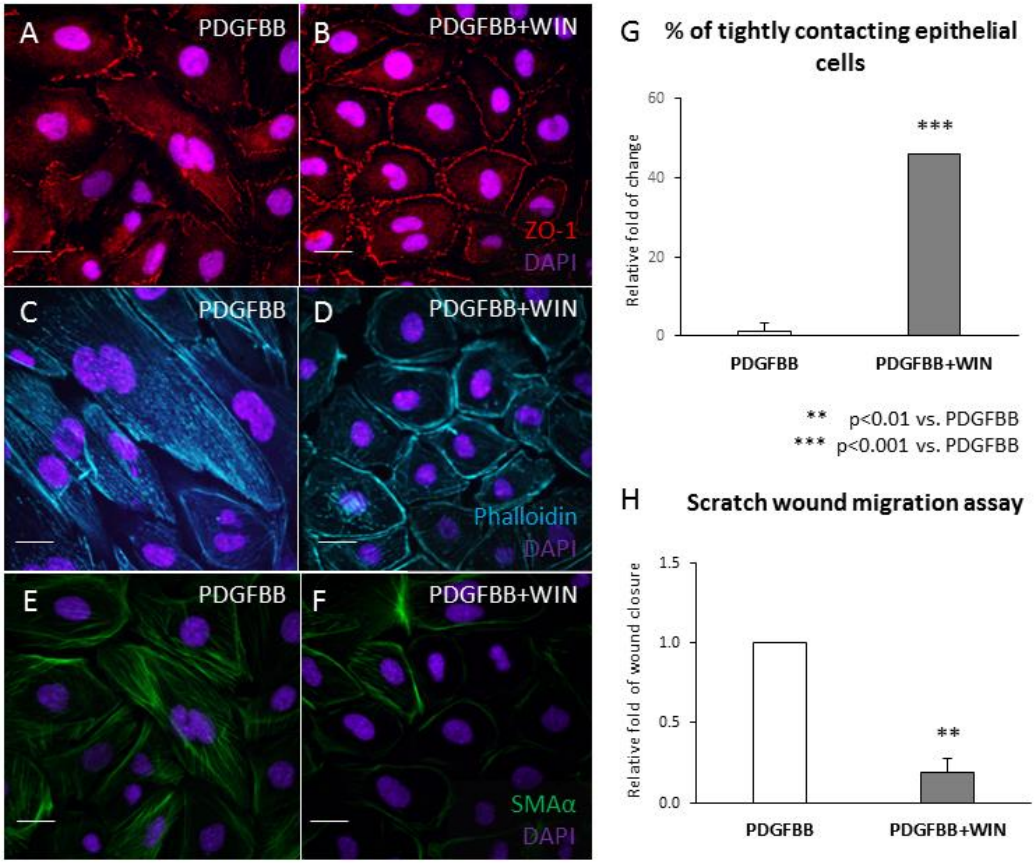

Supplementary Fig 3.5 Inhibition of RA synthesis attenuates PDGFBB-induced cytoskeletal rearrangement and VSMC marker expression in primary epicardial cells.

(**A-F**) In cultures of primary epicardial cells, WIN treatment prevents the PDGFBB-induced relocalization of the epithelial marker ZO-1 (**A,B**), the formation of stress fibers as evidenced by phalloidin staining (**C,D**) and the expression of the VSMC marker SMAα (**E,F**). **PDGFBB+WIN** treatment results in a greater percentage of tightly contacting primary epicardial epithelial cells, as revealed by ZO-1 immunostaining in (**A,B**) and quantified in **G** and expressed as fold-change versus **PDGFBB** alone. The quantification has been performed by a blinded observer. Images (at least 3 pictures per biological replicate) were scrambled and presented to an observer for counting the number of connecting epithelial cells. Numbers of epithelial cells were normalized to the number of nuclei stained by DAPI. At the same time, the migratory capacity of primary epicardial cells treated with **PDGFBB+WIN** is reduced compared to **PDGFBB** alone controls as assessed by a scratch wound-healing

assay and quantification of the percentage of wound closure (**H**), and expressed as fold-change versus **PDGFBB** alone. Scale bars represent 20μm. ** $p<0.01$ *vs*. PDGFBB, *** $p<0.001$ *vs*. PDGFBB. Error bars represent standard deviation for each measurement set in each experimental group. Results are representative from 5 biological replicates. Wound healing assay was performed based on three biological replicates.

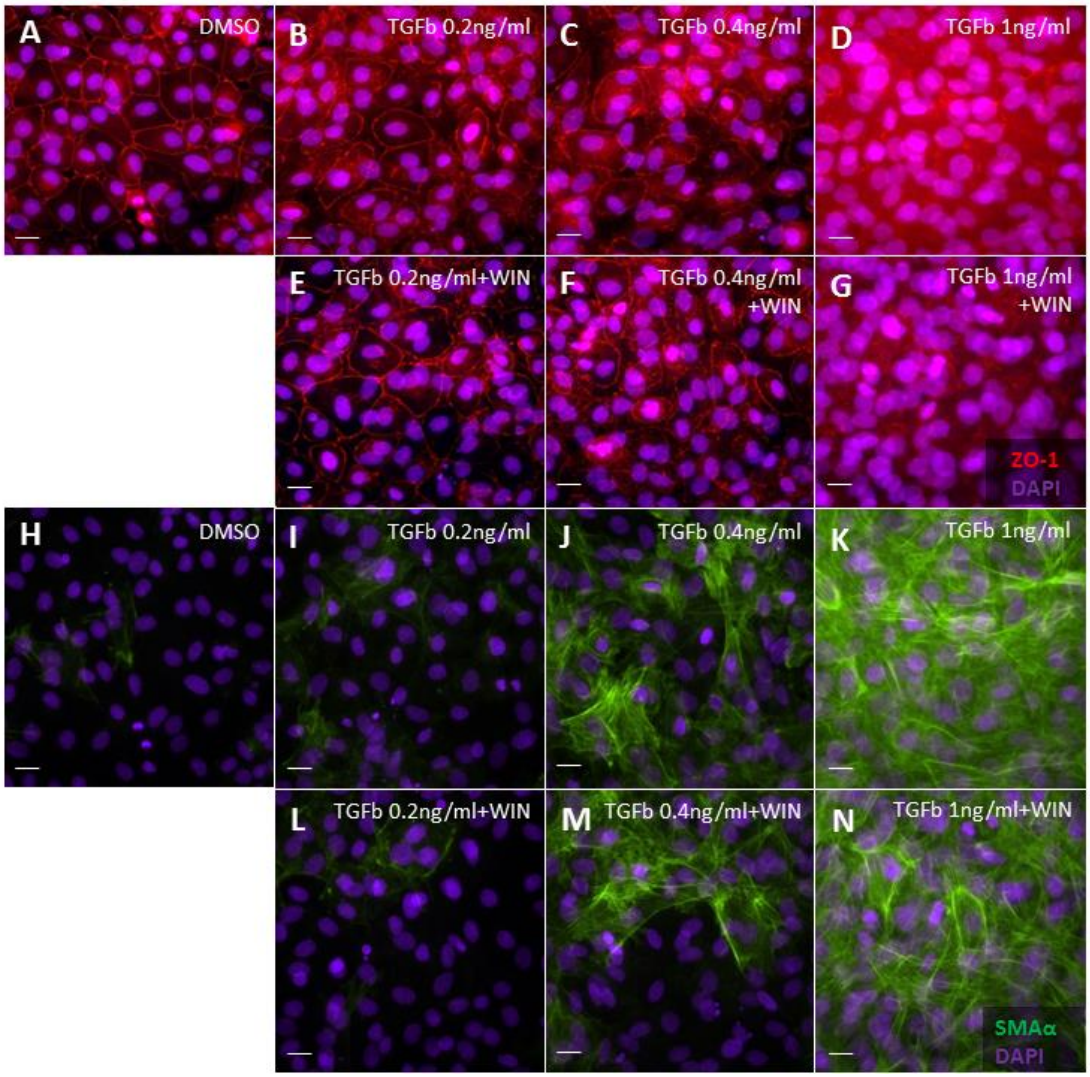

Supplementary Fig 3.6 Effect of WIN on TGFβ-induced EMT.

Inhibition of RA synthesis by WIN in MEC1 cells does not affect TGFβ-induced cytoskeletal reorganization (**A-G**) or TGFβ-induced expresson of VSMC differentiation marker SMAα (**H-N**). MEC1 cell treated with increasing dosages of TGFβ recombinant protein show evident loss of cell contact visualized by ZO-1 immunostainig, as well as VSMC differentiation shown by SMAα staining. These effects were not altered when RA synthesis is blocked by WIN at 16 µM. Scale bars represent 20µm. Each experiment contained two biological replicates per treatment and has been repeated three times.

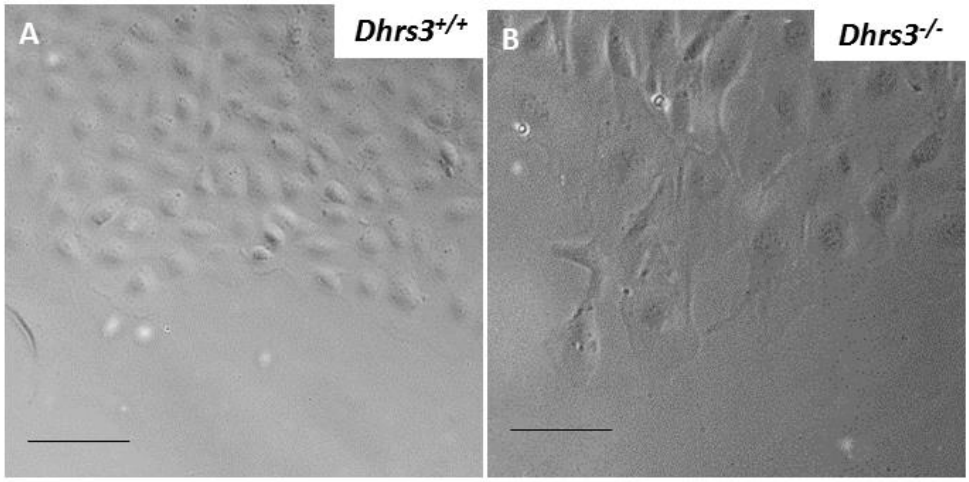

Supplementary Fig 3.7 Deletion of *Dhrs3* causes morphological changes in primary epicardial explant.

Phase contrast images of primary epicardial cells isolated from *Dhrs3*$^{+/+}$ *vs*. *Dhrs3*$^{-/-}$ hearts. Scale bars represent 10 µm. Each experiment contained 5 biological replicates per genotype.

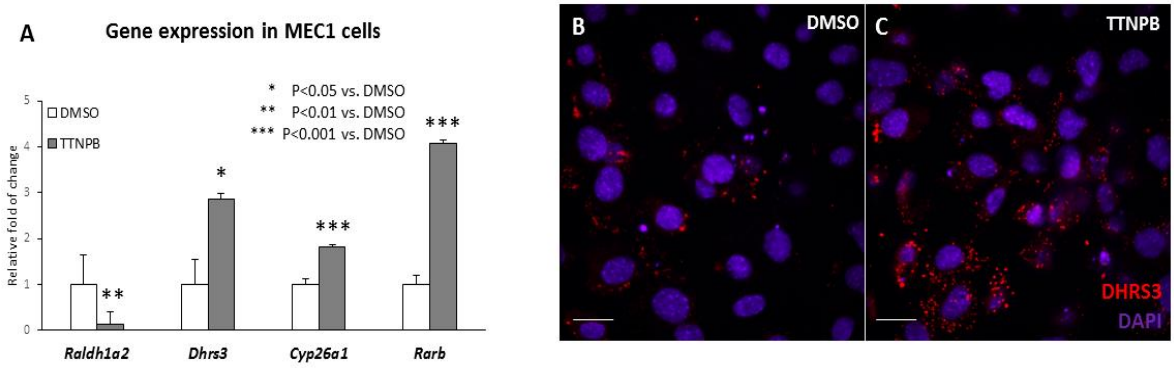

Supplementary Fig 3.8 TTNPB activates RAR signaling causing compensatory responses in RA metabolism in MEC1 cells.

Based qRT-PCR assays, TTNPB treatment of MEC1 cells leads to increased expression of the RAR-targets *Rarb* and *Cyp26a1* and *Dhrs3*, and decreased expression of the RA synthetic enzyme *Raldh1a2* (**A**). The increased expression of DHRS3 is also confirmed by immunohistochemistry of DHRS3 (**B,C**). Scale bars represent 20 μm. *p<0.05 *vs* DMSO, **p<0.01 *vs* DMSO, ***p<0.001 *vs* DMSO. Error bars represent standard deviation for each measurement set in each experimental group. Analyses of gene expression and protein levels are derived from three biological replicates per treatment.

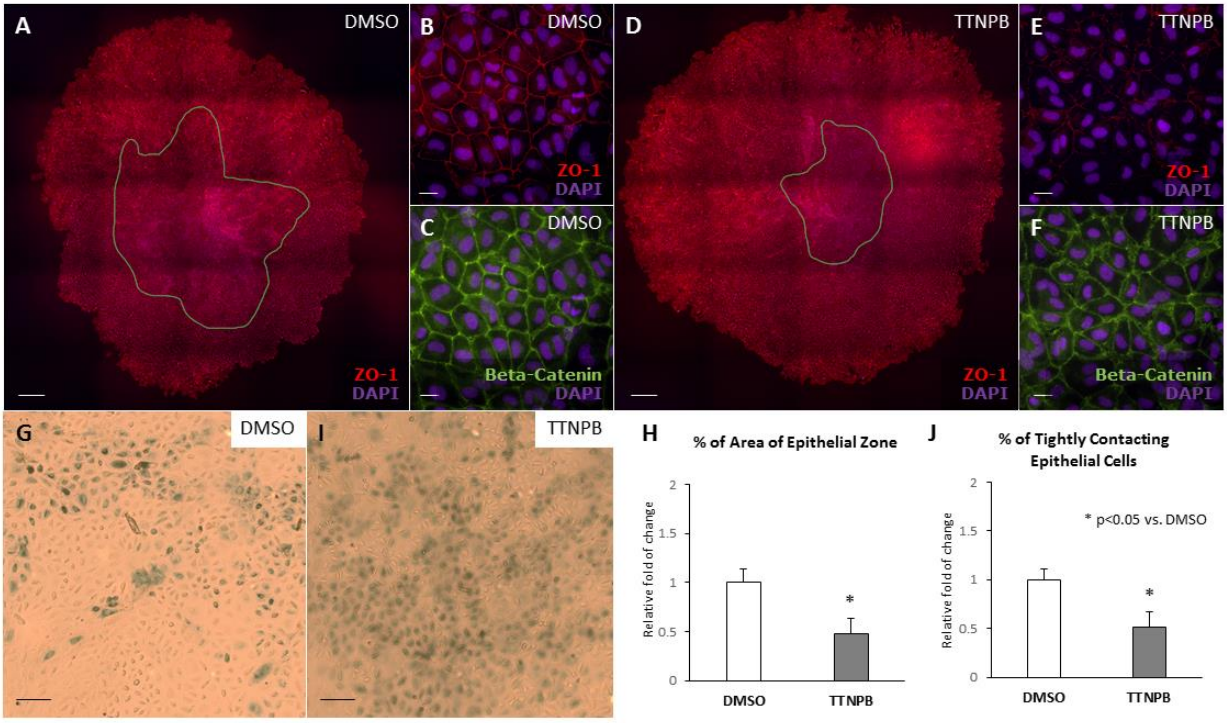

Supplementary Fig 3.9 RAR-agonist TTNPB evidently reduces the epithelial characteristics in primary epicardial cells.

TTNPB at 10nM effectively up-regulated the expression of the LacZ transgene in primary epicardial cells isolated from *RARE-LacZ* embryonic hearts (**G** vs. **I**), suggesting higher levels of RA signaling in TTNPB-treated primary epicardial cells. Addition of TTNPB to primary epicardial cells derived from C57Bl/6 embryos leads to reduced expression of the epithelial markers, ZO-1 (**B** vs. **E**) and beta-catenin (**C** vs. **F**). Cells found in the central area of each explant culture, marked using a green line in **A** and **D**, exhibit clear epithelial characteristics and tight cell-to-cell contact with neighboring cells based on ZO-1 immunostaining. The cells found outside the perimeter marked by the green line show mesothelial characteristics. To assess the number of cells retaining epithelial characteristics we quantified both the relative area of the epithelial zones in relation to the area occupied by the whole explant (**H**), and we also quantified the number of epithelial cells as a percentage of the whole explant (**J**). We then normalized these values to the area occupied by epithelial cells or number of cells with epithelial characteristics in the vehicle control-treated samples. The scale bars in A and D represent 200µm. Scale bars in B, C, E and F

represent 20μm. Scale bars in G-I represent 10μm. * $p<0.05$ *vs*. DMSO. Error bars represent standard deviation for each measurement set in each experimental group. For observation and quantification derived from immunostaining, three biological replicates were included to perform comparison and analysis.

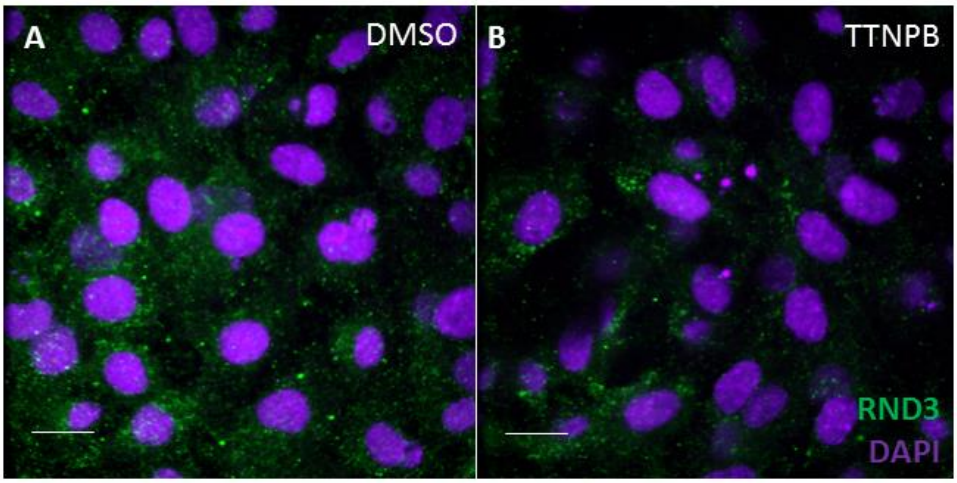

Supplementary Fig 3.10 TTNPB decreases the expression of *Rnd3* in MEC1 cells.

Immunohistochemistry analysis of RND3 in MEC1 cells suggests reduced level of expression in response to TTNPB treatment. Scale bars represent 20 μm. Staining of RND3 has been repeated three times with two biological replicates per treatment per time.

SUPPLEMENTARY TABLES

Supplementary Table 3.1

Host species	Target species	Epitope	Company	Catalog #	Dilution
Rabbit	Mouse	WT1 (C-19)	Santa Cruz	sc-192	1:100 for ICC
					1:1000 for western blotting
Rabbit	Mouse	POD1 (H-75)	Santa Cruz	sc-32914	1:100 for ICC
Mouse	Mouse	αSMA (1A4)	Santa Cruz	sc-32251	1:250 for ICC
Rabbit	Mouse	PDGFR-A (D1E1E)	Cell signaling	3174	1:100 for IF staining on slides
Rabbit	Mouse	DHRS3	Proteintech	15393-AP	1:100 for ICC
Mouse	Mouse	B-ACTIN (C4)	Santa Cruz	sc-47778	1:1000 for western blotting
Mouse	Mouse	RND3	Abcam	ab50316	1:1000 for western blotting
Rabbit	Mouse	ZO-1	Abcam	ab59720	1:250 for ICC
Mouse	Mouse	β-CATENIN	BD Transduction Laboratories	610153	1:250 for ICC
	Mouse	Alexa Fluor 647 Phalloidin	Invitrogen	A22287	2 Unit/ml for ICC
Mouse	Mouse	RhoA	NewEast Biosciences	26007	1:1000 for western blotting
Rabbit	Mouse	Ki67	Abcam	ab15580	1:200 for ICC
Goat	Rabbit	Alexa Fluor 568 Secondary antibody	Invitrogen	A-11011	1:750 for ICC; 1:200 for IF staining on slides
Goat	Mouse	Alexa Fluor 488 Secondary antibody	Invitrogen	R37120	2 drops/ml for ICC
		Wheat Germ Agglutinin	Invitrogen	W11261	1:200 for ICC
Rabbit	Mouse	WT1	Abcam	ab89901	1:100 for IF staining on slides

Supplementary Table 3.2

Gene	Accession number		Sequence (5' to 3')
Cdh1	NM_009864	Forward	CAGCCTTCTTTTCGGAAGACT
		Reverse	GGTAGACAGCTCCCTATGACTG
Cdh1-2	NM_009864	Forward	CAGGTCTCCTCATGGCTTTGC
		Reverse	CTTCCGAAAAGAAGGCTGTCC
Cdh2	NM_007664	Forward	AGCGCAGTCTTACCGAAGG
		Reverse	TCGCTGCTTTCATACTGAACTTT
Rock1	NM_009071	Forward	AAGCTTTTGTTGGCAATCAGC
		Reverse	AACTTTCCTGCAAGCTTTTATCCA
Rock2	NM_009072	Forward	TTGGTTCGTCATAAGGCATCAC
		Reverse	TGTTGGCAAAGGCCATAATATCT
Rnd3	NM_028810	Forward	CAAGATAGTAGTAGTGGGCGACA
		Reverse	AAACACCGTAGGGACGTAATTTT
Krt17	NM_010663	Forward	ACCATCCGCCAGTTTACCTC
		Reverse	CTACCCAGGCCACTAGCTGA
Ppl	NM_008909	Forward	CAAAGGCAAATACAGCCCAAC
		Reverse	TTCCACCTGGTCTGCATTCTT
Axin2	NM_015732	Forward	GCGTGGCCAGTCAGCAGAGG
		Reverse	CCTGGAGCGCGTGGACACTT
Sm22a	NM_011526	Forward	CCACAAACGACCAAGCCTTCT
		Reverse	CGGCTCATGCCGTAGGAT
Rdh10	NM_133832	Forward	CTGGAGTTGAGGATTACTGTGC
		Reverse	TCTGAACATGCCCGTGTCTA
Raldh1a2	NM_009022	Forward	CAGAGAGTGGGAGAGTGTTCC
		Reverse	CACACAGAACCAAGAGAGAAGG
Cyp26a1	NM_007811	Forward	GAACATTCGCGCCAAGATCC
		Reverse	TTAGTGCCTGCATATCCAGCC
Rarb	NM_011243	Forward	CAAGCTCCAAGAACCACTGC
		Reverse	ATTACACGTTCGGCACCTTTC
Dhrs3	NM_001172424	Forward	CAGCCCTCTCACCGTCCCAAT
		Reverse	AGAACAATCTTTCTGGCGCCACGG
Snail	NM_011427	Forward	CACACGCTGCCTTGTGTCT
		Reverse	GGTCAGCAAAAGCACGGTT
Slug	NM_011415	Forward	TGGTCAAGAAACATTTCAACGCC
		Reverse	GGTGAGGATCTCTGGTTTTGGTA
Pdgfra	NM_001347719	Forward	TCATTTACGAGATACCTCGG
		Reverse	TCCTGACATACTCCACTTTG
Pdgfrb	NM_008809	Forward	GATCTCTCGGAACCTCATCG
		Reverse	GGCTTCTTTCGCACAATCTC

Supplementary Table 3.3

Hippo		
Associated Gene Name	log2FoldChange	P-adj
Nf2	0.11487	0.0091775
Stk3	0.29497	9.3202E-06
Lats2	0.44134	3.8815E-30
Mob1b	0.13384	0.0045407
Ppp2ca	-0.16537	0.000073236
Ppp2cb	0.26654	9.8325E-06
Ppp2r2d	-0.22138	0.0028097
Ppp2r2a	-0.1761	4.5826E-05
Ppp2r2b	0.30796	7.6127E-08
Yap1	0.16142	1.9938E-06
Wwtr1	0.46458	6.4321E-50
Ppp1cc	-0.22536	4.6255E-10
Ppp1ca	-0.129	0.00026514
Ppp1cb	0.17385	2.0766E-08
Tead1	0.17218	0.00019772
Tead3	0.30885	6.0188E-06
Tead2	0.56861	4.9145E-24
Smad4	0.19357	0.000042792
Smad3	0.64476	2.1217E-52
Smad1	1.1392	6.0266E-57
Tcf7	1.4429	1.4782E-16
Tcf7l2	0.25347	0.002515
Ctgf	1.8861	1.2741E-41
Itgb2	1.6205	2.1848E-84
Smad7	0.38244	1.1817E-06
Serpine1	0.75762	5.7391E-17
Id1	0.64795	5.0111E-42
Id2	0.35075	7.7474E-06
Axin2	2.1955	5.1378E-89
Myc	0.21197	0.025923
Ccnd3	-0.67774	4.3631E-42
Ccnd2	0.17702	0.00000057
Actb	0.30725	1.315E-19
Actg1	0.28456	5.5438E-23
Ywhab	-0.29144	1.7202E-24
Ywhag	-0.27386	5.7873E-16
Ywhaz	-0.16158	9.3531E-09
Ywhae	-0.15528	3.4221E-07
Ywhah	0.19388	0.00005244
Ctnna1	0.1098	0.00027893
Wtip	0.57055	1.7139E-13
Ajuba	0.33189	2.4996E-09
Trp73	-0.71616	0.016031
Gli2	-0.61564	8.2589E-22
Birc5	-0.81048	3.8971E-23
Nkd1	-0.54278	4.6847E-09

SRF		
Associated Gene Name	log2FoldChange	P-adj
Akap12	2.4355	0
Fhl2	0.79139	6.72E-27
Fhl1	0.96069	7.00E-91
Gda	1.6242	5.44E-125
Gpm6a	-1.1004	3.67E-251
Gsn	0.37975	1.35E-30
Myl9	1.1293	1.40E-168
Pafah1b2	-0.19852	9.65E-10
Pdlim7	0.53614	5.81E-21
Pkhd1l1	-0.43475	5.93E-13
Ptgr1	0.42285	1.48E-07
Tpm1	0.72636	7.15E-192

MMP		
Associated Gene Name	log2FoldChange	P-adj
Mmp23	0.21553	0.044521
Mmp2	1.3239	0
Mmp15	1.6527	1.7674E-15
Mmp3	0.50982	0.011661
Mmp10	2.8513	1.4698E-21
Mmp12	1.0754	0.0018091
Mmp13	1.0278	4.7534E-15
Mmp11	0.39798	1.7484E-10
Mmp14	-0.52734	1.3363E-55
Mmp16	-1.2913	1.9645E-48

Collage *vs.* VSMC		
Associated Gene Name	log2FoldChange	P-adj
Col1a1	-0.82542	4.3505E-97
Col1a2	-0.60451	6.7219E-120
Col6a1	-2.0833	0
Col18a1	-0.67024	2.2154E-06
Col5a3	-1.2081	9.5704E-23
Col6a2	-2.6045	0
Col14a1	-0.95426	0.0072124
Col17a1	-2.4674	7.4473E-17
Col5a2	-0.19501	4.5784E-10
Col3a1	-1.0114	1.9887E-300
Col5a1	-1.9589	1.8926E-248
Col15a1	-1.5135	5.5587E-07
Col4a6	-0.44929	1.1656E-33
Col4a5	-0.21629	3.1732E-12
Col4a2	-0.26542	1.9425E-14
Col6a6	-0.62323	0.0040237
Col27a1	-0.71885	1.1556E-10
Col6a3	-1.4918	1.6152E-10
Col4a4	-1.7594	8.1803E-09
Fn1	-0.29355	0.015872
Itga5	-0.23008	7.8618E-06
Tagln	1.1022	8.3794E-84
Acta2	0.84159	2.8373E-59
Cnn2	0.66978	5.4381E-56
Cnn3	0.68473	3.8832E-87
Cald1	0.34936	1.0164E-32

Chapter 4 Teratogenic Effects of RA in the Development of Coronary Vasculature

Abstract

During the final stages of heart development the myocardium grows and becomes vascularized. These processes rely on paracrine factors and cell progenitors derived from the epicardium. It is not entirely clear which signaling molecules orchestrate epicardial-based developmental programming, but one possible regulator is a metabolite of vitamin A, namely, retinoic acid (RA), which controls gene expression via the RA receptors (RARs) and retinoid X receptors (RXRs). In the current study, we explored the developmental consequences of altered RA signaling in late cardiogenic events that involve the epicardium. For this, we employed a previously characterized model of embryonic RA excess based on mouse embryos deficient in the retinaldehyde reductase DHRS3. To confirm our findings, we also developed a model of embryonic RA deficiency by administering WIN 18,446, a bis-(dichloroacetyl)-diamine inhibitor of RA synthesis, to pregnant dams. Our results demonstrated that alterations in embryonic RA-signaling let to a thin myocardium and aberrant coronary vessel formation and remodeling. Both the cardiac defects and the embryonic lethality associated with RA excess in the *Dhrs3*$^{-/-}$ model could be mitigated by reducing the maternal vitamin A intake. In both models of altered RA-signaling, the endothelial tubes did not become invested with epicardial-derived vascular smooth muscle cells (VSMCs). Through transcriptome profiling of epicardial cells, we found that RA-signaling influenced epicardial signaling pathways relevant to cardiac development. To sum up, we report that RA signaling affects epicardial signaling and plays critical roles in the development of the myocardium and the coronary vasculature.

4.1. Introduction

Retinoic acid (RA), an active metabolite of vitamin A, carries out regulatory roles in many essential processes during both embryonic and postembryonic life (McCollum & Davis, 1913). The activities of RA are mediated by ligand-activated transcription factors, known as retinoic acid receptors (RARs) and

retinoid X receptors (RXRs) found associated with DNA motifs, termed RA response elements (RARE), in the vicinity of target genes (Båvik et al., 1996). Binding of RA to RAR/RXR heterodimers leads to the activation, or repression, of hundreds of genes resulting in pleiotropic effects, which influences cell-signaling and tissue growth, differentiation and repair (Paschaki et al., 2013). RA-signaling is regulated by a complex transport and enzymatic pathway which controls the levels of available cellular RA (reviewed in (Shannon et al., 2017)). Cellular RA levels are also influenced by the health and nutritional status of the individual, which can affect, the dietary availability, uptake or tissue storage of retinol and provitamin A carotenoid precursors (Rubin, Ross, Stephensen, Bohn, & Tanumihardjo, 2017).

Alterations in RA-signaling as a result of excess or deficiency of vitamin A or due to treatment with RAR agonists can lead to congenital disorders manifested as craniofacial, cardiac, limb, thymus, ear and neural tube malformations (Ackermans, Zhou, Carels, Wagener, & Von den Hoff, 2011; Kochhar, 1973; Lammer et al., 1985; Rothman et al., 1995; M. Vieux-Rochas et al., 2007). The magnitude of the teratogenic effects of altered RA-signaling depends on the extent of deficiency or excess and on the developmental stage of the fetus at the time of exposure (Collins & Mao, 1999). The development of the heart is very sensitive to altered RA levels during the early stages of cardiogenesis when RA controls the determination of the cardiogenic progenitor pool and the anteroposterior patterning of the primitive heart tube (reviewed in (Stefanovic & Zaffran, 2017; Xavier-Neto et al., 2015)). As a result, altered RA signaling can induce a series of defects related to looping, outflow tract and chamber formation (Ghyselinck et al., 1997; Kolodzinska et al., 2013; Lammer et al., 1985; Yasui et al., 1997). Paradoxically, some of the defects induced by too much RA can also be brought on by too little RA due to either compensatory mechanisms or for the reason that regardless of excess or deficiency perturbations of RA signaling ultimately result in impaired development (Frenz et al., 2010; Lee et al., 2012; A. Rydeen et al., 2015).

Following the formation of the chambered heart, RA-signaling is involved in several late developmental processes, which include the growth of the myocardial compact zone and the formation of

the coronary vasculature. The main source of RA in the late heart is the epicardium, a mesothelial layer of cells which covers the heart starting at E9.5 in mouse embryos. In addition to producing RA, the epicardium secretes trophic factors which support myocardial expansion. Moreover, epicardial-derived precursor cells (EPDC) undergo epithelial-to-mesenchymal transition giving rise to cardiac vascular smooth muscle cells (VSMCs) and perivascular and interstitial fibroblasts which stabilize the coronary vasculature and provide functionality of the contracting heart (reviewed in (Sharma, Chang, & Red-Horse, 2017)). The formation of the vasculature and the myocardial compaction must proceed in timely an orchestrated manner. Defects in the formation of epicardial derivatives are often associated with both compromised formation of coronary vessels and hypoplastic ventricles (Singh et al., 2016; C. L. Smith et al., 2011; Trembley, Velasquez, de Mesy Bentley, & Small, 2015; von Gise et al., 2011). Studies based on explant studies and on mouse models deficient in the RA-synthetic enzyme RAlDH2, or RXR-signaling suggest that RA is involved in the production of cardiotrophic factors by the epicardium to support the proliferation of the myocardium (Thomas Brade et al., 2011; T. Chen et al., 2002; P. Li et al., 2011; Shen et al., 2015; Ingo Stuckmann et al., 2003). The same mouse models of altered RA-signaling also manifested defects in the formation of the coronary vasculature (S. C. Lin et al., 2010; Merki et al., 2005). Despite this progress many questions remain regarding the mechanism involved in the effects of RA on the late heart development.

Here, we examined the effects of altered RA-signaling during the late development of the heart focusing on coronary vessel formation and myocardial growth Recent studies suggest that RA may control the epicardial EMT and the differentiation of EPDCs ((Azambuja et al., 2010; Caitlin M. Braitsch et al., 2012; Merki et al., 2005) and Chapter 3). Using complementary models of either excess or deficiency of RA we demonstrate that RA plays a role in the development of the primary endothelial plexus and the remodeling of the coronary vasculature. In the presence of excess RA-signaling, PDGFRB-positive VSMC progenitor cells are poorly recruited to the developing vessels and fewer mature VSMCs could be found in the hearts of *Dhrs3*$^{-/-}$ embryos. In addition, *in vivo* excess and

deficiency of RA led a reduction in the ventricular myocardial growth while *in vitro* RA signaling led to changes in the epicardial transcriptome. Taken together, our study describes the effects of altered RA on the development of the coronary vasculature and the myocardium and provides evidence for the requirement of RA during the late development of the heart.

4.2. Materials and Methods

Mice

Dhrs3$^{+/-}$, *RARE-LacZ* and *Dhrs3*$^{+/-}$; *RARE-LacZ* mice have been previously described (Billings et al., 2013). The *RARE-LacZ* carry a *LacZ* gene under the control of an RA-inducible promoter (Rossant et al., 1991) and are available at the Jackson Laboratories identified as strain *RARE-hsp68LacZ*, stock 008477. Unless otherwise noted, mice have been maintained on 2018 chow diet (Envigo) containing 15 IU vitamin A/ gram and kept in rooms with controlled temperature and humidity with a 12 hour light-dark cycle.

After mating female mice were checked for vaginal plugs in the morning and that noon is considered as embryonic day (E0.5). Caesarean sections were performed at designated embryonic stages to harvest pups or embryonic tissues. All animal protocols were approved by the Institutional Animal Care and Use Committee at the University of Kansas.

Generation of *Dhrs3*$^{-/-}$ mice in vitamin A-deficient dams

Dhrs3$^{+/-}$ parent mice were kept on vitamin A sufficient diet (VAS) and their female *Dhrs3*$^{+/-}$ offsprings were reared on vitamin A deficient diet (VAD) from weaning. VAD-fed female *Dhrs3*$^{+/-}$ mice were bred overnight with male *Dhrs3*$^{+/-}$ mice to generate VAD *Dhrs3*$^{-/-}$ embryos. Caesarean sections were performed at designated embryonic stages to harvest pups. Both VAS and VAD diets are derived from AIN-93G growing rodent diet (ref: J. Nutr. 127, 838S–841S). VAS diet contains 4 IU preformed vitamin Aper gram of diet (D13112B, Research Diets) whereas VAD diet is vitamin A-deficient (D13110GC, Research Diets).

Whole-mount PECAM1 staining

Mouse embryonic hearts were isolated in PBS and fixed in 4% paraformaldehyde (PFA) at 4°C overnight. Hearts are dehydrated through a series of increasingly concentrated methanol/PBS. Endogenous horseradish peroxidase activity in the heart was quenched by Dent's bleach (Methanol: DMSO: 30%H_2O_2=4:1:1) at room temperature for 4 hours and then rehydrated through methanol/PBS. Embryonic hearts were blocked in blocking buffer (5% non-fat milk/0.1% Tween 20/PBS) for 2 hours and then incubated with diluted primary antibody against platelet/endothelial cell adhesion molecule 1 (PECAM1) (1:500, Cat# 553370; BD-Pharmingen) for an hour at room temperature and subsequently overnight at 4°C. The specificity of used antibodies has been validated by western blotting. After wash, hearts were incubated with HRP-conjugated secondary antibody diluted in blocking buffer for an hour. Detection of HRP was performed using the DAB Peroxidase substrate kit (Vector Laboratories, Cat# SK-4100) and the stained hearts were photographed and documented by Leica DMS300 Dissection Microscope equipped with digital camera. For each stage, at least 3 distinct mouse embryos were analyzed by whole-mount PECAM1 immunostaining.

Immunofluorescent staining

Embryos at various developmental stages were harvested in ice-cold PBS, fixed in 4% PFA overnight at 4°C and processed for transversal sectioning after being embedded in paraffin. Sample sections were deparaffinized and rehydrated at room temperature. Distinct antigen retrieval methods were then applied in the case of different antigens: for CD31, sections were treated with 0.1mg/ml proteinase K for 5 minutes at room temperature; for PDGFRA/B and COUP-TF II, heat-mediated antigen retrieval was utilized using established protocol. In case of double-labeling, embryonic tissues were fixed for 2 hours at 4°C and processed for frozen section to avoid conflicting antigen retrieval methods. Tissue sections were incubated with 3% H_2O_2 for 5 min to quench endogenous HRP activity. Non-specific binding sites on sections were blocked with blocking buffer (5% normal goat serum/ 0.1% Tween 20/ PBS) for an hour at room temperature. Diluted primary antibody was subsequently added on to slides and incubated at 4°C

overnight. Information about primary antibody was listed in **Table 1**. After washing with 0.1% Tween 20/PBS solution, Alexa Fluor-conjugated secondary antibody was applied to detect the corresponding primary antibody. When signal amplification is needed, HRP-conjugated secondary antibody was used and TSA Plus Fluorescein Evaluation Kit (PerkinElmer, Cat# NEL741E001KT) was used according to manufacturer's protocol. Nuclei were stained with 1Mm DAPI (Life Technologies) and sections were mounted with Vectashield mounting medium (Vector Laboratories, Cat# H-1000). Images were acquired using either an inverted epifluorescent microscope (Olympus IX-81 with ZDC, Olympus Scientific Solutions Americas) with a 20x air objective (0.3NA, Olympus Scientific Solutions Americas) and Hamamatsu Flash 4.0 v1 CMOS camera (Hamamatsu Corporation), or an Olympus 3I spinning disk confocal microscope (Olympus IX-81, Olympus Scientific Solutions Americas) equipped with a 40x oil objective (1.3NA, Olympus Scientific Solutions Americas) and Andor Zyla 4.2 CMOS camera (Andor Technology Ltd). Images were representative of at least 5 images collected from each of three biological replicates per stage. Intensity and contrast of each image were adjusted simultaneously and globally to the same level to accomplish fair comparison between images.

Histology

Mouse embryos were isolated at E14.5 and fixed overnight in 4% paraformaldehyde at 4°C. Fixed embryos were embedded in paraffin and transversally sectioned at 7μm by Leica RM2255 microtome. The slides were stained using hematoxylin and eosin reagents according to previously published protocol (Fischer et al., 2008). Staining results were documented by Leica DMS300 Dissection Microscope equipped with digital camera.

LacZ staining

Dhrs3$^{+/-}$; *RARE-LacZ* mice were mated to produce *Dhrs3*$^{-/-}$; *RARE-LacZ* and *Dhrs3*$^{+/+}$; *RARE-LacZ* embryos which were isolated at various developmental stages to evaluate the activity of LacZ using previously established protocol (Billings et al., 2013). Samples in both experimental and control groups

were processed simultaneously using identical protocol and were documented using Leica DMS300 Dissection Microscope equipped with digital camera.

Transcriptome analysis

MEC1 cells were treated with vehicle (DMSO) or 10nM TTNPB for 48 hours and isolation of RNA using TRIZOL reagent according to manufacturer's protocol. RNA was pretreated with Invitrogen™ DNA-free™ DNA Removal Kit (Cat # AM1906) before submission for cDNA library assembly.

Statistical analysis

Data were represented means ± standard deviation and unpaired Student's *t*-test was utilized to evaluate statistical difference between groups.

4.3. Results

Excess RA affects the late development of the heart

To test the teratogenic effect of excess RA in the development of the heart, we employed a mouse model lacking the enzyme, DHRS3, which reduces the RA precursor, retinaldehyde, to retinol and thus prevents the synthesis of excess RA. Our lab has previously shown that in the absence of DHRS3, RA accumulates and causes alterations in RA-signaling both globally and within the developing hearts of *Dhrs3*$^{-/-}$ embryos ((Billings et al., 2013) and Chapter 3). Here, we first confirmed that *Dhrs3*-ablation results in altered RA-signaling in *Dhrs3*$^{-/-}$ mice at E12.5, a stage marked by the rapid myocardial growth and coronary plexus development. We crossed the *Dhrs3*$^{+/-}$ mice with the *RARE-LacZ* mouse strain which expresses a *LacZ* reporter gene driven by a promoter controlled by a RARE derived from the *Rarb* promoter (Rossant et al., 1991). This was done to allow us to visualize the domains associated with active RA-signaling in the developing embryos. The detection of the activity of *LacZ*-encoded β-galactosidase revealed that at E12.5, ablation of *Dhrs3* causes an evident expansion of RA-signaling domains in the mutant heart (Fig S1A-D), suggesting that the hearts of E12.5 *Dhrs3*$^{-/-}$ embryos, in accordance with the similar findings observed in E10.5 *Dhrs3*$^{-/-}$ embryos ((Shannon et al., 2017) and Chapter 2). The

expanded domains of RA-signaling in the hearts of *Dhrs3*$^{-/-}$ embryos at midgestation are consistent with the observed increases in the global levels of RA as quantified by direct analysis via LC-MS/MS at E12.5 and E14.5 in *Dhrs3*$^{-/-}$ embryos ((Billings et al., 2013) and Chapter 3).

Dhrs3$^{-/-}$ embryos display mid-gestational lethality accompanied by defects in the development of the heart (Supplementary Fig 4.1E *vs.* F). As we have previously reported, global ablation of *Dhrs3* is associated with a membranous ventricular septal defect, a lack of atrial septum and a double outlet right ventricle (DORV) in E14.5 *Dhrs3*$^{-/-}$ embryos (Billings et al., 2013). Examination of the gross morphology of the E14.5 *Dhrs3*$^{-/-}$ embryos indicated that *Dhrs3* mutant embryos showed evidence of peripheral edema suggesting cardiac insufficiency. The ventricular myocardium of E14.5 *Dhrs3*$^{-/-}$ embryos has a 2-fold reduction in the thickness of its compact zone in comparison to wild-type littermates (Fig 4.2A-D, quantified in 4.2E). A hypoplastic ventricular myocardium has been observed in other models with altered RA signaling (S. C. Lin et al., 2010; Merki et al., 2005; Niederreither et al., 2001). Therefore *Dhrs3*-deficiency results in ventricular hypoplasia and defects in heart septation and in alignment of the outflow tract.

Ablation of *Dhrs3* is associated with delays and defects in the formation of the coronary vasculature. *Dhrs3*$^{-/-}$ embryos displayed a 40% reduction in the coronary vessel coverage of the dorsal ventricles when compared to the wild-type littermates as observed at E13.5 (Supplementary Fig 4.2A-B, quantified in S4.2C). As the primitive plexus matures, the vessels of the wild-type heart experienced remodeling including pruning and branching (Fig 4.1K). However, in the *Dhrs3*$^{-/-}$ heart, the vessels remained tortuous, aberrantly enlarged, lacking branching from pre-existing vascular beds (Fig 4.1L). This defect is especially noticeable near the atrioventricular canal (AVC) of the *Dhrs3*$^{-/-}$ hearts, where the vessels formed a single endothelial trunk, which had very few branches (Fig 4.1L, red arrow). Additional related cardiovascular defects become apparent in the *Dhrs3*$^{-/-}$ hearts at E14.5. Most notably, PECAM1-positive endothelial nodules were observed on the ventral side of the ventricles of *Dhrs3*$^{-/-}$ hearts in larger numbers, of greater size and with a broader distribution than seen in wild-type littermates (Fig 4.1F *vs*. G,

quantified in 4.1I). Such epicardial nodules which may originate as ectopic blood islands have been observed in other mouse models that exhibit defects in the development of the coronary vasculature (A. M. Mellgren et al., 2008; N. Smart et al., 2012; Tian et al., 2013; H. Wu et al., 1999; S. P. Wu, Dong, Regan, Su, & Majesky, 2013).

In order to validate that the coronary vessel malformations observed in the *Dhrs3*$^{-/-}$ embryos develop as a consequence of excessive RA, we fed the *Dhrs3*$^{+/-}$ dams with a vitamin A-deficient (VAD) diet since weaning; our hypothesis being that the lower vitamin A intake can reduce the levels of RA being generated and restore normal RA levels and development in the *Dhrs3*$^{-/-}$ embryos. Indeed, feeding dams a VAD diet led to the restoration of the vascular coverage of the dorsal ventricles of *Dhrs3*$^{-/-}$ embryos to normal levels at E14.5. Meanwhile the *Dhrs3*$^{-/-}$ embryos from dams fed a vitamin A-sufficient (VAS) diet experienced developmental delays and reduced coronary vessel coverage of the heart of compared to either wild-type littermates from dams fed on VAS diet or *Dhrs3*$^{-/-}$ embryos from dams fed on VAD diet (Fig 4.1L *vs*. M, vessel coverage is quantified in O) . Feeding dams VAD diet led to both improved vascular remodeling and reduced formation of endothelial nodules in the *Dhrs3*$^{-/-}$ hearts (Fig 4.1G *vs*. H). In fact, feeding dams a VAD diet, allowed us to bypass the embryonic lethality associated with the *Dhrs3*-deficiency to obtain living viable *Dhrs3*$^{-/-}$ pups that survived into adulthood. In conclusion, our data suggest that increased RA formation is the cause of the developmental defects resulting from genetic deletion of *Dhrs3*.

Analysis of the morphology of intramyocardial vessels in the *Dhrs3*$^{-/-}$ hearts indicated a loss of vessel hierarchy. PECAM1 immunostaining of transversal sections indicated that vessels in the Dhrs3$^{-/-}$ hearts showed little distinction between vessels, whereas wild-type hearts developed an extensive arborization of vessels with different calibers (Fig 4.1P *vs*. Q). Both subepicardial and intramyocardial vessels in the *Dhrs3*$^{-/-}$ hearts were consistently enlarged compared to vessels in wild-type hearts (Fig 4.1P *vs*. Q, quantified in N). Because of their aberrant vessel size, *Dhrs3*$^{-/-}$ hearts have a significantly reduced vascular density per area of myocardium (Fig 4.1J). Particularly, there is an accumulation of dilated and

superficial vessels in the subepicardium of *Dhrs3* mutant embryos, which we identified as COUP-TFII-positive veins (Fig 4.1R *vs*. S). *In situ* hybridization of COUP-TFII in *Dhrs3*$^{-/-}$ hearts at E9.5 revealed relatively normal localization and expression levels of COUP-TFII in the primitive *Dhrs3*$^{-/-}$ heart tube, suggesting that the early patterning of the heart was normal (Supplementary Fig 4.3). The enlargement of coronary vessels persisted into late gestation in the few surviving E17.5 *Dhrs3*$^{-/-}$ fetuses which exhibited a combination of normal-sized intramyocardial arteries and very large, collapsed, superficial veins (Supplementary Fig 4.2D-G).

Thus altered RA homeostasis led to perturbations in the hierarchical organization and vascular density of coronary vessels in mouse embryos. Taken together, our results based on suggest that excessive formation of RA in *Dhrs3*$^{-/-}$ embryos affects not only epicardial EMT, but also the subsequent development of coronary vessels.

Excess RA does not affect vessel formation in the placenta and the embryonic yolk sac.

Deletion of *Dhrs3* has been found to cause global elevations of RA levels and expanded RA-signaling ((Billings et al., 2013) and Chapter 3). RA-signaling plays important roles in the development of the placental, and yolk sac vascular plexi (Lai, Bohnsack, Niederreither, & Hirschi, 2003) and the formation of the hematopoietic stem cells from the hemogenic endothelium (Chanda, Ditadi, Iscove, & Keller, 2013). Given the effects of *Dhrs3*-deficiency on the development of the coronary vasculature, we further investigated if *Dhrs3*-deficiency affects the development of vasculature in the placenta and yolk sac.

Histology analysis using hematoxylin and eosin revealed normal placental morphology in *Dhrs3*$^{-/-}$ mice when compared with wild-type littermates at E13.5 and E14.5 (Supplementary Fig 4.4A-D). Quantification of the thickness and density of the vascular labyrinth, did not find any significant difference between wild-type and *Dhrs3* mutant embryos (Supplementary Fig 4.4E,J). Deletion of *Dhrs3* did not impede the formation and branching of vascular tubes from the chorionic plate; neither did it affect the placental vascular patterning (Supplementary Fig 4.4F-I). Hence, the excess RA formed in *Dhrs3*$^{-/-}$ mice has minimal influences on the placental vascular development in mouse embryos.

In addition to the placental vascular system, the vessels in yolk sac have also been found to be critical for embryonic development especially at early embryonic stages (Dominguez et al., 2007). Both *Dhrs3* mutant mice and their stage-matched wild-type littermates had an intact embryonic yolk sac plexus composed of a finely branched and properly developed network as observed by whole-mount PECAM1 immunostaining (Supplementary Fig 4.5A-B). Therefore, the deleterious effects of altered RA-signaling in *Dhrs3*$^{-/-}$ embryos do not affect the vasculogenesis and remodeling of placental and yolk sac plexus.

Excess RA interferes with the recruitment and differentiation of VSMC progenitors

VSMCs and pericytes are critical for coronary vessel morphogenesis and function (Amy M. Mellgren et al., 2008; Trembley et al., 2015). Coronary vascular mural cells, which are derived primarily from the epicardium via EMT, migrate into the myocardium where they are required in vascular stabilization and remodeling (C. L. Smith et al., 2011). We and others have shown that RA-signaling plays a critical role in both the epicardial EMT and the differentiation of VSMC progenitors ((Azambuja et al., 2010; Caitlin M. Braitsch et al., 2012) and Chapter 3). Specifically, *Dhrs3*$^{-/-}$ EPDC were found to migrate deeper into the myocardium of E14.5 *Dhrs3*$^{-/-}$ mice. Studies described herein suggest that *Dhrs3*$^{-/-}$ mice have compromised coronary vessel as a result of RA excess. Therefore, we investigated if the recruitment of VSMC by the coronary plexus is affected in *Dhrs3*$^{-/-}$ hearts.

We investigated the localization and recruitment of VSMC progenitors to the endothelial tubes by double-immunostaining of both PDGFRB and PECAM1 in the wild-type and *Dhrs3*$^{-/-}$ hearts. The staining results suggested that most vessels are associated with PDGFRB-positive vessels in both wild-type control embryos and mutant hearts (Fig 4.2A-H). However, there are more PDGFRB-positive cells not found to be associated with any vessels in the *Dhrs3*$^{-/-}$ hearts. At the same time there are PECAM1-positive endothelial tubes devoid of VSMC progenitors in the *Dhrs3*$^{-/-}$ hearts (Fig 4.2C *vs*. G, yellow arrow). We examined the recruitment of PDGFRB-positive VSMC progenitors in surviving E17.5 embryos. Consistent with earlier stages, PECAM1 immunostaining revealed that *Dhrs3*$^{-/-}$ hearts consisted of malformed, large caliber vessels. Though at E14.5, some VSMC progenitors were found to be in the

vicinity of endothelial tubes, PDGFRB immunostaining at E17.5 revealed a surprising absence of VSMC progenitors near the PECAM1-positive vessels in the *Dhrs3* mutant hearts (Fig 4.2I-P) suggesting that excess RA-signaling affects the recruitment and stability of VSMC progenitors on the endothelial tubes. The large subepicardial veins still observable in *Dhrs3*$^{-/-}$ hearts at E17.5 (Supplementary Fig 4.2E, G) were the most severely affected and found to be devoid of mural PDGFRB-positive cells (Fig 4.2O-P). PDGFRB marks not only progenitors of VSMCs but also pericytes that are recruited to capillaries and postcapillary venules. In contrast to larger vessels, PDGFRB-positive mural cells were found to be in direct contact with the PECAM1-positive endothelial cells of capillaries (Fig 4.2J *vs*. N) though this colocalization does not provide information about whether the two types of cells have established proper communication. Furthermore, VSMC progenitors failed to differentiate into mature VSMC in *Dhrs3*$^{-/-}$ hearts when compared to wild-type hearts, as revealed by the lack of expression of SM22α in mural cells around major vessels (Fig 4.3). Thus, excess RA influences the recruitment, stabilization and differentiation of PDGFRB-positive VSMC progenitors.

RA deficiency leads to defective formation of the myocardium and the coronary vessels

Previously we have described the establishment of the mid-gestational RA deficiency model by by administration of Win 18, 446 (WIN), an inhibitor of the aldehyde dehydrogenase 1A family of enzymes which convert retinaldehyde to RA. WIN, previously investigated as a potential male contraceptive (Heller, Moore, & Paulsen, 1961), is a potent inducer of congenital heart defects including coronary defects, yet, the cause for such defects remains poorly understood (Binder, 1985; Fujino et al., 2005; Hanato et al., 2011; Ito et al., 1992; Jackson, Connell, Smith, Drury, & Anderson, 1995; Kilburn, Hess, Lesser, & Oster, 1982; Kise et al., 2005; Kuribayashi & Roberts, 1993; Nishijima et al., 2000; Okamoto et al., 2004; Okishima, Takamura, Matsuoka, Ohdo, & Hayakawa, 1992; Oster et al., 1974; Tasaka et al., 1991). We found that administration of WIN between E9.5 and E13.5 dramatically reduced the amount of RA and alters RA-signaling in developing mouse embryos and their heart (Chapter 3). Importantly, we found that administration of WIN affects the epicardial EMT and migration of EPDC into the

myocardium (Chapter 3). Examination of the gross morphology of WIN-treated embryos showed signs of imminent heart failure as evidenced by the accumulation of body fluid on the back of the embryo (Fig 4.4A *vs*. B). Histology analysis of vehicle- or WIN-treated embryos suggested a normal development of the heart chamber in response to WIN-treatment at mid-gestation, yet, the WIN-treated animals had myocardial hypoplasia manifested as a 50% thinner myocardium compact zone when compared to the vehicle control-treated group (Fig 4.4C *vs*. D, quantified in 4K).

We next investigated if inadequate formation of RA during mid-gestation can affect coronary development. Whole-mount immunostaining of endothelial cells via PECAM1 suggested that whereas vessels developed and sprouted normally in the vehicle control group, coronary vessels failed to fully expand to the ventricular apices in the WIN-treated hearts (Fig 4.4E *vs*. F). Quantification of vessel coverage revealed a 20% reduction in the hearts of the WIN-treated group compared to the control (Fig 4.4L). In addition, RA deficiency also altered the vascular hierarchy of the coronary plexus. At E14.5, vehicle-treated embryonic hearts displayed a well-organized coronary vessel network with several major vessels developing from the AVC coursing towards the apex and branching out to smaller vessels. In contrast, WIN-treated embryos showed evidence of defects in the formation and maturation of the vascular network marked by few clearly distinguishable major branches and a conspicuous absence of the interventricular artery (Fig 4.4M). Upon examining intramyocardial vessel morphology we found that WIN treatment led to excessive formation of vessels of small diameter (Fig 4.4G-J, quantified in 4N). Consistent with the reduced vascular coverage observed with the whole-mount PECAM1 staining, the myocardium near the apices in E14.5 WIN-treated embryos is devoid of vessels and the density of intramyocardial vessels is overall reduced (Fig 4.4H *vs*. J, density quantified in 4O).

We next investigated the recruitment of VSMC progenitors to the coronary vessels at E14.5 in vehicle and WIN-treated embryos. Endothelial cells and VSMC progenitors were visualized by double immunostaining of PECAM1 (green) and PDGFRB (red) at E14.5 in embryonic hearts (Fig 4.5). Previously, we reported reduced migration of EPDC in response to WIN treatment in both *in vivo* and *in*

vitro models (Chapter 3). As a consequence, there are fewer PDGFRB-positive cells in the myocardium surrounding coronary vessels of WIN-treated embryos (Fig 4.5A vs. E). However, the PDGFRB-positive EPDCs that have infiltrated the myocardium were found to be near or adjacent to the endothelial tubes, which indicates that the initial recruitment of VSMC progenitors to the coronary vessels is not severely affected by the reduced RA formation in the WIN-treated group.

RA-signaling regulates the epicardial transcriptome

Both fetal and postnatal epicardium secretes signaling molecules that stimulate the growth and repair of the heart (Olivey & Svensson; B. Zhou et al., 2011). RA-signaling can stimulate epicardial cells to produce trophic factors to enhance the proliferation of cardiomyocytes (Thomas Brade et al., 2011; T. Chen et al., 2002; Merki et al., 2005; Shen et al., 2015; Ingo Stuckmann et al., 2003).

To define the effects of altered RA-signaling on epicardial cell signaling we performed transcriptome profiling on a ventricular epicardial cell line, MEC1, treated for 48 hours with 10nM TTNPB, a stable RAR pan-agonist (Chapter 3). Upon analysis we identified 6,931 genes being differentially regulated in MEC1 cells by TTNPB treatment compared to the vehicle control-treated group. TTNPB led to the RA-signaling by up-regulating the expression of multiple known RA-modulated genes, including *Rarβ*, *Rbp1* and *Hoxa1* (Fig 4.6A). TTNPB treatment also induced compensatory responses in RA metabolism to inhibit its synthesis and activate its degradation; such an effect is commonly seen in models of excessive RA-signaling. Within the list of differentially expressed genes, we also found the RAR-agonist treatment of MEC1 cells induced the expression of cardiotrophic factors such as *Fgf2* and *Fgf9* as well as mediators of FGF signaling (Fig 4.6B; altered genes are listed in Supplementary Table 4.1). Activation of RAR in MEC1 epicardial cells leads to down-regulation of the expression of *Igf2* by over 75% (Fig 4.6C) which supports the regulation of this particular cardiotrophic pathway by extra-cardiac RA signaling. Pathway analysis of the transcriptome data derived from TTNPB-treated MEC1 cells versus control revealed that HIF-1α signaling was broadly attenuated by activation of RAR in epicardial cells. This was evident as a down-regulation of *Hif1α* as well as multiple known effectors of HIF-1α signaling, such as *Vegfα*, *Tgfα*

and *Hyou1* (Fig 4.6D). The expression of several angiopoietin and angiopoietin-like proteins known to be hypoxia-responsive were also observed to be altered in response to TTNPB-treatment in MEC1 epicardial cells. Therefore, analysis of the RNAseq data revealed that RA alters the gene expression profile of MEC1 resulting in alterations in growth-promoting and angiogenic pathways. Collectively, our results suggest that besides its better understood roles in early cardiogenesis, RA-signaling also plays critical roles in the regulation of the growth of the myocardium and the formation and maturation of the coronary vasculature.

4.4. Discussion

We report here that alterations of RA-signaling can cause defects and delays in the formation of the coronary vasculature. These defects are observable in the case of either excess or deficiency of RA. First, using *Dhrs3*$^{-/-}$ embryos, a mouse model exhibiting mildly elevated embryonic RA (Billings et al., 2013), we showed that excess RA caused delays in the formation of the coronary vascular plexus and abnormalities in coronary vessel morphology and branching. The most severe consequences of *Dhrs3*-ablation were the formation of ectopic endothelial nodules and of large aberrant subepicardal veins, the latter of which persisted in the few *Dhrs3*$^{-/-}$ embryos surviving to late gestation. The defects seen in *Dhrs3*$^{-/-}$ embryos could be averted by reducing the maternal vitamin A intake of the dam, thus, demonstrating that the effects of *Dhrs3*-ablation on heart development were indeed the result of excess RA. In a second approach, starting at midgestation, we administered WIN to block RA synthesis. By doing so, we avoided the lethality and early cardiogenic defects resulting from RA deficiency and observed in early WIN-treated embryos (Oster et al., 1974). Late WIN-treated embryonic hearts were properly chambered and had similar gross morphology when compared to the vehicle-treated group, yet, experienced a 60% reduction in the global levels of all-*trans*-RA and showed very restricted RA-signaling in the E14.5 heart (Chapter 3). Importantly, RA deficiency caused by WIN administration led to the formation of predominantly small-caliber vessels with few major arterial branches. Both deficiency and excess of RA caused defects in coronary vascular remodeling leading to alterations in coronary vessel

hierarchy and the intramyocardial vascular density. Important many of the intramyocardial vessels failed to become invested with mural cells expressing markers of mature VSMCs. Our results therefore establish a critical role for RA in the formation, remodeling and maturation of the coronary vasculature.

Both deficiency and excess RA can result in various cardiovascular malformations in developing embryos (Lammer et al., 1985; Niederreither et al., 2001; L. Ryckebusch et al., 2008). Due to the essential roles of RA during early embryogenesis, extensive changes in embryonic RA-signaling often result in embryonic lethality. As a result, the role of RA in the later stages of heart development is less well understood. The main source of cardiac RA in the late heart development of the heart is the epicardium (J. B. Moss et al., 1998; Niederreither, Fraulob, Garnier, Chambon, & Dolle, 2002; J. M. Perez-Pomares et al., 2002). The epicardium is responsible for the growth of the myocardial compact zone and for generating precursors of primarily VSMCs, and cardiac fibroblasts. Therefore, alterations in RA formation during late heart development affect primarily epicardial RA-signaling and have the potential of influencing important epicardial-related events in late heart development.

RA generated from cardiac (epicardial) and extra-cardiac sources influences the secretion of cardiotrophic factors by the epicardium. The ventricular myocardium grows during mid-gestation and has been found to be sensitive to altered levels of RA-signaling in the heart (S. C. Lin et al., 2010; Lohnes et al., 1994; Merki et al., 2005). The growth of the myocardium is dependent among other factors on cardiotrophic factors, such as IGF2, first proposed to be secreted by the epicardium in response to cell-autonomous RA-signaling (T. Chen et al., 2002; Merki et al., 2005; Ingo Stuckmann et al., 2003), but later shown to be secreted in response to RA-signaling in extra-cardiac (liver and placental) tissues (Thomas Brade et al., 2011; Shen et al., 2015). One possible explanation of thinned myocardium in *Dhrs3*$^{-/-}$ mice is that aberrant RA-signaling in either cardiac or extra-cardiac tissues causes alterations in the epicardial transcriptome. In our transcriptome analysis of RAR agonist-treated epicardial MEC1 cells we observed that RA-signaling causes the up-regulation of the expression of several mitogenic proteins, including FGF2 and FGF9 and follistatin-like 1 (FSTL1), previously proposed to be involved in

myocardial growth and coronary vascularization (K. J. Lavine et al., 2005; D. J. Pennisi & Mikawa, 2005; Vega-Hernandez, Kovacs, De Langhe, & Ornitz, 2011; Wei et al., 2015). The expression of the epicardial secreted cardiotrophic factor, IGF2, as well as its receptor IGFR2 was down-regulated in response to induction of RA-signaling in epicardial cells (Supplementary Fig 5) suggesting that IGF2 secretion relies on secondary signaling from RA produced by extra-cardiac sources (Thomas Brade et al., 2011; Shen et al., 2015). In addition, the expression of proteins antagonizing IGF functions, namely IGF binding proteins, was found to be highly induced in RAR agonist-treated MEC1 cells. The possibly reduced IGF signaling might contribute to the teratogenic effects of altered RA in the myocardial growth.

RA affects the development of EPDCs and epicardial-derived lineages which are necessary for the proper development of the coronary vasculature. We have previously shown that RA signaling controls the cytoskeletal reorganization of epicardial cells via Rho-signaling (Chapter 3). *In vivo*, both excess or deficiency of RA affect the extent and timing of the infiltration of the myocardium by EPDCs. In addition, RA-signaling acting via TCF21 delays the differentiation of VSMCs (Azambuja et al., 2010; Caitlin M. Braitsch et al., 2012). Recruitment of mural cells in the form of VSMCs and pericytes is required for the proper angiogenic remodeling and maturation of vessels (reviewed in(Gaengel, Genove, Armulik, & Betsholtz, 2009)) and defects in VSMC/pericyte formation or recruitment often lead to endothelial defects and vascular abnormalities and decreased ventricular vascular coverage (Hellstrom et al., 2001; Hellstrom, Kalen, Lindahl, Abramsson, & Betsholtz, 1999; A. M. Mellgren et al., 2008; C. L. Smith et al., 2011; Trembley et al., 2015; Volz et al., 2015Trembley, 2015 #3852). Likewise, defects in VSMC/pericyte formation or recruitment observed in the hearts of *Dhrs3*$^{-/-}$ or WIN-treated embryos could account for the compromised coronary vessel remodeling and maturation seen in these models. However, these interesting possibilities require further investigation.

Alterations in RA-signaling during the late heart development often translate into defects or delays in both myocardial growth and the formation of the coronary vasculature. For example, a hypoplastic ventricle and coronary vascular defects have been observed in mice with either an epicardial-ablation of

RXR (Merki et al., 2005) and in mice deficient in the RA synthetic enzyme RALDH2 (S. C. Lin et al., 2010). Here, we show that embryos affected by RA excess or RA deficiency had defects and delays in the formation and the primary coronary vessels and that their coronary vessels did not become invested with mature VSMCs. In all above mentioned examples the coronary vascular defects are accompanied by hypoplastic myocardium and, in some cases, by other cardiac defects in outflow tract formation, chamber formation and septation ((S. C. Lin et al., 2010; Lohnes et al., 1994) and Chapter 4). Since the growth of the compact zone of the myocardium is dependent on the proper provision of oxygen and nutrients provided by the coronary vasculature, the hypoxia resulting from coronary defects may compromise its growth (Ream, Ray, Chandra, & Chikaraishi, 2008). Nonetheless, induction of HIF1α-signaling is important for fetal growth and angiogenesis and for proper coronary vessel formation (Tomanek, Lund, & Yue, 2003; Tomanek, Ratajska, Kitten, Yue, & Sandra, 1999; Wikenheiser, Doughman, Fisher, & Watanabe, 2006; Yue & Tomanek, 1999). In addition, we observed that RA treatment of MEC1 epicardial cells caused alterations in the expression of factors involved in HIF1α-signaling and angiopoiesis. The causal relationship among congenital coronary anomalies and other congenital cardiac defects is not understood but it is quite possible that they share common pathogenic mechanisms and that they influence each other through reciprocal interactions (Cano et al., 2016).

In summary, our results demonstrate the importance RA-signaling in the development of the coronary vasculature and ventricular myocardium. RA-signaling influences the secretion of epicardial cardiotrophic factors and the development, recruitment and differentiation of EPDCs. Sharing a common signaling mediator allows the aforementioned cardiogenic pathways to simultaneously orchestrate the growth and vascularization of the heart. Future studies focused on the downstream effectors of RA-signaling will be able to differentiate its mitogenic and angiogenic pathways. Deficiency of vitamin A or administration of retinoid-based therapies during pregnancy can expose fetuses to high risks of congenital heart diseases with the most sensitive window having been proposed to be during early embryogenesis (Lammer et al., 1985). Studies presented here and elsewhere caution that mid-gestation exposure to

retinoid therapies or to excess or vitamin A deficiency could lead to late heart maturation defects including congenital coronary anomalies and hypoplastic myocardium and therefore these considerations could contribute to the roadmap for mechanism-based dietary recommendations during gestation.

FIGURES

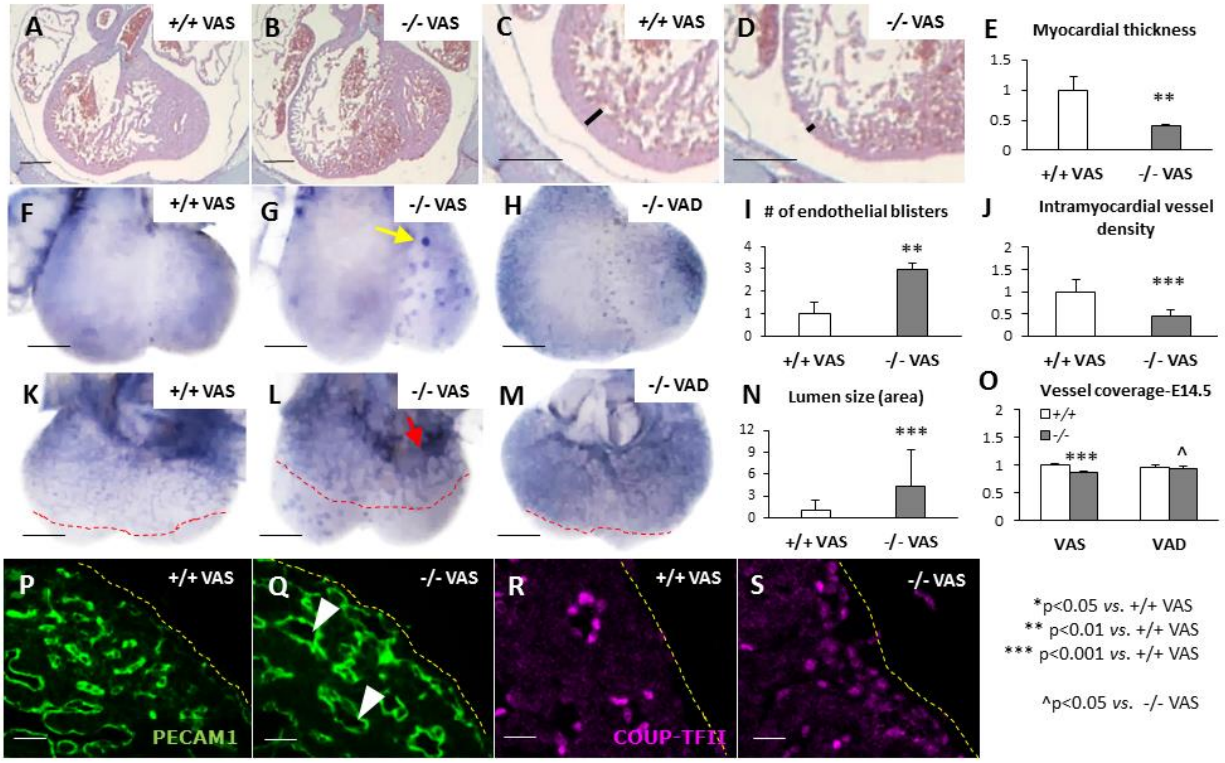

Figure 4.1 Ablation of *Dhrs3* compromises myocardial growth and coronary vessel formation via excess formation of RA.

Examination of heart morphology at E14.5 revealed an evident reduction in myocardial thickness in ventricles of *Dhrs3*$^{-/-}$ (-/-) embryos when compared to wild-type (+/+) controls (**A**-**D** enlarged and marked by **black bars** in **C** *vs.* **D** quantified in **E**). Whole-mount PECAM1 staining (*purple*) of endothelial cells suggest that E14.5 *Dhrs3*$^{-/-}$ embryos developed more numerous and larger ectopic endothelial nodules on the ventral side of the heart (**F** *vs.* **G**, *yellow arrow*, numbers of nodules quantified in **I**). At E14.5 *Dhrs3*$^{-/-}$ embryos had a compromised vascular network morphology as well as reduced vascular expansion towards the apices (**K** *vs.* **L**, quantified in **O**; *red dashed lines* mark the apical edges of the plexi). Near the AVC of *Dhrs3*$^{-/-}$ hearts, the vessels fused to form a large diffuse endothelial trunk (Fig 2L, *red arrow*). Feeding VAD diet to the dam restored the vascular coverage of E14.5 *Dhrs3*$^{-/-}$ embryos and decreased size and number of endothelial blisters compared to *Dhrs3*$^{-/-}$ embryos from dams on VAS diet

(**L** *vs*. **M**, **G** vs **H**, vascular coverage quantified in **O**). At E14.5 *Dhrs3*-deficiency resulted in enlargement of both intramyocardial and subepicardial coronary vessels (**P** *vs*. **Q**, *white arrowhead*, lumen sizes are quantified in **N**), accumulation of superficially localized-veins (**R** *vs*. **S,** *yellow dashed line* marks the surface of the heart) and reduced intramyocardial vessel density (**J**) as observed via PECAM1 (in **P**, **Q**, *green*) and COUP-TFII (in **R,S,** *violet*) immunostaining of sections of transversal sections. Analyses were performed based on at least three biological replicates. Scale bars represent 200μm in A-D, 400μm in F-H and K-M, 20μm in P-S. Error bars represent standard deviation. * $p<0.05$ *vs*. VAS-WT; ** $p<0.01$ *vs*. VAS-WT; *** $P<0.001$ *vs*. VAS-WT; ^ $p<0.05$ *vs* VAS-Dhrs3 KO.

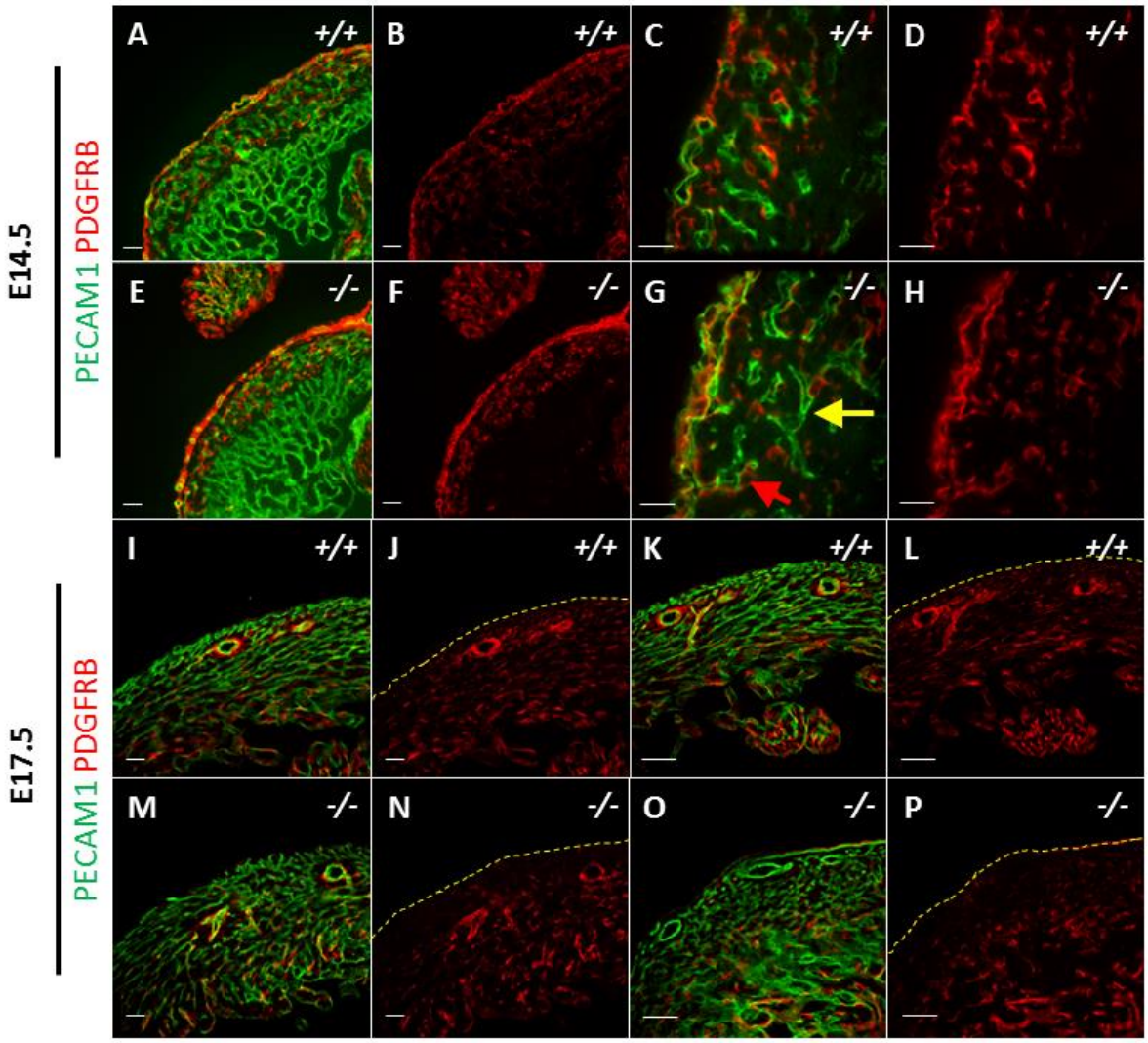

Figure 4.2 *Dhrs3*-deficiency affects the recruitment of PDGFRB-positive VMSC progenitor cells to endothelial tubes.

At E14.5, PDGFRB-positive (*red*) cells were found to be near PECAM1-positive (*green*) endothelial tubules of wild-type (+/+) embryos (**A-D**). In *Dhrs3*$^{-/-}$ (-/-) embryos, PDGFRB-positive cells were found near the superficially-localized vessels (**E-H**) including close juxtaposition with vascular endothelia (**G,** *red arrow*) but there are vessels devoid of PDGFRB-positive cells (**G,** *yellow arrow*). At E17.5 large-caliber intramyocardial vessels in the wild-type embryos were surrounded by a layer of PDGFRB-positive, VMSC progenitor cells (**I-L** *yellow dashed line* marks the surface of the heart). In contrast, vessels of similar sizes in *Dhrs3*$^{-/-}$ embryos had a thin, sparse coverage of PDGFRB-positive cells. Many

of the abnormally enlarged superficial, subepicardial vessels were found to be devoid of coverage by VMSCs (**M-P)**. Scale bars represent 50μm in A-B, E-F, I-J and M-N; 20μm in C-D, G-H, K-L and O-P. Images are representative of at least three embryos per genotype per stage examined.

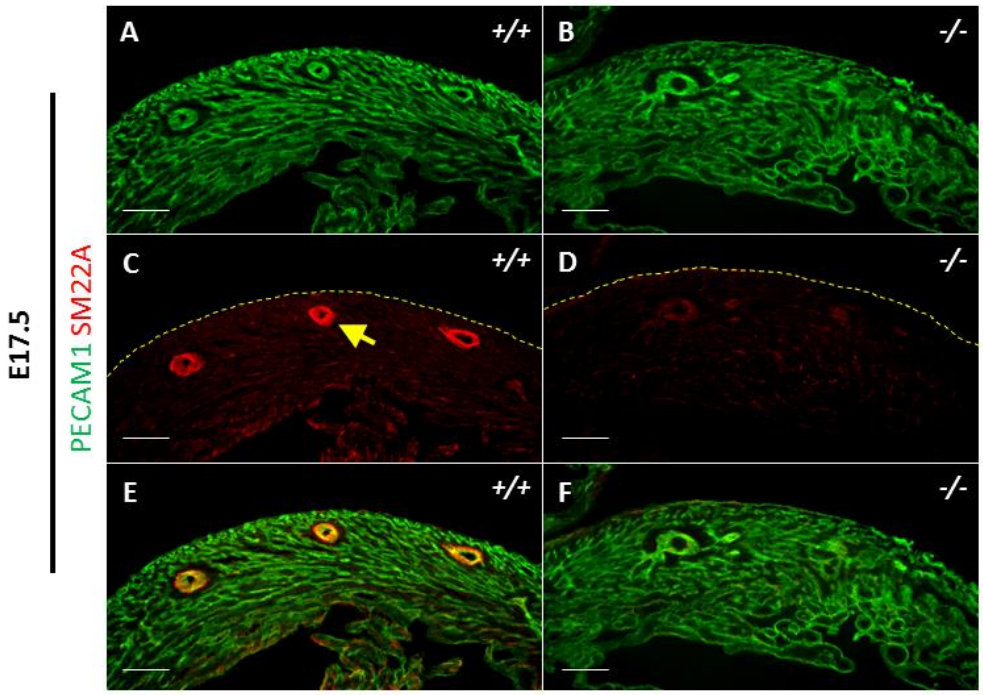

Figure 4.3 *Dhrs3*-deficiency affects the differentiation and recruitment of VSMCs.

Double labeling of PECAM1 (*green*) and VSMC marker SM22A (*red*) in *Dhrs3*$^{-/-}$ (-/-) and wild-type (+/+) embryonic hearts at E17.5 revealed a reduced expression of SM22A in the mural vascular cells of *Dhrs3*$^{-/-}$ embryos in contrast to the presence of SM22A-positive around vessels in the wild-type hearts (**C**, *yellow arrow*). A *yellow dashed line* marks the surface of the heart. Scale bars represent 100um. Images are representative of at least three embryos per genotype.

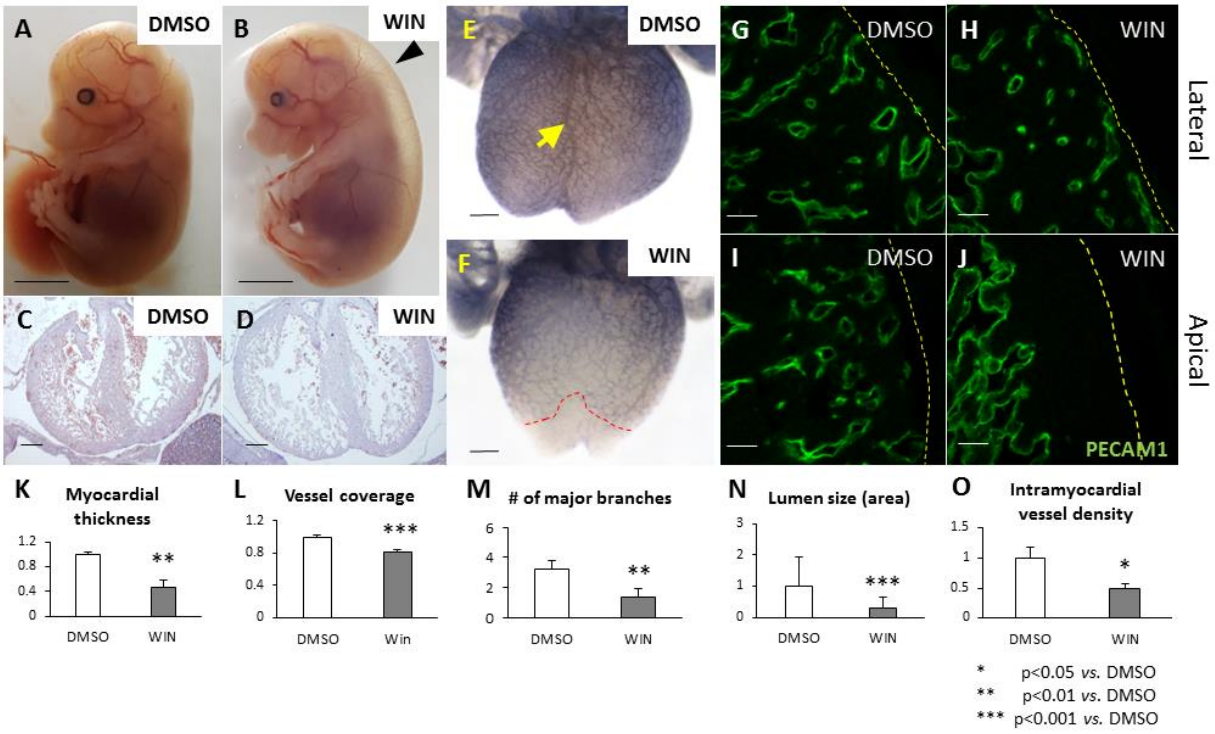

Figure 4.4 RA deficiency compromises myocardial growth and coronary vessel formation.

Embryos from dams treated with vehicle (**DMSO**) or WIN 18,446 (**WIN**) from E9.5 to E13.5 were isolated at E14.5. Embryos from the WIN-treated group showed evident subcutaneous edema (**A** *vs*. **B**), and significantly compromised growth of the ventricular myocardium as visualized by Hematoxylin and Eosin staining (**C** *vs*. **D**, quantified in **K**). Whole-mount PECAM1 immunostaining (**E, F**, *purple*) indicated that vehicle control-treated embryos develop a finely branched and a well-organized vascular network (**E** *vs*. **F**, number of major branches was quantified in **M**). In comparison, WIN treatment drastically altered the number and localization of the major branches of vessels that sprout towards the apex of the heart including the absence of the interventricular coronary artery branch (**E** *vs*. **F,** marked by *yellow arrow* in **E**). WIN treatment resulted in a 20% reduction in vascular coverage of the ventricles when compared to the vehicle group (**E** *vs*. **F**, quantified in **L,** a *red dashed line* marks the apical edge of the vascular network on the dorsal side of ventricles) leading to avascular areas near the ventricular apices (**I** *vs*. **J**). Administration of WIN led to a reduction in the density and caliber of intramyocardial vessels (**G** *vs*. **H**, lumen sizes quantified in **N**, vessel density per area in the myocardium quantified in **O**) as

revealed by PECAM1 (**G,I**, *green*) immunostaining of transversal sections (*yellow dashed line* marks the surface of the heart). Scale bars represent 2mm in A-B , 200μm in C-F , 20μm in G-J. Images are representative of at least three embryos per treatment.

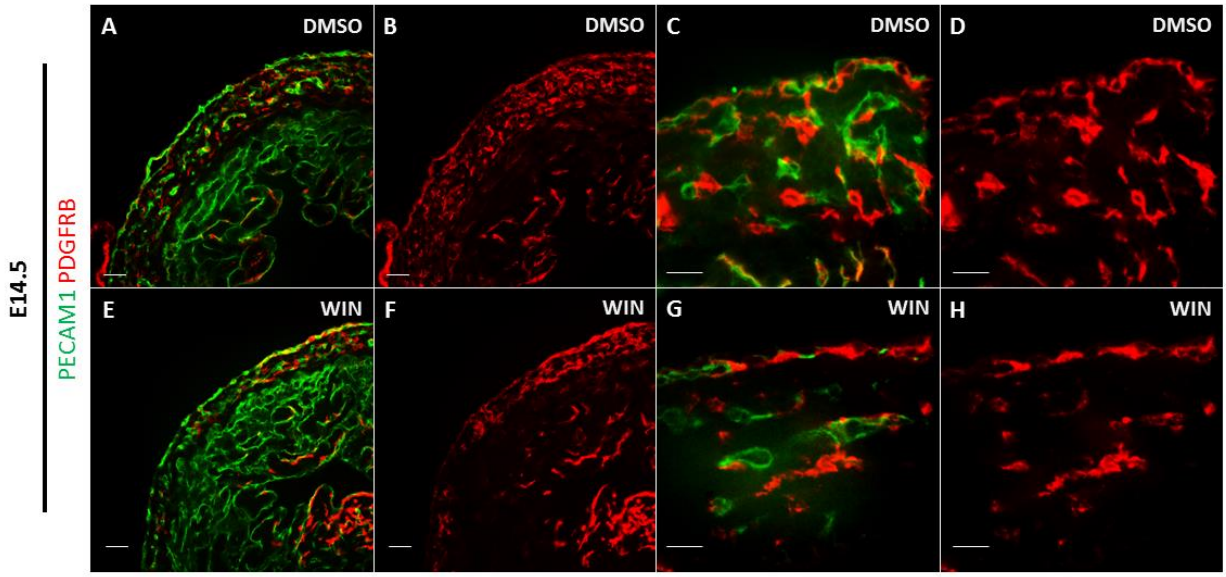

Figure 4.5 RA deficiency affects the migration of epicardial-derived VSMC progenitor cells in WIN-treated embryonic hearts.

Endothelial cells and VSMC progenitors were visualized by double immunostaining of PECAM1 (*green*) and PDGFRB (*red*) at E14.5 in embryonic hearts. When compared to vehicle control group, WIN-treated embryos have evidently thinned myocardium and fewer coronary vessels in the myocardium, accompanied with decreased number of PDGFRB-positive VSMC progenitor cells in the myocardium (**B** *vs*. **F**; **D** *vs*. **H**). Though lower in number, the intramyocardial PDGFRB-positive cells in WIN-treated embryos were found to either surround or in adjacent to vessels, similar to the vehicle control group, suggesting that the initial recruitment of VSMC cells to immature endothelial tubes is minimally affected by deficiency of RA during heart development. Scale bars in A-B and E-F represent 50μm and those in C-D and G-H represent 20μm. Images are representative of 4 biological replicates per treatment.

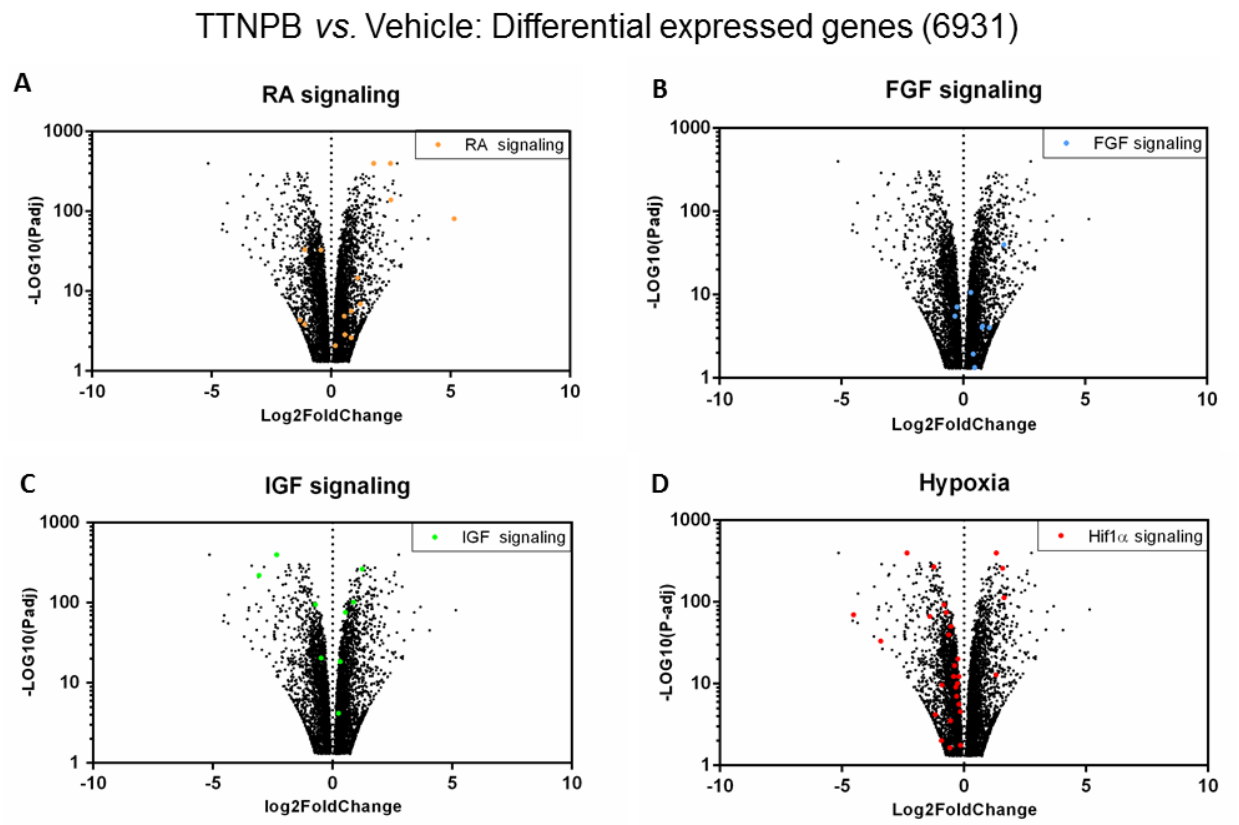

Figure 4.6 RNAseq analysis in MEC1 cells treated with RA for 48 hours.

Differentially regulated genes with adjusted p-value smaller than 0.05 are mapped in volcano plot. Genes involved in FGF signaling are color-coded blue (**B**), those belonging to IGF signaling are in green (**C**) and those in red represent genes in HIF1α-signaling (**D**). RNAseq was performed in quadruplicate for each treatment.

SUPPLEMENTARY FIGURES

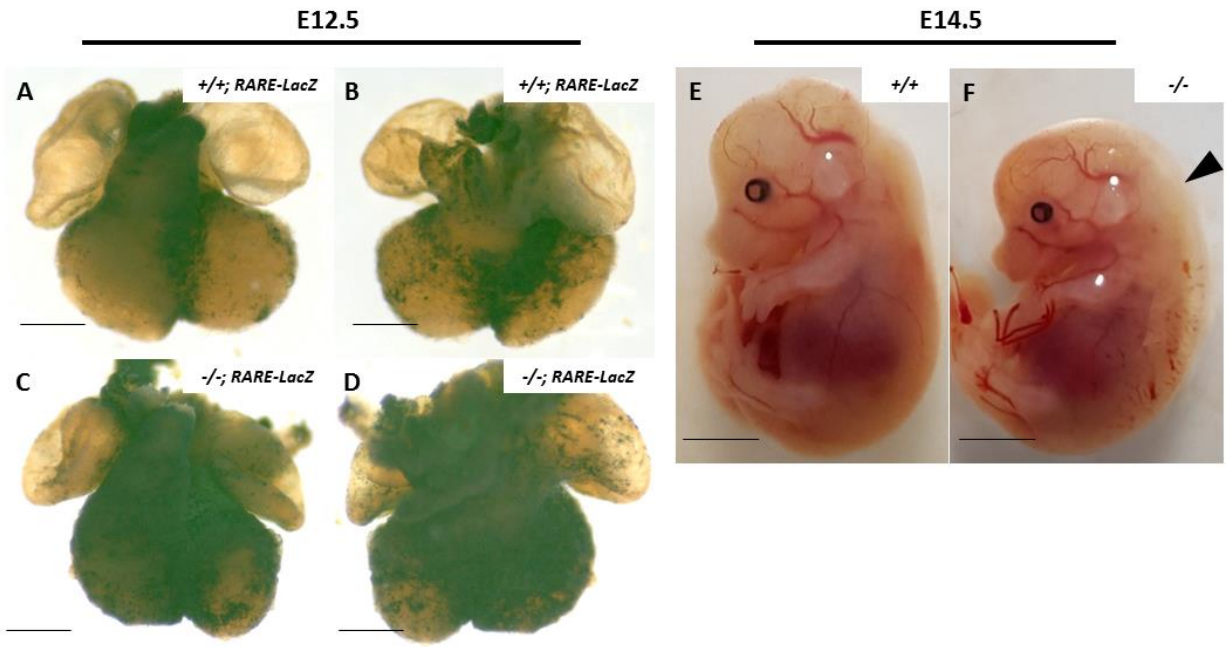

Supplementary Fig 4.1 *Dhrs3*$^{-/-}$ hearts have increase RA signaling and edema.

Genetic ablation of *Dhrs3* leads to expansion of RA-signaling domains in the developing heart at E12.5 (**A**-**D**) and subcutaneous edema at E14.5 (**E**-**F**). The domains associated with active RA-signaling were visualized through the X-gal staining *RARE-LacZ* dams Scale bars represent in 200μm in A-D, and 2mm in E-F. Observation was derived from at least three biological replicates per genotype at each developmental stage.

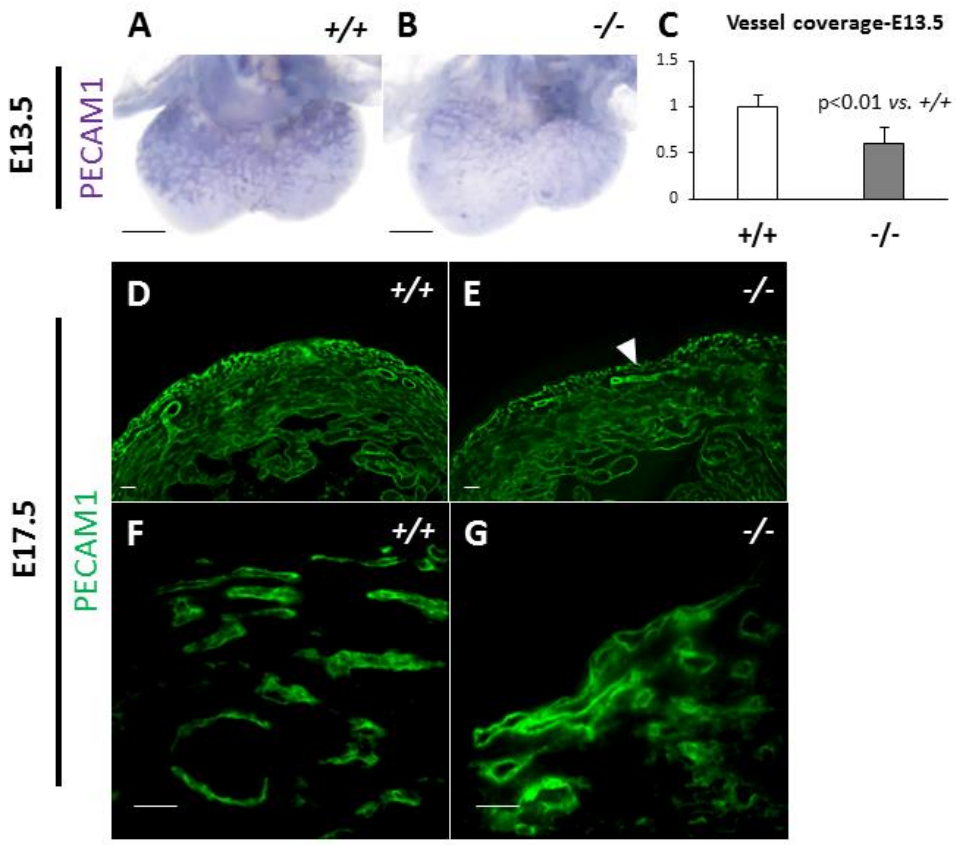

Supplementary Fig 4.2 *Dhrs3*$^{-/-}$ embryos have defects in coronary vessels.

Dhrs3$^{-/-}$ mice exhibited reduced vessel coverage on ventricles at E13.5 and aberrantly enlarged vessels at E17.5 (marked by white arrow head), when compared to wild-type littermates. Scale bars represent 200μm in A-B, and 20μm in D-G. Images are representative of at least three embryos per genotype per stage.

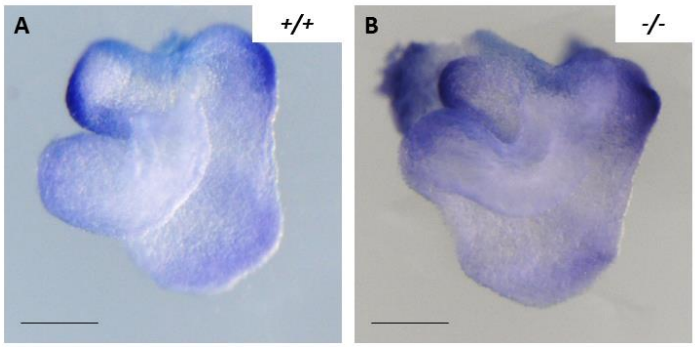

Supplementary Fig 4.3 Deletion of *Dhrs3* did not alter COUP-TFII expression at early stages.

In *situ* hybridization of COUP-TF II demonstrated that the early patterning of heart tube was not affected by the ablation of *Dhrs3*. Scale bars represent 500μm. Images are representative of at least three embryos per genotype.

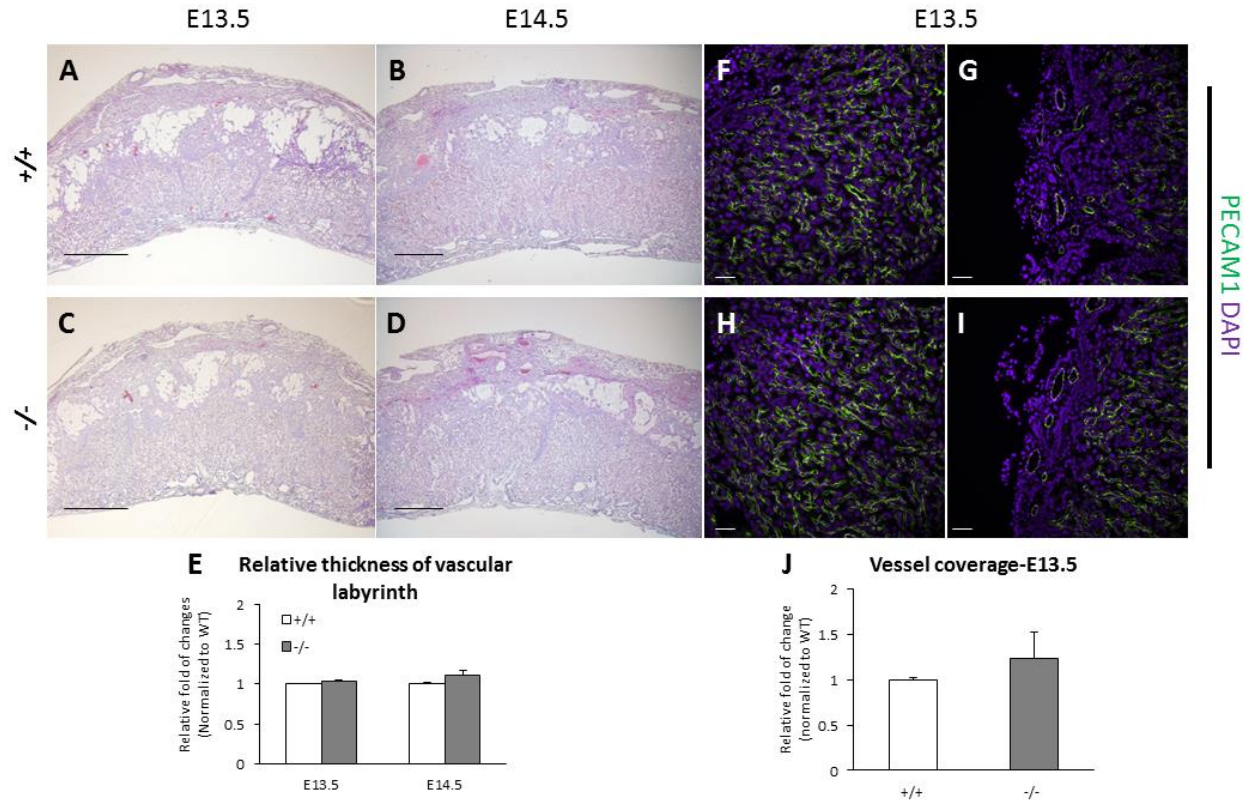

Supplementary Fig 4.4 Development of placenta is minimally affected by the ablation of *Dhrs3*.

Histology of placenta from *Dhrs3*$^{-/-}$ and wildtype embryos at E13.5 (**A** *vs*. **C**) and E14.5 (**B** *vs*. **D**). Analysis of the thickness of labyrinth suggested that mutation of *Dhrs3* does not significantly alter the development of vascular labyrinth layer (**E**). Vascularization of placenta was observed to be sufficient in both wildtype and mutant embryos, revealed by PECAM1 immunostaining of transversal section of placenta. Vessel density was quantified in **J** and found to be comparable between *Dhrs3*$^{-/-}$ and wildtype embryos. Scale bars in F-I represent 50μm. Images are representative of at least three embryos per genotype per stage.

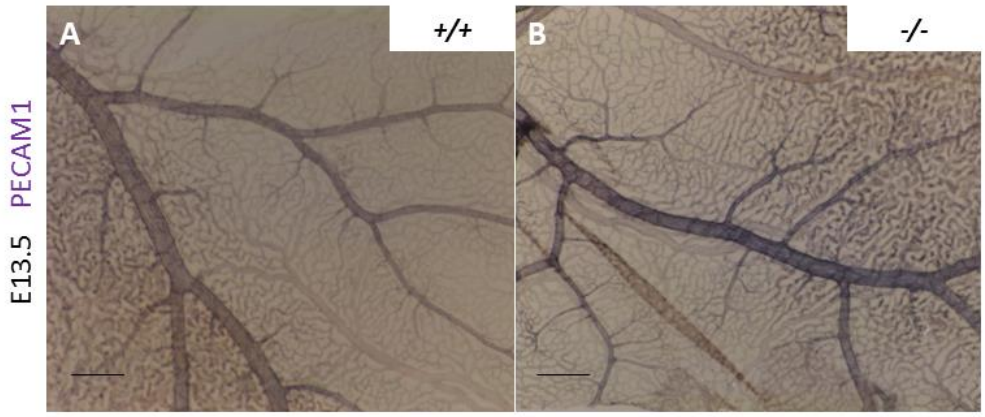

Supplementary Fig 4.5 Analysis of the development of vessels in the yolk sac at E13.5.

Vessel morphology was analyzed by whole-mount PECAM1 staining of yolk sac membranes collected from *Dhrs3*$^{-/-}$ and wild-type embryos. The branching pattern and vessel density were compared between *Dhrs3*$^{-/-}$ and wildtype embryos and found to be comparable. Images are representative of three biological replicates per genotype.

SUPPLEMENTARY TABLES

Supplementary Table 4.1

Hypoxia		
Associated Gene Name	log2FoldChange	P-adj
Vegfa	-0.62744	2.52E-40
Angptl2	-1.4029	1.73E-67
Angptl7	-1.2361	5.68E-270
Angptl6	-1.1779	6.71E-05
Angptl4	-0.90227	2.39E-10
Angpt4	1.3124	1.45E-13
Hif1a	-0.2144	5.33E-13
Hif3a	-4.5305	2.47E-70
Hif1an	-0.21281	2.54E-06
Bdnf	1.0735	2.98E-40
Hyou1	-0.14187	0.017402
Egln1	-0.33523	8.42E-10
Edn1	1.6404	7.54E-114
Adm	-0.93242	0.0096117
Aldoc	-3.4138	5.60E-34
Gapdh	-0.15644	2.81E-05
Hk1	-0.42851	4.98E-13
Igf2	-2.341	0
Krt14	-0.55102	0.00030709
Krt18	1.5796	5.29E-260
Ldha	-0.73195	4.07E-75
Mmp2	1.3239	0
Pfkl	-0.30129	9.38E-08
Pgk1	-0.82	2.84E-93
Pkm	-0.25103	6.98E-21
Tgfa	-0.58123	0.022861
Tgfb3	-0.27286	8.07E-11
Tpi1	-0.54061	7.16E-51
Vim	-0.38362	2.27E-17

IGF		
Associated Gene Name	log2FoldChange	P-adj
Igf1	-3.0723	1.42E-221
Igf2	-2.341	0
Igfbp4	-0.71926	1.05E-95
Igf2r	-0.47864	3.19E-21
Igf2bp1	0.24389	6.64E-05
Igf2bp2	0.32245	3.72E-19
Igfbp3	0.53729	1.14E-76
Igfbp6	0.87303	5.82E-103
Igfbp7	1.2386	7.88E-264

FGF		
Associated Gene Name	log2FoldChange	P-adj
Fgf10	-0.34718	2.77E-06
Fgfr2	-0.26003	7.10E-08
Fgfr1	0.30019	2.05E-11
Fgfr3	0.40221	0.011388
Fgfbp3	0.45978	0.045881
Fgf18	0.75993	8.79E-05
Fgf2	0.78712	6.19E-05
Fgf11	1.0591	9.13E-05
Fgf9	1.6623	1.07E-40

RA metabolism		
Associated Gene Name	log2FoldChange	P-adj
Rdh10	-1.1082	5.18E-34
Dhrs3	2.498	3.97E-140
Aldh1a2	-1.3079	4.54E-05
Aldh1a1	-0.43237	1.34E-33
Cyp26a1	0.83829	0.0023821
Cyp26b1	5.1489	1.30E-81
Rarg	0.18046	0.0083629
Rarb	2.4766	0
Rbp4	-1.1015	0.000138
Rbp1	1.7751	0
Hoxa3	1.1014	2.03E-15
Hoxd3	1.2174	1.17E-07
Hoxb4	0.54631	1.32E-05
Hoxc9	0.84526	2.29E-06

Chapter 5 : Conclusions and Future Directions

Role of DHRS3 in preventing excess formation of RA and embryogenesis

The indispensability of DHRS3 in RA metabolism during embryogenesis was reported in Chapter 2. Based on the expression of *RARE-LacZ* transgene in *Dhrs3*$^{+/+}$ and *Dhrs3*$^{-/-}$ embryos at various developmental stages, the data demonstrated that deficiency of *Dhrs3* led to an increased RA signaling in mouse embryos as early as E10, and such an increase persisted to E12.5 as well as E14.5 (Chapter 2 and (Billings et al., 2013)). Measurement of endogenous retinoids further validated the accumulation of RA in *Dhrs3*$^{-/-}$ embryos at E12.5, which agrees with my lab's previously published observation of altered RA metabolism in E14.5 *Dhrs3*$^{-/-}$ embryos (Billings et al., 2013). These data collectively support a non-redundant role of *Dhrs3* in RA metabolism in preventing excessive accumulation of RA and RA signaling.

DHRS3 plays critical roles in the development of multiple fetal organs, specifically via regulating RA metabolism. *Dhrs3*$^{-/-}$ embryos die during mid- to late-gestation and were found to possess a spectrum of malformations, most of which resembling defects induced by teratogenic doses of RA. During early developmental stages, ablation of *Dhrs3* disrupted the outgrowth and patterning of hindbrain-derived cranial nerves with incomplete penetrance. Similar neuronal defects have been reported previous in animals with altered RA signaling due to genetic manipulation or pharmacological treatment. When examined at mid-gestation, *Dhrs3*-null mutant mice were found to show evident subcutaneous edema, which indicates cardiac dysfunction and is consistent with previous observation of multiple defects in the heart, i.e. DORV, VSD as well as ASD (Billings et al., 2013). A detailed analysis of cardiac development was carried out in Chapter 3 and 4. *Dhrs3*$^{-/-}$ embryos also display skeletal defects including defective formation of cervical vertebrae and delayed ossification in the skull as well as rib cage. Importantly, treating *Dhrs3*$^{+/-}$ dam with a vitamin A deficient diet was found to partially correct the defect in cervical vertebrae as well as ossification process. A prolonged VAD treatment successfully corrected most of the

congenital defects in *Dhrs3*$^{-/-}$ embryos and rescued the embryonically lethal *Dhrs3*-null mice to fully grown adults with normal growth rate. These results, together with our lab's previous observations made at E14.5, consistently support that DHRS3 is physiologically important for normal embryogenesis due to its critical role in preventing the formation of excess RA (Billings et al., 2013). This finding would not only enrich the current understanding of the molecular mechanisms regulating RA metabolism, but also be relevant in the case of patients who present symptoms as a result of Dhrs3 mutation.

Roles of RA in regulating the migration of epicardial cell

Studies presented in Chapter 3 focus on understanding the biological functions of RA in the epicardium and migrating EPDCs. Though the major synthetic enzyme of RA, i.e. RALDH2, is exclusively expressed in the epicardium and has been widely used as an epicardial marker, the physiological roles played by RA in epicardial cells remains an important, yet, unsolved question. In the current dissertation, multiple *in vivo* and *in vitro* models were employed to address this question. In both primary epicardial explant culture and MEC1 cell line, inhibition of RA synthesis greatly attenuated PDGFBB-induced phenotypes associated with EMT such as loss of epithelial characteristics and polymerization of F-actin. Deficiency of RA signaling also disrupted the assembly of focal adhesion junctions and the formation of filopodia that are essential components of remodeling cytoskeleton and are indispensable for cellular movement. As a result of the failure in cytoskeletal reorganization, epicardial cells that are deficient in RA migrated poorly, which further demonstrated that RA is functionally required for the EMT of epicardial cells. Activation of RA signaling in epicardial cells *in vitro* induced a series of morphological changes that are directly linked with elevated EMT, such as accumulation of stress fibers, formation of filopodia and the loss of expression of epithelial markers. The conclusion of RA being able to facilitate the cytoskeletal rearrangement and the epicardial EMT was further supported by data derived from *in vivo* models. Epicardial cells experiencing high RA signaling migrated deeper into the myocardium in *Dhrs3*$^{-/-}$ embryos whereas those in RA deficient environment move slower in WIN-treated embryos. Consistent observations derived from complementary models of RA signaling,

establish that epicardial RA signaling affects epicardial EMT through modulating cytoskeletal actin remodeling. The influence of RA signaling on the delamination of EPDCs from the epicardium and their migration is represented in Figure 5.1.

Further molecular analysis argues that RA signaling primes cytoskeleton remodeling in epicardial cells through the RhoA-ROCK pathway. RhoA and its downstream effectors have been well-established as classic modulators of cytoskeletal actin in the event of EMT (Amano et al., 1997; Maekawa et al., 1999). Activation of the RhoA pathway leads to the formation of stress fiber, filopodia and lamellipodia, which was also observed in epicardial cells with elevated RA signaling (Amano et al., 1997). Upon more in-depth studies, we not only noted that up-regulation of RA signaling potently induced the binding of GTP to RhoA but we also noted that RA signaling potently induced the expression of numerous RhoA effectors, whose roles are directly linked with the EMT and the remodeling of the cytoskeleton. Specifically, within these altered RhoA effectors, ROCK2 and RND3 were previously reported to be potential RA direct target genes due to the identification of RARE in the promoter regions of these gene (Delacroix et al., 2010; E. Moutier et al., 2012). To further identify epicardial expressed RA target genes that that involved in the RhoA pathway and/or epicardial EMT, future studies employing chromatin-immunoprecipitation based techniques are warranted.

Interestingly, activation of RA in MEC1 cells was observed to induce cell differentiation preferentially towards VSMCs over fibroblasts. In response to treatment of RAR agonist, several mature VSMC markers were highly induced meanwhile the expression of collagens was suppressed in RA-treated MEC1 cells. However, inhibition of RA signaling was previously reported to enhance the differentiation of proepicardial cells into VSMC and Braitsch *et al*. proposed that RA suppresses VSMC differentiation via inducing *Tcf21*, which favors differentiation towards fibroblasts (Azambuja et al., 2010; C. M. Braitsch, M. D. Combs, S. E. Quaggin, & K. E. Yutzey, 2012). The discrepancy between our observations and the previous reports might be explained by the difference in the types of progenitors found in the proepicardium versus epicardium. The proepicardium is a heterogenous progenitor pool that

gives rise to the epicardium and multiple other cell lineages that collectively facilitate the late cardiogenic events (Carmona et al., 2010; Katz et al., 2012; Perez-Pomares & de la Pompa, 2011). Cells isolated from these two tissues do not necessarily behave completely the same: proepicardial cells migrate as a sheet (in chick) or as a cluster of epithelial cells (in mouse) to the myocardium whereas the epicardial cells transform into mesenchymal cells and delaminate individually into the myocardium (Reese, Mikawa, & Bader, 2002). Though the epicardium develops from the proepicardium, the epicardial cells may not follow exactly the same morphogenic signals. To fully address the question about the roles of RA in epicardial differentiation, future studies should be carried out to determine if proepicardial cells and epicardial cells respond similarly to the same level of RA signaling and more importantly, to test the effect of RA in VSMC/fibroblast differentiation in more physiological settings.

Lastly, a transcriptomic approach revealed potential interaction of RA signaling with developmentally important pathways in epicardial cells. Several developmentally important signaling pathways were identified as RA-responsive, including IGF and Hippo signaling pathways. These data suggest additional molecular mechanisms of regulation of epicardial cell behavior, and subsequent epicardial-regulated cardiogenic events, by RA. It would be highly informative and interesting if future studies could combine models deficient in signaling of, for example Hippo pathways, with RA deficiency/excess models to gain an more in-depth understanding of the molecular regulatory mechanism of cardiogenesis.

Role of RA in the development of coronary vessels

Congenital heart diseases (CHDs) are some of the most common causes of embryonic or newborn lethality (Hoffman, 1995). Among the maternal risk factors of CHDs one is the fetal excess or deficiency of vitamin A (Lammer et al., 1985). As a critical signaling molecule, RA has been known to regulate early cardiogenesis with evidence reported by numerous excellent studies (reviewed in (Stéphane Zaffran, Robrini, & Bertrand, 2014)). However, the exact involvement and the regulatory functions of RA in heart maturation remain elusive, hindering the progress in understanding the mechanisms underlying the

teratology of RA. In the current study, I employed novel mouse models that allowed for the investigation of the role of RA signaling in the late developmental stages of the heart.

Results presented in Chapter 4 demonstrate the importance of proper levels of RA signaling in coronary vessel formation and are depicted in Figure 5.1. The establishment of coronary vasculature is highly sensitive to changes in the microenvironment of the heart and perturbations of RA signaling have been observed to be related to defects in coronary vessel formation (S. C. Lin et al., 2010; Merki et al., 2005). When RA synthesis is inhibited only during mid-gestation, the formation of coronary vessel hierarchy was evidently compromised, shown as a lack of major vascular branches and tightly restrained vascular calibers (Chapter 4). In the opposite model, excess RA signaling in *Dhrs3*$^{-/-}$ embryos severely impairs vessel budding and branching, rendering the coronary vessels ubiquitously enlarged and lack of proper structure. Since the formation of coronary vessels requires molecular guidance and signaling cues from various tissues, it would be important to understand the spatial and temporal distribution of endogenous RA signaling in terms of both vasculogenesis and angiogenesis and by examining both the angiogenic environment and cellular components of the developing coronary vasculature.

Failure of remodeling the endothelial network in both RA excess and RA deficiency models is further accompanied with a lack of perivascular supporting cells, which may acerbate the existing vascular defects. The interaction between immature endothelial cells and perivascular supporting cells in both models with coronary defects needs further investigation. Based on the current data it is not entirely clear if the vascular defects seen in the case of altered RA signaling are attributable to either defects in the formation of the primary endothelial plexus or due to remodeling defects related to the lack of perivascular cells. In addition, as reported both here and elsewhere, RA affects the arteriovenous identity of coronary vessels with a preference towards venous characteristics. However, COUP-TFII staining at E10.5 revealed no changes in inflow/outflow partitioning. To understand the effect of RA on vascular identity it would require a more detailed molecular analysis utilizing various atrial or venous markers and

genes that have been found to be involved in arteriovenous decision can be screened for RA downstream target genes in regulating coronary vessel formation.

Besides the direct influence of altered RA signaling on endothelial cells/perivascular cells, another possible cause of coronary defects could be a defect in epicardial-derived developmental signaling pathways. One of the most affected is the hypoxia-related pathway in response to elevated RA signaling in the epicardial cells. Hif1α signaling, as well as genes that were previously identified to be hypoxia-responsive, was broadly down-regulated by the activation of RA signaling in epicardial cells. A physiologically hypoxic environment is critical for the proper development of vessels and embryonic growth (Nanka, Valasek, Dvorakova, & Grim, 2006; Patterson & Zhang, 2010; Ream et al., 2008). Thus, perturbation of hypoxia-related signaling pathways could be a contributing factor to the defective angiogenesis and thin myocardium seen in the *Dhrs3*$^{-/-}$ embryos. Another possibility is the SRF signaling pathway that is highly up-regulated by RA signaling. SRF pathway actively participates and is required in multiple aspects of cardiogenesis including the epicardial EMT, coronary vessel development as well as cardiomyocyte proliferation (Parlakian et al., 2004; Trembley et al., 2015). Over-activation of the SRF a pathway by RA might disrupt the physiological homeostasis of signaling network which orchestrates the various processes of heart maturation. Though the causal relationship between abnormally altered hypoxia or SRF-signaling pathways and defective heart development in *Dhrs3*$^{-/-}$ and WIN-models remain to be tested in *in vivo* settings, these interesting observations provide clues of how RA modulates epicardial-dependent cardiogenic events and might contribute to the mechanisms of the teratology of RA during heart maturation.

Role of RA in the development of myocardium

Concomitant with coronary defects are ventricular hypoplasia in response to perturbation of normal RA signaling in the heart. In both *in vivo* models of RA deficiency and RA excess, the ventricular myocardium was observed to be critically thin (Chapter 4 and (S.-C. Lin et al., 2010)). The fact that both excess and deficiency of RA results in a similar range of congenital defects has been previously

documented and discussed, yet the mechanism remains elusive (Billings et al., 2013; Davis & Sadler, 1981; Frenz et al., 2010; Lee et al., 2012; A. Rydeen et al., 2015). In the case of the thin myocardium seen in *Dhrs3*$^{-/-}$ and WIN models, poor vascular nourishment resulting from malformations in coronary vessels observed in both models could be one plausible explanation for these co-occurring phenotype (S. C. Lin et al., 2010; Merki et al., 2005; Olivey & Svensson, 2010). First, it would be important to establish that the connection between the coronary vasculature and the aorta is properly established in the *Dhrs3*$^{-/-}$ and WIN models. Further studies focusing on the levels of hypoxia in the myocardium of the *Dhrs3*$^{-/-}$ and WIN models could also help us understand whether the thin myocardium is caused by the poor vascularization.

Another possible cause of the thin myocardium in response to altered RA signaling could be related to changes in the secretion of RA-dependent epicardial-derived trophic factors. Numerous studies have demonstrated that RA stimulates the epicardium to produce peptide-based molecule(s) that can boost cardiomyocyte proliferation (T. Brade et al., 2011; T. Chen et al., 2002; I. Stuckmann, S. Evans, & A. B. Lassar, 2003). Our RNA-seq analysis revealed cardiogenic-relevant transcriptomic changes in ventricular epicardial cells (MEC1) in response to activation of RA signaling. For example, RA caused the up-regulation of FGF signaling and inhibition of IGF pathway (Chapter 4). FGF as well as IGF proteins have been previously identified to be epicardial-derived trophic factors involved in boosting cardiomyocyte proliferation (K. J. Lavine et al., 2005; P. Li et al., 2011). The expression of several FGF proteins, including FGF2 and FGF9, were positively related to RA signaling and, thus, could account for the myocardial thinning seen in the WIN-treated model. Surprisingly, expression of IGFs, especially IGF2, was found to be dramatically down-regulated by RA signaling (Chapter 4). Elevated RA signaling also strongly induced the expression of IGF binding protein 1 (IGFBP1) in *Dhrs3*$^{-/-}$ embryos, revealed by microarray analysis. IGF2 is required for cardiomyocyte proliferation and has been proposed as a critical epicardial-derived trophic factor in the myocardial development (T. Brade et al., 2011; Y. Huang et al., 2013). Changes in the expression of these previously identified trophic factors might contribute

considerably to the defective myocardial compact zone morphogenesis seen in the *Dhrs3*$^{-/-}$ and WIN models. However, the involvement and the precise roles of FGF and IGF pathways in RA-induced cardiac malformations require further studies. Furthermore, as mentioned above, hypoxia-related genes were seen to be down-regulated in the presence of an RAR agonist. Hypoxia was found to be indispensable for the proliferation of embryonic cardiomyocytes and suppression of hypoxia-induces transcriptional responses in the heart by altered RA signaling may be a cause of the defective myocardial growth (Guimarães-Camboa et al., 2015).

Potential roles of RA in the post-injury heart regeneration

Heart is one of the least regenerative organs in adult mammals, in contrast to the robust cardioregenerative potential of zebrafish and neonatal mouse models. Studying what makes the latter models successful in recovering cardiac function could provide a fruitful roadmap to discovering new treatments for myocardial infarction/injury(K. Kikuchi et al., 2011; Poss, Wilson, & Keating, 2002). Hearts of zebrafish and neonatal mice form fully a functional myocardium and vasculature in the injured area instead of forming a fibrotic scar as observed in adult mammals. Interestingly enough, the regenerative capacity of neonatal mice is rapidly lost after a week of postnatal life, which is consistent with the observation that human infants have the highest potential to recover cardiac functions from surgery early rather than later (Michielon et al., 2003). An increasing number of studies have started to adopt neonatal mice as models to understand the mechanism underlying heart regeneration due to the clinical relevance of this mammalian model suggested by its similarity in loss of regenerative capacity to human cases.

It is believed that by re-activating the developmentally important pathways that govern the heart maturation, adult zebrafish hearts may revisit embryonic growth and thus accelerate their recovery. Work in zebrafish model indicated that the post-injury heart regeneration program involves reactivation of the epicardial markers (Wt1, Tbx18 and Raldh2), cardiomyocyte proliferation and revascularization of newly formed myocardium, which largely recapitulates the late development of the heart (Marin-Juez et al.,

2016; Masters & Riley, 2014). Relevant to our work, synthesis of RA via RALDH2 is significantly elevated in the epicardium of non-regenerative adult mouse hearts but such an increase was found to be in both endocardium and epicardium of regenerative zebrafish hearts (D. Bilbija et al., 2012; K. Kikuchi et al., 2011). Since mammals do not express RA synthetic enzymes in the endocardium it might interesting to conditionally overexpress *Raldh2* in adult mouse endocardium and explore the biological consequences of elevation of endocardial RA production in a mouse myocardial infarction model. As RA signaling is activated in post-injury hearts of both neonatal (capable of cardioregeneration) and adult mouse hearts (not capable of cardioregeneration), a future comprehensive comparison of the targets and distribution of RA signaling between these two developmental stages models would be a good starting point in deciphering the roles of RA during wound healing in adult mouse hearts. Considering RA signaling appears to be activated but ineffectively so in the post-injury hearts of adult mice, this knowledge would also be beneficial for the studies aiming at accelerating tissue recovery in wounded adult hearts.

It remains unclear if activated epicardial cells delaminate and migrate into the wounded area and if so, whether such a migration follows similar developmental signaling pathways. In the regenerative hearts of zebrafish, the activated epicardium gives rise to migratory EPDCs via EMT and those EPDCs were observed to invade into the wounded area and contribute to endothelial cells and perivascular cells (Lepilina et al., 2006). In adult mice however, activation of epicardium only induces thickening of epicardium in adult mice, as reported by Zhou *et al*.(B. Zhou et al., 2011). Interestingly, in neonatal mice, heart injury leads to activation of Wnt pathway and infiltration of migratory EPDCs in the subepicardial space (Mizutani, Wu, & Nusse, 2016). Based on these data, it is reasonable to speculate that the increased regenerative capacity is associated with increased EPDC formation and migration. This observation needs to be validated in models by investigating the level of heart regeneration when epicardial EMT is blocked. Based on data presented in Chapter 3 in this dissertation, RA is found to regulate cytoskeleton remodeling and migration of EPDCs during embryonic development. Since activation of RA signaling along in the adult mouse heart is not associated with increased EPDC formation or migration (B. Zhou et

al., 2011), it would be interesting to investigate 1) if RA plays conserved role in epicardial EMT during heart regeneration in neonatal mice as it does in embryogenesis; and 2) if RA can potentiate the pro-migratory effects of other EMT inducers on EPDCs in the adult heart. Aside from the epicardial EMT, it is clear that both injury response and regenerative response includes the secretion of epicardial derived signaling molecules but the composition of epicardial secretome remains unclear (Masters & Riley, 2014; Raya et al., 2003; B. Zhou et al., 2011). Through the implementation of system biology approaches we can envision a discovery process based on studying the success of the highly regenerative zebrafish or neonatal mouse models, or the differences between epicardial cells from regenerative and non-regenerative hearts. RNAseq analysis of MEC1 cells treated with RAR agonist suggested that activation of RA signaling affects multiple developmentally important pathways, several of which have been found to be critically involved in heart regeneration program. For example, Hippo pathway was found to impede heart regeneration and is revealed by RNAseq data presented here to be highly activated by RA in MEC1 cells. This link of Hippo pathway and RA signaling pathway should be emphasized in the future and needs to be investigated in depth (Heallen et al., 2013).

In summary, this dissertation provides new insight into the teratology of RA by revealing novel roles of RA in the formation of coronary vasculature and the myocardial growth during the late development of the heart. Results presented here show indispensable roles for RA in regulating the intramyocardial migration of epicardial cells. A better understanding of the regulatory functions of RA in epicardial EMT, coronary vessel formation and cardiomyocyte proliferation during embryogenesis can shed light into future studies of post-injury heart regeneration in adulthood and contribute to the identification of novel therapeutic targets in the treatment of cardiac diseases.

FIGURES

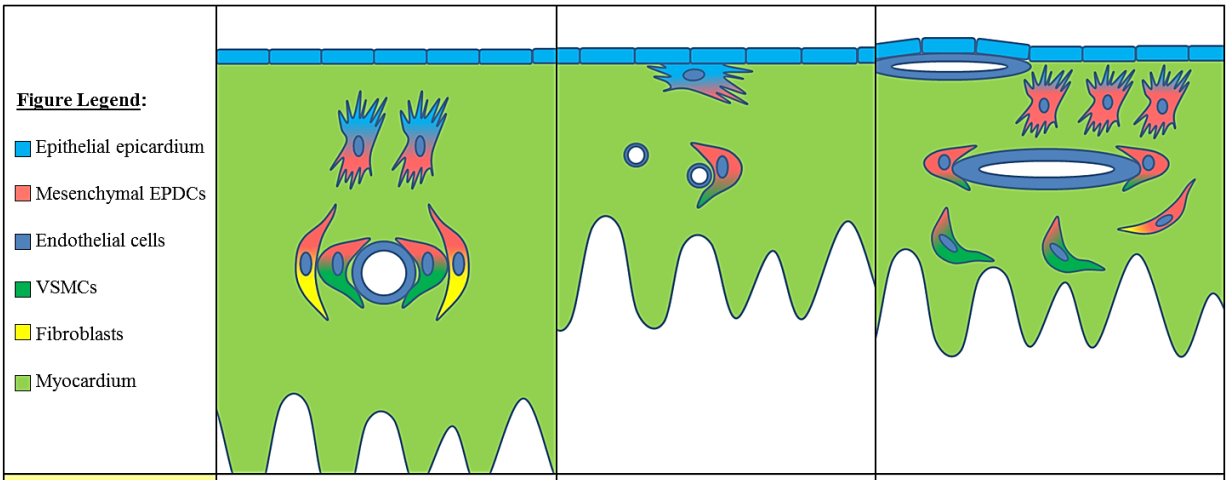

RA status	Normal	Deficiency	Excess
E14.5	Phenotype compared to normal heart	Thin myocardium	Thin myocardium
		Formation of microvessels at the expense of large vessels	Formation of large vessel at the expense of microvessels
		Low EMT	High EMT
		Lack of perivascular EPDCs	Excess EPDCs that are not associated with vessels
E17.5	Phenotype compared to normal heart	N/A	Lack of VSMCs

Figure 5.1 Conclusion of roles of RA in late heart development.

During normal embryogenesis, mesenchymal EPDCs delaminate from the epicardium and migrate to support the maturation of coronary vasculature. Epicardium also functions to support the growth and compaction of myocardium. RA promotes the loss of epithelial characteristics and regulates cytoskeletal rearrangement in epicardial cells, thus facilitating the migration of EPDCs. Status of RA correlates with the caliber of intramyocardial vessels, and aberrant RA signaling disrupts vascular hierarchy. Consistent with the development of coronary vessels, the thickening of ventricular myocardium is also sensitive to alterations in RA signaling. Paradoxically, excess or deficiency in RA can result in hypoplastic myocardium in mouse embryos. In addition, RA signaling regulates the recruitment of VSMCs to immature endothelia in coronary vessels, as well as the differentiation of mature perivascular cells. Collectively, RA signaling is not only actively involved but also indispensable in the late heart development.

Reference

Abu-Abed, S., Dolle, P., Metzger, D., Beckett, B., Chambon, P., & Petkovich, M. (2001). The retinoic acid-metabolizing enzyme, CYP26A1, is essential for normal hindbrain patterning, vertebral identity, and development of posterior structures. *Genes Dev, 15*(2), 226-240.

Abu-Abed, Suzan, Dollé, Pascal, Metzger, Daniel, Beckett, Barbara, Chambon, Pierre, & Petkovich, Martin. (2001). The retinoic acid-metabolizing enzyme, CYP26A1, is essential for normal hindbrain patterning, vertebral identity, and development of posterior structures. *Genes & Development, 15*(2), 226-240. doi: 10.1101/gad.855001

Abu-Abed, Suzan S., Beckett, Barbara R., Chiba, Hideki, Chithalen, James V., Jones, Glenville, Metzger, Daniel, . . . Petkovich, Martin. (1998). Mouse P450RAI (CYP26) Expression and Retinoic Acid-inducible Retinoic Acid Metabolism in F9 Cells Are Regulated by Retinoic Acid Receptor γ and Retinoid X Receptor α. *Journal of Biological Chemistry, 273*(4), 2409-2415. doi: 10.1074/jbc.273.4.2409

Abu-Issa, Radwan, Smyth, Graham, Smoak, Ida, Yamamura, Ken-ichi, & Meyers, Erik N. (2002). Fgf8 is required for pharyngeal arch and cardiovascular development in the mouse. *Development, 129*(19), 4613-4625.

Acharya, A., Baek, S. T., Huang, G., Eskiocak, B., Goetsch, S., Sung, C. Y., . . . Tallquist, M. D. (2012). The bHLH transcription factor Tcf21 is required for lineage-specific EMT of cardiac fibroblast progenitors. *Development, 139*(12), 2139-2149. doi: 10.1242/dev.079970

Ackermans, M. M., Zhou, H., Carels, C. E., Wagener, F. A., & Von den Hoff, J. W. (2011). Vitamin A and clefting: putative biological mechanisms. *Nutr Rev, 69*(10), 613-624. doi: 10.1111/j.1753-4887.2011.00425.x

Adams, M. K., Belyaeva, O. V., Wu, L., & Kedishvili, N. Y. (2014). The retinaldehyde reductase activity of DHRS3 is reciprocally activated by retinol dehydrogenase 10 to control retinoid homeostasis. *J Biol Chem, 289*(21), 14868-14880. doi: 10.1074/jbc.M114.552257

Agarwal, P., Wylie, J. N., Galceran, J., Arkhitko, O., Li, C., Deng, C., . . . Bruneau, B. G. (2003). Tbx5 is essential for forelimb bud initiation following patterning of the limb field in the mouse embryo. *Development, 130*(3), 623-633.

Alapatt, P., Guo, F., Komanetsky, S. M., Wang, S., Cai, J., Sargsyan, A., . . . Graham, T. E. (2013). Liver retinol transporter and receptor for serum retinol-binding protein (RBP4). *J Biol Chem, 288*(2), 1250-1265. doi: 10.1074/jbc.M112.369132

Amano, M., Chihara, K., Kimura, K., Fukata, Y., Nakamura, N., Matsuura, Y., & Kaibuchi, K. (1997). Formation of actin stress fibers and focal adhesions enhanced by Rho-kinase. *Science, 275*(5304), 1308-1311.

Arnold, S. L., Kent, T., Hogarth, C. A., Griswold, M. D., Amory, J. K., & Isoherranen, N. (2015). Pharmacological inhibition of ALDH1A in mice decreases all-trans retinoic acid concentrations in a tissue specific manner. *Biochem Pharmacol, 95*(3), 177-192. doi: 10.1016/j.bcp.2015.03.001

Artamonov, M. V., Jin, L., Franke, A. S., Momotani, K., Ho, R., Dong, X. R., . . . Somlyo, A. V. (2015). Signaling pathways that control rho kinase activity maintain the embryonic epicardial progenitor state. *J Biol Chem, 290*(16), 10353-10367. doi: 10.1074/jbc.M114.613190

Austin, Anita F., Compton, Leigh A., Love, Joseph D., Brown, Christopher B., & Barnett, Joey V. (2008). Primary and immortalized mouse epicardial cells undergo differentiation in response to TGFβ. *Developmental Dynamics, 237*(2), 366-376. doi: 10.1002/dvdy.21421

Azambuja, A. P., Portillo-Sanchez, V., Rodrigues, M. V., Omae, S. V., Schechtman, D., Strauss, B. E., . . . Xavier-Neto, J. (2010). Retinoic acid and VEGF delay smooth muscle relative to endothelial differentiation to coordinate inner and outer coronary vessel wall morphogenesis. *Circ Res, 107*(2), 204-216. doi: 10.1161/CIRCRESAHA.109.214650

Båvik, C., Ward, S. J., & Chambon, P. (1996). Developmental abnormalities in cultured mouse embryos deprived of retinoic by inhibition of yolk-sac retinol binding protein synthesis. *Proceedings of the National Academy of Sciences of the United States of America, 93*(7), 3110-3114.

Bax, N. A., Bleyl, S. B., Gallini, R., Wisse, L. J., Hunter, J., Van Oorschot, A. A., . . . Gittenberger-de Groot, A. C. (2010). Cardiac malformations in Pdgfralpha mutant embryos are associated with increased expression of WT1 and Nkx2.5 in the second heart field. *Dev Dyn, 239*(8), 2307-2317. doi: 10.1002/dvdy.22363

Beard, R. L., Chandraratna, R. A., Colon, D. F., Gillett, S. J., Henry, E., Marler, D. K., . . . et al. (1995). Synthesis and structure-activity relationships of stilbene retinoid analogs substituted with heteroaromatic carboxylic acids. *J Med Chem, 38*(15), 2820-2829.

Berry, D. C., Jacobs, H., Marwarha, G., Gely-Pernot, A., O'Byrne, S. M., DeSantis, D., . . . Ghyselinck, N. B. (2013). The STRA6 receptor is essential for retinol-binding protein-induced insulin resistance but not for maintaining vitamin A homeostasis in tissues other than the eye. *J Biol Chem, 288*(34), 24528-24539. doi: 10.1074/jbc.M113.484014

Bertrand, N., Roux, M., Ryckebusch, L., Niederreither, K., Dolle, P., Moon, A., . . . Zaffran, S. (2011). Hox genes define distinct progenitor sub-domains within the second heart field. *Dev Biol, 353*(2), 266-274. doi: 10.1016/j.ydbio.2011.02.029

Biesalski, H. K., Frank, J., Beck, S. C., Heinrich, F., Illek, B., Reifen, R., . . . Zrenner, E. (1999). Biochemical but not clinical vitamin A deficiency results from mutations in the gene for retinol binding protein. *Am J Clin Nutr, 69*(5), 931-936.

Bilbija, D., Haugen, F., Sagave, J., Baysa, A., Bastani, N., Levy, F. O., . . . Valen, G. (2012). Retinoic acid signalling is activated in the postischemic heart and may influence remodelling. *PLoS One, 7*(9), e44740. doi: 10.1371/journal.pone.0044740

Bilbija, Dusan, Haugen, Fred, Sagave, Julia, Baysa, Anton, Bastani, Nasser, Levy, Finn Olav, . . . Valen, Guro. (2012). Retinoic Acid Signalling Is Activated in the Postischemic Heart and May Influence Remodelling. *PLoS ONE, 7*(9), e44740. doi: 10.1371/journal.pone.0044740

Billings, S. E., Pierzchalski, K., Butler Tjaden, N. E., Pang, X. Y., Trainor, P. A., Kane, M. A., & Moise, A. R. (2013). The retinaldehyde reductase DHRS3 is essential for preventing the formation of

excess retinoic acid during embryonic development. *FASEB J, 27*(12), 4877-4889. doi: 10.1096/fj.13-227967

Binder, M. (1985). The teratogenic effects of a bis(dichloroacetyl)diamine on hamster embryos. Aortic arch anomalies and the pathogenesis of the DiGeorge syndrome. *Am J Pathol, 118*(2), 179-193.

Bouillet, Philippe, Sapin, Vincent, Chazaud, Claire, Messaddeq, Nadia, Décimo, Didier, Dollé, Pascal, & Chambon, Pierre. (1997). Developmental expression pattern of Stra6, a retinoic acid-responsive gene encoding a new type of membrane protein. *Mechanisms of Development, 63*(2), 173-186. doi: http://dx.doi.org/10.1016/S0925-4773(97)00039-7

Brade, T., Kumar, S., Cunningham, T. J., Chatzi, C., Zhao, X., Cavallero, S., . . . Duester, G. (2011). Retinoic acid stimulates myocardial expansion by induction of hepatic erythropoietin which activates epicardial Igf2. *Development, 138*(1), 139-148. doi: 10.1242/dev.054239

Brade, Thomas, Kumar, Sandeep, Cunningham, Thomas J., Chatzi, Christina, Zhao, Xianling, Cavallero, Susana, . . . Duester, Gregg. (2011). Retinoic acid stimulates myocardial expansion by induction of hepatic erythropoietin which activates epicardial Igf2. *Development (Cambridge, England), 138*(1), 139-148. doi: 10.1242/dev.054239

Braitsch, C. M., Combs, M. D., Quaggin, S. E., & Yutzey, K. E. (2012). Pod1/Tcf21 is regulated by retinoic acid signaling and inhibits differentiation of epicardium-derived cells into smooth muscle in the developing heart. *Dev Biol, 368*(2), 345-357. doi: 10.1016/j.ydbio.2012.06.002

Braitsch, Caitlin M., Combs, Michelle D., Quaggin, Susan E., & Yutzey, Katherine E. (2012). Pod1/Tcf21 is regulated by retinoic acid signaling and inhibits differentiation of epicardium-derived cells into smooth muscle in the developing heart. *Developmental Biology, 368*(2), 345-357. doi: http://dx.doi.org/10.1016/j.ydbio.2012.06.002

Bruneau, B. G. (2008). The developmental genetics of congenital heart disease. *Nature, 451*(7181), 943-948. doi: 10.1038/nature06801

Bruneau, B. G., Logan, M., Davis, N., Levi, T., Tabin, C. J., Seidman, J. G., & Seidman, C. E. (1999). Chamber-specific cardiac expression of Tbx5 and heart defects in Holt-Oram syndrome. *Dev Biol, 211*(1), 100-108. doi: 10.1006/dbio.1999.9298

Cai, C. L., Liang, X., Shi, Y., Chu, P. H., Pfaff, S. L., Chen, J., & Evans, S. (2003). Isl1 identifies a cardiac progenitor population that proliferates prior to differentiation and contributes a majority of cells to the heart. *Dev Cell, 5*(6), 877-889.

Cai, C. L., Martin, J. C., Sun, Y., Cui, L., Wang, L., Ouyang, K., . . . Evans, S. M. (2008). A myocardial lineage derives from Tbx18 epicardial cells. *Nature, 454*(7200), 104-108. doi: 10.1038/nature06969

Calmont, A., Ivins, S., Van Bueren, K. L., Papangeli, I., Kyriakopoulou, V., Andrews, W. D., . . . Scambler, P. J. (2009). Tbx1 controls cardiac neural crest cell migration during arch artery development by regulating Gbx2 expression in the pharyngeal ectoderm. *Development, 136*(18), 3173-3183. doi: 10.1242/dev.028902

Cano, Elena, Carmona, Rita, Ruiz-Villalba, Adrián, Rojas, Anabel, Chau, You-Ying, Wagner, Kay D., . . . Pérez-Pomares, José M. (2016). Extracardiac septum transversum/proepicardial endothelial cells pattern embryonic coronary arterio–venous connections. *Proceedings of the National Academy of Sciences, 113*(3), 656-661. doi: 10.1073/pnas.1509834113

Carmona, R., Guadix, J. A., Cano, E., Ruiz-Villalba, A., Portillo-Sanchez, V., Perez-Pomares, J. M., & Munoz-Chapuli, R. (2010). The embryonic epicardium: an essential element of cardiac development. *J Cell Mol Med, 14*(8), 2066-2072. doi: 10.1111/j.1582-4934.2010.01088.x

Chablais, F., & Jazwinska, A. (2012). The regenerative capacity of the zebrafish heart is dependent on TGFbeta signaling. *Development, 139*(11), 1921-1930. doi: 10.1242/dev.078543

Chanda, B., Ditadi, A., Iscove, N. N., & Keller, G. (2013). Retinoic acid signaling is essential for embryonic hematopoietic stem cell development. *Cell, 155*(1), 215-227. doi: 10.1016/j.cell.2013.08.055

Chapman, D. L., Garvey, N., Hancock, S., Alexiou, M., Agulnik, S. I., Gibson-Brown, J. J., . . . Papaioannou, V. E. (1996). Expression of the T-box family genes, Tbx1-Tbx5, during early mouse development. *Dev Dyn, 206*(4), 379-390. doi: 10.1002/(sici)1097-0177(199608)206:4<379::aid-aja4>3.0.co;2-f

Chawla, B., Schley, E., Williams, A. L., & Bohnsack, B. L. (2016). Retinoic Acid and Pitx2 Regulate Early Neural Crest Survival and Migration in Craniofacial and Ocular Development. *Birth Defects Res B Dev Reprod Toxicol, 107*(3), 126-135. doi: 10.1002/bdrb.21177

Chazaud, C., Chambon, P., & Dolle, P. (1999). Retinoic acid is required in the mouse embryo for left-right asymmetry determination and heart morphogenesis. *Development, 126*(12), 2589-2596.

Chen, F., Marquez, H., Kim, Y. K., Qian, J., Shao, F., Fine, A., . . . Cardoso, W. V. (2014). Prenatal retinoid deficiency leads to airway hyperresponsiveness in adult mice. *J Clin Invest, 124*(2), 801-811. doi: 10.1172/JCI70291

Chen, Felicia, Marquez, Hector, Kim, Youn-Kyung, Qian, Jun, Shao, Fengzhi, Fine, Alan, . . . Cardoso, Wellington V. (2014). Prenatal retinoid deficiency leads to airway hyperresponsiveness in adult mice. *The Journal of Clinical Investigation, 124*(2), 801-811. doi: 10.1172/JCI70291

Chen, J., Kubalak, S. W., & Chien, K. R. (1998). Ventricular muscle-restricted targeting of the RXRalpha gene reveals a non-cell-autonomous requirement in cardiac chamber morphogenesis. *Development, 125*(10), 1943.

Chen, N., & Napoli, J. L. (2008). All-trans-retinoic acid stimulates translation and induces spine formation in hippocampal neurons through a membrane-associated RARalpha. *FASEB J, 22*(1), 236-245. doi: 10.1096/fj.07-8739com

Chen, T., Chang, T. C., Kang, J. O., Choudhary, B., Makita, T., Tran, C. M., . . . Sucov, H. M. (2002). Epicardial induction of fetal cardiomyocyte proliferation via a retinoic acid-inducible trophic factor. *Dev Biol, 250*(1), 198-207.

Chou, C. M., Nelson, C., Tarle, S. A., Pribila, J. T., Bardakjian, T., Woods, S., . . . Glaser, T. (2015). Biochemical Basis for Dominant Inheritance, Variable Penetrance, and Maternal Effects in RBP4 Congenital Eye Disease. *Cell, 161*(3), 634-646. doi: 10.1016/j.cell.2015.03.006

Christoffels, Vincent M, Grieskamp, Thomas, Norden, Julia, Mommersteeg, Mathilda TM, Rudat, Carsten, & Kispert, Andreas. (2009). Tbx18 and the fate of epicardial progenitors. *Nature, 458*(7240), E8-E9.

Clagett-Dame, M., & DeLuca, H. F. (2002). The role of vitamin A in mammalian reproduction and embryonic development. *Annu Rev Nutr, 22*, 347-381. doi: 10.1146/annurev.nutr.22.010402.102745E

Collins, Michael D, & Mao, Gloria E. (1999). Teratology of retinoids. *Annual review of pharmacology and toxicology, 39*(1), 399-430.

Collop, A. H., Broomfield, J. A., Chandraratna, R. A., Yong, Z., Deimling, S. J., Kolker, S. J., . . . Drysdale, T. A. (2006). Retinoic acid signaling is essential for formation of the heart tube in Xenopus. *Dev Biol, 291*(1), 96-109. doi: 10.1016/j.ydbio.2005.12.018

Cordero, Dwight R., Brugmann, Samantha, Chu, Yvonne, Bajpai, Ruchi, Jame, Maryam, & Helms, Jill A. (2011). CRANIAL NEURAL CREST CELLS ON THE MOVE: THEIR ROLES IN CRANIOFACIAL DEVELOPMENT. *American journal of medical genetics. Part A, 155*(2), 270-279. doi: 10.1002/ajmg.a.33702

Couchman, J. R., & Rees, D. A. (1979). The behaviour of fibroblasts migrating from chick heart explants: changes in adhesion, locomotion and growth, and in the distribution of actomyosin and fibronectin. *J Cell Sci, 39*, 149-165.

Cukras, Catherine, Gaasterland, Terry, Lee, Pauline, Gudiseva, Harini V., Chavali, Venkata R. M., Pullakhandam, Raghu, . . . Ayyagari, Radha. (2012). Exome Analysis Identified a Novel Mutation in the RBP4 Gene in a Consanguineous Pedigree with Retinal Dystrophy and Developmental Abnormalities. *PLOS ONE, 7*(11), e50205. doi: 10.1371/journal.pone.0050205

D'Aniello, E., & Waxman, J. S. (2014). Input overload: contributions of retinoic acid signaling feedback mechanisms to heart development and teratogenesis. *Dev Dyn*. doi: 10.1002/dvdy.24232

Davis, L. A., & Sadler, T. W. (1981). Effects of vitamin A on endocardial cushion development in the mouse heart. *Teratology, 24*(2), 139-148. doi: 10.1002/tera.1420240205

de Paiva, Sergio Alberto Rupp, Zornoff, Leonardo Antonio Mamede, Okoshi, Marina Politi, Okoshi, Katashi, Matsubara, Luiz Shiguero, Matsubara, Beatriz Bojikian, . . . Campana, Alvaro Oscar. (2003). Ventricular remodeling induced by retinoic acid supplementation in adult rats. *American Journal of Physiology - Heart and Circulatory Physiology, 284*(6), H2242-H2246.

Delacroix, L., Moutier, E., Altobelli, G., Legras, S., Poch, O., Choukrallah, M. A., . . . Davidson, I. (2010). Cell-specific interaction of retinoic acid receptors with target genes in mouse embryonic fibroblasts and embryonic stem cells. *Mol Cell Biol, 30*(1), 231-244. doi: 10.1128/MCB.00756-09

Deltour, L., Foglio, M. H., & Duester, G. (1999). Metabolic deficiencies in alcohol dehydrogenase Adh1, Adh3, and Adh4 null mutant mice. Overlapping roles of Adh1 and Adh4 in ethanol clearance and metabolism of retinol to retinoic acid. *J Biol Chem, 274*(24), 16796-16801.

Dersch, H., & Zile, M. H. (1993). Induction of normal cardiovascular development in the vitamin A-deprived quail embryo by natural retinoids. *Dev Biol, 160*(2), 424-433. doi: 10.1006/dbio.1993.1318

Dickman, Eileen D., & Smith, Susan M. (1996). Selective regulation of cardiomyocyte gene expression and cardiac morphogenesis by retinoic acid. *Developmental Dynamics, 206*(1), 39-48. doi: 10.1002/(SICI)1097-0177(199605)206:1<39::AID-AJA4>3.0.CO;2-1

Dolle, P. (2009). Developmental expression of retinoic acid receptors (RARs). *Nucl Recept Signal, 7*, e006. doi: 10.1621/nrs.07006

Dolle, P., Fraulob, V., Gallego-Llamas, J., Vermot, J., & Niederreither, K. (2010). Fate of retinoic acid-activated embryonic cell lineages. *Dev Dyn, 239*(12), 3260-3274. doi: 10.1002/dvdy.22479

Dominguez, Melissa G., Hughes, Virginia C., Pan, Li, Simmons, Mary, Daly, Christopher, Anderson, Keith, . . . Gale, Nicholas W. (2007). Vascular endothelial tyrosine phosphatase (VE-PTP)-null mice undergo vasculogenesis but die embryonically because of defects in angiogenesis. *Proceedings of the National Academy of Sciences, 104*(9), 3243-3248. doi: 10.1073/pnas.0611510104

Duim, S. N., Kurakula, K., Goumans, M. J., & Kruithof, B. P. (2015). Cardiac endothelial cells express Wilms' tumor-1: Wt1 expression in the developing, adult and infarcted heart. *J Mol Cell Cardiol, 81*, 127-135. doi: 10.1016/j.yjmcc.2015.02.007

Eggenschwiler, Jonathan, Ludwig, Thomas, Fisher, Peter, Leighton, Philip A., Tilghman, Shirley M., & Efstratiadis, Argiris. (1997). Mouse mutant embryos overexpressing IGF-II exhibit phenotypic features of the Beckwith–Wiedemann and Simpson–Golabi–Behmel syndromes. *Genes & Development, 11*(23), 3128-3142. doi: 10.1101/gad.11.23.3128

Emoto, Y., Wada, H., Okamoto, H., Kudo, A., & Imai, Y. (2005). Retinoic acid-metabolizing enzyme Cyp26a1 is essential for determining territories of hindbrain and spinal cord in zebrafish. *Dev Biol, 278*(2), 415-427. doi: 10.1016/j.ydbio.2004.11.023

Ericson, J., Rashbass, P., Schedl, A., Brenner-Morton, S., Kawakami, A., van Heyningen, V., . . . Briscoe, J. (1997). Pax6 controls progenitor cell identity and neuronal fate in response to graded Shh signaling. *Cell, 90*(1), 169-180. doi: https://doi.org/10.1016/S0092-8674(00)80323-2

Fang, M., Xiang, F. L., Braitsch, C. M., & Yutzey, K. E. (2016). Epicardium-derived fibroblasts in heart development and disease. *J Mol Cell Cardiol, 91*, 23-27. doi: 10.1016/j.yjmcc.2015.12.019

Feng, L., Hernandez, R. E., Waxman, J. S., Yelon, D., & Moens, C. B. (2010). Dhrs3a Regulates Retinoic Acid Biosynthesis through a Feedback Inhibition Mechanism. *Developmental biology, 338*(1), 1-14. doi: 10.1016/j.ydbio.2009.10.029

Fischer, Andrew H., Jacobson, Kenneth A., Rose, Jack, & Zeller, Rolf. (2008). Hematoxylin and Eosin Staining of Tissue and Cell Sections. *Cold Spring Harbor Protocols, 2008*(5), pdb.prot4986. doi: 10.1101/pdb.prot4986

Franco, P. J., Farooqui, M., Seto, E., & Wei, L. N. (2001). The orphan nuclear receptor TR2 interacts directly with both class I and class II histone deacetylases. *Mol Endocrinol, 15*(8), 1318-1328. doi: 10.1210/mend.15.8.0682

Frenz, D. A., Liu, W., Cvekl, A., Xie, Q., Wassef, L., Quadro, L., . . . Shanske, A. (2010). Retinoid signaling in inner ear development: A "Goldilocks" phenomenon. *Am J Med Genet A, 152A*(12), 2947-2961. doi: 10.1002/ajmg.a.33670

Fujino, H., Nakagawa, M., Nishijima, S., Okamoto, N., Hanato, T., Watanabe, N., . . . Takeuchi, Y. (2005). Morphological differences in cardiovascular anomalies induced by bis-diamine between Sprague-Dawley and Wistar rats. *Congenit Anom (Kyoto), 45*(2), 52-58. doi: 10.1111/j.1741-4520.2005.00063.x

Gaengel, K., Genove, G., Armulik, A., & Betsholtz, C. (2009). Endothelial-mural cell signaling in vascular development and angiogenesis. *Arterioscler Thromb Vasc Biol, 29*(5), 630-638. doi: 10.1161/atvbaha.107.161521

Gallego, O., Ruiz, F. X., Ardevol, A., Dominguez, M., Alvarez, R., de Lera, A. R., . . . Pares, X. (2007). Structural basis for the high all-trans-retinaldehyde reductase activity of the tumor marker AKR1B10. *Proc Natl Acad Sci U S A, 104*(52), 20764-20769. doi: 10.1073/pnas.0705659105

Galli, D., Dominguez, J. N., Zaffran, S., Munk, A., Brown, N. A., & Buckingham, M. E. (2008). Atrial myocardium derives from the posterior region of the second heart field, which acquires left-right identity as Pitx2c is expressed. *Development, 135*(6), 1157-1167. doi: 10.1242/dev.014563

Ghatpande, S., Brand, T., Zile, M., & Evans, T. (2006). Bmp2 and Gata4 function additively to rescue heart tube development in the absence of retinoids. *Dev Dyn, 235*(8), 2030-2039. doi: 10.1002/dvdy.20836

Ghatpande, Satish K., Zhou, Hui-Ren, Cakstina, Inese, Carlson, Christopher, Rondini, Elizabeth A., Romeih, Mahmoud, & Zile, Maija H. (2010). Transforming growth factor β2 is negatively regulated by endogenous retinoic acid during early heart morphogenesis. *Development, Growth & Differentiation, 52*(5), 433-455. doi: 10.1111/j.1440-169X.2010.01183.x

Ghyselinck, N. B., Dupe, V., Dierich, A., Messaddeq, N., Garnier, J. M., Rochette-Egly, C., . . . Mark, M. (1997). Role of the retinoic acid receptor beta (RARbeta) during mouse development. *Int J Dev Biol, 41*(3), 425-447.

Ghyselinck, N. B., Wendling, O., Messaddeq, N., Dierich, A., Lampron, C., Decimo, D., . . . Mark, M. (1998). Contribution of retinoic acid receptor beta isoforms to the formation of the conotruncal septum of the embryonic heart. *Dev Biol, 198*(2), 303-318.

Giguere, V., Ong, E. S., Segui, P., & Evans, R. M. (1987). Identification of a receptor for the morphogen retinoic acid. *Nature, 330*(6149), 624-629. doi: 10.1038/330624a0

Giovannone, Dion, Reyes, Michelle, Reyes, Rachel, Correa, Lisa, Martinez, Darwin, Ra, Hannah, . . . de Bellard, Maria Elena. (2012). Slits Affect the Timely Migration of Neural Crest Cells via Robo Receptor. *Developmental dynamics : an official publication of the American Association of Anatomists, 241*(8), 1274-1288. doi: 10.1002/dvdy.23817

Gittenberger-de Groot, Adriana C., Vrancken Peeters, Mark-Paul F.M., Mentink, Monica M.T., Gourdie, Robert G., & Poelmann, Robert E. (1998). Epicardium-Derived Cells Contribute a Novel Population to the Myocardial Wall and the Atrioventricular Cushions. *Circulation Research, 82*(10), 1043-1052. doi: 10.1161/01.res.82.10.1043

Glover, J. C., Renaud, J. S., & Rijli, F. M. (2006). Retinoic acid and hindbrain patterning. *J Neurobiol, 66*(7), 705-725. doi: 10.1002/neu.20272

Grandel, H., Lun, K., Rauch, G. J., Rhinn, M., Piotrowski, T., Houart, C., . . . Brand, M. (2002). Retinoic acid signalling in the zebrafish embryo is necessary during pre-segmentation stages to pattern the anterior-posterior axis of the CNS and to induce a pectoral fin bud. *Development, 129*(12), 2851-2865.

Grieskamp, Thomas, Rudat, Carsten, Lüdtke, Timo H.-W., Norden, Julia, & Kispert, Andreas. (2011). Notch Signaling Regulates Smooth Muscle Differentiation of Epicardium-Derived Cells. *Circulation Research, 108*(7), 813-823. doi: 10.1161/circresaha.110.228809

Guadix, J. A., Ruiz-Villalba, A., Lettice, L., Velecela, V., Munoz-Chapuli, R., Hastie, N. D., . . . Martinez-Estrada, O. M. (2011). Wt1 controls retinoic acid signalling in embryonic epicardium through transcriptional activation of Raldh2. *Development, 138*(6), 1093-1097. doi: 10.1242/dev.044594

Guadix, Juan A, Carmona, Rita, Muñoz-Chápuli, Ramón, & Pérez-Pomares, José M. (2006). In vivo and in vitro analysis of the vasculogenic potential of avian proepicardial and epicardial cells†. *Developmental dynamics, 235*(4), 1014-1026.

Guadix, Juan A., Carmona, Rita, Muñoz-Chápuli, Ramón, & Pérez-Pomares, José M. (2006). In vivo and in vitro analysis of the vasculogenic potential of avian proepicardial and epicardial cells†. *Developmental Dynamics, 235*(4), 1014-1026. doi: 10.1002/dvdy.20685

Guimarães-Camboa, Nuno, Stowe, Jennifer, Aneas, Ivy, Sakabe, Noboru, Cattaneo, Paola, Henderson, Lindsay, . . . Zambon, Alexander C. (2015). HIF1α Represses Cell Stress Pathways to Allow Proliferation of Hypoxic Fetal Cardiomyocytes. *Developmental Cell, 33*(5), 507-521. doi: https://doi.org/10.1016/j.devcel.2015.04.021

Haeseleer, F., Huang, J., Lebioda, L., Saari, J. C., & Palczewski, K. (1998). Molecular characterization of a novel short-chain dehydrogenase/reductase that reduces all-trans-retinal. *J Biol Chem, 273*(34), 21790-21799.

Hale, Fred. (1937). The relation of maternal vitamin A deficiency to microphthalmia in pigs. *Texas State Journal of Medicine, 33*, 228-232.

Hanato, T., Nakagawa, M., Okamoto, N., Nishijima, S., Fujino, H., Shimada, M., . . . Imanaka-Yoshida, K. (2011). Developmental defects of coronary vasculature in rat embryos administered bis-diamine. *Birth Defects Res B Dev Reprod Toxicol, 92*(1), 10-16. doi: 10.1002/bdrb.20279

Heallen, T., Morikawa, Y., Leach, J., Tao, G., Willerson, J. T., Johnson, R. L., & Martin, J. F. (2013). Hippo signaling impedes adult heart regeneration. *Development, 140*(23), 4683-4690. doi: 10.1242/dev.102798

Hector, A. Marquez, Felicia, Chen, Yuxia, Cao, & Wellington, V. Cardoso. (2013). Regulation Of Airway Smooth Muscle Differentiation By Retinoic Acid In The Developing Lung *C69. PATHWAYS TO LUNG DEVELOPMENT AND DISEASE* (pp. A4776-A4776): American Thoracic Society.

Heine, U. I., Roberts, A. B., Munoz, E. F., Roche, N. S., & Sporn, M. B. (1985). Effects of retinoid deficiency on the development of the heart and vascular system of the quail embryo. *Virchows Arch B Cell Pathol Incl Mol Pathol, 50*(2), 135-152.

Heller, C. G., Moore, D. J., & Paulsen, C. A. (1961). Suppression of spermatogenesis and chronic toxicity in men by a new series of bis(dichloroacetyl) diamines. *Toxicol Appl Pharmacol, 3*, 1-11.

Hellstrom, M., Gerhardt, H., Kalen, M., Li, X., Eriksson, U., Wolburg, H., & Betsholtz, C. (2001). Lack of pericytes leads to endothelial hyperplasia and abnormal vascular morphogenesis. *J Cell Biol, 153*(3), 543-553.

Hellstrom, M., Kalen, M., Lindahl, P., Abramsson, A., & Betsholtz, C. (1999). Role of PDGF-B and PDGFR-beta in recruitment of vascular smooth muscle cells and pericytes during embryonic blood vessel formation in the mouse. *Development, 126*(14), 3047-3055.

Hessel, S., Eichinger, A., Isken, A., Amengual, J., Hunzelmann, S., Hoeller, U., . . . Wyss, A. (2007). CMO1 deficiency abolishes vitamin A production from beta-carotene and alters lipid metabolism in mice. *J Biol Chem, 282*(46), 33553-33561. doi: 10.1074/jbc.M706763200

Hochgreb, T., Linhares, V. L., Menezes, D. C., Sampaio, A. C., Yan, C. Y., Cardoso, W. V., . . . Xavier-Neto, J. (2003). A caudorostral wave of RALDH2 conveys anteroposterior information to the cardiac field. *Development, 130*(22), 5363-5374. doi: 10.1242/dev.00750

Hochgreb, Tatiana, Linhares, Vania L., Menezes, Diego C., Sampaio, Allysson C., Yan, Chao Y. I., Cardoso, Wellington V., . . . Xavier-Neto, José. (2003). A caudorostral wave of RALDH2 conveys anteroposterior information to the cardiac field. *Development, 130*(22), 5363-5374.

Hoffman, J. I. (1995). Incidence of congenital heart disease: I. Postnatal incidence. *Pediatr Cardiol, 16*(3), 103-113. doi: 10.1007/BF00801907

Hoffman, J. I., & Kaplan, S. (2002). The incidence of congenital heart disease. *J Am Coll Cardiol, 39*(12), 1890-1900.

Hoover, L. L., Burton, E. G., Brooks, B. A., & Kubalak, S. W. (2008). The expanding role for retinoid signaling in heart development. *ScientificWorldJournal, 8,* 194-211. doi: 10.1100/tsw.2008.39

Huang, G. N., Thatcher, J. E., McAnally, J., Kong, Y., Qi, X., Tan, W., . . . Olson, E. N. (2012). C/EBP transcription factors mediate epicardial activation during heart development and injury. *Science, 338*(6114), 1599-1603. doi: 10.1126/science.1229765

Huang, Y., Harrison, M. R., Osorio, A., Kim, J., Baugh, A., Duan, C., . . . Lien, C. L. (2013). Igf Signaling is Required for Cardiomyocyte Proliferation during Zebrafish Heart Development and Regeneration. *PLoS One, 8*(6), e67266. doi: 10.1371/journal.pone.0067266

Hutson, M. R., & Kirby, M. L. (2007). Model systems for the study of heart development and disease. Cardiac neural crest and conotruncal malformations. *Semin Cell Dev Biol, 18*(1), 101-110. doi: 10.1016/j.semcdb.2006.12.004

Ilagan, Roger, Abu-Issa, Radwan, Brown, Doris, Yang, Yu-Ping, Jiao, Kai, Schwartz, Robert J., . . . Meyers, Erik N. (2006). Fgf8 is required for anterior heart field development. *Development, 133*(12), 2435-2445.

Ishiguro, A., Inagaki, M., & Kaga, M. (2007). Stereotypic circling behavior in mice with vestibular dysfunction: asymmetrical effects of intrastriatal microinjection of a dopamine agonist. *Int J Neurosci, 117*(7), 1049-1064. doi: 10.1080/00207450600936874

Isken, A., Golczak, M., Oberhauser, V., Hunzelmann, S., Driever, W., Imanishi, Y., . . . von Lintig, J. (2008). RBP4 disrupts vitamin A uptake homeostasis in a STRA6-deficient animal model for Matthew-Wood syndrome. *Cell Metab, 7*(3), 258-268. doi: 10.1016/j.cmet.2008.01.009

Ito, H., Iwasaki, K., Ikeda, T., Sakai, H., Shimokawa, I., & Matsuo, T. (1992). HNK-1 expression pattern in normal and bis-diamine induced malformed developing rat heart: three dimensional reconstruction analysis using computer graphics. *Anat Embryol (Berl), 186*(4), 327-334.

Jackson, M., Connell, M. G., Smith, A., Drury, J., & Anderson, R. H. (1995). Common arterial trunk and pulmonary atresia: close developmental cousins? results from a teratogen induced animal model. *Cardiovasc Res, 30*(6), 992-1000.

Jiang, Xiaobing, Choudhary, Bibha, Merki, Esther, Chien, Kenneth R., Maxson, Robert E., & Sucov, Henry M. (2002). Normal fate and altered function of the cardiac neural crest cell lineage in retinoic acid receptor mutant embryos. *Mechanisms of Development, 117*(1–2), 115-122. doi: http://dx.doi.org/10.1016/S0925-4773(02)00206-X

Kam, R. K., Chen, Y., Chan, S. O., Chan, W. Y., Dawid, I. B., & Zhao, H. (2010). Developmental expression of Xenopus short-chain dehydrogenase/reductase 3. *Int J Dev Biol, 54*(8-9), 1355-1360. doi: 10.1387/ijdb.092984rk

Kam, R. K., Shi, W., Chan, S. O., Chen, Y., Xu, G., Lau, C. B., . . . Zhao, H. (2013). Dhrs3 protein attenuates retinoic acid signaling and is required for early embryonic patterning. *J Biol Chem, 288*(44), 31477-31487. doi: 10.1074/jbc.M113.514984

Kam, Richard Kin Ting, Shi, Weili, Chan, Sun On, Chen, Yonglong, Xu, Gang, Lau, Clara Bik-San, . . . Zhao, Hui. (2013). Dhrs3 Protein Attenuates Retinoic Acid Signaling and Is Required for Early Embryonic Patterning. *The Journal of Biological Chemistry, 288*(44), 31477-31487. doi: 10.1074/jbc.M113.514984

Kambe, T., Tada-Kambe, J., Kuge, Y., Yamaguchi-Iwai, Y., Nagao, M., & Sasaki, R. (2000). Retinoic acid stimulates erythropoietin gene transcription in embryonal carcinoma cells through the direct repeat of a steroid/thyroid hormone receptor response element half-site in the hypoxia-response enhancer. *Blood, 96*(9), 3265-3271.

Kane, M. A., Chen, N., Sparks, S., & Napoli, J. L. (2005). Quantification of endogenous retinoic acid in limited biological samples by LC/MS/MS. *Biochem J, 388*(Pt 1), 363-369. doi: 10.1042/BJ20041867

Kane, M. A., & Napoli, J. L. (2010). Quantification of endogenous retinoids. *Methods Mol Biol, 652*, 1-54. doi: 10.1007/978-1-60327-325-1_1

Kang, Jione, Gu, Ying, Li, Peng, Johnson, Betsy L, Sucov, Henry M, & Thomas, Penny S. (2008). PDGF-A as an epicardial mitogen during heart development. *Developmental Dynamics, 237*(3), 692-701.

Kardami, E., & Fandrich, R. R. (1989). Basic fibroblast growth factor in atria and ventricles of the vertebrate heart. *J Cell Biol, 109*(4 Pt 1), 1865-1875.

Kastner, P., Messaddeq, N., Mark, M., Wendling, O., Grondona, J. M., Ward, S., . . . Chambon, P. (1997). Vitamin A deficiency and mutations of RXRalpha, RXRbeta and RARalpha lead to early differentiation of embryonic ventricular cardiomyocytes. *Development, 124*(23), 4749-4758.

Katz, T. C., Singh, M. K., Degenhardt, K., Rivera-Feliciano, J., Johnson, R. L., Epstein, J. A., & Tabin, C. J. (2012). Distinct compartments of the proepicardial organ give rise to coronary vascular endothelial cells. *Dev Cell, 22*(3), 639-650. doi: 10.1016/j.devcel.2012.01.012

Kedishvili, N. Y. (2013). Enzymology of retinoic acid biosynthesis and degradation. *J Lipid Res, 54*(7), 1744-1760. doi: 10.1194/jlr.R037028

Keegan, Brian R., Feldman, Jessica L., Begemann, Gerrit, Ingham, Philip W., & Yelon, Deborah. (2005). Retinoic Acid Signaling Restricts the Cardiac Progenitor Pool. *Science, 307*(5707), 247-249. doi: 10.1126/science.1101573

Kelly, M., Widjaja-Adhi, M. A., Palczewski, G., & von Lintig, J. (2016). Transport of vitamin A across blood-tissue barriers is facilitated by STRA6. *FASEB J, 30*(8), 2985-2995. doi: 10.1096/fj.201600446R

Kelly, R. G. (2012). The second heart field. *Curr Top Dev Biol, 100*, 33-65. doi: 10.1016/b978-0-12-387786-4.00002-6

Kennedy-Lydon, T., & Rosenthal, N. (2015). Cardiac regeneration: epicardial mediated repair. *Proc Biol Sci, 282*(1821), 20152147. doi: 10.1098/rspb.2015.2147

Kessel, Michael, & Gruss, Peter. (1991). Homeotic transformations of murine vertebrae and concomitant alteration of Hox codes induced by retinoic acid. *Cell, 67*(1), 89-104. doi: https://doi.org/10.1016/0092-8674(91)90574-I

Kikuchi, K., Holdway, J. E., Major, R. J., Blum, N., Dahn, R. D., Begemann, G., & Poss, K. D. (2011). Retinoic acid production by endocardium and epicardium is an injury response essential for zebrafish heart regeneration. *Dev Cell, 20*(3), 397-404. doi: 10.1016/j.devcel.2011.01.010

Kikuchi, Kazu, Gupta, Vikas, Wang, Jinhu, Holdway, Jennifer E., Wills, Airon A., Fang, Yi, & Poss, Kenneth D. (2011). tcf21 epicardial cells adopt non-myocardial fates during zebrafish heart development and regeneration. *Development, 138*(14), 2895-2902. doi: 10.1242/dev.067041

Kilburn, K. H., Hess, R. A., Lesser, M., & Oster, G. (1982). Perinatal death and respiratory apparatus dysgenesis due to a bis (dichloroacetyl) diamine. *Teratology, 26*(2), 155-162. doi: 10.1002/tera.1420260207

Kim, J., Wu, Q., Zhang, Y., Wiens, K. M., Huang, Y., Rubin, N., . . . Lien, C. L. (2010). PDGF signaling is required for epicardial function and blood vessel formation in regenerating zebrafish hearts. *Proc Natl Acad Sci U S A, 107*(40), 17206-17210. doi: 10.1073/pnas.0915016107

Kise, K., Nakagawa, M., Okamoto, N., Hanato, T., Watanabe, N., Nishijima, S., . . . Shiraishi, I. (2005). Teratogenic effects of bis-diamine on the developing cardiac conduction system. *Birth Defects Res A Clin Mol Teratol, 73*(8), 547-554. doi: 10.1002/bdra.20163

Kliewer, S. A., Umesono, K., Mangelsdorf, D. J., & Evans, R. M. (1992). Retinoid X receptor interacts with nuclear receptors in retinoic acid, thyroid hormone and vitamin D3 signalling. *Nature, 355*(6359), 446-449. doi: 10.1038/355446a0

Kochhar, D. M. (1973). Limb development in mouse embryos. I. Analysis of teratogenic effects of retinoic acid. *Teratology, 7*(3), 289-298. doi: 10.1002/tera.1420070310

Kolodzinska, A., Heleniak, A., & Ratajska, A. (2013). Retinoic acid-induced ventricular non-compacted cardiomyopathy in mice. *Kardiol Pol, 71*(5), 447-452. doi: 10.5603/KP.2013.0090

Koop, Demian, Holland, Nicholas D., Sémon, Marie, Alvarez, Susana, de Lera, Angel Rodriguez, Laudet, Vincent, . . . Schubert, Michael. (2010). Retinoic acid signaling targets Hox genes during the amphioxus gastrula stage: Insights into early anterior–posterior patterning of the chordate body plan. *Developmental Biology, 338*(1), 98-106. doi: http://dx.doi.org/10.1016/j.ydbio.2009.11.016

Kostetskii, I., Jiang, Y., Kostetskaia, E., Yuan, S., Evans, T., & Zile, M. (1999). Retinoid signaling required for normal heart development regulates GATA-4 in a pathway distinct from cardiomyocyte differentiation. *Dev Biol, 206*(2), 206-218. doi: 10.1006/dbio.1998.9139

Kostetskii, I., Yuan, S. Y., Kostetskaia, E., Linask, K. K., Blanchet, S., Seleiro, E., . . . Zile, M. (1998). Initial retinoid requirement for early avian development coincides with retinoid receptor coexpression in the precardiac fields and induction of normal cardiovascular development. *Dev Dyn, 213*(2), 188-198. doi: 10.1002/(SICI)1097-0177(199810)213:2<188::AID-AJA4>3.0.CO;2-C

Krust, A., Kastner, P., Petkovich, M., Zelent, A., & Chambon, P. (1989). A third human retinoic acid receptor, hRAR-gamma. *Proc Natl Acad Sci U S A, 86*(14), 5310-5314.

Kumar, S., & Duester, G. (2014). Retinoic acid controls body axis extension by directly repressing Fgf8 transcription. *Development, 141*(15), 2972-2977. doi: 10.1242/dev.112367

Kumar, S., Sandell, L. L., Trainor, P. A., Koentgen, F., & Duester, G. (2012). Alcohol and aldehyde dehydrogenases: retinoid metabolic effects in mouse knockout models. *Biochim Biophys Acta, 1821*(1), 198-205. doi: 10.1016/j.bbalip.2011.04.004

Kuribayashi, T., & Roberts, W. C. (1993). Tetralogy of Fallot, truncus arteriosus, abnormal myocardial architecture and anomalies of the aortic arch system induced by bis-diamine in rat fetuses. *J Am Coll Cardiol, 21*(3), 768-776.

Lai, L., Bohnsack, B. L., Niederreither, K., & Hirschi, K. K. (2003). Retinoic acid regulates endothelial cell proliferation during vasculogenesis. *Development, 130*(26), 6465-6474. doi: 10.1242/dev.00887

Lamalice, Laurent, Le Boeuf, Fabrice, & Huot, Jacques. (2007). Endothelial Cell Migration During Angiogenesis. *Circulation Research, 100*(6), 782-794. doi: 10.1161/01.RES.0000259593.07661.1e

Lammer, E. J., Chen, D. T., Hoar, R. M., Agnish, N. D., Benke, P. J., Braun, J. T., . . . et al. (1985). Retinoic acid embryopathy. *N Engl J Med, 313*(14), 837-841. doi: 10.1056/NEJM198510033131401

Lavine, K. J., Yu, K., White, A. C., Zhang, X., Smith, C., Partanen, J., & Ornitz, D. M. (2005). Endocardial and epicardial derived FGF signals regulate myocardial proliferation and differentiation in vivo. *Dev Cell, 8*(1), 85-95. doi: 10.1016/j.devcel.2004.12.002

Lavine, Kory J., Yu, Kai, White, Andrew C., Zhang, Xiuqin, Smith, Craig, Partanen, Juha, & Ornitz, David M. (2005). Endocardial and Epicardial Derived FGF Signals Regulate Myocardial Proliferation and Differentiation In Vivo. *Developmental Cell, 8*(1), 85-95. doi: http://dx.doi.org/10.1016/j.devcel.2004.12.002

Lee, L. M., Leung, C. Y., Tang, W. W., Choi, H. L., Leung, Y. C., McCaffery, P. J., . . . Shum, A. S. (2012). A paradoxical teratogenic mechanism for retinoic acid. *Proc Natl Acad Sci U S A, 109*(34), 13668-13673. doi: 10.1073/pnas.1200872109

Lepilina, A., Coon, A. N., Kikuchi, K., Holdway, J. E., Roberts, R. W., Burns, C. G., & Poss, K. D. (2006). A dynamic epicardial injury response supports progenitor cell activity during zebrafish heart regeneration. *Cell, 127*(3), 607-619. doi: 10.1016/j.cell.2006.08.052

Li, E., Sucov, H. M., Lee, K. F., Evans, R. M., & Jaenisch, R. (1993). Normal development and growth of mice carrying a targeted disruption of the alpha 1 retinoic acid receptor gene. *Proceedings of the National Academy of Sciences of the United States of America, 90*(4), 1590-1594.

Li, P., Cavallero, S., Gu, Y., Chen, T. H., Hughes, J., Hassan, A. B., . . . Sucov, H. M. (2011). IGF signaling directs ventricular cardiomyocyte proliferation during embryonic heart development. *Development, 138*(9), 1795-1805. doi: 10.1242/dev.054338

Li, P., Pashmforoush, M., & Sucov, H. M. (2010). Retinoic acid regulates differentiation of the secondary heart field and TGFbeta-mediated outflow tract septation. *Dev Cell, 18*(3), 480-485. doi: 10.1016/j.devcel.2009.12.019

Li, Peng, Cavallero, Susana, Gu, Ying, Chen, Tim H. P., Hughes, Jennifer, Hassan, A. Bassim, . . . Sucov, Henry M. (2011). IGF signaling directs ventricular cardiomyocyte proliferation during embryonic heart development. *Development, 138*(9), 1795-1805. doi: 10.1242/dev.054338

Liberatore, C. M., Searcy-Schrick, R. D., & Yutzey, K. E. (2000). Ventricular expression of tbx5 inhibits normal heart chamber development. *Dev Biol, 223*(1), 169-180. doi: 10.1006/dbio.2000.9748

Lie-Venema, H., Eralp, I., Markwald, R. R., van den Akker, N. M., Wijffels, M. C., Kolditz, D. P., . . . Gittenberger-de Groot, A. C. (2008). Periostin expression by epicardium-derived cells is involved in the development of the atrioventricular valves and fibrous heart skeleton. *Differentiation, 76*(7), 809-819. doi: 10.1111/j.1432-0436.2007.00262.x

Lie-Venema, H., van den Akker, N. M., Bax, N. A., Winter, E. M., Maas, S., Kekarainen, T., . . . Gittenberger-de Groot, A. C. (2007). Origin, fate, and function of epicardium-derived cells (EPDCs) in normal and abnormal cardiac development. *ScientificWorldJournal, 7*, 1777-1798. doi: 10.1100/tsw.2007.294

Lin, S. C., Dolle, P., Ryckebusch, L., Noseda, M., Zaffran, S., Schneider, M. D., & Niederreither, K. (2010). Endogenous retinoic acid regulates cardiac progenitor differentiation. *Proc Natl Acad Sci U S A, 107*(20), 9234-9239. doi: 10.1073/pnas.0910430107

Lin, Song-Chang, Dollé, Pascal, Ryckebüsch, Lucile, Noseda, Michela, Zaffran, Stéphane, Schneider, Michael D., & Niederreither, Karen. (2010). Endogenous retinoic acid regulates cardiac progenitor differentiation. *Proceedings of the National Academy of Sciences of the United States of America, 107*(20), 9234-9239. doi: 10.1073/pnas.0910430107

Liu, Q., Yan, H., Dawes, N. J., Mottino, G. A., Frank, J. S., & Zhu, H. (1996). Insulin-like growth factor II induces DNA synthesis in fetal ventricular myocytes in vitro. *Circ Res, 79*(4), 716-726.

Lobo, G. P., Hessel, S., Eichinger, A., Noy, N., Moise, A. R., Wyss, A., . . . von Lintig, J. (2010). ISX is a retinoic acid-sensitive gatekeeper that controls intestinal beta,beta-carotene absorption and vitamin A production. *FASEB J, 24*(6), 1656-1666. doi: 10.1096/fj.09-150995

Lockhart, Marie M., Phelps, Aimee L., van den Hoff, Maurice J. B., & Wessels, Andy. (2014). The Epicardium and the Development of the Atrioventricular Junction in the Murine Heart. *Journal of developmental biology, 2*(1), 1-17. doi: 10.3390/jdb2010001

Lohnes, D., Mark, M., Mendelsohn, C., Dolle, P., Dierich, A., Gorry, P., . . . Chambon, P. (1994). Function of the retinoic acid receptors (RARs) during development (I). Craniofacial and skeletal abnormalities in RAR double mutants. *Development, 120*(10), 2723-2748.

Lu, J., Landerholm, T. E., Wei, J. S., Dong, X. R., Wu, S. P., Liu, X., . . . Majesky, M. W. (2001). Coronary smooth muscle differentiation from proepicardial cells requires rhoA-mediated actin reorganization and p160 rho-kinase activity. *Dev Biol, 240*(2), 404-418. doi: 10.1006/dbio.2001.0403

Maclean, G., Dolle, P., & Petkovich, M. (2009). Genetic disruption of CYP26B1 severely affects development of neural crest derived head structures, but does not compromise hindbrain patterning. *Dev Dyn, 238*(3), 732-745. doi: 10.1002/dvdy.21878

Maclean, Glenn, Dollé, Pascal, & Petkovich, Martin. (2009). Genetic disruption of CYP26B1 severely affects development of neural crest derived head structures, but does not compromise hindbrain patterning. *Developmental Dynamics, 238*(3), 732-745. doi: 10.1002/dvdy.21878

Maden, Malcolm, Gale, Emily, Kostetskii, Igor, & Zile, Maija. (1996). Vitamin A-deficient quail embryos have half a hindbrain and other neural defects. *Current Biology, 6*(4), 417-426. doi: 10.1016/s0960-9822(02)00509-2

Maekawa, M., Ishizaki, T., Boku, S., Watanabe, N., Fujita, A., Iwamatsu, A., . . . Narumiya, S. (1999). Signaling from Rho to the actin cytoskeleton through protein kinases ROCK and LIM-kinase. *Science, 285*(5429), 895-898.

Manabe, I., & Owens, G. K. (2001). Recruitment of serum response factor and hyperacetylation of histones at smooth muscle-specific regulatory regions during differentiation of a novel P19-derived in vitro smooth muscle differentiation system. *Circ Res, 88*(11), 1127-1134.

Marin-Juez, R., Marass, M., Gauvrit, S., Rossi, A., Lai, S. L., Materna, S. C., . . . Stainier, D. Y. (2016). Fast revascularization of the injured area is essential to support zebrafish heart regeneration. *Proc Natl Acad Sci U S A, 113*(40), 11237-11242. doi: 10.1073/pnas.1605431113

Marques, S. R., Lee, Y., Poss, K. D., & Yelon, D. (2008). Reiterative roles for FGF signaling in the establishment of size and proportion of the zebrafish heart. *Dev Biol, 321*(2), 397-406. doi: 10.1016/j.ydbio.2008.06.033

Martínez-Estrada, Ofelia M, Lettice, Laura A, Essafi, Abdelkader, Guadix, Juan Antonio, Slight, Joan, Velecela, Víctor, . . . Hohenstein, Peter. (2010). Wt1 is required for cardiovascular progenitor cell formation through transcriptional control of Snail and E-cadherin. *Nature genetics, 42*(1), 89-93.

Mason, Karl E. (1935). Foetal death, prolonged gestation, and difficult parturition in the rat as a result of vitamin A-deficiency. *American Journal of Anatomy, 57*(2), 303-349.

Masters, Megan, & Riley, Paul R. (2014). The epicardium signals the way towards heart regeneration. *Stem Cell Research, 13*(3), 683-692. doi: 10.1016/j.scr.2014.04.007

Matt, N., Schmidt, C. K., Dupe, V., Dennefeld, C., Nau, H., Chambon, P., . . . Ghyselinck, N. B. (2005). Contribution of cellular retinol-binding protein type 1 to retinol metabolism during mouse development. *Dev Dyn, 233*(1), 167-176. doi: 10.1002/dvdy.20313

McCollum, Elmer Verner, & Davis, Marguerite. (1913). The necessity of certain lipids in the diet during growth.

Mellgren, A. M., Smith, C. L., Olsen, G. S., Eskiocak, B., Zhou, B., Kazi, M. N., . . . Tallquist, M. D. (2008). Platelet-derived growth factor receptor beta signaling is required for efficient epicardial cell migration and development of two distinct coronary vascular smooth muscle cell populations. *Circ Res, 103*(12), 1393-1401. doi: 10.1161/CIRCRESAHA.108.176768

Mellgren, Amy M., Smith, Christopher L., Olsen, Gregory S., Eskiocak, Banu, Zhou, Bin, Kazi, Michelle N., . . . Tallquist, Michelle D. (2008). PDGFRβ signaling is required for efficient epicardial cell migration and development of two distinct coronary vascular smooth muscle cell populations. *Circulation research, 103*(12), 1393-1401. doi: 10.1161/CIRCRESAHA.108.176768

Mendez, M. G., Kojima, S., & Goldman, R. D. (2010). Vimentin induces changes in cell shape, motility, and adhesion during the epithelial to mesenchymal transition. *Faseb j, 24*(6), 1838-1851. doi: 10.1096/fj.09-151639

Mercader, N., Fischer, S., & Neumann, C. J. (2006). Prdm1 acts downstream of a sequential RA, Wnt and Fgf signaling cascade during zebrafish forelimb induction. *Development, 133*(15), 2805-2815. doi: 10.1242/dev.02455

Merki, E., Zamora, M., Raya, A., Kawakami, Y., Wang, J., Zhang, X., . . . Ruiz-Lozano, P. (2005). Epicardial retinoid X receptor alpha is required for myocardial growth and coronary artery formation. *Proc Natl Acad Sci U S A, 102*(51), 18455-18460. doi: 10.1073/pnas.0504343102

Metzler, M. A., & Sandell, L. L. (2016). Enzymatic Metabolism of Vitamin A in Developing Vertebrate Embryos. *Nutrients, 8*(12). doi: 10.3390/nu8120812

Mic, F. A., Molotkov, A., Fan, X., Cuenca, A. E., & Duester, G. (2000). RALDH3, a retinaldehyde dehydrogenase that generates retinoic acid, is expressed in the ventral retina, otic vesicle and olfactory pit during mouse development. *Mech Dev, 97*(1-2), 227-230.

Mic, Felix A., Haselbeck, Robert J., Cuenca, Arnold E., & Duester, Gregg. (2002). Novel retinoic acid generating activities in the neural tube and heart identified by conditional rescue of Raldh2 null mutant mice. *Development, 129*(9), 2271.

Michielon, G., Di Carlo, D., Brancaccio, G., Guccione, P., Mazzera, E., Toscano, A., & Di Donato, R. M. (2003). Anomalous coronary artery origin from the pulmonary artery: correlation between surgical timing and left ventricular function recovery. *Ann Thorac Surg, 76*(2), 581-588; discussion 588.

Mikawa, T, & Fischman, D A. (1992). Retroviral analysis of cardiac morphogenesis: discontinuous formation of coronary vessels. *Proceedings of the National Academy of Sciences, 89*(20), 9504-9508. doi: 10.1073/pnas.89.20.9504

Minicucci, M. F., Azevedo, P. S., Oliveira, S. A., Jr., Martinez, P. F., Chiuso-Minicucci, F., Polegato, B. F., . . . Zornoff, L. A. (2010). Tissue vitamin A insufficiency results in adverse ventricular

remodeling after experimental myocardial infarction. *Cell Physiol Biochem, 26*(4-5), 523-530. doi: 10.1159/000322320

Minoux, M., & Rijli, F. M. (2010). Molecular mechanisms of cranial neural crest cell migration and patterning in craniofacial development. *Development, 137*(16), 2605-2621. doi: 10.1242/dev.040048

Mizutani, Makiko, Wu, Joseph C., & Nusse, Roeland. (2016). Fibrosis of the Neonatal Mouse Heart After Cryoinjury Is Accompanied by Wnt Signaling Activation and Epicardial-to-Mesenchymal Transition. *Journal of the American Heart Association, 5*(3). doi: 10.1161/jaha.115.002457

Moasser, Mark M., & Dmitrovsky, Ethan. The retinoids: Biology, chemistry, and medicine, second edition. *Trends in Endocrinology & Metabolism, 6*(5), 185-186. doi: 10.1016/1043-2760(95)90051-9

Mollard, Richard, Viville, Stéphane, Ward, Simon J., Décimo, Didier, Chambon, Pierre, & Dollé, Pascal. (2000). Tissue-specific expression of retinoic acid receptor isoform transcripts in the mouse embryo. *Mechanisms of Development, 94*(1–2), 223-232. doi: http://dx.doi.org/10.1016/S0925-4773(00)00303-8

Morriss-Kay, G. (1993). Retinoic acid and craniofacial development: molecules and morphogenesis. *Bioessays, 15*(1), 9-15. doi: 10.1002/bies.950150103

Moss, J. B., Xavier-Neto, J., Shapiro, M. D., Nayeem, S. M., McCaffery, P., Drager, U. C., & Rosenthal, N. (1998). Dynamic patterns of retinoic acid synthesis and response in the developing mammalian heart. *Dev Biol, 199*(1), 55-71. doi: 10.1006/dbio.1998.8911

Moss, Jennifer B, Xavier-Neto, José, Shapiro, Michael D, Nayeem, Sara M, McCaffery, Peter, Dräger, Ursula C, & Rosenthal, Nadia. (1998). Dynamic patterns of retinoic acid synthesis and response in the developing mammalian heart. *Developmental biology, 199*(1), 55-71.

Moutier, E., Ye, T., Choukrallah, M. A., Urban, S., Osz, J., Chatagnon, A., . . . Davidson, I. (2012). Retinoic acid receptors recognize the mouse genome through binding elements with diverse spacing and topology. *J Biol Chem, 287*(31), 26328-26341. doi: 10.1074/jbc.M112.361790

Moutier, Emmanuel, Ye, Tao, Choukrallah, Mohamed-Amin, Urban, Sylvia, Osz, Judit, Chatagnon, Amandine, . . . Moras, Dino. (2012). Retinoic acid receptors recognize the mouse genome through binding elements with diverse spacing and topology. *Journal of Biological Chemistry, 287*(31), 26328-26341.

Nanka, O., Valasek, P., Dvorakova, M., & Grim, M. (2006). Experimental hypoxia and embryonic angiogenesis. *Dev Dyn, 235*(3), 723-733. doi: 10.1002/dvdy.20689

Narematsu, Mayu, Kamimura, Tatsuya, Yamagishi, Toshiyuki, Fukui, Mitsuru, & Nakajima, Yuji. (2015). Impaired Development of Left Anterior Heart Field by Ectopic Retinoic Acid Causes Transposition of the Great Arteries. *Journal of the American Heart Association, 4*(5). doi: 10.1161/jaha.115.001889

Niederreither, K., Abu-Abed, S., Schuhbaur, B., Petkovich, M., Chambon, P., & Dolle, P. (2002). Genetic evidence that oxidative derivatives of retinoic acid are not involved in retinoid signaling during mouse development. *Nat Genet, 31*(1), 84-88. doi: 10.1038/ng876

Niederreither, K., Fraulob, V., Garnier, J. M., Chambon, P., & Dolle, P. (2002). Differential expression of retinoic acid-synthesizing (RALDH) enzymes during fetal development and organ differentiation in the mouse. *Mech Dev, 110*(1-2), 165-171.

Niederreither, K., McCaffery, P., Drager, U. C., Chambon, P., & Dolle, P. (1997). Restricted expression and retinoic acid-induced downregulation of the retinaldehyde dehydrogenase type 2 (RALDH-2) gene during mouse development. *Mech Dev, 62*(1), 67-78.

Niederreither, K., Subbarayan, V., Dolle, P., & Chambon, P. (1999). Embryonic retinoic acid synthesis is essential for early mouse post-implantation development. *Nat Genet, 21*(4), 444-448. doi: 10.1038/7788

Niederreither, K., Vermot, J., Fraulob, V., Chambon, P., & Dolle, P. (2002). Retinaldehyde dehydrogenase 2 (RALDH2)- independent patterns of retinoic acid synthesis in the mouse embryo. *Proc Natl Acad Sci U S A, 99*(25), 16111-16116. doi: 10.1073/pnas.252626599

Niederreither, K., Vermot, J., Messaddeq, N., Schuhbaur, B., Chambon, P., & Dolle, P. (2001). Embryonic retinoic acid synthesis is essential for heart morphogenesis in the mouse. *Development, 128*(7), 1019-1031.

Niederreither, Karen, Subbarayan, Vemparala, Dollé, Pascal, & Chambon, Pierre. (1999). Embryonic retinoic acid synthesis is essential for early mouse post-implantation development. *Nature genetics, 21*(4), 444-448.

Niederreither, Karen, Vermot, Julien, Roux, Isabelle Le, Schuhbaur, Brigitte, Chambon, Pierre, & Dollé, Pascal. (2003). The regional pattern of retinoic acid synthesis by RALDH2 is essential for the development of posterior pharyngeal arches and the enteric nervous system. *Development, 130*(11), 2525.

Nishijima, S., Nakagawa, M., Fujino, H., Hanato, T., Okamoto, N., & Shimada, M. (2000). Teratogenic effects of bis-diamine on early embryonic rat heart: an in vitro study. *Teratology, 62*(2), 115-122. doi: 10.1002/1096-9926(200008)62:2<115::AID-TERA8>3.0.CO;2-#

Okamoto, N., Nakagawa, M., Fujino, H., Nishijima, S., Hanato, T., Narita, T., . . . Imanaka-Yoshida, K. (2004). Teratogenic effects of bis-diamine on the developing myocardium. *Birth Defects Res A Clin Mol Teratol, 70*(3), 132-141. doi: 10.1002/bdra.20001

Okishima, T., Takamura, K., Matsuoka, Y., Ohdo, S., & Hayakawa, K. (1992). Cardiovascular anomalies in chick embryos produced by bis-diamine in dimethylsulfoxide. *Teratology, 45*(2), 155-162. doi: 10.1002/tera.1420450209

Olivey, H. E., & Svensson, E. C. (2010). Epicardial-myocardial signaling directing coronary vasculogenesis. *Circ Res, 106*(5), 818-832. doi: 10.1161/CIRCRESAHA.109.209197

Osmond, M. K., Butler, A. J., Voon, F. C., & Bellairs, R. (1991). The effects of retinoic acid on heart formation in the early chick embryo. *Development, 113*(4), 1405-1417.

Oster, G., Salgo, M. P., & Taleporos, P. (1974). Embryocidal action of a bis(dichloroacetyl)-diamine: an oral abortifacient for rats. *Am J Obstet Gynecol, 119*(5), 583-588.

Osumi, N., Hirota, A., Ohuchi, H., Nakafuku, M., Iimura, T., Kuratani, S., . . . Eto, K. (1997). Pax-6 is involved in the specification of hindbrain motor neuron subtype. *Development, 124*(15), 2961.

Paik, J., Haenisch, M., Muller, C. H., Goldstein, A. S., Arnold, S., Isoherranen, N., . . . Amory, J. K. (2014). Inhibition of retinoic acid biosynthesis by the bisdichloroacetyldiamine WIN 18,446 markedly suppresses spermatogenesis and alters retinoid metabolism in mice. *J Biol Chem, 289*(21), 15104-15117. doi: 10.1074/jbc.M113.540211

Paiva, S. A., Matsubara, L. S., Matsubara, B. B., Minicucci, M. F., Azevedo, P. S., Campana, A. O., & Zornoff, L. A. (2005). Retinoic acid supplementation attenuates ventricular remodeling after myocardial infarction in rats. *J Nutr, 135*(10), 2326-2328.

Papaioannou, Virginia E, & Behringer, Richard R. (2005). *Mouse phenotypes: a handbook of mutation analysis*: Cold Spring Harbor Laboratory Press.

Park, Eon Joo, Ogden, Lisa A., Talbot, Amy, Evans, Sylvia, Cai, Chen-Leng, Black, Brian L., . . . Moon, Anne M. (2006). Required, tissue-specific roles for Fgf8 in outflow tract formation and remodeling. *Development, 133*(12), 2419-2433.

Parlakian, Ara, Tuil, David, Hamard, Ghislaine, Tavernier, Geneviève, Hentzen, Daniele, Concordet, Jean-Paul, . . . Daegelen, Dominique. (2004). Targeted Inactivation of Serum Response Factor in the Developing Heart Results in Myocardial Defects and Embryonic Lethality. *Molecular and Cellular Biology, 24*(12), 5281-5289. doi: 10.1128/MCB.24.12.5281-5289.2004

Paschaki, M., Schneider, C., Rhinn, M., Thibault-Carpentier, C., Dembele, D., Niederreither, K., & Dolle, P. (2013). Transcriptomic analysis of murine embryos lacking endogenous retinoic acid signaling. *PLoS One, 8*(4), e62274. doi: 10.1371/journal.pone.0062274

Patterson, A. J., & Zhang, L. (2010). Hypoxia and fetal heart development. *Curr Mol Med, 10*(7), 653-666.

Pennimpede, T., Cameron, D. A., MacLean, G. A., Li, H., Abu-Abed, S., & Petkovich, M. (2010). The role of CYP26 enzymes in defining appropriate retinoic acid exposure during embryogenesis. *Birth Defects Res A Clin Mol Teratol, 88*(10), 883-894. doi: 10.1002/bdra.20709

Pennisi, D. J., & Mikawa, T. (2005). Normal patterning of the coronary capillary plexus is dependent on the correct transmural gradient of FGF expression in the myocardium. *Dev Biol*, *279*(2), 378-390. doi: 10.1016/j.ydbio.2004.12.028

Pennisi, David J., Ballard, Victoria L. T., & Mikawa, Takashi. (2003). Epicardium is required for the full rate of myocyte proliferation and levels of expression of myocyte mitogenic factors FGF2 and its receptor, FGFR-1, but not for transmural myocardial patterning in the embryonic chick heart. *Developmental Dynamics*, *228*(2), 161-172. doi: 10.1002/dvdy.10360

Perez-Pomares, J. M., & de la Pompa, J. L. (2011). Signaling during epicardium and coronary vessel development. *Circ Res*, *109*(12), 1429-1442. doi: 10.1161/CIRCRESAHA.111.245589

Perez-Pomares, J. M., Phelps, A., Sedmerova, M., Carmona, R., Gonzalez-Iriarte, M., Munoz-Chapuli, R., & Wessels, A. (2002). Experimental studies on the spatiotemporal expression of WT1 and RALDH2 in the embryonic avian heart: a model for the regulation of myocardial and valvuloseptal development by epicardially derived cells (EPDCs). *Dev Biol*, *247*(2), 307-326.

Pérez-Pomares, J. M., Phelps, A., Sedmerova, M., Carmona, R., González-Iriarte, M., Muñoz-Chápuli, R., & Wessels, A. (2002). Experimental Studies on the Spatiotemporal Expression of WT1 and RALDH2 in the Embryonic Avian Heart: A Model for the Regulation of Myocardial and Valvuloseptal Development by Epicardially Derived Cells (EPDCs). *Developmental Biology*, *247*(2), 307-326. doi: http://dx.doi.org/10.1006/dbio.2002.0706

Perez-Pomares, Jose-Maria, Carmona, Rita, Gonzalez-Iriarte, Mauricio, Atencia, Gerardo, Wessels, Andy, & Munoz-Chapuli, Ramon. (2002). Origin of coronary endothelial cells from epicardial mesothelium in avian embryos. *International Journal of Developmental Biology*, *46*(8), 1005-1013.

Petkovich, M., Brand, N. J., Krust, A., & Chambon, P. (1987). A human retinoic acid receptor which belongs to the family of nuclear receptors. *Nature*, *330*(6147), 444-450. doi: 10.1038/330444a0

Porrello, Enzo R., Mahmoud, Ahmed I., Simpson, Emma, Hill, Joseph A., Richardson, James A., Olson, Eric N., & Sadek, Hesham A. (2011). Transient Regenerative Potential of the Neonatal Mouse Heart. *Science, 331*(6020), 1078-1080. doi: 10.1126/science.1200708

Porté, Sergio, Ruiz, F Xavier, Giménez, Joan, Molist, Iago, Alvarez, Susana, Domínguez, Marta, . . . Farrés, Jaume. (2013). Aldo–keto reductases in retinoid metabolism: Search for substrate specificity and inhibitor selectivity. *Chemico-biological interactions, 202*(1), 186-194.

Poss, K. D., Wilson, L. G., & Keating, M. T. (2002). Heart regeneration in zebrafish. *Science, 298*(5601), 2188-2190. doi: 10.1126/science.1077857

Pratt, R. M., Goulding, E. H., & Abbott, B. D. (1987). Retinoic acid inhibits migration of cranial neural crest cells in the cultured mouse embryo. *J Craniofac Genet Dev Biol, 7*(3), 205-217.

Qian, Li, Huang, Yu, Spencer, C. Ian, Foley, Amy, Vedantham, Vasanth, Liu, Lei, . . . Srivastava, Deepak. (2012). In vivo reprogramming of murine cardiac fibroblasts into induced cardiomyocytes. *Nature, 485*(7400), 593-598. doi: http://www.nature.com/nature/journal/v485/n7400/abs/nature11044.html#supplementary-information

Quadro, L., Hamberger, L., Gottesman, M. E., Colantuoni, V., Ramakrishnan, R., & Blaner, W. S. (2004). Transplacental delivery of retinoid: the role of retinol-binding protein and lipoprotein retinyl ester. *Am J Physiol Endocrinol Metab, 286*(5), E844-851. doi: 10.1152/ajpendo.00556.2003

Quadro, L., Hamberger, L., Gottesman, M. E., Wang, F., Colantuoni, V., Blaner, W. S., & Mendelsohn, C. L. (2005). Pathways of vitamin A delivery to the embryo: insights from a new tunable model of embryonic vitamin A deficiency. *Endocrinology, 146*(10), 4479-4490. doi: 10.1210/en.2005-0158

Quaggin, S. E., Vanden Heuvel, G. B., & Igarashi, P. (1998). Pod-1, a mesoderm-specific basic-helix-loop-helix protein expressed in mesenchymal and glomerular epithelial cells in the developing kidney. *Mech Dev, 71*(1-2), 37-48.

Raya, A., Koth, C. M., Buscher, D., Kawakami, Y., Itoh, T., Raya, R. M., . . . Izpisua-Belmonte, J. C. (2003). Activation of Notch signaling pathway precedes heart regeneration in zebrafish. *Proc Natl Acad Sci U S A, 100 Suppl 1*, 11889-11895. doi: 10.1073/pnas.1834204100

Ream, Margie, Ray, Alisa M., Chandra, Rashmi, & Chikaraishi, Dona M. (2008). *Early fetal hypoxia leads to growth restriction and myocardial thinning* (Vol. 295).

Reese, D. E., Mikawa, T., & Bader, D. M. (2002). Development of the coronary vessel system. *Circ Res, 91*(9), 761-768.

Reeves, P. G. (1997). Components of the AIN-93 diets as improvements in the AIN-76A diet. *J Nutr, 127*(5 Suppl), 838S-841S.

Reifers, F., Walsh, E. C., Leger, S., Stainier, D. Y., & Brand, M. (2000). Induction and differentiation of the zebrafish heart requires fibroblast growth factor 8 (fgf8/acerebellar). *Development, 127*(2), 225-235.

Rhinn, M., Schuhbaur, B., Niederreither, K., & Dolle, P. (2011). Involvement of retinol dehydrogenase 10 in embryonic patterning and rescue of its loss of function by maternal retinaldehyde treatment. *Proc Natl Acad Sci U S A, 108*(40), 16687-16692. doi: 10.1073/pnas.1103877108

Rhinn, Muriel, & Dollé, Pascal. (2012). Retinoic acid signalling during development. *Development, 139*(5), 843-858. doi: 10.1242/dev.065938

Ribes, V., Fraulob, V., Petkovich, M., & Dolle, P. (2007). The oxidizing enzyme CYP26a1 tightly regulates the availability of retinoic acid in the gastrulating mouse embryo to ensure proper head development and vasculogenesis. *Dev Dyn, 236*(3), 644-653. doi: 10.1002/dvdy.21057

Riento, K., Villalonga, P., Garg, R., & Ridley, A. (2005). Function and regulation of RhoE. *Biochem Soc Trans, 33*(Pt 4), 649-651. doi: 10.1042/BST0330649

Romand, Raymond, Kondo, Takako, Fraulob, Valérie, Petkovich, Martin, Dollé, Pascal, & Hashino, Eri. (2006). Dynamic expression of retinoic acid-synthesizing and-metabolizing enzymes in the developing mouse inner ear. *Journal of Comparative Neurology, 496*(5), 643-654.

Romeih, M., Cui, J., Michaille, J. J., Jiang, W., & Zile, M. H. (2003). Function of RARgamma and RARalpha2 at the initiation of retinoid signaling is essential for avian embryo survival and for distinct events in cardiac morphogenesis. *Dev Dyn, 228*(4), 697-708. doi: 10.1002/dvdy.10419

Rosenkranz, Stephan. (2004). TGF-β1 and angiotensin networking in cardiac remodeling. *Cardiovascular Research, 63*(3), 423-432. doi: 10.1016/j.cardiores.2004.04.030

Rossant, J., Zirngibl, R., Cado, D., Shago, M., & Giguere, V. (1991). Expression of a retinoic acid response element-hsplacZ transgene defines specific domains of transcriptional activity during mouse embryogenesis. *Genes Dev, 5*(8), 1333-1344.

Rothman, K. J., Moore, L. L., Singer, M. R., Nguyen, U. S., Mannino, S., & Milunsky, A. (1995). Teratogenicity of high vitamin A intake. *N Engl J Med, 333*(21), 1369-1373. doi: 10.1056/NEJM199511233332101

Rubin, L. P., Ross, A. C., Stephensen, C. B., Bohn, T., & Tanumihardjo, S. A. (2017). Metabolic Effects of Inflammation on Vitamin A and Carotenoids in Humans and Animal Models. *Adv Nutr, 8*(2), 197-212. doi: 10.3945/an.116.014167

Rudat, C., Norden, J., Taketo, M. M., & Kispert, A. (2013). Epicardial function of canonical Wnt-, Hedgehog-, Fgfr1/2-, and Pdgfra-signalling. *Cardiovasc Res, 100*(3), 411-421. doi: 10.1093/cvr/cvt210

Rudat, Carsten, & Kispert, Andreas. (2012). Wt1 and Epicardial Fate Mapping. *Circulation Research, 111*(2), 165-169. doi: 10.1161/circresaha.112.273946

Ruiz-Villalba, A., & Perez-Pomares, J. M. (2012). The expanding role of the epicardium and epicardial-derived cells in cardiac development and disease. *Curr Opin Pediatr, 24*(5), 569-576. doi: 10.1097/MOP.0b013e328357a532

Ruiz, F. X., Gallego, O., Ardevol, A., Moro, A., Dominguez, M., Alvarez, S., . . . Farres, J. (2009). Aldo-keto reductases from the AKR1B subfamily: retinoid specificity and control of cellular retinoic acid levels. *Chem Biol Interact, 178*(1-3), 171-177. doi: 10.1016/j.cbi.2008.10.027

Ruiz, F. X., Porte, S., Gallego, O., Moro, A., Ardevol, A., Del Rio-Espinola, A., . . . Pares, X. (2011). Retinaldehyde is a substrate for human aldo-keto reductases of the 1C subfamily. *Biochem J, 440*(3), 335-344. doi: 10.1042/BJ20111286

Ryckebusch, L., Wang, Z., Bertrand, N., Lin, S. C., Chi, X., Schwartz, R., . . . Niederreither, K. (2008). Retinoic acid deficiency alters second heart field formation. *Proc Natl Acad Sci U S A, 105*(8), 2913-2918. doi: 10.1073/pnas.0712344105

Ryckebusch, Lucile, Wang, Zengxin, Bertrand, Nicolas, Lin, Song-Chang, Chi, Xuan, Schwartz, Robert, . . . Niederreither, Karen. (2008). Retinoic acid deficiency alters second heart field formation. *Proceedings of the National Academy of Sciences, 105*(8), 2913-2918. doi: 10.1073/pnas.0712344105

Rydeen, A. B., & Waxman, J. S. (2014). Cyp26 enzymes are required to balance the cardiac and vascular lineages within the anterior lateral plate mesoderm. *Development, 141*(8), 1638-1648. doi: 10.1242/dev.105874

Rydeen, A., Voisin, N., D'Aniello, E., Ravisankar, P., Devignes, C. S., & Waxman, J. S. (2015). Excessive feedback of Cyp26a1 promotes cell non-autonomous loss of retinoic acid signaling. *Dev Biol, 405*(1), 47-55. doi: 10.1016/j.ydbio.2015.06.008

Sakabe, M., Kokubo, H., Nakajima, Y., & Saga, Y. (2012). Ectopic retinoic acid signaling affects outflow tract cushion development through suppression of the myocardial Tbx2-Tgfbeta2 pathway. *Development, 139*(2), 385-395. doi: 10.1242/dev.067058

Sakai, Y., Meno, C., Fujii, H., Nishino, J., Shiratori, H., Saijoh, Y., . . . Hamada, H. (2001). The retinoic acid-inactivating enzyme CYP26 is essential for establishing an uneven distribution of retinoic acid along the anterio-posterior axis within the mouse embryo. *Genes Dev, 15*(2), 213-225.

Sandell, L. L., Sanderson, B. W., Moiseyev, G., Johnson, T., Mushegian, A., Young, K., . . . Trainor, P. A. (2007). RDH10 is essential for synthesis of embryonic retinoic acid and is required for limb, craniofacial, and organ development. *Genes Dev, 21*(9), 1113-1124. doi: 10.1101/gad.1533407

Sandell, Lisa L., Lynn, Megan L., Inman, Kimberly E., McDowell, William, & Trainor, Paul A. (2012). RDH10 Oxidation of Vitamin A Is a Critical Control Step in Synthesis of Retinoic Acid during Mouse Embryogenesis. *PLoS ONE, 7*(2), e30698. doi: 10.1371/journal.pone.0030698

Sapin, Vincent, Bègue, René-Jean, Dastugue, Bernard, Chambon, Pierre, & Dollé, Pascal. (1998). Trophoblast Research. The maternal-fetal interfaceRetinoids and mouse placentation. *Placenta, 19*, 57-76. doi: http://dx.doi.org/10.1016/S0143-4004(98)80033-7

Satre, M. A., & Kochhar, D. M. (1989). Elevations in the endogenous levels of the putative morphogen retinoic acid in embryonic mouse limb-buds associated with limb dysmorphogenesis. *Developmental Biology, 133*(2), 529-536. doi: https://doi.org/10.1016/0012-1606(89)90055-9

Schmidt, Annette, Brixius, Klara, & Bloch, Wilhelm. (2007). Endothelial Precursor Cell Migration During Vasculogenesis. *Circulation Research, 101*(2), 125-136. doi: 10.1161/circresaha.107.148932

Shannon, S. R., Moise, A. R., & Trainor, P. A. (2017). New insights and changing paradigms in the regulation of vitamin A metabolism in development. *Wiley Interdiscip Rev Dev Biol, 6*(3). doi: 10.1002/wdev.264

Sharma, B., Chang, A., & Red-Horse, K. (2017). Coronary Artery Development: Progenitor Cells and Differentiation Pathways. *Annu Rev Physiol, 79*, 1-19. doi: 10.1146/annurev-physiol-022516-033953

Shen, H., Cavallero, S., Estrada, K. D., Sandovici, I., Kumar, S. R., Makita, T., . . . Sucov, H. M. (2015). Extracardiac control of embryonic cardiomyocyte proliferation and ventricular wall expansion. *Cardiovasc Res, 105*(3), 271-278. doi: 10.1093/cvr/cvu269

Shenefelt, RE. (1972). Gross congenital malformations. Animal model: treatment of various species with a large dose of vitamin A at known stages in pregnancy. *The American journal of pathology, 66*(3), 589.

Shirakami, Y., Lee, S. A., Clugston, R. D., & Blaner, W. S. (2012). Hepatic metabolism of retinoids and disease associations. *Biochim Biophys Acta, 1821*(1), 124-136. doi: 10.1016/j.bbalip.2011.06.023

Singh, A., Ramesh, S., Cibi, D. M., Yun, L. S., Li, J., Li, L., . . . Singh, M. K. (2016). Hippo Signaling Mediators Yap and Taz Are Required in the Epicardium for Coronary Vasculature Development. *Cell Rep, 15*(7), 1384-1393. doi: 10.1016/j.celrep.2016.04.027

Sirbu, Ioan Ovidiu, Zhao, Xianling, & Duester, Gregg. (2008). Retinoic Acid Controls Heart Anteroposterior Patterning by Downregulating Isl1 through the Fgf8 Pathway. *Developmental dynamics : an official publication of the American Association of Anatomists, 237*(6), 1627-1635. doi: 10.1002/dvdy.21570

Smart, N., Bollini, S., Dube, K. N., Vieira, J. M., Zhou, B., Riegler, J., . . . Riley, P. R. (2012). Myocardial regeneration: expanding the repertoire of thymosin beta4 in the ischemic heart. *Ann N Y Acad Sci, 1269*, 92-101. doi: 10.1111/j.1749-6632.2012.06708.x

Smart, Nicola, Bollini, Sveva, Dubé, Karina N, Vieira, Joaquim M, Zhou, Bin, Davidson, Sean, . . . Lythgoe, Mark F. (2011). De novo cardiomyocytes from within the activated adult heart after injury. *Nature, 474*(7353), 640-644.

Smith, C. L., Baek, S. T., Sung, C. Y., & Tallquist, M. D. (2011). Epicardial-derived cell epithelial-to-mesenchymal transition and fate specification require PDGF receptor signaling. *Circ Res, 108*(12), e15-26. doi: 10.1161/CIRCRESAHA.110.235531

Smith, Susan M., Dickman, Eileen D., Power, Susan C., & Lancman, Joseph. (1998). Retinoids and Their Receptors in Vertebrate Embryogenesis. *The Journal of Nutrition, 128*(2), 467S-470S.

Smith, Susan M., Dickman, Eileen D., Thompson, Robert P., Sinning, Allan R., Wunsch, Ann M., & Markwald, Roger R. (1997). Retinoic Acid Directs Cardiac Laterality and the Expression of Early Markers of Precardiac Asymmetry. *Developmental Biology, 182*(1), 162-171. doi: http://dx.doi.org/10.1006/dbio.1996.8474

Sorrell, M. R., & Waxman, J. S. (2011). Restraint of Fgf8 signaling by retinoic acid signaling is required for proper heart and forelimb formation. *Dev Biol, 358*(1), 44-55. doi: 10.1016/j.ydbio.2011.07.022

Soshnikova, Natalia, Dewaele, Romain, Janvier, Philippe, Krumlauf, Robb, & Duboule, Denis. (2013). Duplications of hox gene clusters and the emergence of vertebrates. *Developmental Biology, 378*(2), 194-199. doi: http://dx.doi.org/10.1016/j.ydbio.2013.03.004

Stefanovic, S., & Zaffran, S. (2017). Mechanisms of retinoic acid signaling during cardiogenesis. *Mech Dev, 143*, 9-19. doi: 10.1016/j.mod.2016.12.002

Stuckmann, I., Evans, S., & Lassar, A. B. (2003). Erythropoietin and retinoic acid, secreted from the epicardium, are required for cardiac myocyte proliferation. *Dev Biol, 255*(2), 334-349. doi: http://dx.doi.org/10.1016/S0012-1606(02)00078-7

Stuckmann, Ingo, Evans, Samuel, & Lassar, Andrew B. (2003). Erythropoietin and retinoic acid, secreted from the epicardium, are required for cardiac myocyte proliferation. *Developmental Biology, 255*(2), 334-349. doi: http://dx.doi.org/10.1016/S0012-1606(02)00078-7

Subbarayan, V., Kastner, P., Mark, M., Dierich, A., Gorry, P., & Chambon, P. (1997). Limited specificity and large overlap of the functions of the mouse RAR gamma 1 and RAR gamma 2 isoforms. *Mech Dev, 66*(1-2), 131-142.

Sun, Xin, Meyers, Erik N., Lewandoski, Mark, & Martin, Gail R. (1999). Targeted disruption of Fgf8 causes failure of cell migration in the gastrulating mouse embryo. *Genes & Development, 13*(14), 1834-1846.

Swindell, E. C., Thaller, C., Sockanathan, S., Petkovich, M., Jessell, T. M., & Eichele, G. (1999). Complementary domains of retinoic acid production and degradation in the early chick embryo. *Dev Biol, 216*(1), 282-296. doi: 10.1006/dbio.1999.9487

Tallquist, M. D., & Molkentin, J. D. (2017). Redefining the identity of cardiac fibroblasts. *Nat Rev Cardiol, 14*(8), 484-491. doi: 10.1038/nrcardio.2017.57

Tasaka, H., Takenaka, H., Okamoto, N., Onitsuka, T., Koga, Y., & Hamada, M. (1991). Abnormal development of cardiovascular systems in rat embryos treated with bisdiamine. *Teratology, 43*(3), 191-200. doi: 10.1002/tera.1420430303

Tevosian, S. G., Deconinck, A. E., Tanaka, M., Schinke, M., Litovsky, S. H., Izumo, S., . . . Orkin, S. H. (2000). FOG-2, a cofactor for GATA transcription factors, is essential for heart morphogenesis and development of coronary vessels from epicardium. *Cell*, *101*(7), 729-739.

Tian, X., Hu, T., Zhang, H., He, L., Huang, X., Liu, Q., . . . Zhou, B. (2013). Subepicardial endothelial cells invade the embryonic ventricle wall to form coronary arteries. *Cell Res*, *23*(9), 1075-1090. doi: 10.1038/cr.2013.83

Tickle, C., Lee, J., & Eichele, G. (1985). A quantitative analysis of the effect of all-trans-retinoic acid on the pattern of chick wing development. *Developmental Biology*, *109*(1), 82-95. doi: http://dx.doi.org/10.1016/0012-1606(85)90348-3

Tomanek, R. J., Lund, D. D., & Yue, X. (2003). Hypoxic induction of myocardial vascularization during development. *Adv Exp Med Biol*, *543*, 139-149.

Tomanek, R. J., Ratajska, A., Kitten, G. T., Yue, X., & Sandra, A. (1999). Vascular endothelial growth factor expression coincides with coronary vasculogenesis and angiogenesis. *Dev Dyn*, *215*(1), 54-61. doi: 10.1002/(SICI)1097-0177(199905)215:1<54::AID-DVDY6>3.0.CO;2-0

Trembley, M. A., Velasquez, L. S., de Mesy Bentley, K. L., & Small, E. M. (2015). Myocardin-related transcription factors control the motility of epicardium-derived cells and the maturation of coronary vessels. *Development*, *142*(1), 21-30. doi: 10.1242/dev.116418

Twal, W., Roze, L., & Zile, M. H. (1995). Anti-retinoic acid monoclonal antibody localizes all-trans-retinoic acid in target cells and blocks normal development in early quail embryo. *Dev Biol*, *168*(2), 225-234. doi: 10.1006/dbio.1995.1075

Uehara, M., Yashiro, K., Mamiya, S., Nishino, J., Chambon, P., Dolle, P., & Sakai, Y. (2007). CYP26A1 and CYP26C1 cooperatively regulate anterior-posterior patterning of the developing brain and the production of migratory cranial neural crest cells in the mouse. *Dev Biol*, *302*(2), 399-411. doi: 10.1016/j.ydbio.2006.09.045

Uehara, Masayuki, Yashiro, Kenta, Takaoka, Katsuyoshi, Yamamoto, Masamichi, & Hamada, Hiroshi. (2009). Removal of maternal retinoic acid by embryonic CYP26 is required for correct Nodal expression during early embryonic patterning. *Genes & development, 23*(14), 1689-1698.

van Wijk, Bram, Gunst, Quinn D., Moorman, Antoon F. M., & van den Hoff, Maurice J. B. (2012). Cardiac Regeneration from Activated Epicardium. *PLoS ONE, 7*(9), e44692. doi: 10.1371/journal.pone.0044692

Vega-Hernandez, M., Kovacs, A., De Langhe, S., & Ornitz, D. M. (2011). FGF10/FGFR2b signaling is essential for cardiac fibroblast development and growth of the myocardium. *Development, 138*(15), 3331-3340. doi: 10.1242/dev.064410

Vieux-Rochas, M., Coen, L., Sato, T., Kurihara, Y., Gitton, Y., Barbieri, O., . . . Levi, G. (2007). Molecular dynamics of retinoic acid-induced craniofacial malformations: implications for the origin of gnathostome jaws. *PLoS One, 2*(6), e510. doi: 10.1371/journal.pone.0000510

Vieux-Rochas, Maxence, Coen, Laurent, Sato, Takahiro, Kurihara, Yukiko, Gitton, Yorick, Barbieri, Ottavia, . . . Levi, Giovanni. (2007). Molecular Dynamics of Retinoic Acid-Induced Craniofacial Malformations: Implications for the Origin of Gnathostome Jaws. *PLoS ONE, 2*(6), e510. doi: 10.1371/journal.pone.0000510

Vincent, S. D., & Buckingham, M. E. (2010). How to make a heart: the origin and regulation of cardiac progenitor cells. *Curr Top Dev Biol, 90*, 1-41. doi: 10.1016/s0070-2153(10)90001-x

Volz, K. S., Jacobs, A. H., Chen, H. I., Poduri, A., McKay, A. S., Riordan, D. P., . . . Red-Horse, K. (2015). Pericytes are progenitors for coronary artery smooth muscle. *Elife, 4*. doi: 10.7554/eLife.10036

von Gise, A., & Pu, W. T. (2012). Endocardial and epicardial epithelial to mesenchymal transitions in heart development and disease. *Circ Res, 110*(12), 1628-1645. doi: 10.1161/CIRCRESAHA.111.259960

von Gise, A., Zhou, B., Honor, L. B., Ma, Q., Petryk, A., & Pu, W. T. (2011). WT1 regulates epicardial epithelial to mesenchymal transition through beta-catenin and retinoic acid signaling pathways. *Dev Biol, 356*(2), 421-431. doi: 10.1016/j.ydbio.2011.05.668

von Lintig, J., & Vogt, K. (2000). Filling the gap in vitamin A research. Molecular identification of an enzyme cleaving beta-carotene to retinal. *J Biol Chem, 275*(16), 11915-11920.

Vrancken Peeters, M. P., Gittenberger-de Groot, A. C., Mentink, M. M., Hungerford, J. E., Little, C. D., & Poelmann, R. E. (1997). The development of the coronary vessels and their differentiation into arteries and veins in the embryonic quail heart. *Dev Dyn, 208*(3), 338-348. doi: 10.1002/(SICI)1097-0177(199703)208:3<338::AID-AJA5>3.0.CO;2-J

Wakino, Shu, Kintscher, Ulrich, Kim, Sarah, Jackson, Simon, Yin, Fen, Nagpal, Sunil, . . . Law, Ronald E. (2001). Retinoids Inhibit Proliferation of Human Coronary Smooth Muscle Cells by Modulating Cell Cycle Regulators. *Arteriosclerosis, Thrombosis, and Vascular Biology, 21*(5), 746-751. doi: 10.1161/01.atv.21.5.746

Wang, Hao-Jie, Zhu, Yi-Chun, & Yao, Tai. (2002). Effects of all-trans retinoic acid on angiotensin II-induced myocyte hypertrophy. *Journal of Applied Physiology, 92*(5), 2162-2168. doi: 10.1152/japplphysiol.01192.2001

Ward, C., Stadt, H., Hutson, M., & Kirby, M. L. (2005). Ablation of the secondary heart field leads to tetralogy of Fallot and pulmonary atresia. *Dev Biol, 284*(1), 72-83. doi: 10.1016/j.ydbio.2005.05.003

Waxman, J. S., Keegan, B. R., Roberts, R. W., Poss, K. D., & Yelon, D. (2008). Hoxb5b acts downstream of retinoic acid signaling in the forelimb field to restrict heart field potential in zebrafish. *Dev Cell, 15*(6), 923-934. doi: 10.1016/j.devcel.2008.09.009

Waxman, J. S., & Yelon, D. (2009). Increased Hox activity mimics the teratogenic effects of excess retinoic acid signaling. *Dev Dyn, 238*(5), 1207-1213. doi: 10.1002/dvdy.21951

Waxman, Joshua S., Keegan, Brian R., Roberts, Richard W., Poss, Kenneth D., & Yelon, Deborah. (2008). Hoxb5b acts downstream of retinoic acid signaling in the forelimb field to restrict heart

field potential in zebrafish. *Developmental cell, 15*(6), 923-934. doi: 10.1016/j.devcel.2008.09.009

Wei, K., Serpooshan, V., Hurtado, C., Diez-Cunado, M., Zhao, M., Maruyama, S., . . . Ruiz-Lozano, P. (2015). Epicardial FSTL1 reconstitution regenerates the adult mammalian heart. *Nature, 525*(7570), 479-485. doi: 10.1038/nature15372

Wendler, Christopher C., Schmoldt, Angela, Flentke, George R., Case, Lauren C., Quadro, Loredana, Blaner, William S., . . . Smith, Susan M. (2003). Increased Fibronectin Deposition in Embryonic Hearts of Retinol-Binding Protein–Null Mice. *Circulation Research, 92*(8), 920-928. doi: 10.1161/01.res.0000069030.30886.8f

White, J. C., Shankar, V. N., Highland, M., Epstein, M. L., DeLuca, H. F., & Clagett-Dame, M. (1998). Defects in embryonic hindbrain development and fetal resorption resulting from vitamin A deficiency in the rat are prevented by feeding pharmacological levels of all-trans-retinoic acid. *Proc Natl Acad Sci U S A, 95*(23), 13459-13464.

White, Jeffrey C., Highland, Margaret, Kaiser, Mary, & Clagett-Dame, Margaret. (2000). Vitamin A Deficiency Results in the Dose-Dependent Acquisition of Anterior Character and Shortening of the Caudal Hindbrain of the Rat Embryo. *Developmental Biology, 220*(2), 263-284. doi: https://doi.org/10.1006/dbio.2000.9635

Wikenheiser, J., Doughman, Y. Q., Fisher, S. A., & Watanabe, M. (2006). Differential levels of tissue hypoxia in the developing chicken heart. *Dev Dyn, 235*(1), 115-123. doi: 10.1002/dvdy.20499

Wilson, James G, Roth, Carolyn B, & Warkany, Josef. (1953a). An analysis of the syndrome of malformations induced by maternal vitamin A deficiency. Effects of restoration of vitamin A at various times during gestation. *American Journal of Anatomy, 92*(2), 189-217.

Wilson, James G, Roth, Carolyn B, & Warkany, Josef. (1953b). An analysis of the syndrome of malformations induced by maternal vitamin A deficiency. Effects of restoration of vitamin A at various times during gestation. *Developmental Dynamics, 92*(2), 189-217.

Wilson, James G, & Warkany, Josef. (1948). Malformations in the genito-urinary tract induced by maternal vitamin a deficiency in the rat. *Developmental Dynamics, 83*(3), 357-407.

Wu, H., Lee, S. H., Gao, J., Liu, X., & Iruela-Arispe, M. L. (1999). Inactivation of erythropoietin leads to defects in cardiac morphogenesis. *Development, 126*(16), 3597-3605.

Wu, S. P., Dong, X. R., Regan, J. N., Su, C., & Majesky, M. W. (2013). Tbx18 regulates development of the epicardium and coronary vessels. *Dev Biol, 383*(2), 307-320. doi: 10.1016/j.ydbio.2013.08.019

Wyss, A., Wirtz, G., Woggon, W., Brugger, R., Wyss, M., Friedlein, A., . . . Hunziker, W. (2000). Cloning and expression of beta,beta-carotene 15,15'-dioxygenase. *Biochem Biophys Res Commun, 271*(2), 334-336. doi: 10.1006/bbrc.2000.2619

Xavier-Neto, J., Neville, C. M., Shapiro, M. D., Houghton, L., Wang, G. F., Nikovits, W., Jr., . . . Rosenthal, N. (1999). A retinoic acid-inducible transgenic marker of sino-atrial development in the mouse heart. *Development, 126*(12), 2677-2687.

Xavier-Neto, J., Shapiro, M. D., Houghton, L., & Rosenthal, N. (2000). Sequential programs of retinoic acid synthesis in the myocardial and epicardial layers of the developing avian heart. *Dev Biol, 219*(1), 129-141. doi: 10.1006/dbio.1999.9588

Xavier-Neto, J., Sousa Costa, A. M., Figueira, A. C., Caiaffa, C. D., Amaral, F. N., Peres, L. M., . . . Castillo, H. A. (2015). Signaling through retinoic acid receptors in cardiac development: Doing the right things at the right times. *Biochim Biophys Acta, 1849*(2), 94-111. doi: 10.1016/j.bbagrm.2014.08.003

Xu, Huansheng, Morishima, Masae, Wylie, John N., Schwartz, Robert J., Bruneau, Benoit G., Lindsay, Elizabeth A., & Baldini, Antonio. (2004). Tbx1 has a dual role in the morphogenesis of the cardiac outflow tract. *Development, 131*(13), 3217-3227.

Yang, J. T., Rayburn, H., & Hynes, R. O. (1995). Cell adhesion events mediated by alpha 4 integrins are essential in placental and cardiac development. *Development, 121*(2), 549-560.

Yashiro, Kenta, Zhao, Xianling, Uehara, Masayuki, Yamashita, Kimiyo, Nishijima, Misae, Nishino, Jinsuke, . . . Hamada, Hiroshi. (2004). Regulation of Retinoic Acid Distribution Is Required for Proximodistal Patterning and Outgrowth of the Developing Mouse Limb. *Developmental Cell, 6*(3), 411-422. doi: 10.1016/s1534-5807(04)00062-0

Yasui, H., Nakazawa, M., Morishima, M., Ando, M., Takao, A., & Aikawa, E. (1997). Cardiac outflow tract septation process in the mouse model of transposition of the great arteries. *Teratology, 55*(6), 353-363. doi: 10.1002/(SICI)1096-9926(199706)55:6<353::AID-TERA1>3.0.CO;2-Z

Yu, Shuiliang, Levi, Liraz, Siegel, Ruth, & Noy, Noa. (2012). Retinoic Acid Induces Neurogenesis by Activating Both Retinoic Acid Receptors (RARs) and Peroxisome Proliferator-activated Receptor β/δ (PPARβ/δ). *The Journal of Biological Chemistry, 287*(50), 42195-42205. doi: 10.1074/jbc.M112.410381

Yue, X., & Tomanek, R. J. (1999). Stimulation of coronary vasculogenesis/angiogenesis by hypoxia in cultured embryonic hearts. *Dev Dyn, 216*(1), 28-36. doi: 10.1002/(SICI)1097-0177(199909)216:1<28::AID-DVDY5>3.0.CO;2-U

Yutzey, K. E., Rhee, J. T., & Bader, D. (1994). Expression of the atrial-specific myosin heavy chain AMHC1 and the establishment of anteroposterior polarity in the developing chicken heart. *Development, 120*(4), 871-883.

Zaffran, S., Kelly, R. G., Meilhac, S. M., Buckingham, M. E., & Brown, N. A. (2004). Right ventricular myocardium derives from the anterior heart field. *Circ Res, 95*(3), 261-268. doi: 10.1161/01.RES.0000136815.73623.BE

Zaffran, Stéphane, Robrini, Nicolas El, & Bertrand, Nicolas. (2014). Retinoids and cardiac development. *Journal of Developmental Biology, 2*(1), 50-71.

Zhao, Dayao, McCaffery, Peter, Ivins, Kathryn J, Neve, Rachael L, Hogan, Patrick, Chin, William W, & Dräger, Ursula C. (1996). Molecular identification of a major retinoic-acid-synthesizing enzyme, a retinaldehyde-specific dehydrogenase. *The FEBS Journal, 240*(1), 15-22.

Zhou, B., Honor, L. B., He, H., Ma, Q., Oh, J. H., Butterfield, C., . . . Pu, W. T. (2011). Adult mouse epicardium modulates myocardial injury by secreting paracrine factors. *J Clin Invest, 121*(5), 1894-1904. doi: 10.1172/JCI45529

Zhou, B., Ma, Q., Rajagopal, S., Wu, S. M., Domian, I., Rivera-Feliciano, J., . . . Pu, W. T. (2008). Epicardial progenitors contribute to the cardiomyocyte lineage in the developing heart. *Nature, 454*(7200), 109-113. doi: 10.1038/nature07060

Zhou, Bin, Honor, Leah B., He, Huamei, Ma, Qing, Oh, Jin-Hee, Butterfield, Catherine, . . . Pu, William T. (2011). Adult mouse epicardium modulates myocardial injury by secreting paracrine factors. *The Journal of Clinical Investigation, 121*(5), 1894-1904. doi: 10.1172/JCI45529

Zhou, Bin, & Pu, William T. (2012). Genetic Cre-loxP assessment of epicardial cell fate using Wt1-driven Cre Alleles. *Circulation research, 111*(11), e276-e280. doi: 10.1161/CIRCRESAHA.112.275784

Zhou, Bin, von Gise, Alexander, Ma, Qing, Hu, Yong Wu, & Pu, William T. (2010). Genetic fate mapping demonstrates contribution of epicardium-derived cells to the annulus fibrosis of the mammalian heart. *Developmental Biology, 338*(2), 251-261. doi: https://doi.org/10.1016/j.ydbio.2009.12.007

Zhou, M., Sutliff, R. L., Paul, R. J., Lorenz, J. N., Hoying, J. B., Haudenschild, C. C., . . . Doetschman, T. (1998). Fibroblast growth factor 2 control of vascular tone. *Nat Med, 4*(2), 201-207.

Zile, M. H. (1999). Avian Embryo as Model for Retinoid Function in Early Development. In H. Nau & W. S. Blaner (Eds.), *Retinoids: The Biochemical and Molecular Basis of Vitamin A and Retinoid Action* (pp. 443-464). Berlin, Heidelberg: Springer Berlin Heidelberg.